doi.org/10.26434/chemrxiv.12613823.v1

Semisynthetic Analogs of the Antibiotic Fidaxomicin – Design, Synthesis, and Biological Evaluation

Andrea Dorst, Regina Berg, Christoph Gertzen, Daniel Schäfle, katja zerbe, myriam gwerder, Simon Schnell, Peter Sander, Holger Gohlke, Karl Gademann

Submitted date: 06/07/2020 • Posted date: 07/07/2020

Citation information: Dorst, Andrea; Berg, Regina; Gertzen, Christoph; Schäfle, Daniel; zerbe, katja; gwerder, myriam; et al. (2020): Semisynthetic Analogs of the Antibiotic Fidaxomicin – Design, Synthesis, and Biological Evaluation. ChemRxiv. Preprint. https://doi.org/10.26434/chemrxiv.12613823.v1

The glycoslated macrocyclic antibiotic fidaxomicin (1, tiacumicin B, lipiarmycin A3) displays good to excellent activity against Gram-positive bacteria and was approved for the treatment of Clostridium difficile infections (CDI). Main limitations of the compound include low water solubility, which impacts further clinical use. We report on the synthesis of new fidaxomicin derivatives based on structural design and utilizing an operationally simple one-step protecting group-free preparative approach from the natural product. An increase in solubility of up to 25-fold with largely retained activity was observed. Furthermore, hybrid antibiotics were prepared that show improved antibiotic activities

Semisynthetic Analogs of the Antibiotic Fidaxomicin – Design, Synthesis, and Biological Evaluation

Andrea Dorst,[‡a] Regina Berg,[‡a] Christoph G. W. Gertzen,[b] Daniel Schäfle,[c] Katja Zerbe,[a] Myriam Gwerder,[a] Simon D. Schnell,[a] Peter Sander,[c,d] Holger Gohlke,[b] and Karl Gademann*[a]

[a] Department of Chemistry, University of Zurich, Winterthurerstrasse 190, 8057 Zürich, Switzerland. E-mail: karl.gademann@chem.uzh.ch

[b] Institute for Pharmaceutical and Medicinal Chemistry, Heinrich Heine University Düsseldorf, Universitätsstr. 1, 40225 Düsseldorf and John von Neumann Institute for Computing (NIC), Institute of Biological Information Processing (IBI-7: Structural Biochemistry) & Jülich Supercomputing Centre (JSC), Forschungszentrum Jülich, 52425 Jülich, Germany.

[c] Institute of Medical Microbiology, University of Zurich, Gloriastrasse 28/30, 8006 Zurich, Switzerland

[d] National Center for Mycobacteria, University of Zurich, Gloriastrasse 28/30, 8006 Zurich, Switzerland

KEYWORDS fidaxomicin, antibiotics, semisynthesis, homology modeling, water solubility

ABSTRACT: The glycoslated macrocyclic antibiotic fidaxomicin (**1**, tiacumicin B, lipiarmycin A3) displays good to excellent activity against Gram-positive bacteria and was approved for the treatment of *Clostridium difficile* infections (CDI). Main limitations of the compound include low water solubility, which impacts further clinical use. We report on the synthesis of new fidaxomicin derivatives based on structural design and utilizing an operationally simple one-step protecting group-free preparative approach from the natural product. An increase in solubility of up to 25-fold with largely retained activity was observed. Furthermore, hybrid antibiotics were prepared that show improved antibiotic activities.

Fidaxomicin (**1**, tiacumicin B, lipiarmycin A3) is a glycosylated macrocyclic lactone produced by actinomycetes and has been isolated from four different soil bacteria.[1–7] Fidaxomicin shows good antibiotic activity in vitro against many Gram-positive bacteria, with minimum inhibitory concentration (MIC) values between 0.012 μg/mL and 0.25 μg/mL for *Clostridium difficile*,[8,9] a pathogen causing nosocomial diarrhea. Since 2011, fidaxomicin has been approved for the treatment of inflammations of the intestine caused by *C. difficile*.[10–12] Furthermore, excellent activity against multi-resistant *M. tuberculosis* and *S. aureus* has been reported.[7,13] Due to the low water solubility of fidaxomicin (**1**) and in consequence its poor systemic absorption, its application for the treatment of systemic infections has not yet been achieved. The development of semisynthetic derivatives is therefore a promising approach to render this class of antibiotics available for such treatments of systemic infections, in particular by improving water solubility.

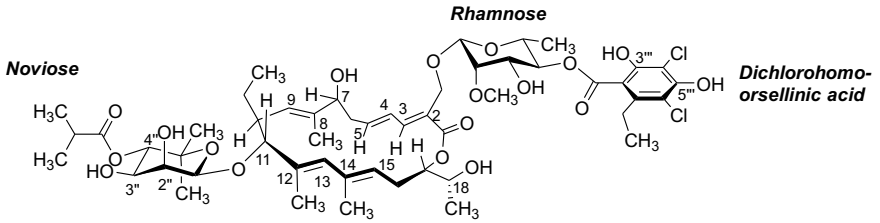

Fidaxomicin (**1**, tiacumicin B, lipiarmycin A3)

Figure 1. Structure of fidaxomicin (tiacumicin B, lipiarmycin A3).

With regard to its aglycon ring system, fidaxomicin (**1**) structurally belongs to the macrocyclic lactone antibiotics (Figure 1), but features a larger 18-membered ring.[14,15] The aglycon is connected to a modified noviose (isobutyl ester instead of a methoxy group in 4''-position) as well as to a rhamnose substituent, which is esterified to a dichlorohomoorsellinic acid subunit. The complex structure and the remarkable biological properties of fidaxomicin (**1**) aroused the interest of many research groups and led to several synthetic studies towards the preparation of the aglycon[16–20] and finally the first total synthesis of this natural product reported by some of us,[21] and subsequently by others.[22] Furthermore, investigations of the mechanism of action revealed that fidaxomicin, in contrast to other macrolide antibiotics, does not affect ribosomal protein synthesis, but rather inhibits the transcription process catalyzed by bacterial RNA-Polymerase (RNAP).[8,23–30] In order to identify promising semisynthetic target molecules based on structural considerations, docking calculations of fidaxomicin on a homology model of *M. tuberculosis* RNAP, as well as stability assays[31] under various conditions were carried out first.

We started our work with the prediction of the binding mode of fidaxomicin in a structural model of *M. tuberculosis* RNAP. We applied multi-template homology modeling and a multi-model docking approach.[32,33] In the predicted complex, fidaxomicin forms one direct and three indirect interactions (mediated by water) with an RNAP residue whose mutation triggered resistance (Figure 2).[7,26,34–36] The dichlorohomoorsellinic acid is located outside the binding pocket and its phenolic hydroxy groups do not take part in any of these interactions. This led to the hypothesis that modifications at these positions represent a promising strategy when aiming to improve water solubility. Furthermore, these hydroxy groups are in proximity to the binding pocket of the antibiotic rifampicin (Figure S1) and we used our binding mode prediction to calculate the optimal linker length (24 atoms of a polyethylene glycol chain) to covalently connect the two antibiotics in order to target both binding sites at the same time. The actual binding mode of fidaxomicin in *M. tuberculosis* RNAP was recently elucidated using cryo-electron microscopy (cryo-EM).[29,30] A comparison with our binding mode prediction revealed that the macrocycles are overlapping, but the resorcinol moieties point in opposite directions (Figure S2). However, the cryo-EM structure also revealed a solvent pocket around the dichlorohomoorsellinic acid subunit, thus further corroborating the hypothesis that this part is a suitable site for modifications.

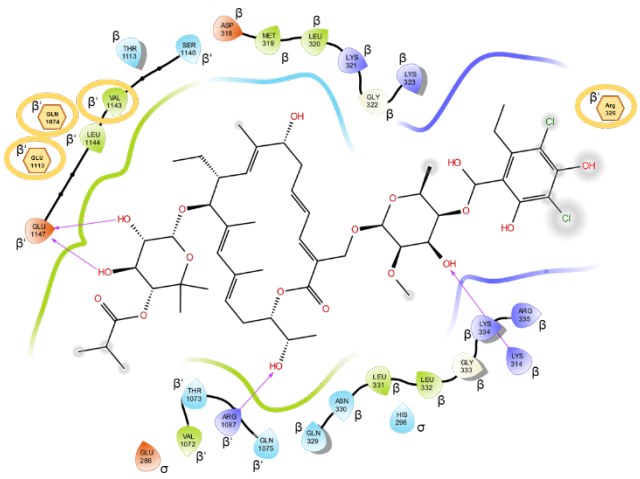

Figure 2. Interaction diagram of the predicted fidaxomicin binding mode in *M. tuberculosis* RNAP. The protein subunits are given in Greek letters. Grey circles around atoms show exposition to solvent. Orange circles show residues that lead to resistance when mutated, indirectly affected residues are displayed as hexagons.

According to our binding mode prediction, 3'''- and 5'''-positions displayed promising sites for modifications as they are exposed to solvent. Furthermore, functionalizations in these positions turned out to be synthetically feasible without the use of any protecting group, thus analogs were accessible with only one preparative step.[37] Therefore, fidaxomicin (**1**) was treated with different electrophiles under slightly basic conditions in DMF at elevated temperatures (Scheme 1). The products **2**–**10** were obtained as separable mixtures of mono- and disubstituted compounds (except **9b**[38]). Under basic conditions, formation of trace amounts of isomers, which proved to be the transacylated isobutyric ester, could not be prevented.[31] After purification by preparative HPLC, the desired compounds were obtained in moderate to good yields (28–81%).

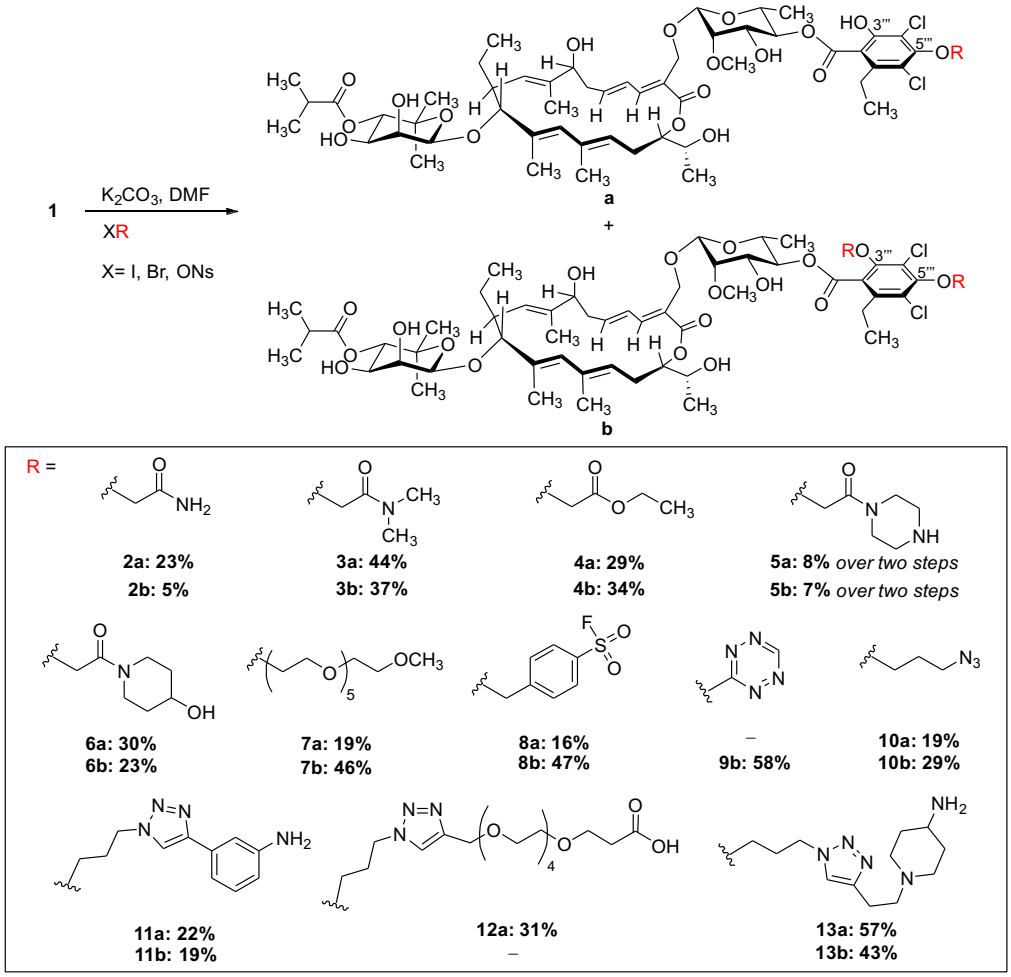

Scheme 1. Functionalization at positions 3''' and 5''' of the resorcinol unit. (Ns = Nosyl).

The substituents in compounds **2**–**7** were installed for their high polarity and their common use in medicinal chemistry. The sulfonyl fluorides **8a**/**8b** were synthesized for their ability to form covalent bonds with the enzyme of interest (SuFEx-Click chemistry),[39] which might also be useful for MS-based studies on the binding site. In the context of a study on labeling of macromolecules with tetrazine moieties, we synthesized tetrazine-fidaxomicin **9b**.[38] Furthermore, we reacted the nosylated azidopropanol to obtain azide derivatives **10a**/**b**, which were used as a platform to connect several structurally diverse alkynes to the resorcinol moiety using Click chemistry (CuAAC) with a dicopper-catalyst developed by Straub and coworkers[40] or commercially available Cu(I)OAc. Using azide **10a** as starting material, anilines **11**, alkyne-PEG5-acid **12a** and piperidinamine **13a**/**b** were obtained, which showed improved water solubility in comparison with fidaxomicin (see below).

In addition to the derivatives discussed so far, hybrids of fidaxomicin with other antibiotics were synthesized. These either have different targets or interact with different binding sites within a common target. Fluoroquinolones are common components of hybrid antibiotics due to their stability in a great variety of reaction conditions and their broad spectrum of activity.[41,42] Modifications on the amine of the piperazine moiety were shown to barely influence the activity.[43] Therefore, this position was chosen for covalently connecting ciprofloxacin to fidaxomicin, thus expecting only minor influences on both molecules' biological properties. For the synthesis of the fidaxomicin-ciprofloxacin hybrid **15**, ciprofloxacin was first transformed into the corresponding bromoacetyl-ciprofloxacin **14** using bromoacetyl bromide (Scheme 2). Subsequent exposure to basic conditions (K_2CO_3 in DMF) together with fidaxomicin resulted in the desired hybrid **15**.

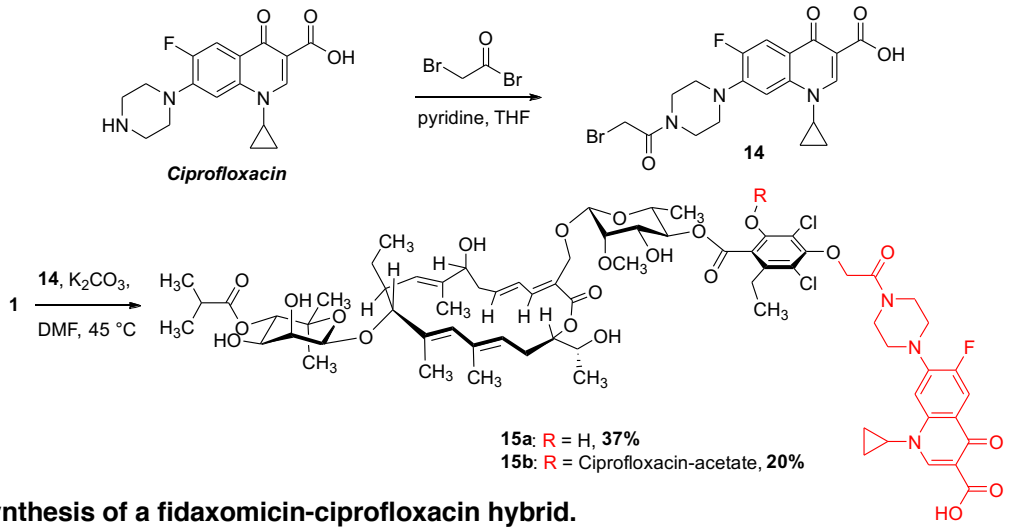

Scheme 2. Synthesis of a fidaxomicin-ciprofloxacin hybrid.

As fidaxomicin and rifampicin share the same target enzyme (RNAP), but interact with different binding sites (Figure S1),[8] we synthesized a fidaxomicin-rifampicin hybrid. Based on our calculations on the predicted binding mode, an octaethyleneglycol linker was deemed suitable in order to covalently connect the two antibiotics while

retaining their ability to interact with their respective binding sites at the same time. Starting from fidaxomicin (**1**) and nosylated octaethyleneglycol azide **16,** the octaethlyene glycol linker was introduced and azide **17** was then connected with literature known alkynylated rifampicin **18**[44] using a Cu(I)-catalyst[40] to give the desired fidaxomicin-rifampicin hybrid **19** (Scheme 3).

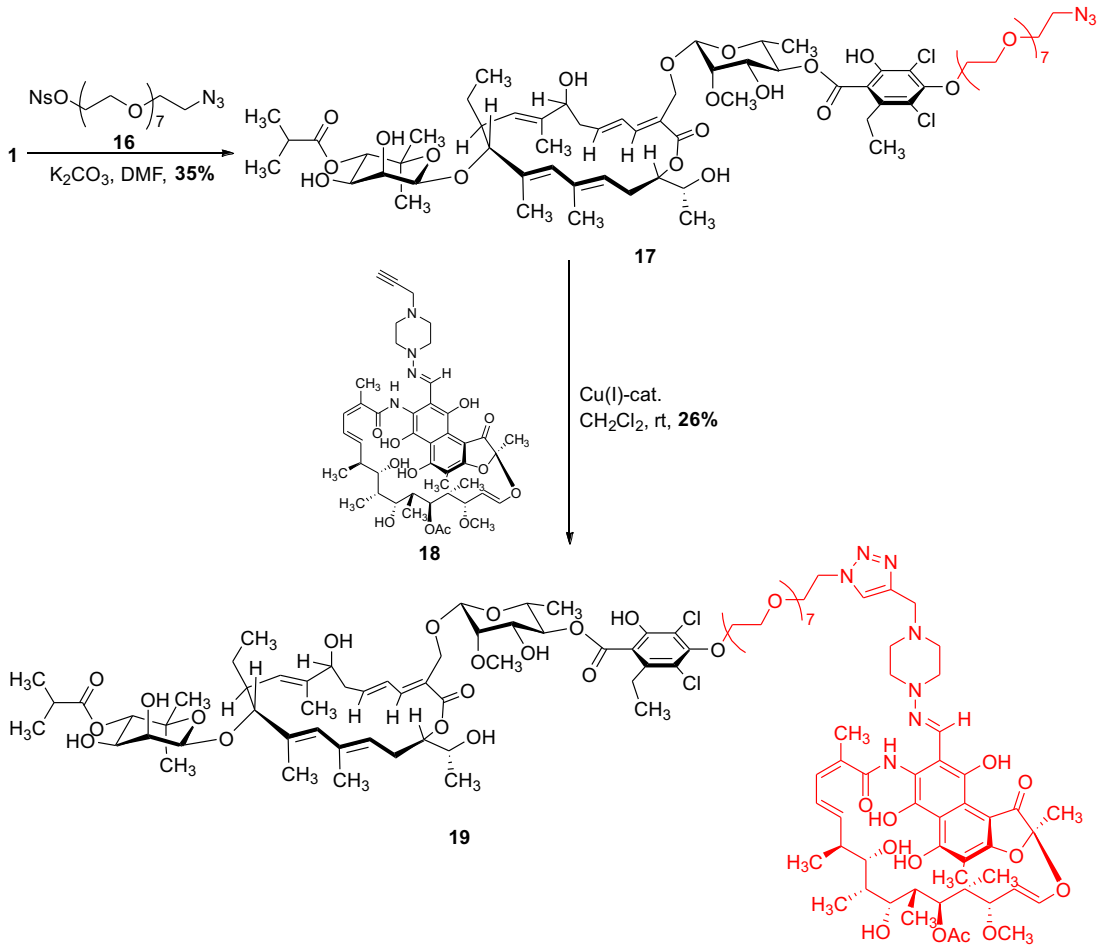

Scheme 3. Synthesis of the fidaxomicin-rifampicin hybrid 19.

We investigated the antibiotic activity of the synthesized derivatives on different bacterial strains such as *B. subtilis* (DSM3256), *S. aureus* (ATCC29213) and *M. tuberculosis* by evaluation of the minimum inhibitory concentration (MIC) (see SI). Derivatives that showed promising antibiotic activity in these tests where further assessed for their antibiotic activity against several isolates of *C. difficile* (Table 1). Although some of the derivatives did not retain their antibiotic activity, it was demonstrated that large substituents on the resorcinol do not necessarily impair the biological activity, which is shown by the good biological activities of derivatives **4a/b**, **5a, 9b, 13a** and hybrids **15a** and **19**. Although derivatives **4a/b** and **13a/b** display decreased activity against *C. difficile*, some promising activity was observed against *M. tuberculosis, S. aureus* and *B. subtilis*. Moreover, compounds **5a** and **9b** retained excellent activity against *C. difficile*.

Table 1. Summary of the minimum inhibitory concentrations (MIC) of selected derivatives.

Compound	MIC in μg/mL												
	C. difficile ATCC 43255	*C. difficile ATCC 700057*	*C. difficile BAA-1805*	*C. difficile* BAA-1875	*C. difficile* ATCC 9689 (rt 001)	*C. difficile* 8260 (rt 017)	*C. difficile* 8282 (rt 017)	*C. difficile* 5680 (rt 027)	*C. difficile* 8264 (rt 027)	*C. difficile* 8290 (rt 078)	*M. tuberculosis*	*S.aureus* ATCC 29213	*B. subtilis* DSM3256
1	0.03	0.03	0.12	0.03	≤0.015	0.06	0.03	0.06	0.12	0.03	0.25	8–16	8–16
4a	>16	8	>16	8	2	16	8	>16	>16	16	2	16	32
4b	>16	16	>16	16	4	16	16	>16	>16	16	0.5–1	32	8
5a	0.5	0.25	0.5	0.5	0.03	0.03	0.06	0.5	0.5	0.25	1-2	>64	>64
9b	0.12	0.06	0.25	0.25	0.03	0.12	0.06	0.5	0.25	0.12	n.d.	n.d.	n.d.
13a	4	2	8	2	0.5	4	1	8	8	4	4-8	>64	>64
13b	>16	>16	>16	>16	>16	>16	>16	>16	>16	>16	16–32	>64	8
15a	0.03	0.06	0.12	0.06	≤0.015	0.03	0.03	0.12	0.12	0.12	1-2	>64	32 –
19	≤0.015	≤0.015	≤0.015	≤0.015	≤0.015	≤0.015	4	≤0.015	0.03	0.03	0.5	4	4–16
Rifampicin	≤0.015	≤0.015	≤0.015	≤0.015	≤0.015	>16	>16	≤0.015	≤0.015	≤0.015	0.004	0.008	0.25
Ciprofloxacin	>16	>16	>16	>16	16	>16	>16	>16	>16	>16	1	n.d.	n.d.

The fidaxomicin-rifampicin hybrid **19** shows an improved activity compared to fidaxomicin against all investigated strains and similar activity against *C. difficile* when compared to rifampicin. Interestingly, hybrid **19** retains its biological activity even against strains which are not susceptible to rifampicin (*C. difficile* 8260 and 8282). Though no antibiotic activity against *S. aureus* and *B. subtilis* has been observed, the fidaxomicin-ciprofloxacin hybrid **15a** retains its excellent activity against all *C. difficile* strains even though ciprofloxacin itself is inactive against the latter.

Additionally, we investigated the water solubility of the obtained derivatives at pH = 7 by HPLC. For this purpose, saturated solutions of the derivatives in phosphate buffer were prepared and the concentration was determined after filtration of the resulting suspensions. The results (Figure 3) provide evidence for higher water solubility of PEG-derivatives **7b** and **12a**, piperidinol **6a/b** and piperidinamine **13b**. Thus, PEG5-acid **12a** acid displays 25-fold and amine **13b** 5-fold increase in water solubility, though its antibiotic activity is reduced.

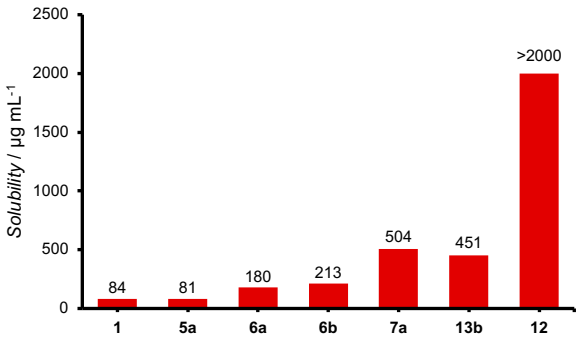

Figure 3. Solubility of selected derivatives in phosphate buffer (pH = 7).

In conclusion, apart from methylations[45] and benzylations[30] at the phenolic hydroxy groups and diversely substituted benzylidene-acetals[46] at the diol of the noviose, the new analogs presented here are, to our knowledge, the first examples of complex semisynthetic derivatives of fidaxomicin obtained via phenolic modifications. Other derivatives reported are obtained by fermentation[47,48] and fermentation of gene-knockout mutants.[49–52] Based on our predictions of a binding mode of fidaxomicin in a homology model of *M. tuberculosis* RNAP, which suggested that modifications on the dichlorohomoorsellinic acid would be promising, several analogs have been synthesized and tested for their biological activity and water solubility. Some of these compounds showed improved water solubility with maintained antibiotic activity. The synthesized hybrid antibiotics **14** and **18** show improved activity compared to fidaxomicin, while also retaining activity against strains, that show resistance against the attached antibiotic itself. Access to a great variety of derivatives of this complex natural product was

achieved by using easy and reliable synthetic methods. These derivatives could provide an important contribution in ongoing efforts to reduce the rate of antibiotic resistance development in bacteria and broaden the scope of application of fidaxomicin.

ASSOCIATED CONTENT

Supporting Information

The Supporting Information is available free of charge on the ACS Publications website.

Supplementary Figures S1 and S2, experimental procedures and methods, characterization data, ^{1}H and ^{13}C NMR spectra, supplementary MIC tables, computational details. (PDF)

AUTHOR INFORMATION

Corresponding Author

Karl Gademann - Department of Chemistry, University of Zurich, Winterthurerstrasse 190, 8057 Zürich. E-mail: karl.gademann@chem.uzh.ch

Author Contributions

The manuscript was written through contributions of all authors. All authors have given approval to the final version of the manuscript.

‡These authors contributed equally.

Notes

A patent application (WO2019135010A1, EP18150671.8A) was filed Jan 8th, 2018 that includes antibiotics presented in this work.

ACKNOWLEDGMENT

We thank the Swiss National Science Foundation for financial support (200021_182043 (K.G.) and 31003A_153349/1 (P.S.)). Work in the laboratory of P.S. is supported by Swiss Lung Association (2018-02). We acknowledge partial financial support by the DFG (GRK 2158, P4 for H.G.). We gratefully acknowledge the NMR- und MS services of the University of Zurich and F. Fazzi und G. Uzunidis for skillful laboratory assistance. We further thank Dr. A. Siegle and Prof. Dr. O. Trapp (LMU München) for using the HPLC in their research groups and Dr. R. Wehlauch and J. Michel for proofreading the manuscript.

ABBREVIATIONS

CDI C. difficile infection, MIC minimum inhibitory concentration, RNAP RNA polymerase, cryo-EM cryo-electron microscopy, HPLC high performance liquid chromatography, PEG polyethylene glycol.

REFERENCES

(1) Parenti, F.; Pagani, H.; Beretta, G. Lipiarmycin, A New Antibiotic From Actinoplanes I. Description of the Producer Strain and Fermentation Studies. *J. Antibiot.* **1975**, *28*, 247–252.

(2) Coronelli, C.; White, R. J.; Lancini, G. C.; Parenti, F. Lipiarmycin, A New Antibiotic from Actinoplanes II. Isolation, Chemical, Biological and Biochemical Charaterization. *J. Antibiot.* **1975**, *28*, 253–259.

(3) Õmura, S.; Imamura, N.; Õiwa, R.; Kuga, H.; Iwata, R.; Masuma, R.; Iwai, Y. Clostomicins, New Antibiotics Produced by Micromonospora Echinospora Subsp. Armeniaca Subsp. Nov. I. Production, Isolation, and Physico-Chemical and Biological Properties. *J. Antibiot.* **1986**, *39*, 1407–1412.

(4) Takashi, Y.; Iwai, Y.; Õmura, S. Clostomicins, New Antibiotics Produced by Micromonospora Echinospora Subsp. Armeniaca Subsp. Nov. II. Taxonomic Study of the Producing Microorganism. *J. Antibiot.* **1986**, *39*, 1413–1418.

(5) Hochlowski, J. E.; Swanson, S. J.; Ranfranz, L. M.; Whittern, D. N.; Buko, A. M.; McAlpine, J. B. Tiacumicins, a Novel Complex of 18-Membered Macrolides II. Isolation and Structure Determination. *J. Antibiot.* **1987**, *40*, 575–588.

(6) Theriault, R. J.; Karwowski, J. P.; Jackson, M.; Girolami, R. L.; Sunga, G. N.; Vojtko, C. M.; Coen, L. J. Tiacumicins, a Novel Complex of 18-Membered Macrolide Antibiotics I. Taxonomy, Fermentation and Antibacterial Activity. *J. Antibiot.* **1987**, *40*, 567–574.

(7) Kurabachew, M.; Lu, S. H. J.; Krastel, P.; Schmitt, E. K.; Suresh, B. L.; Goh, A.; Knox, J. E.; Ma, N. L.; Jiricek, J.; Beer, D.; Cynamon, M.; Petersen, F.; Dartois, V.; Keller, T.; Dick, T.; Sambandamurthy, V.

K. Lipiarmycin Targets RNA Polymerase and Has Good Activity against Multidrug-Resistant Strains of Mycobacterium Tuberculosis. *J. Antimicrob. Chemother.* **2008**, *62*, 713–719.

(8) Srivastava, A.; Talaue, M.; Liu, S.; Degen, D.; Ebright, R. Y.; Sineva, E.; Chakraborty, A.; Druzhinin, S. Y.; Chatterjee, S.; Mukhopadhyay, J.; Ebright, Y. W.; Zozula, A.; Shen, J.; Sengupta, S.; Niedfeldt, R. R.; Xin, C.; Kaneko, T.; Irschik, H.; Jansen, R.; Donadio, S.; Connell, N.; Ebright, R. H. New Target for Inhibition of Bacterial RNA Polymerase: "Switch Region." *Curr. Opin. Microbiol.* **2011**, *14*, 532–543.

(9) Babakhani, F.; Gomez, A.; Robert, N.; Sears, P. Killing Kinetics of Fidaxomicin and Its Major Metabolite, OP-1118, against Clostridium Difficile. *J. Med. Microbiol.* **2011**, *60*, 1213–1217.

(10) Erb, W.; Zhu, J. From Natural Product to Marketed Drug: The Tiacumicin Odyssey. *Nat. Prod. Rep.* **2013**, *30*, 161–174.

(11) Dorst, A.; Gademann, K. Chemistry and Biology of the Clinically Used Macrolactone Antibiotic Fidaxomicin. *Helv. Chim. Acta* **2020**, *103*, e2000038.

(12) Dorst, A.; Jung, E.; Gademann, K. Recent Advances in Mode of Action and Biosynthesis Studies of the Clinically Used Antibiotic Fidaxomicin. *Chimia* **2020**, *74*, 270–273.

(13) Biedenbach, D. J.; Ross, J. E.; Putnam, S. D.; Jones, R. N. In Vitro Activity of Fidaxomicin (OPT-80) Tested against Contemporary Clinical Isolates of Staphylococcus Spp. and Enterococcus Spp. *Antimicrob. Agents Chemother.* **2010**, *54*, 2273–2275.

(14) Arnone, A.; Nasini, G.; Cavalleri, B. Structure Elucidation of the Macrocyclic Antibiotic Lipiarmycin. *J. Chem. Soc. Perkin Trans. I* **1987**, 1353–1359.

(15) Serra, S.; Malpezzi, L.; Bedeschi, A.; Fuganti, C.; Fonte, P. Final Demonstration of the Co-Identity of Lipiarmycin A3 and Tiacumicin B (Fidaxomicin) through Single Crystal X-Ray Analysis. *Antibiotics* **2017**, *6*, 7.

(16) Glaus, F.; Altmann, K. H. Total Synthesis of the Tiacumicin B (Lipiarmycin A3/Fidaxomicin) Aglycone. *Angew. Chem. Int. Ed.* **2015**, *54*, 1937–1940.

(17) Miyatake-Ondozabal, H.; Kaufmann, E.; Gademann, K. Total Synthesis of the Protected Aglycon of Fidaxomicin (Tiacumicin B, Lipiarmycin A3). *Angew. Chem. Int. Ed.* **2015**, *54*, 1933–1936.

(18) Erb, W.; Grassot, J. M.; Linder, D.; Neuville, L.; Zhu, J. Enantioselective Synthesis of Putative Lipiarmycin Aglycon Related to Fidaxomicin/Tiacumicin B. *Angew. Chem. Int. Ed.* **2015**, *54*, 1929–1932.

(19) Jeanne-Julien, L.; Masson, G.; Astier, E.; Genta-Jouve, G.; Servajean, V.; Beau, J. M.; Norsikian, S.; Roulland, E. Synthesis of a Tiacumicin B Protected Aglycone. *Org. Lett.* **2017**, *19*, 4006–4009.

(20) Jeanne-Julien, L.; Masson, G.; Astier, E.; Genta-Jouve, G.; Servajean, V.; Beau, J.-M.; Norsikian, S.;

Roulland, E. Study of the Construction of the Tiacumicin B Aglycone. *J. Org. Chem.* **2018**, *83*, 921–929.

(21) Kaufmann, E.; Hattori, H.; Miyatake-Ondozabal, H.; Gademann, K. Total Synthesis of the Glycosylated Macrolide Antibiotic Fidaxomicin. *Org. Lett.* **2015**, *17*, 3514–3517.

(22) Norsikian, S.; Tresse, C.; François-Eude, M.; Jeanne-Julien, L.; Masson, G.; Servajean, V.; Genta-Jouve, G.; Beau, J.-M.; Roulland, E. Total Synthesis of Tiacumicin B: Implementing H-Bond-Directed Acceptor Delivery for Highly Selective β-Glycosylations. *Angew. Chem. Int. Ed.* **2020**, *59*, 6612–6616.

(23) Talpaert, M.; Campagnari, F.; Clerici, L. Lipiarmycin: An Antibiotic Inhibiting Nucleic Acid Polymerases. *Biochem. Biophys. Res. Commun.* **1975**, *63*, 328–334.

(24) Sonenshein, A. L.; Alexander, H. B.; Rothstein, D. M.; Fisher, S. H. Lipiarmycin-Resistant Ribonucleic Acid Polymerase Mutants of Bacillus Subtilis. *J. Bacteriol.* **1977**, *132*, 73–79.

(25) Sonenshein, A. L.; Alexander, H. B. Initiation of Transcription in Vitro Is Inhibited by Lipiarmycin. *J. Mol. Biol.* **1979**, *127*, 55–72.

(26) Tupin, A.; Gualtieri, M.; Leonetti, J. P.; Brodolin, K. The Transcription Inhibitor Lipiarmycin Blocks DNA Fitting into the RNA Polymerase Catalytic Site. *EMBO J.* **2010**, *29*, 2527–2537.

(27) Artsimovitch, I.; Seddon, J.; Sears, P. Fidaxomicin Is an Inhibitor of the Initiation of Bacterial RNA Synthesis. *Clin. Infect. Dis.* **2012**, *55*, 127–131.

(28) Morichaud, Z.; Chaloin, L.; Brodolin, K. Regions 1.2 and 3.2 of the RNA Polymerase σ Subunit Promote DNA Melting and Attenuate Action of the Antibiotic Lipiarmycin. *J. Mol. Biol.* **2016**, *428*, 463–476.

(29) Boyaci, H.; Chen, J.; Lilic, M.; Palka, M.; Mooney, R. A.; Landick, R.; Darst, S. A.; Campbell, E. A. Fidaxomicin Jams Mycobacterium Tuberculosis RNA Polymerase Motions Needed for Initiation via RbpA Contacts. *Elife* **2018**, *7*, e34823

(30) Lin, W.; Das, K.; Degen, D.; Zhang, C.; Ebright, R. H.; Lin, W.; Das, K.; Degen, D.; Mazumder, A.; Duchi, D.; Wang, D.; Ebright, Y. W. Structural Basis of Transcription Inhibition by Fidaxomicin (Lipiarmycin A3). *Mol. Cell* **2018**, *70*, 60–71.

(31) Hattori, H.; Kaufmann, E.; Miyatake-Ondozabal, H.; Berg, R.; Gademann, K. Total Synthesis of Tiacumicin A. Total Synthesis, Relay Synthesis, and Degradation Studies of Fidaxomicin (Tiacumicin B, Lipiarmycin A3). *J. Org. Chem.* **2018**, *83*, 7180–7205.

(32) Gertzen, C. G. W.; Spomer, L.; Smits, S. H. J.; Häussinger, D.; Keitel, V.; Gohlke, H. Mutational Mapping of the Transmembrane Binding Site of the G-Protein Coupled Receptor TGR5 and Binding Mode Prediction of TGR5 Agonists. *Eur. J. Med. Chem.* **2015**, *104*, 57–72.

(33) Milić, D.; Dick, M.; Mulnaes, D.; Pfleger, C.; Kinnen, A.; Gohlke, H.; Groth, G. Recognition Motif and

Mechanism of Ripening Inhibitory Peptides in Plant Hormone Receptor ETR1. *Sci. Rep.* **2018**, *8*, 3890.

(34) Gualtieri, M.; Tupin, A.; Brodolin, K.; Leonetti, J. P. Frequency and Characterisation of Spontaneous Lipiarmycin-Resistant Enterococcus Faecalis Mutants Selected in Vitro. *Int. J. Antimicrob. Agents* **2009**, *34*, 605–616.

(35) Ebright, R. H. RNA-Exit Channel: Target and Method for Inhibition of Bacterial RNA. WO2005/001034, **2005**.

(36) Babakhani, F.; Seddon, J.; Sears, P. Comparative Microbiological Studies of Transcription Inhibitors Fidaxomicin and the Rifamycins in Clostridium Difficile. *Antimicrob. Agents Chemother.* **2014**, *58*, 2934–2937.

(37) Gademann, K.; Berg, R.; Meier, A. Glycosylated Macrolides and Their Use as Antibiotics. WO 2019/135010 A1, **2019**.

(38) Schnell, S. D.; Hoff, L. V.; Panchagnula, A.; Wurzenberger, M. H. H.; Klapötke, T. M.; Sieber, S.; Linden, A.; Gademann, K. 3-Bromotetrazine: Labelling of Macromolecules via Monosubstituted Bifunctional s-Tetrazines. *Chem. Sci.* **2020**, *11*, 3042–3047.

(39) Liu, Z.; Li, J.; Li, S.; Li, G.; Sharpless, K. B.; Wu, P. SuFEx Click Chemistry Enabled Late-Stage Drug Functionalization. *J. Am. Chem. Soc.* **2018**, *140*, 2919–2925.

(40) Berg, R.; Straub, J.; Schreiner, E.; Mader, S.; Rominger, F.; Straub, B. F. Highly Active Dinuclear Copper Catalysts for Homogeneous Azide-Alkyne Cycloadditions. *Adv. Synth. Catal.* **2012**, *354*, 3445–3450.

(41) Hu, Y. Q.; Zhang, S.; Xu, Z.; Lv, Z. S.; Liu, M. L.; Feng, L. S. 4-Quinolone Hybrids and Their Antibacterial Activities. *Eur. J. Med. Chem.* **2017**, *141*, 335–345.

(42) Pokrovskaya, V.; Baasov, T. Dual-Acting Hybrid Antibiotics: A Promising Strategy to Combat Bacterial Resistance. *Expert Opin. Drug Discov.* **2010**, *5*, 883–902.

(43) Gootz, T. D.; Brighty, K. E. Fluoroquinolone Antibacterials: SAR, Mechanism of Action, Resistance, and Clinical Aspects. *Med. Res. Rev.* **1996**, *16*, 433–486.

(44) Cochrane, S. A.; Li, X.; He, S.; Yu, M.; Wu, M.; Vederas, J. C. Synthesis of Tridecaptin-Antibiotic Conjugates with in Vivo Activity against Gram-Negative Bacteria. *J. Med. Chem.* **2015**, *58*, 9779–9785.

(45) McAlpine, J. E.; Hochlowski, J. E. Dialkyltiacumicin Compounds. US 5,583,115, **1996**.

(46) Wu, M.-C.; Huang, C.-C.; Lu, Y.-C.; Fan, W.-J. Derivatives of Tiacumicin B as Anti-Cancer Agents. US 2009/0110718 A1, **2008**.

(47) Hochlowski, J. E.; Jackson, M.; Rasmussen, R. R.; Buko, A. M.; Clement, J. J.; Whittern, D. N.; McAlpine, J. B. Production of Brominated Tiacumicin Derivatives. *J. Antibiot.* **1997**, *50*, 201–205.

(48) Hochlowski, J. E.; Jackson, M.; McAlpine, J. B.; Rasmussen, R. R. Bromotiacumicin Compounds. US 5,767,096, **1998**.

(49) Xiao, Y.; Li, S.; Niu, S.; Ma, L.; Zhang, G.; Zhang, H.; Zhang, G.; Ju, J.; Zhang, C. Characterization of Tiacumicin B Biosynthetic Gene Cluster Affording Diversified Tiacumicin Analogues and Revealing a Tailoring Dihalogenase. *J. Am. Chem. Soc.* **2011**, *133*, 1092–1105.

(50) Niu, S.; Hu, T.; Li, S.; Xiao, Y.; Ma, L.; Zhang, G.; Zhang, H.; Yang, X.; Ju, J.; Zhang, C. Characterization of a Sugar-O-Methyltransferase TiaS5 Affords New Tiacumicin Analogues with Improved Antibacterial Properties and Reveals Substrate Promiscuity. *ChemBioChem* **2011**, *12*, 1740–1748.

(51) Zhang, H.; Tian, X.; Pu, X.; Zhang, Q.; Zhang, W.; Zhang, C. Tiacumicin Congeners with Improved Antibacterial Activity from a Halogenase-Inactivated Mutant. *J. Nat. Prod.* **2018**, *81*, 1219–1224.

(52) Yu, Z.; Zhang, H.; Yuan, C.; Zhang, Q.; Khan, I.; Zhu, Y.; Zhang, C. Characterizing Two Cytochrome P450s in Tiacumicin Biosynthesis Reveals Reaction Timing for Tailoring Modifications. *Org. Lett.* **2019**, *21*, 7679–7683.

Supporting Information

Semisynthetic Analogs of the Antibiotic Fidaxomicin – Design, Synthesis and Biological Evaluation

Andrea Dorst,[‡a] Regina Berg,[‡a] Christoph G. W. Gertzen,[b] Daniel Schäfle,[c] Katja Zerbe,[a] Myriam Gwerder,[a] Simon D. Schnell,[a] Peter Sander,[c,d] Holger Gohlke,[b] and Karl Gademann*[a]

[a] Department of Chemistry, University of Zurich, Winterthurerstrasse 190, 8057 Zürich, Switzerland. E-mail: karl.gademann@chem.uzh.ch

[b] Institute for Pharmaceutical and Medicinal Chemistry, Heinrich Heine University Düsseldorf, Universitätsstr. 1, 40225 Düsseldorf and John von Neumann Institute for Computing (NIC), Institute of Biological Information Processing (IBI-7: Structural Biochemistry) & Jülich Supercomputing Centre (JSC), Forschungszentrum Jülich, 52425 Jülich, Germany.

[c] Institute of Medical Microbiology, University of Zurich, Gloriastrasse 28/30, 8006 Zurich, Switzerland

[d] National Center for Mycobacteria, University of Zurich, Gloriastrasse 28/30, 8006 Zurich, Switzerland

[†] These authors contributed equally to this work.

Table of Content

Synthesis of Fidaxomicin Derivatives

General Experimental

Unless otherwise stated, all chemicals were of reagent grade and purchased from *Sigma-Aldrich, Merck, Fluorochem, Honeywell,* or *Thommen Furler AG*. Fidaxomicin was either obtained by fermentation from *Actinoplanes deccanensis* (ATCC 21983) or purchased from commercial suppliers. Reactions were carried out under protecting gas (N2 or Ar) in oven-dried (120 °C) glass equipment and monitored for completion by TLC or UHPLC-MS (ESI). Solvents for reactions were of p.a. grade. Evaporation of solvents *in vacuo* was carried out on a rotary evaporator at 40 °C bath temperature and appropriate pressure. **Thin layer chromatography** (TLC): *Merck* TLC plates silica gel *60* on glass with the indicated solvent system; the spots were visualized by UV light (254 nm) and cerium ammonium molybdate or KMnO4 stain. **Ultra high-performance liquid chromatography coupled to mass spectrometry** (UHPLC-MS): *Ultimate 3000 LC* instrument (*Thermo Fisher Scientific*) coupled to a triple quadrupole *Quantum Ultra EMR* MS (*Thermo Fisher Scientific*) using a reversed-phase column (*Kinetex*® EVO C18; 1.7 µm; 100 Å, 50 x 2.1 mm; *Phenomenex*). The LC was equipped with an *HPG-3400RS* pump, a *WPS-3000TRS* autosampler, a *TCC-3000RS* column oven and a *Vanquish DAD* detector (all *Thermo Fisher Scientific*). The following solvents were applied: H2O + 0.1 % HCOOH (A), MeCN + 0.1 % HCOOH (B). Samples were prepared using HPLC grade solvents (MeCN, MeOH, H_2O) and filtered over a 4 mm syringe filter, PTFE (hydrophilic), pore size: 0.22 µm obtained from BGB Analytik AG. The MS was equipped with an H-ESI II ion source. The source temperature was 250 °C, the capillary temperature 270 °C and capillary voltage 3500 V, and datasets were acquired at resolution 0.7 on Q3 in centroid mode. **High-performance liquid chromatography** (HPLC):
Prominence modular HPLC instrument (*Shimadzu*) coupled to an *SPD-20A* UV/Vis detector (*Shimadzu*) using a reversed-phase column (*Gemini-NX* C18, 3 µm, 10 Å, 150 mm x 4.6 mm; *Phenomenex, Synergy Hydro*) for analytical HPLC, and a reversed-phase column (*Gemini NX* C18, 5 µm, 110 Å, 250 mm x 21.2 mm; *Phenomenex Synergi Hydro-RP*, 10 µ, 80 Å, 250 mm x 21.2 mm; *Phenomenex Synergi Hydro-RP*, 10 µ, 80 Å, 250 mm x 4.60 mm) for (semi-) preparative HPLC. The LC was equipped with a *CBM-20A* system controller, *LC-20A* solvent delivery unit, a *DGU-20A* degassing unit, *FRC-10A* fraction collector(all *Shimadzu*). The following solvents were used: H2O + 0.1 % HCOOH (A), MeCN + 0.1 % HCOOH (B). **Specific optical rotation** $[\alpha]_D^T$: *Jasco P-2000 Polarimeter*; measured at the indicated temperature *T*. All given values for $[\alpha]_D^T$ have the dimension ° mL dm^{-1} g^{-1}. **Infrared spectra** (IR): *SpectrumTwo FT-IR Spectrometer* (*Perkin–Elmer*) equipped with a *Specac Golden Gate™ ATR* (attenuated total reflection) accessory; applied as neat samples or as films; $1/\lambda$ in cm^{-1}. **UV-Vis Spectroscopy**: UV-Vis spectra were measured in the spectral region from λ = 200 nm to λ = 800 nm on the instrument *Shimadzu UV Spectrophotometer*, model: UV-1800 240V IVDD, using quartz cuvettes of length d = 1 cm. **Nuclear magnetic resonance spectra** (NMR): ^{1}H NMR spectra were recorded in $CDCl_3$, CD_2Cl_2, CD_3OD, acetone-d_6 or DMSO-d_6 on the instruments *Bruker AV-600* (600 MHz), *AV-500* (500 MHz) or *AV-400* (400 MHz); chemical shift δ in ppm relative to solvent signals (δ = 7.26 ppm for $CDCl_3$, 5.32 ppm for CD_2Cl_2, 3.31 ppm for CD_3OD, 2.05 ppm for acetone-d_6

and 2.50 for DMSO-d_6),[1] coupling constant J is given in Hz. ^{13}C NMR spectra were recorded in $CDCl_3$, CD_2Cl_2, CD_3OD, acetone-d_6 or DMSO-d_6 on the instruments *Bruker AV-600* (150 MHz), *AV-500* (125 MHz) or *AV-400* (100 MHz); chemical shift δ in ppm relative to solvent signals (δ = 77.16 ppm for $CDCl_3$, 53.84 ppm for CD_2Cl_2, 49.00 ppm for CD_3OD, 29.84 ppm for acetone-d_6 and 39.52 for DMSO-d_6);[1] multiplicities from DEPT-135 experiments. **High-resolution electrospray ionization mass spectra** (HRMS): *QExactive* (*Thermo Fisher Scientific*) with a heated ESI source connected to a *Dionex Ultimate 3000* UHPLC system. Samples dissolved in MeOH; injection on-flow with an auto-sampler (mobile phase: MeOH + 0.1 % HCOOH or MeCN/H2O 2:8 + 0.1 % HCOOH; flow rate: 120 μL/min); ion source parameters: spray voltage 3.0 kV, capillary temperature 320 °C, sheath gas rate: 5 L/min, s-lens RF level 55.0; full scan MS in alternating (+)/(–)-ESI mode; mass ranges 80–1200, 133–2000, or 200–3000 amu; resolution (full width half-maximum) 70'000; automatic gain control (AGC) target $3.00 \cdot 10^6$; maximum allowed ion transfer time (IT) 30 ms; mass calibration <2 ppm accuracy for *m/z* 130.06619–1621.96509 in (+)-ESI and for *m/z* 265.14790–1779.96528 in (–)-ESI with *Pierce*® ESI calibration solutions (*Thermo Fisher Scientific*); lock masses: ubiquitous erucamide (*m/z* 338.34174, (+)-ESI) and palmitic acid (*m/z* 255.23295, (–)-ESI).

Fidaxomicin Acetamide (2a) and Fidaxomicin Bis(acetamide) (2b)

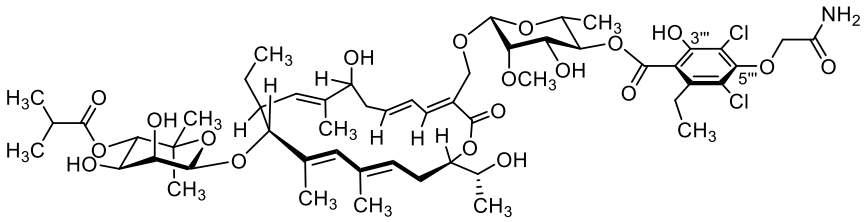

2a

Chemical Formula: $C_{54}H_{77}Cl_2NO_{19}$

Exact Mass: 1113.4467

Molecular Weight: 1115.0980

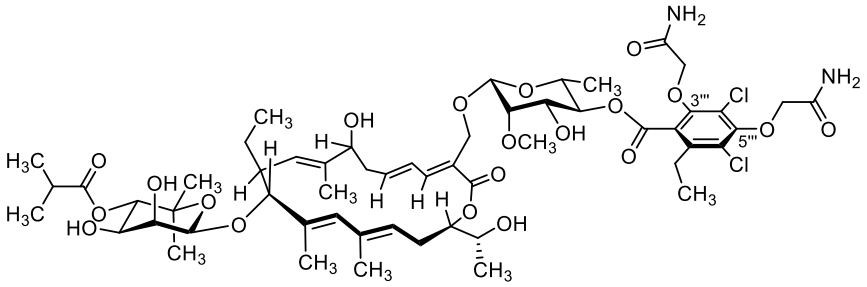

2b

Chemical Formula: $C_{56}H_{80}Cl_2N_2O_{20}$

Exact Mass: 1170.4681

Molecular Weight: 1172.1500

In a flame-dried flask under argon atmosphere, fidaxomicin (**1**, 100 mg, 94.5 µmol, 1.0 equiv.) and K_2CO_3 (52.2 mg, 0.378 mmol, 4.0 equiv.) were dissolved in dry DMF (1.2 mL). Iodoacetamide (22.7 mg, 0.123 mmol, 1.3 equiv.) was added and the yellow reaction mixture was stirred at 45 °C for 5 hours. The reaction mixture was diluted with EtOAc (2.0 mL) and a saturated aqueous solution of NH_4Cl (3.0 mL) was added. The layers were separated and the aqueous layer was extracted with EtOAc (3x). The combined organic phases were washed with a saturated aqueous solution of NaCl (3x) and dried over anhydrous $MgSO_4$. After filtration of the drying agent, the solvent was evaporated under reduced pressure to afford a mixture of mono- and disubstituted fidaxomicin acetamide. The two compounds **2a** and **2b** were separated by preparative RP-HPLC (Gemini NX C18, 10 µ, 110 Å, 250 mm x 21.2 mm; solvent A: H_2O+0.1 % HCOOH, solvent B: MeCN+0.1 % HCOOH; 20 mL/min; 47 % B for 50 min) to afford **2a** (t_R = 16.25 min, 24.0 mg, 21.5 µmol, 23 %) and **2b** (t_R = 9.50 min, 6.0 mg, 5.1 µmol, 5 %) as colourless solids after lyophilization.

2a

R_f (pentane/acetone 1:4) = 0.44; **Specific Rotation** $[\alpha]_D^{25°C}$ = −91.31 (β = 0.61 g/100 mL, $CHCl_3$); **FT-IR** $\tilde{\nu}$ (film) 3474, 2974, 2936, 1734, 1689, 1383, 1247, 1070, 1028, 904 cm^{-1}; **^{1}H NMR** (500 MHz, acetone-d_6) δ 7.23 (d, *J* = 11.5 Hz, 1H), 7.21 (s, 1H), 6.91 (s, 1H), 6.63 (m, 1H), 5.96 (ddd, *J* = 14.5, 9.9, 5.1 Hz, 1H), 5.83 (s, 1H), 5.62 (t, *J* = 8.3 Hz, 1H), 5.21 (d, *J* = 10.5 Hz, 1H), 5.07 (t, *J* = 9.7 Hz, 1H), 5.00 (d, *J* = 10.1 Hz, 1H), 4.77 (s, 1H), 4.73 (q, *J* = 5.4 Hz, 1H), 4.67 (s, 1H), 4.60 (d, *J* = 11.4 Hz, 1H), 4.47 (s, 2H), 4.41 (d, *J* = 11.4 Hz, 1H), 4.27 (br m, 1H), 4.10–3.99 (m, 1H), 3.96 (d, *J* = 3.3 Hz, 1H), 3.85 (s, br, 1H), 3.79–3.71 (m, 3H), 3.61 (d, *J* = 3.4 Hz, 1H), 3.60–3.54 (m, 1H), 3.52 (s, 3H), 2.95–2.83 (m, 2H), 2.79–2.60 (m, 3H), 2.56 (sept, *J* = 7.1 Hz, 1H), 2.53–2.39 (m, 2H), 1.99–1.90 (m, 1H), 1.81 (s, 3H), 1.73 (s, 3H), 1.65 (s, 3H), 1.33 (d, *J* = 6.1 Hz, 3H), 1.30–1.22 (m, 1H), 1.21–1.07 (m, 15H), 1.09 (s, 3H), 0.82 (t, *J* = 7.1 Hz, 3H) ppm; **^{13}C NMR** (126 MHz, acetone-d_6) δ 176.8, 169.7, 167.8, 167.5, 153.4, 153.1, 145.4, 143.4, 141.4, 136.9, 136.1, 133.8, 128.1, 126.3, 125.3, 123.9, 120.4, 119.1, 115.7, 101.8, 96.7, 93.3, 81.5, 78.2, 77.5, 75.7, 73.8, 72.84, 72.78, 72.4, 71.8, 70.6, 70.1, 67.7, 63.4, 61.7, 42.0, 37.2, 34.8, 28.7, 28.3, 26.5, 25.8, 20.7, 19.4, 19.2, 18.6, 18.1, 17.5, 15.2, 14.5, 13.8, 11.2 ppm; **HRMS** ESI− (MeOH), calculated for $C_{54}H_{76}Cl_2NO_{19}$ $[M-H]^-$: 1112.43941, found: 1112.44043.

2b

R_f (pentane/acetone 1:4) = 0.38; **Specific Rotation** $[\alpha]_D^{25°C}$ = −25.68 (β = 0.48 g/100 mL, $CHCl_3$); **FT-IR** $\tilde{\nu}$ (film) 3474, 2977, 2935, 1734, 1688, 1406, 1253, 1069, 1026 cm^{-1}; **^{1}H NMR** (500 MHz, acetone-d_6) δ 7.25 (d, *J* = 11.5 Hz, 1H), 7.20 (s, 2H), 7.17 (s, 1H), 6.90 (s, 1H), 6.86 (s, 1H), 6.61 (dd, *J* = 14.9, 11.9 Hz, 1H), 5.96 (ddd, *J* = 14.4, 10.0, 4.9 Hz, 1H), 5.82 (s, 1H), 5.63 (t, *J* = 8.3 Hz, 1H), 5.21 (d, *J* = 10.5 Hz, 1H), 5.05 (t, *J* = 9.6 Hz, 1H), 4.99 (d, *J* = 10.1 Hz, 1H), 4.77 (s, 1H), 4.73 (q, *J* = 5.1 Hz, 1H), 4.60 (s, 1H), 4.58–4.52 (m, 2H), 4.49 (s, 3H), 4.45–4.39 (m, 2H), 4.28 (m, br, 1H), 4.07–4.00 (m, 3H), 3.97–3.94 (m, 1H), 3.87–3.82 (m, 2H), 3.76–3.67 (m, 3H), 3.57–3.51 (m, 2H), 3.52 (s, 3H), 3.26 (d, *J* = 9.4 Hz, 1H), 2.87–2.76 (m, 2H), 2.76–2.60 (m, 3H), 2.56 (sept, *J* = 7.0 Hz, 1H), 2.52–2.46 (m, 1H), 2.46–2.40 (m, 1H), 1.98–1.88 (m, 1H), 1.81 (d, *J* = 1.2 Hz, 3H), 1.71 (d, *J* = 1.3 Hz, 3H), 1.65 (s, 3H), 1.34 (d, *J* = 6.1 Hz, 3H), 1.30–1.21 (m, 1H), 1.21–1.07 (m, 15H), 1.09 (s, 3H), 0.82 (t, *J* = 7.5 Hz, 3H) ppm; **^{13}C NMR** (126 MHz, acetone-d_6) δ 176.8, 169.9, 169.6, 167.7, 166.1, 153.1, 150.9, 145.7, 143.7, 140.6, 136.8, 136.11, 136.05, 133.7, 128.6, 128.0, 126.24, 126.23, 125.0, 123.9, 121.7, 101.1, 96.8, 93.3, 81.8, 78.1, 78.0, 75.7, 73.8, 73.6, 72.83, 72.81, 72.3, 72.0, 70.6, 70.2, 67.7, 62.9, 61.7, 42.0, 37.4, 34.8, 28.7, 28.3, 26.5, 25.7, 20.8, 19.4, 19.2, 18.6, 18.4, 17.5, 15.2, 14.3, 13.8, 11.2 ppm; **HRMS** ESI+, (MeOH) calculated for $C_{56}H_{80}Cl_2N_2O_{20}Na$ $[M+Na]^+$: 1193.45737, found: 1193.45811.

Fidaxomicin Dimethylacetamide (3a) and Fidaxomicin Bis(dimethylacetamide) (3b)

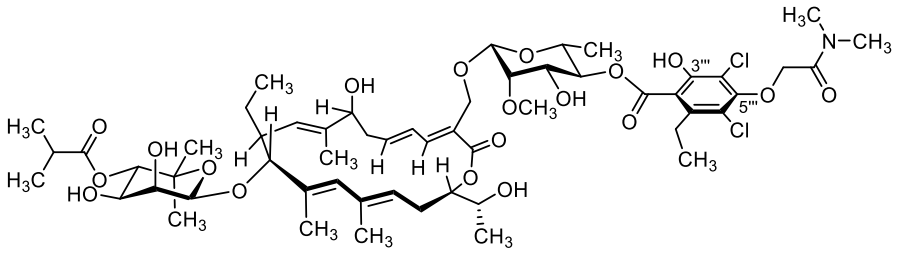

3a

Chemical Formula: $C_{56}H_{81}Cl_2NO_{19}$

Exact Mass: 1141.4780

Molecular Weight: 1143.1520

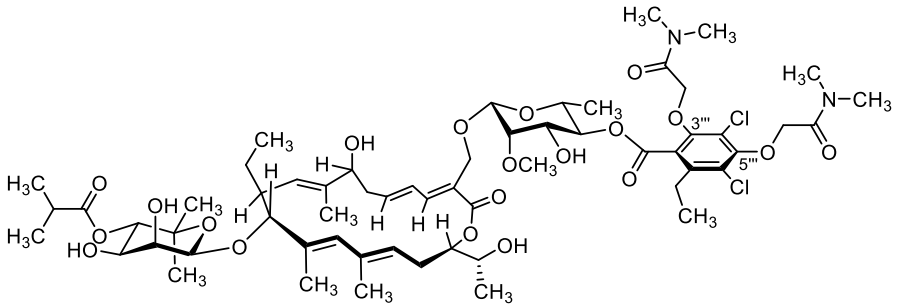

3b

Chemical Formula: $C_{60}H_{88}Cl_2N_2O_{20}$

Exact Mass: 1226.5307

Molecular Weight: 1228.2580

An flame-dried flask was charged with fidaxomicin (**1**, 20.0 mg, 18.9 µmol, 1.0 equiv.) and K_2CO_3 (10.4 mg, 75.6 µmol, 4.0 equiv.) was added under argon atmosphere. The solids were dissolved in dry DMF (0.8 mL) and 2-iodo-*N*,*N*-dimethylacetamide (4 µL, 34 µmol, 1.8 equiv.) was added. The dark brown mixture was stirred at 45 °C for 7 hours. The reaction mixture was diluted with EtOAc (1.0 mL) and a saturated aqueous solution of NH_4Cl (1.0 mL) was added. The phases were separated and the aqueous phase was extracted with EtOAc (3x). The combined organic layers were washed with a saturated aqueous solution of NaCl (2x) and dried over anhydrous $MgSO_4$. After filtration of the drying agent, the solvent was evaporated under reduced pressure. A mixture of mono- and disubstituted fidaxomicin-*N*,*N*-dimethylacetamide **3a** and **3b** was obtained. The two compounds were separated by RP-HPLC (Gemini NX C18, 10 µ, 110 Å, 250 mm x 21.2 mm; solvent A: H_2O+0.1 % HCOOH, solvent B: MeCN+0.1 % HCOOH; 20 mL/min; 47 % B for 50 min) to afford, after lyophilization, **3a** (t_R = 23.83 min, 9.5 mg, 8.3 µmol, 44 %) and **3b** (t_R = 16.88 min, 8.5 mg, 6.9 µmol, 37 %) as colourless solids.

3a

R_f (pentane/acetone 1:4) = 0.84; **Specific Rotation** $[\alpha]_D^{24^\circ C}$ = −18.53 (β = 0.17 g/100 mL, $CHCl_3$); **FT-IR** $\tilde{\nu}$ (film) 3423, 2976, 2934, 1700, 1644, 1384, 1244, 1200, 1069, 1028, 901, 800 cm^{-1}; **^{1}H NMR** (500 MHz, acetone-d_6) δ 7.23 (d, *J* = 11.5 Hz, 1H), 6.68–6.58 (m, 1H), 5.96 (ddd, *J* = 14.6, 9.5, 4.6 Hz, 1H), 5.83 (s, 1H), 5.62 (t, *J* = 8.3 Hz, 1H), 5.21 (d, *J* = 10.4, 1H), 5.06 (t, *J* = 9.7 Hz, 1H), 4.99 (d, *J* = 10.2 Hz, 1H), 4.79–4.69 (m, 1H), 4.73 (s, 2H), 4.66 (s, 1H), 4.58 (d, *J* = 11.5 Hz, 1H), 4.41 (d, *J* = 11.5 Hz, 1H), 4.27 (m, br, 1H), 4.06–3.99 (m, 1H), 3.98–3.93 (m, 1H), 3.79–3.69 (m, 3H), 3.62–3.54 (m, 2H), 3.52 (s, 3H), 3.17 (s, 3H), 2.93 (s, 3H), 2.91–2.70 (m, 3H), 2.70–2.67 (m, 1H), 2.67–2.63 (m, 1H), 2.56 (sept, *J* = 6.9 Hz, 1H), 2.54–2.47 (m, 1H), 2.53–2.40 (ddd, *J* = 13.9, 9.2, 4.5 Hz, 1H), 1.98–1.89 (m, 1H), 1.81 (s, 3H), 1.73 (s, 3H), 1.66 (s, 3H), 1.33 (d, *J* = 6.2 Hz, 3H), 1.28–1.21 (m, 1H), 1.21–1.12 (m, 15H), 1.09 (s, 3H), 0.82 (t, *J* = 7.4 Hz, 2H) ppm; **^{13}C NMR** (126 MHz, acetone-d_6) δ 176.8, 167.83, 167.77, 166.8, 154.4, 151.7, 145.4, 143.4, 141.3, 136.9, 136.12, 136.10, 133.8, 128.2, 126.4, 125.3, 124.0, 120.3 (from HMBC), 118.9 (from HMBC), 115.8, 101.8, 96.8, 93.3, 81.6, 78.2, 77.5, 75.7, 73.8, 72.8, 72.7, 72.4, 72.2, 70.6, 70.2, 67.7, 63.4, 61.7, 42.0, 37.3, 36.7, 35.3, 34.8, 28.7, 28.4, 26.5, 25.9, 20.7, 19.4, 19.2, 18.6, 18.1, 17.5, 15.2, 14.5, 13.8, 11.2 ppm; **HRMS** ESI− (MeOH), calculated for $C_{56}H_{80}Cl_2NO_{19}$ $[M-H]^-$: 1140.47071, found: 1140.47231.

3b

R_f (pentane/acetone 4:1) = 0.68; **Specific Rotation** $[\alpha]_D^{24^\circ C}$ = −18.54 (β = 0.37 g/100 mL, $CHCl_3$); **FT-IR** $\tilde{\nu}$ (film) 3431, 2976, 2935, 2877, 1734, 1645, 1369, 1251, 1069, 1027, 904 cm^{-1}; **^{1}H NMR** (500 MHz, acetone-d_6) δ 7.26 (d, *J* = 11.5 Hz, 1H), 6.66–6.58 (m, 1H), 5.96 (ddd, *J* = 14.6, 9.8, 4.5 Hz, 1H), 5.82 (s, 1H), 5.62 (t, *J* = 8.3 Hz, 1H), 5.22 (d, *J* = 10.6 Hz, 1H), 5.03–4.98 (m, 2H), 4.79–4.71 (m, 6H), 4.56 (s, 1H), 4.55 (d, *J* = 11.5 Hz, 1H), 4.43 (d, *J* = 11.6 Hz, 1H), 4.31–4.28 (br m, 1H), 4.17 (d, *J* = 9.4 Hz, 1H), 4.06–3.99 (m, 2H), 3.95 (d, *J* = 3.3 Hz, 1H), 3.89 (d, *J* = 4.2 Hz, 1H), 3.86–3.80 (m, 1H), 3.76–3.70 (m, 2H), 3.68–3.63 (m, 1H), 3.52 (s, 3H), 3.52–3.47 (m, 2H), 3.26 (d, *J* = 9.0 Hz, 1H), 3.16 (s, 3H), 3.06 (s, 3H), 2.94 (s, 3H), 2.93 (s, 3H), 2.88–2.74 (m, 2H), 2.74–2.68 (m, 2H), 2.68–2.61 (m, 1H), 2.61–2.48 (m, 2H), 2.43 (ddd, *J* = 14.3, 9.5, 4.6 Hz, 1H), 1.98–1.89 (m, 1H), 1.81 (d, *J* = 1.3 Hz, 3H), 1.70 (s, 3H), 1.66 (s, 3H), 1.30 (d, *J* = 6.1 Hz, 3H), 1.28–1.21 (m, 1H), 1.19–1.12 (m, 15H), 1.09 (s, 3H), 0.82 (t, *J* = 7.5 Hz, 3H) ppm; **^{13}C NMR** (126 MHz, acetone-d_6) δ 176.8, 167.7, 167.1, 166.7, 166.2, 153.8, 151.7, 145.8, 143.8, 140.3, 136.8, 136.11, 136.08, 133.7, 128.5, 128.0, 126.13, 126.07, 124.9, 124.0, 122.0, 101.0, 96.8, 93.3, 82.0, 78.1, 77.9, 75.7, 73.8, 72.9, 72.8, 72.7, 72.4, 72.3, 70.8, 70.2, 67.7, 62.8, 61.7, 42.0, 37.5, 36.7, 36.3, 35.4, 35.3, 34.8, 28.7, 28.4, 26.6, 25.7, 20.8, 19.4, 19.2, 18.6, 18.5, 17.5, 15.2, 14.4, 13.8, 11.2 ppm; **HRMS** ESI+ (MeOH), calculated for $C_{60}H_{88}Cl_2N_2O_{20}Na$ $[M+Na]^+$: 1249.51997, found: 1249.51806.

Fidaxomicin Ethylacetat (4a) and Fidaxomicin Bis(ethylacetate) (4b)

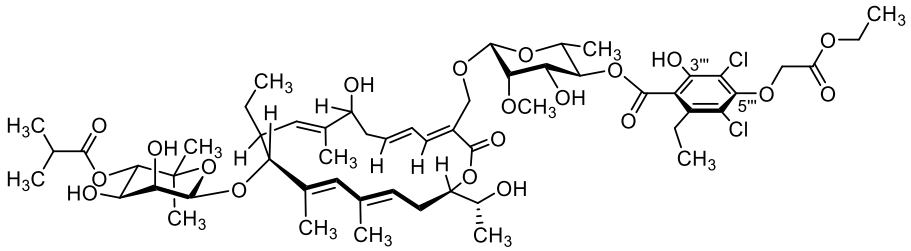

4a

Chemical Formula: $C_{56}H_{80}Cl_2O_{20}$

Exact Mass: 1142.4620

Molecular Weight: 1144.1360

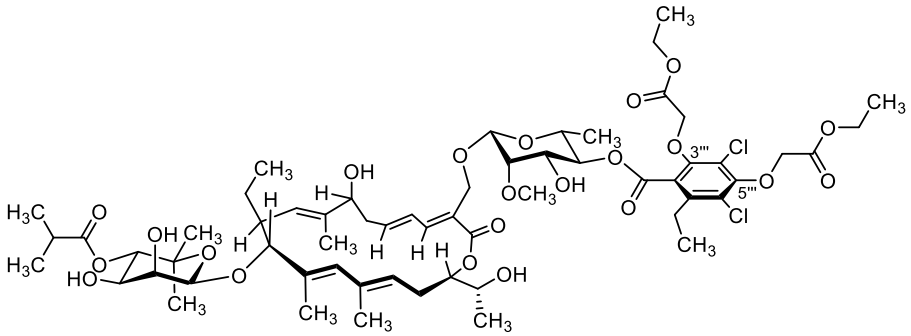

4b

Chemical Formula: $C_{60}H_{86}Cl_2O_{22}$

Exact Mass: 1228.4988

Molecular Weight: 1230.2260

A flame-dried flask was charged with fidaxomicin (20.0 mg, 18.9 µmol, 1.0 equiv.) and K_2CO_3 (10.4 mg, 75.6 µmol, 4.0 equiv.). The solids were dissolved in dry DMF (0.8 mL) and ethyliodoacetate (3 µL, 25 µmol, 1.3 equiv.) was added. The slightly yellow reaction mixture was stirred at 45 °C under argon atmosphere for 6.5 hours. The reaction mixture was diluted with EtOAc (1.0 mL) and a saturated aqueous solution of NH_4Cl (1.0 mL) was added. The layers were separated and the aqueous phase was extracted with EtOAc (3x). The combined organic phases were washed with a saturated aqueous solution of NaCl (2x) and dried over anhydrous $MgSO_4$. After filtration of the drying agent, the solvent was evaporated under reduced pressure to afford fidaxomicin derivatives **4a** and **4b** as a mixture. The compounds were separated by flash column chromatography (SiO_2, pentane/acetone 3:2) to afford **4a** (6.2 mg, 5.4 µmol, 29 %) and **4b** (7.8 mg, 6.3 mmol, 34 %) as colourless solids.

4a

R_f (pentane/acetone 3:2) = 0.37; **Specific Rotation** $[\alpha]_D^{26°C}$ = −31.90 (β = 0.41 g/100 mL, $CHCl_3$); **FT-IR** $\tilde{\nu}$ (film) 3474, 2978, 2935, 1737, 1642, 1581, 1384, 1243, 1202, 1146, 1117, 1069, 1028, 902, 770 cm^{-1}; **^{1}H NMR** (500 MHz, acetone-*d_6*) δ 7.23 (d, *J* = 11.5 Hz, 1H), 6.69–6.54 (m, 1H), 5.96 (ddd, *J* = 14.6, 9.5, 4.6 Hz, 1H), 5.83 (s, 1H), 5.63 (t, *J* = 8.3 Hz, 1H), 5.21 (d, *J* = 10.5 Hz, 1H), 5.06 (t, *J* = 9.7 Hz, 1H), 4.99 (d, *J* = 10.1 Hz, 1H), 4.77 (s, 1H), 4.73 (q, *J* = 5.1 Hz, 1H), 4.70 (s, 2H), 4.67 (s, 1H), 4.60 (d, *J* = 11.5 Hz, 1H), 4.41 (d, *J* = 1.5 Hz, 1H), 4.27 (m, br, 1H), 4.25 (q, *J* = 7.1 Hz, 2H), 4.10–3.99 (m, 2H), 3.97–3.94 (m, 1H), 3.83 (d, *J* = 3.6 Hz, 1H), 3.79–3.70 (m, 3H), 3.62–3.55 (m, 2H), 3.52 (s, 3H), 3.32–3.25 (m, 1H), 2.93–2.78 (m, 2H), 2.78–2.60 (m, 3H), 2.56 (sept, *J* = 7.0 Hz, 1H), 2.53–2.40 (m, 2H), 1.98–1.89 (m, 1H), 1.81 (d, *J* = 1.4 Hz, 3H), 1.73 (d, *J* = 1.3 Hz, 3H), 1.66 (s, 3H), 1.33 (d, *J* = 6.1 Hz, 3H), 1.28 (t, *J* = 7.2 Hz, 3H), 1.30–1.22 (m, 1H), 1.21–1.11 (m, 15H), 1.09 (s, 3H), 0.82 (t, *J* = 7.4 Hz, 3H) ppm; **^{13}C NMR** (126 MHz, acetone-*d_6*) δ 176.8, 168.0, 167.8, 167.6, 153.8, 152.9, 145.4, 143.4, 141.4, 136.9, 136.11, 136.09, 133.8, 128.2, 126.3, 125.3, 124.0, 120.8, 118.8, 115.7, 101.8, 96.8, 93.3, 81.6, 78.2, 77.5, 75.7, 73.8, 72.9, 72.8, 72.4, 70.6, 70.2, 70.0, 67.7, 63.4, 61.7, 61.6, 42.0, 37.3, 34.8, 28.7, 28.4, 26.5, 25.9, 20.7, 19.4, 19.2, 18.6, 18.1, 17.5, 15.2, 14.5, 13.8, 11.2 ppm; **HRMS** ESI+ (MeOH), calculated for $C_{56}H_{80}Cl_2O_{20}Na$ $[M+Na]^+$: 1165.45122, found: 1165.44810.

4b

R_f (pentane/acetone 3:2) = 0.29; **Specific Rotation** $[\alpha]_D^{24°C}$ = −33.68 (β = 0.34 g/100 mL, $CHCl_3$); **FT-IR** $\tilde{\nu}$ (film) 3493, 2977, 2936, 2877,1737, 1641, 1384, 1251, 1204, 1121, 1070, 1030, 901, 795 cm^{-1}; **^{1}H NMR** (500 MHz, acetone-*d_6*) δ 7.23 (d, *J* = 11.4 Hz, 1H), 6.62 (m, 1H), 5.96 (ddd, *J* = 14.6, 9.5, 4.6 Hz, 1H), 5.83 (s, 1H), 5.62 (t, *J* = 8.3 Hz, 1H), 5.21 (dt, *J* = 10.5, 1.7 Hz, 1H), 5.04–4.97 (m, 2H), 4.77 (s, 1H), 4.75–4.69 (m, 3H), 4.68 (s, 1H), 4.64–4.60 (m, 2H), 4.59 (d, *J* = 11.5 Hz, 1H), 4.40 (d, *J* = 11.5 Hz, 1H), 4.29–4.20 (m, 5H), 4.05–3.99 (m, 2H), 3.97–3.93 (m, 1H), 3.87 (d, *J* = 10.0 Hz, 1H), 3.80 (d, *J* = 3.7 Hz, 1H), 3.75–3.66 (m, 4H), 3.56–3.52 (m, 2H), 3.52 (s, 3H), 3.24 (d, *J* = 9.4 Hz, 1H), 2.93–2.75 (m, 2H), 2.74–2.61 (m, 3H), 2.56 (sept, *J* = 7.0 Hz, 1H), 2.54–2.46 (m, 1H), 2.44 (ddd, *J* = 13.9, 9.5, 4.7 Hz, 1H). 1.97–1.89 (m, 1H), 1.81 (d, *J* = 1.4 Hz, 3H), 1.73 (s, 3H), 1.66 (s, 3H), 1.33 (d, *J* = 6.2 Hz, 3H), 1.30–1.26 (m, 7H), 1.19–1.12 (m, 15H), 1.09 (s, 3H), 0.82 (t, *J* = 7.4 Hz, 3H) ppm; **^{13}C NMR** (126 MHz, acetone-*d_6*) 176.8, 167.98, 167.96, 167.8, 166.1, 153.4, 151.1, 145.4, 143.4, 140.4, 136.9, 136.1, 133.8, 128.6, 128.2, 126.4, 126.2, 125.4, 124.0, 121.8, 101.7, 96.7, 93.3, 81.9, 79.2, 78.2, 77.8, 75.7, 73.8, 72.9, 72.8, 72.4, 71.5, 70.7, 70.2, 70.1, 67.7, 63.3, 61.73, 61.66, 61.6, 42.0, 37.3, 34.8, 28.7, 28.4, 26.5, 25.6, 20.7, 19.4, 19.2, 18.6, 18.2, 17.5, 15.2, 14.52, 14.47, 14.3, 13.8, 11.1 ppm; **HRMS** ESI+ (MeOH), calculated for $C_{60}H_{90}Cl_2O_{22}N$ $[M+NH_4]^+$: 1246.53261, found: 1246.53412.

Allyl 4-(2-chloroacetyl)piperazine-1-carboxylate[2]

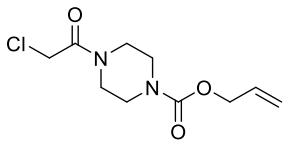

Chemical Formula: $C_{10}H_{15}ClN_2O_3$
Exact Mass: 246.0771
Molecular Weight: 246.6910

In a flame-dried flask, a solution of chloroacetyl chloride (59 µL, 0.73 mmol, 1.0 equiv.) in dry THF (590 µL) was added to a stirred solution of alloc-protected piperazin[3,4] (125 mg, 0.734 mmol, 1.0 equiv.) and freshly distilled diisopropylethyl amine (146 µL, 0.881 mmol, 1.2 equiv.) in THF (2.3 mL) at 0 °C. Upon addition of chloroacetyl chloride, the clear solution turned pink and a colourless solid precipitated. The mixture was stirred at 0 °C for 1 hour and was then allowed to warm to rt and stirred for another 2.5 hours. The solvent was evaporated under reduced pressure and the residue was dissolved in chloroform. The organic phase was washed with H_2O (3x), the combined aqueous layers were extracted with chloroform and the combined organic phases dried over anhydrous $MgSO_4$. After filtration of the drying agent, the solvent was removed *in vacuo* and the crude product was purified by flash column chromatography (SiO_2, pentane/EtOAc 1:1) to afford the desired product (130 mg, 0.527 mmol, 72 %) as a colourless oil.

R_f (pentane/EtOAc 1:1) = 0.20; **FT-IR** $\tilde{\nu}$ (film) 2866, 1701, 1654, 1466, 1432, 1417, 1287, 1250, 1230, 1149, 1127, 1080, 970, 766 cm^{-1}; **^{1}H NMR** (400 MHz, $CDCl_3$) δ 5.94 (ddt, *J* = 17.2, 10.4, 5.6 Hz, 1H), 5.34–5.27 (m, 1H), 5.26–5.21 (m, 1H), 4.62 (dt, *J* = 5.6, 1.4 Hz, 2H), 4.08 (s, 2H), 3.65–3.47 (m, 8H) ppm; **^{13}C NMR** (101 MHz, $CDCl_3$) δ 165.5, 155.1, 132.8, 118.1, 66.6, 46.2, 43.9, 43.6, 42.1, 40.9 ppm; **HRMS** ESI+ (MeOH), calculated for $C_{10}H_{16}ClN_2O_3$ $[M+H]^+$: 247.08440, found: 247.08442.

Allyl 4-(2-iodoacetyl)piperazine-1-carboxylate

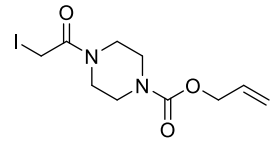

Chemical Formula: $C_{10}H_{15}IN_2O_3$

Exact Mass: 338.0127

Molecular Weight: 338.1455

In a flame-dried flask equipped with a reflux condenser, allyl 4-(2-chloroacetyl)piperazine-1-carboxylate (80.0 mg, 0.324 mmol, 1.0 equiv.) was dissolved in dry MeCN (1.0 mL) and NaI (219 mg, 1.46 mmol, 4.5 equiv.) was added. The mixture immediately turned cloudy yellow and was stirred at 60 °C for 3 hours under argon atmosphere. H_2O (3.0 mL) was added to the reaction mixture, and MeCN was removed under reduced pressure. EtOAc (3.0 mL) was added and the phases were separated. The aqueous phase was extracted with EtOAc (3x). The combined yellow organic layers were dried over anhydrous $MgSO_4$. After filtration of the drying agent, the solvent was evaporated under reduced pressure. The crude product was purified by flash column chromatography (SiO_2, pentane/EtOAc 1:1) to afford the desired product (83.0 mg, 0.246 mmol, 76 %) as a yellow oil.

R_f (pentane/EtOAc 1:1) = 0.19; **FT-IR** $\tilde{\nu}$ (film) 2863, 1694, 1635, 1457, 1430, 1412, 1356, 1285, 1226, 1175, 1131, 1104, 1069, 967, 929, 795, 605, 541 cm^{-1}; **^{1}H NMR** (400 MHz, $CDCl_3$) δ 5.88 (ddt, *J* = 17.2, 10.4, 5.6 Hz, 1H), 5.24 (dq, *J* = 17.2, 1.5 Hz, 1H), 5.17 (dq, *J* = 10.4, 1.3 Hz, 1H), 4.55 (dt, *J* = 5.7, 1.4 Hz, 2H), 3.69 (s, 2H), 3.58–3.52 (m, 4H), 3.46–3.36 (m, 4H) ppm; **^{13}C NMR** (101 MHz, $CDCl_3$) δ 166.7, 154.9, 132.7, 117.9, 66.4, 46.9, 43.2, 43.1, 41.8, −4.22 ppm; **HRMS** ESI+ (MeOH), calculated for $C_{10}H_{16}IN_2O_3$ $[M+H]^+$: 339.02001, found: 339.01996.

Fidaxomicin Piperazine and Fidaxomicin Di(piperazine) with alloc Protecting Group

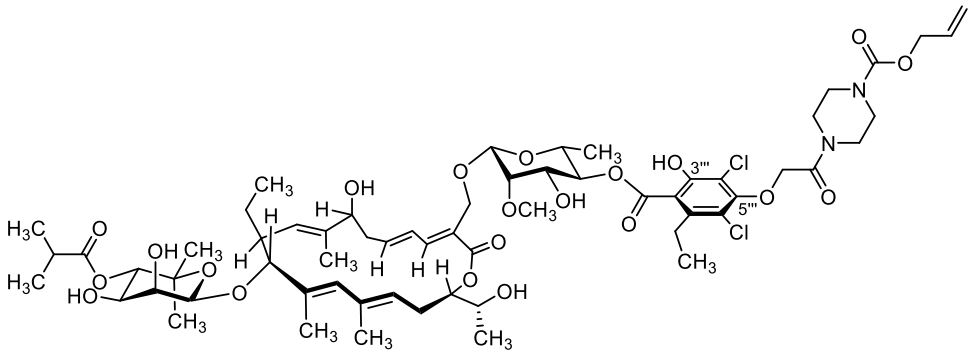

A

Chemical Formula: $C_{62}H_{88}Cl_2N_2O_{21}$

Exact Mass: 1266.52566

Molecular Weight: 1268.27900

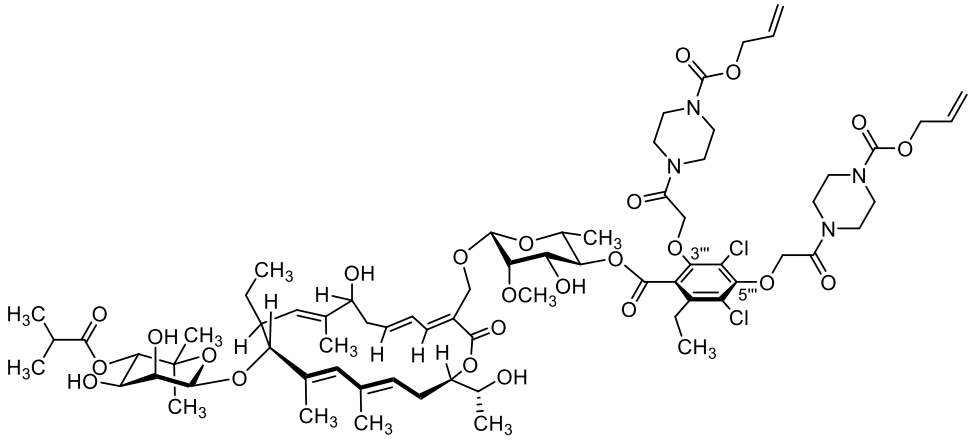

B

Chemical Formula: $C_{72}H_{102}Cl_2N_4O_{24}$

Exact Mass: 1476.6261

Molecular Weight: 1478.5120

A flame-dried flask was charged with fidaxomicin (100 mg, 94.5 µmol, 1.0 equiv.) and K_2CO_3 (52.2 mg, 0.378 mmol, 4.0 equiv.). The solids were dissolved in dry DMF (4.0 mL) and allyl 4-(2-iodoacetyl)piperazine-1-carboxylate (47.9 mg, 0.142 mmol, 1.5 equiv.) was added. The brown reaction mixture was stirred at 45 °C under argon atmosphere for 7.5 hours. The reaction mixture was diluted with EtOAc and a saturated aqueous solution of NH_4Cl was added. The layers were separated and the aqueous phase was extracted with EtOAc (3x). The combined organic phases were dried over anhydrous $MgSO_4$. After filtration of the drying agent, the solvent was evaporated under reduced pressure to afford mono- and disubstituted products **A** and **B** as a mixture. The two compounds

were separated by RP-HPLC [Gemini NX C18, 10 µ, 110 Å, 250 mm x 21.2 mm, solvent A: H_2O+0.1 % HCOOH, solvent B: MeCN+0.1 % HCOOH; 20 mL/min; LC time program (min – % B): 0.0 – 45 %, 3.0 – 45 %,46.0 – 55 %, 55.0 – 100 %] to afford, after lyophilization, **A** (t_R = 35.6 min, 32.3 mg, 25.5 µmol, 27 %) and **B** (t_R = 38.0 min, 42.8 mg, 28.9 µmol, 31 %) as colourless solids.

A

R_f (CH_2Cl_2/MeOH 9:1) = 0.42; **Specific Rotation** $[\alpha]_D^{24^\circ C}$ = −49.52 (β = 0.35 g/100 mL, $CHCl_3$); **FT-IR** $\tilde{\nu}$ (film) 3452, 2978, 2936, 2877, 1736, 1697, 1647, 1580, 1416, 1370, 1234, 1069, 1006, 901, 768 cm^{-1}; **^{1}H NMR** (500 MHz, acetone-d_6) δ 7.23 (d, *J* = 11.3 Hz, 1 H), 6.67–6.58 (m, 1H), 6.02–5.92 (m, 2H), 5.83 (s, 1H), 5.62 (t, *J* = 8.4 Hz, 1H), 5.31 (dq, *J* = 17.3, 1.7 Hz, 1H), 5.23–5.16 (m, 2H), 5.06 (t, *J* = 9.8 Hz, 1H), 4.99 (d, *J* = 10.1 Hz, 1H), 4.80 (s, 2H), 4.77 (s, 1H), 4.73 (q, *J* = 5.3Hz, 1H), 4.67 (s, 1H), 4.62–4.57 (m, 3H), 4.41 (d, *J* = 11.5 Hz, 1H), 4.27 (m, br, 1H), 4.05–3.99 (m, 1H), 3.97–3.94 (m, 1H), 3.83–3.67 (m, 7H), 3.65–3.54 (m, 6H), 3.52 (s, 3H), 2.97–2.81 (m, 2H), 2.79–2.61 (m, 3H), 2.56 (sept, *J* = 6.9 Hz, 1H), 2.54–2.39 (m, 2H), 1.99–1.89 (m, 1H), 1.81 (d, *J* = 1.3 Hz, 3H), 1.73 (s, 3H), 1.66 (s, 3H), 1.33 (d, *J* = 6.2 Hz, 3H), 1.31–1.22 (m, 1H), 1.21–1.11 (m, 15H), 1.09 (s, 3H), 0.83 (t, *J* = 7.5 Hz, 3H) ppm; **^{13}C NMR** (126 MHz, acetone-d_6) δ 176.8, 167.8, 167.6, 165.8, 155.4, 154.3, 152.9, 145.4, 143.4, 141.4, 136.9, 136.1, 134.4, 133.8, 128.1, 126.4, 125.3, 124.0, 120.8, 118.8, 117.3, 115.8, 101.8, 96.7, 93.3, 81.5, 78.2, 77.5, 75.7, 73.8, 72.9, 72.8, 72.40, 72.38, 70.6, 70.2, 67.7, 66.4, 63.4, 61.7, 45.8, 44.7, 44.3, 42.2, 42.0, 37.3, 34.8, 28.7, 28.4, 26.5, 25.9, 20.7, 19.4, 19.2, 18.6, 18.1, 17.5, 15.2, 14.5, 13.8, 11.2 ppm; **HRMS** ESI+ (MeOH), calculated for $C_{62}H_{88}Cl_2N_2O_{21}Na$ $[M+Na]^+$: 1289.51488, found: 1289.51544.

B

R_f (CH_2Cl_2/MeOH 4:1) = 0.76; **Specific Rotation** $[\alpha]_D^{24^\circ C}$ = −40.24 (β = 0.96 g/100 mL, $CHCl_3$); **FT-IR** $\tilde{\nu}$ (film) 3452, 2976, 2935, 2876, 1733, 1699, 1646, 1468, 1432, 1368, 1287, 1246, 1229, 1128, 1067, 1025, 902, 766 cm^{-1}; **^{1}H NMR** (500 MHz, acetone-d_6) δ 7.24 (d, *J* = 11.4 Hz, 1H), 6.66–6.57 (m, 1H), 6.03–5.90 (m, 3H), 5.82 (s, 1H), 5.62 (t, *J* = 8.7 Hz, 1H), 5.65–5.58 (m, 2H), 5.23–5.16 (m, 3H), 5.04–4.97 (m, 2H), 4.86–4.78 (m, 4H), 4.76 (s, 1H), 4.73 (q, *J* = 4.9 Hz, 1H), 4.60–4.54 (m, 6H), 4.41 (d, *J* = 11.5 Hz, 1H), 4.28 (m, br, 1H), 4.11 (d, *J* = 9.7 Hz, 1H), 4.08–3.99 (m, 1H), 3.97–3.94 (m, 1H), 3.90–3.81 (m, br, 1H), 3.76–3.64 (m, 3H), 3.64–3.47 (18 H), 3.52 (s, 3H), 2.91–2.76 (m, 2H), 2.75–2.61 (m, 3H), 2.56 (sept, *J* = 7.0 Hz, 1H), 2.53–2.47 (m, 1H), 2.43 (ddd, *J* = 14.0, 9.3, 4.5 Hz, 1H), 1.98–1.89 (m, 1H), 1.80 (d, *J* = 1.3 Hz, 3H), 1.70 (s, 3H), 1.65 (s, 3H), 1.31 (d, *J* = 6.1 Hz, 3H), 1.28–1.20 (m, 1H), 1.19–1.12 (m, 15H), 1.09 (s, 3H), 0.83 (t, *J* = 7.3 Hz, 3H) ppm; **^{13}C NMR** (126 MHz, acetone-d_6) δ 176.8, 167.7, 166.1, 166.0, 165.7, 155.4, 153.7, 151.6, 145.6, 143.6, 140.4, 136.8, 136.1, 136.0, 134.32, 134.30, 133.7, 128.5, 128.0, 126.2, 126.1, 125.0, 123.9, 122.0, 117.37, 117.34, 101.3, 96.7, 93.2, 81.9, 78.1, 77.9, 75.7, 73.7, 73.1, 72.82, 72.77, 72.5, 72.3, 70.7, 70.2, 67.6, 66.45, 66.43, 63.0, 61.7, 45.8, 45.4, 44.7, 44.3, 42.1, 42.0, 37.4, 34.7, 28.7, 28.3, 26.5, 25.7, 20.7, 19.4, 19.2, 18.6, 18.5, 17.5, 15.2, 14.4, 13.8, 11.2 ppm; **HRMS** ESI+ (MeOH), calculated for $C_{72}H_{102}Cl_2N_4O_{24}Na$ $[M+Na]^+$: 1499.61533, found: 1499.61505.

Fidaxomicin Piperazine (5a)

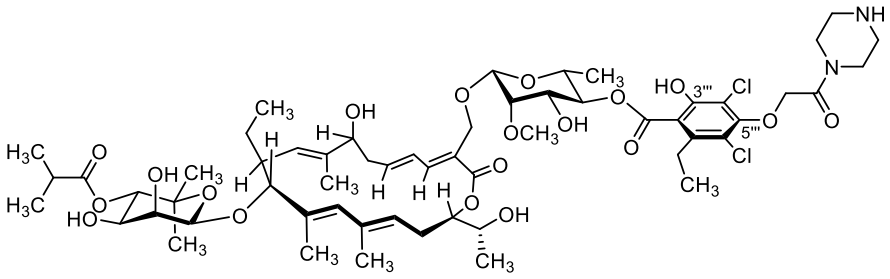

Chemical Formula: $C_{58}H_{84}Cl_2N_2O_{19}$

Exact Mass: 1182.5045

Molecular Weight: 1184.2050

In a flame-dried flask under argon atmosphere, mono-substituted alloc-piperazine-fidaxomicin (20.0 mg, 15.8 µmol, 1.0 equiv.) was dissolved in dry CH_2Cl_2 (1.5 mL) and 1,3-dimethylbarbituric acid (5.9 mg, 38 µmol, 2.4 equiv.) was added. The reaction mixture was cooled to 0 °C and tetrakis(triphenylphosphine)palladium(0) (0.9 mg, 0.8 µmol, 5 mol%) was added. The mixture was stirred at 0 °C for 30 min. After completion of the reaction, the mixture was diluted with CH_2Cl_2 and H_2O was added. The phases were separated and the aqueous phase was extracted with CH_2Cl_2 (3x). The combined organic layers were dried over anhydrous $MgSO_4$. After filtration of the drying agent, the solvent was removed under reduced pressure and the crude product was purified by flash column chromatography (SiO_2, CH_2Cl_2/MeOH 9:1 to 4:1) to afford the desired amine **5a** (9.50 mg, 8.0 µmol, 51 %) as a colourless solid.

R_f (CH_2Cl_2/MeOH 4:1) = 0.28; **Specific Rotation** $[\alpha]_D^{24°C}$ = −2.79 (β = 0.35 g/100 mL, MeOH); **FT-IR** $\tilde{\nu}$ (film) 3414, 2975, 2928, 2875, 1692, 1640, 1557, 1410, 1371, 1245, 1202, 1112, 1068, 1027, 901 cm^{-1}; **^{1}H NMR** (500 MHz, CD_3OD) δ 7.22 (d, *J* = 11.4 Hz, 1H), 6.63–6.56 (m, 1H), 5.95 (ddd, *J* = 14.5, 9.4, 4.8 Hz, 1H), 5.83 (s, 1H), 5.57 (t, *J* = 8.2 Hz, 1H), 5.16–5.11 (m, 1H), 5.05 (t, *J* = 9.7 Hz, 1H), 5.01 (d, *J* = 10.2 Hz, 1H), 4.77–4.68 (m, 4H), 4.63–4.57 (m, 2H), 4.42 (d, *J* = 11.4 Hz, 1H), 4.25–4.20 (m, 1H), 4.02 (m, 1H), 3.93 (dd, *J* = 3.2, 1.1 Hz, 1H), 3.80–3.68 (m, 7H), 3.59–3.57 (m, 1H), 3.56 (s, 3H), 3.54–3.50 (m, 1H), 3.13–3.05 (m, 4H), 2.86–2.65 (m, 5H), 2.60 (sept, *J* = 7.0 Hz, 1H), 2.52–2.38 (m, 2H), 2.04–1.96 (m, 1H), 1.81 (s, 3H), 1.76 (s, 3H), 1.66 (s, 3H), 1.37 (d, *J* = 6.2 Hz, 3H), 1.32–1.25 (m, 1H), 1.20–1.11 (m, 18H), 0.87 (t, *J* = 7.5 Hz, 3H) ppm; **^{13}C NMR** (126 MHz, CD_3OD) δ 178.4, 169.1, 168.9, 168.0, 157.2, 153.5, 146.2, 143.7, 140.6, 137.1, 137.0, 136.3, 134.6, 128.5, 126.9, 125.6, 124.6, 122.2, 121.4, 116.9, 102.2, 97.2, 94.3, 82.3, 78.6, 77.0, 75.9, 74.5, 73.5, 73.2, 72.9, 72.0, 71.5, 70.5, 68.3, 63.8, 62.1, 45.7, 45.3, 42.5, 42.0, 41.9, 37.3, 35.4, 28.7, 28.4, 26.9, 26.0, 20.2, 19.5, 19.1, 18.7, 18.0, 17.5, 15.4, 14.6, 13.9, 11.3 ppm; **HRMS** ESI+ (MeOH), calculated for $C_{58}H_{85}Cl_2N_2O_{19}$ $[M+H]^+$: 1183.51181, found: 1183.51223.

Fidaxomicin Dipiperazine (5b)

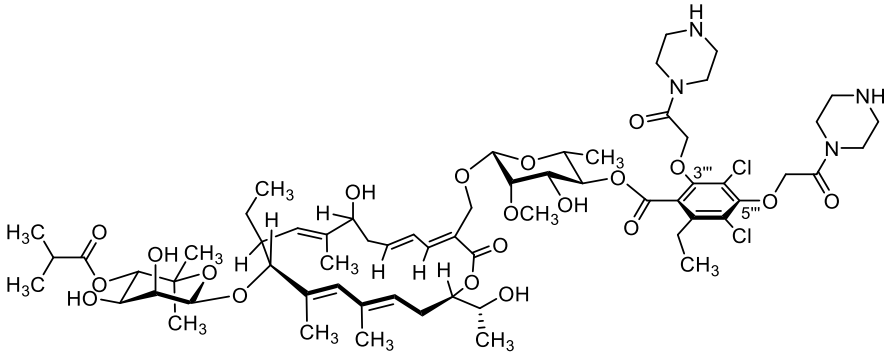

Chemical Formula: $C_{64}H_{94}Cl_2N_4O_{20}$

Exact Mass: 1308.5838

Molecular Weight: 1310.3640

In a flame-dried flask, disubstituted alloc-protected fidaxomicin di(piperazine) (15.4 mg, 10.4 µmol, 1.0 equiv.) was dissolved in dry CH_2Cl_2 (1.0 mL) and 1,3-dimethylbarbituric acid (3.9 mg, 25 µmol, 2.4 equiv.) was added. The reaction mixture was cooled to 0 °C and tetrakis(triphenylphosphine)palladium(0) (0.6 mg, 0.5 µmol, 5 mol%) was added. The mixture was stirred at 0 °C for 1 hour. CH_2Cl_2 and H_2O were added. The phases were separated and the aqueous phase was washed with CH_2Cl_2 (3x). The desired product **5b** (9.50 mg crude) was obtained by lyophilization of the aqueous phase.

R_f (CH_2Cl_2/MeOH 3:2) = 0.14; **^{1}H NMR** (500 MHz, CD_3OD) δ 7.21 (d, *J* = 11.5 Hz, 1H), 6.63–6.54 (m, 1H), 5.95 (ddd, *J* = 14.6, 9.2, 4.9 Hz, 1H), 5.83 (s, 1H), 5.57 (t, *J* = 8.2 Hz, 1H), 5.14 (dt, *J* = 10.5, 1.5 Hz, 1H), 5.03 (t, *J* = 9.7 Hz, 1H), 5.01 (d, *J* = 10.2 Hz, 1H), 4.85–4.78 (m, 4H), 4.73–4.69 (m, 2H), 4.62–4.58 (m, 2H), 4.42 (d, *J* = 11.5 Hz, 1H), 4.22 (s, br, 1H), 4.01 (m, 1H), 3.92 (d, *J* = 3.2 Hz, 1H), 3.87–3.75 (m, 6H), 3.74 (d, *J* = 3.3 Hz, 1H), 3.87–3.75 (m, 2H), 3.56 (s, 3H), 3.54 (d, 1H), 3.52–3.46 (m, 2H), 3.24–3.10 (m, 8H), 2.86 (sept, *J* = 6.9 Hz, 2H), 2.76–2.66 (m, 3H), 2.59 (sept, *J* = 7.0 Hz, 1H), 2.52–2.46 (m, 1H), 2.46–2.39 (m, 1H), 2.05–1.96 (m, 1H), 1.81 (d, *J* = 1.3 Hz, 3H), 1.75 (d, *J* = 1.4 Hz 3H), 1.65 (d, *J* = 1.3 Hz, 3H), 1.32 (d, *J* = 6.2 Hz, 3H), 1.30–1.22 (m, 1H), 1.22–1.15 (m, 12H), 1.14 (s, 3H), 1.12 (s, 3H), 0.87 (t, *J* = 7.4 Hz, 3H) ppm; **^{13}C NMR** (126 MHz, CD_3OD) δ 178.4, 168.7, 167.81, 167.76, 166.8, 154.0, 151.9, 146.2, 143.8, 141.2, 137.0, 136.9, 136.4, 134.6, 129.0, 128.4, 126.9, 126.8, 125.7, 124.6, 122.4, 102.2, 97.2, 94.3, 82.6, 78.6, 77.8, 75.9, 74.6, 73.5, 73.3, 73.0, 72.7, 72.1, 71.4, 70.5, 68.3, 63.9, 62.3, 44.8, 44.6, 44.1, 42.5, 40.6, 37.3, 35.4, 28.7, 28.4, 26.9, 26.1, 20.3, 19.5, 19.1, 18.7, 18.4, 17.5, 15.4, 14.4, 13.9, 11.3 ppm; **HRMS** ESI(+) (MeOH) calculated for $C_{64}H_{95}Cl_2N_4O_{20}$ $[M+H]^+$: 1309.59112, found: 1309.59286; $C_{64}H_{96}Cl_2N_4O_{20}$ $[M+2H]^{2+}$: 655.29920, found: 655.29992.

1-(4-Hydroxypiperidin-1-yl)-2-iodoethan-1-one

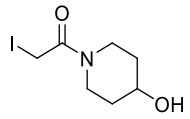

Chemical Formula: $C_7H_{12}INO_2$

Exact Mass: 268.9913

Molecular Weight: 269.0825

In a flame-dried flask equipped with a reflux condenser, 2-chloro-1-(4-hydroxycyclohexyl)ethan-1-one[5] (200 mg, 1.13 mmol, 1.0 equiv.) was dissolved in dry MeCN (3.5 mL) and NaI (762 mg, 5.08 mmol, 4.5 equiv.) was added. The mixture immediately turned cloudy yellow and was stirred at 60 °C for 3 hours. After completion of the reaction, MeCN was removed under reduced pressure. The residue was dissolved in CH_2Cl_2 and H_2O (10 mL) was added. The aqueous layer was extracted with CH_2Cl_2 (3x). The combined yellow organic layers were dried over anhydrous $MgSO_4$. After filtration of the drying agent, the solvent was evaporated under reduced pressure. The crude brown oil was purified by flash column chromatography (SiO_2, pentane/EtOAc 5:95) to afford 2-iodo-1-(4-hydroxycyclohexyl)ethan-1-one as a dark brown oil (170 mg, 0.63 mmol, 56 %).

R_f (pentane/EtOAc 1:9) = 0.21; **FT-IR** (film) $\tilde{\nu}$ = 3393, 2943, 2865, 1616, 1451, 1266, 1068, 1016 cm^{-1}; **^{1}H NMR** (400 MHz, $CDCl_3$) δ 4.02–3.92 (m, 2H), 3.75 (s, 2H), 3.72–3.64 (m, 1H), 3.35–3.19 (m, 2H), 2.01–1.92 (m, 1H), 1.90–1.81 (m, 1H), 1.71–1.60 (m, 1H), 1.57–1.46 (m, 1H) ppm; **^{13}C NMR** (101 MHz, $CDCl_3$) δ 166.6, 66.7, 44.6, 39.5, 33.9, 33.6, −3.9 ppm; **HRMS** ESI(+) (MeOH) calculated for $C_7H_{13}INO_2$ $[M+H]^+$: 269.99855, found: 269.99826.

Fidaxomicin Piperidin-4-ol (6a) and Fidaxomicin Di(piperidin-4-ol) (6b)

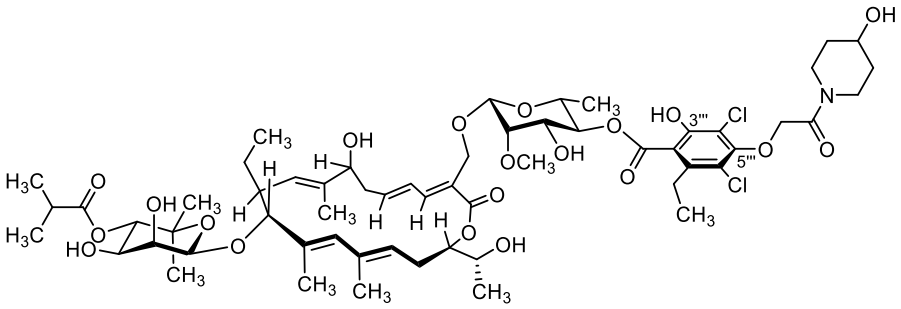

6a

Chemical Formula: $C_{59}H_{85}Cl_2NO_{20}$

Exact Mass: 1197.5042

Molecular Weight: 1199.2160

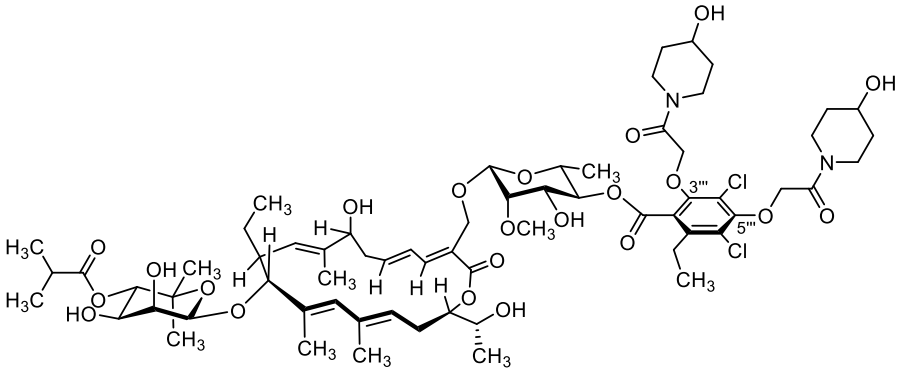

6b

Chemical Formula: $C_{66}H_{96}Cl_2N_2O_{22}$

Exact Mass: 1338.5832

Molecular Weight: 1340.3860

A flame-dried flask under an atmosphere of argon was charged with fidaxomicin (**1**, 30.0 mg, 28.4 µmol, 1.0 equiv.), K_2CO_3 (15.7 mg, 0.114 mmol, 4.0 equiv.) and 2-iodo-1-(4-hydroxycyclohexyl)ethan-1-one (11.5 mg, 42.6 µmol, 1.5 equiv.). The solids were dissolved in dry DMF (1.2 mL) and the brown reaction mixture was stirred at 45 °C for 9 hours. The reaction mixture was diluted with EtOAc and a saturated aqueous solution of NH_4Cl was added. The layers were separated and the aqueous phase was extracted with EtOAc (3x). The combined organic phases were dried over anhydrous $MgSO_4$. After filtration of the drying agent, the solvent was evaporated under reduced pressure. The crude mixture of mono- and disubstituted products was purified by RP-HPLC [Gemini NX C18, 10 µ, 110 Å, 250 mm x 21.2 mm, solvent A: H_2O+0.1 % HCOOH, solvent B: MeCN+0.1 % HCOOH; 20 mL/min; LC time

program (min – % B): 2.0 min – 40 %, 45.0 min – 45 %, 46.0 min – 100 %] to afford, after lyophilization, **6a** (t_R = 30.2 min, 10.3 mg, 8.59 µmol, 30 %) and **6b** (t_R = 16.0 min, 8.8 mg, 6.6 µmol, 23 %) as colourless solids.

6a

R_f (CH_2Cl_2/MeOH 9:1) = 0.33; **Specific Rotation** $[\alpha]_D^{24°C}$ = −31.81 (β = 0.59 g/100 mL, $CHCl_3$); **FT-IR** (film) $\tilde{\nu}$ = 3425, 2976, 2935, 2735, 1967, 1640, 1580, 1454, 1416, 1369, 1246, 1069, 1026, 902, 767 cm^{-1}; **^{1}H NMR** (500 MHz, acetone-d_6) δ 7.23 (d, *J* = 11.5 Hz, 1H), 6.66–6.59 (m, 1H), 5.96 (ddd, *J* = 14.6, 9.5, 4.7 Hz, 1H), 5.83 (s, 1H), 5.65–5.59 (m, 1H), 5.24–5.19 (m, 1H), 5.06 (t, *J* = 9.7 Hz, 1H), 4.99 (d, *J* = 10.1 Hz, 1H), 4.77 (s, 1H), 4.75–4.71 (m, 1H), 4.74 (s, 2H), 4.66 (s, 1H), 4.59 (d, *J* = 11.5 Hz, 1H), 4.41 (d, *J* = 11.5 Hz, 1H), 4.28–4.24 (m, 1H), 4.06–3.97 (m, 3H), 3.95 (d, *J* = 3.4 Hz, 1H), 3.90 (tt, *J* = 8.0, 3.8 Hz, 1H), 3.78–3.70 (m, 3H), 3.61–3.54 (m, 2H), 3.52 (s, 3H), 3.46–3.38 (m, 1H), 3.24–3.17 (m, 1H), 2.95–2.80 (m, 2H), 2.78–2.61 (m, 3H), 2.60–2.47 (m, 2H), 2.44 (ddd, *J* = 13.9, 9.3, 4.6 Hz, 1H), 1.93–1.89 (m, 2H), 1.87–1.79 (m, 1H), 1.82 (s, 3H), 1.73 (s, 3H), 1.66 (s, 3H), 1.61–1.53 (m, 1H), 1.50–1.41 (m, 1H), 1.33 (d, *J* = 6.1 Hz, 3H), 1.29–1.23 (m, 1H), 1.21–1.11 (m, 15H), 1.09 (s, 3H), 0.83 (d, *J* = 7.3 Hz, 3H) ppm; **^{13}C NMR** (126 MHz, acetone-d_6) δ 176.8, 167.8, 167.7, 165.3, 154.4, 153.2, 145.4, 143.4, 141.3, 136.9, 136.1, 133.8, 128.2, 126.4, 125.3, 124.0, 120.6, 118.8, 115.8, 101.8, 96.8, 93.3, 81.6, 78.2, 77.5, 75.7, 73.8, 72.9, 72.8, 72.5, 72.4, 70.6, 70.2, 67.7, 67.1, 63.4, 61.7, 43.3, 42.0, 39.9, 37.3, 35.6, 34.8, 28.7, 28.4, 26.5, 25.9, 20.7, 19.4, 19.2, 18.6, 18.1, 17.5, 15.2, 14.5, 13.8, 11.2 ppm; **HRMS** ESI(+) (MeOH) calculated for $C_{59}H_{85}Cl_2NO_{20}Na$ $[M+Na]^+$: 1220.49342, found: 1220.49393.

6b

R_f (CH_2Cl_2/MeOH 9:1) = 0.23; **Specific Rotation** $[\alpha]_D^{24°C}$ = −38.23 (β = 0.47 g/100 mL, $CHCl_3$); **FT-IR** (film) $\tilde{\nu}$ = 3420, 2975, 2935, 2876, 1733, 1700, 1639, 1452, 1405, 1369, 1331, 1248, 1068, 1004, 902, 771 cm^{-1}; **^{1}H NMR** (500 MHz, acetone-d_6) δ 7.26 (d, *J* = 11.5 Hz, 4H), 6.66–6.58 (m, 1H), 5.96 (ddd, *J* = 14.6, 9.7, 4.5 Hz, 1H), 5.82 (s, 1H), 5.62 (t, *J* = 8.3 Hz, 1H), 5.24–5.19 (m, 1H), 5.04–4.97 (m, 2H), 4.78–4.76 (m, 5H), 4.73 (q, *J* = 5.0 Hz, 1H), 4.58–4.53 (m, 2H), 4.43 (d, *J* = 11.6 Hz, 1H), 4.31–4.27 (m, 1H), 4.18–4.10 (m, 1H), 4.06–3.86 (m, 6H), 3.86–3.78 (m, 2H), 3.75–3.70 (m, 2H), 3.69–3.64 (m, 1H), 3.52 (s, 3H), 3.52–3.47 (m, 2H), 3.44–3.17 (m, 4H), 2.89–2.77 (m, 2H), 2.76–2.61 (m, 3H), 2.61–2.48 (m, 1H), 2.56 (sept, *J* = 7.0 Hz, 1H), 2.43 (ddd, *J* = 14.1, 9.3, 4.5 Hz, 1H), 1.97–1.82 (m, 5H), 1.81 (s, 3H), 1.70 (s, 3H), 1.66 (s, 3H), 1.60–1.41 (m, 4H), 1.31 (d, *J* = 6.1 Hz, 3H), 1.28–1.22 (m, 1H), 1.20–1.11 (m, 15H), 1.09 (s, 3H), 0.82 (t, *J* = 7.4 Hz, 3H) ppm; **^{13}C NMR** (126 MHz, acetone-d_6) δ 176.8, 167.7, 166.2, 165.5, 165.3, 153.9, 151.7, 145.8, 143.8, 140.4, 136.7, 136.10, 136.07, 133.7, 128.5, 128.0, 126.2, 126.1, 125.0, 124.0, 122.0, 101.1, 96.8, 93.3, 82.0, 78.1, 77.9, 75.7, 73.8, 73.1, 73.0, 72.9, 72.8, 72.6, 72.4, 70.8, 70.2, 67.6, 67.1, 67.0, 62.9, 61.7, 43.3, 42.9, 42.0, 40.0, 39.9, 37.5, 35.61, 35.57, 34.8, 28.7, 28.4, 26.5, 25.7, 20.8, 19.4, 19.2, 18.6, 17.5, 15.2, 14.4, 13.8, 11.2 ppm; **HRMS** ESI(+) (MeOH) calculated for $C_{66}H_{96}Cl_2N_2O_{22}Na$ $[M+Na]^+$: 1361.57240, found: 1361.57256.

2,5,8,11,14,17-Hexaoxanonadecan-19-yl 4-nitrobenzenesulfonate

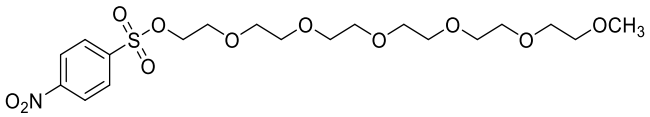

Chemical Formula: $C_{19}H_{31}NO_{11}S$

Exact Mass: 481.1618

Molecular Weight: 481.5130

In a flame-dried 10 mL Schlenk tube, hexaethyleneglycol monomethyl ether (163 mg, 0.550 mmol, 1.0 equiv.) was dissolved in dry THF (0.3 mL). NEt_3 (150 µL, 1.11 mmol, 2.0 equiv.) and *N*,*N*-dimethylaminopyridine (16.3 mg, 0.133 mmol, 0.13 equiv.) were added and the flask was cooled in an ice bath. A solution of nosyl chloride (222 mg, 1.00 mmol, 1.8 equiv.) in dry THF (1.0 mL) was slowly added by syringe. After the addition, the reaction mixture was stirred at 0 °C for five minutes and then allowed to warm to room temperature. After 18 hours of stirring at room temperature, the reaction mixture was filtered and the solid residue washed with THF (3 x 10 mL). The filtrate was concentrated under reduced pressure. The oily residue was dissolved in CH_2Cl_2 (15 mL) and washed with a saturated aqueous solution of NaCl (15 mL). The aqueous phase was extracted with CH_2Cl_2 (3 x 15 mL). The combined organic phases were dried over anhydrous $MgSO_4$. After filtration of the drying agent, the solvent was evaporated under reduced pressure. The crude product was further purified by flash column chromatography (SiO_2, CH_2Cl_2/MeOH 96:4) to give the product as a yellow oil (239 mg, 0.496 mmol, 90 %).

R_f (CH_2Cl_2/MeOH 96:4) = 0.28; **FT-IR** (film) $\tilde{\nu}$ = 2872, 1608, 1532, 1453, 1403, 1350, 1310, 1249, 1185, 1094, 1011, 921, 855, 789, 746, 733, 685, 614, 578, 532, 464 cm^{-1}; **^{1}H NMR** (400 MHz, $CDCl_3$) δ 8.41–8.31 (m, 2H), 8.15–8.05 (m, 2H), 4.30–4.20 (m, 2H), 3.69–3.65 (m, 2H), 3.62–3.54 (m, 14H), 3.53–3.47 (m, 6H), 3.32 (s, 3H) ppm; **^{13}C NMR** (101 MHz, $CDCl_3$) δ 150.7, 141.9, 129.4, 124.4, 71.9, 70.7, 70.62, 70.59, 70.56, 70.54, 70.50, 70.47, 68.5, 59.0 ppm; **HRMS** ESI(+) (MeOH) calculated for $C_{19}H_{32}NO_{11}S$ $[M+H]^+$: 482.16906, found: 482.16923.

HEG-Fidaxomicin (7a) and Bis(HEG)-Fidaxomicin (7b)

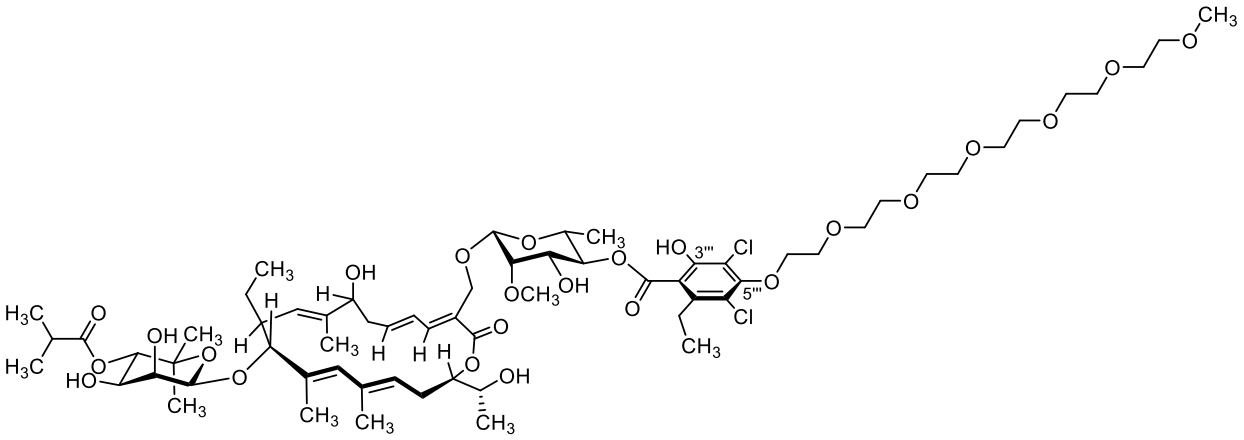

7a

Chemical Formula: $C_{65}H_{100}Cl_2O_{24}$

Exact Mass: 1334.5982

Molecular Weight: 1336.3910

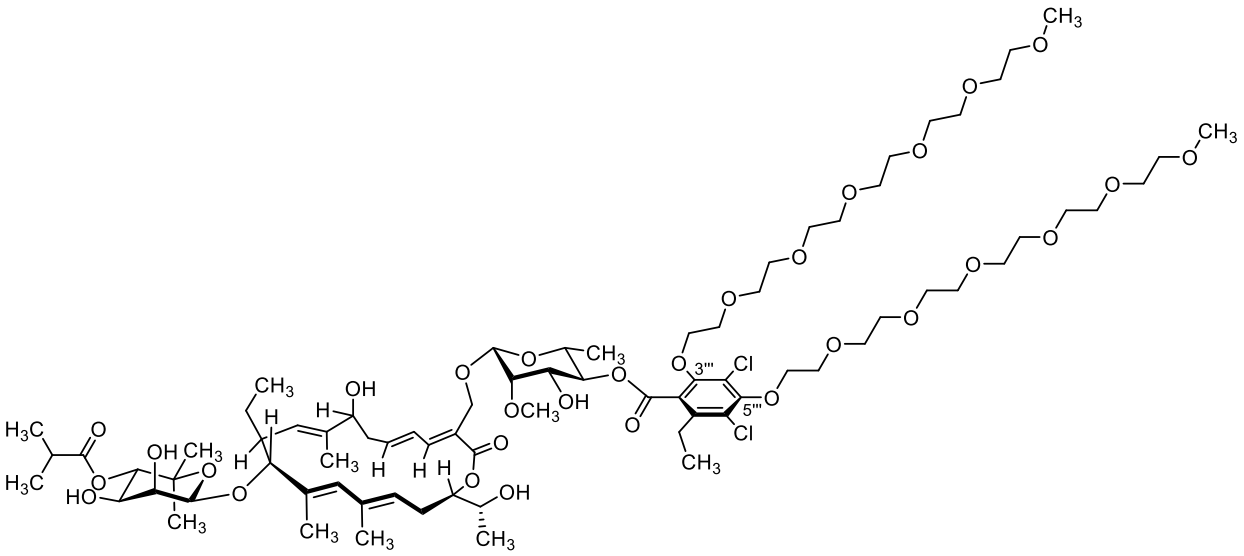

7b

Chemical Formula: $C_{78}H_{126}Cl_2O_{30}$

Exact Mass: 1612.7711

Molecular Weight: 1614.7360

A flame-dried Schlenk tube was charged with fidaxomicin (**1**, 58.0 mg, 54.8 μmol, 1.0 equiv.) and the solid was dissolved in dry DMF (0.3 mL). 2,5,8,11,14,17-Hexaoxanonadecan-19-yl 4-nitrobenzenesulfonate (186 mg, 0.386 mmol, 7.0 equiv.) was dissolved in dry DMF (0.7 mL) and this solution was added to the reaction flask *via* microliter syringe. Solid K_2CO_3 (31.0 mg, 0.224 mmol, 4.0 equiv.) was added followed by another portion of dry

DMF (0.4 mL). The reaction mixture was stirred at 45 °C. The reaction was monitored by analyzing aliquot samples by UHPLC-MS. After 2.5 hours, the reaction mixture was diluted with EtOAc (10 mL) and washed with a saturated aqueous solution of NH_4Cl (15 mL). The aqueous phase was extracted with EtOAc (2 x 10 mL) and the combined organic phases were dried over anhydrous $MgSO_4$. After filtration of the drying agent, the solvent was evaporated under reduced pressure. The crude product was subjected to preparative RP-HPLC [Synergi Hydro-RP, 10 µ, 80 Å, 250 mm x 21.2 mm, solvent A: H_2O +0.1 % HCOOH, solvent B: MeCN+0.1 % HCOOH; 25 mL/min; LC time program (min – % B): 4.0 min – 47 %, 52.0 min – 53 %, 58.0 min – 80 %, 58.1 min – 100 %, 63.00 min – 100 %; λ = 270 nm] to give the monosubstitution product **17a** as a colourless solid (t_R = 32.54–35.33 min, 14.3 mg, 10.7 µmol, 19 %) and the disubstitution product **17b** as a colourless resin (t_R = 32.54–35.33 min, 41.2 mg, 25.5 µmol, 46 %).

7a

Specific Rotation $[\alpha]_D^{24°C}$ = −38.6 (β = 0.45 g/100 mL, $CHCl_3$); **FT-IR** $\tilde{\nu}$ (film) 3454, 2972, 2930, 2875, 1736, 1702, 1641, 1581, 1455, 1414, 1384, 1369, 1349, 1296, 1243, 1199, 1092, 1068, 1024, 949, 901, 857, 800, 769, 732, 583, 506 cm^{-1}; **^{1}H NMR** (600 MHz, acetone-d_6) δ 7.23 (d, *J* = 11.4 Hz, 1H), 6.66–6.59 (m, 1H), 5.96 (ddd, *J* = 14.6, 9.5, 4.7 Hz, 1H), 5.83 (s, 1H), 5.65–5.60 (m, 1H), 5.21 (dt, *J* = 10.6, 1.6 Hz, 1H), 5.06 (t, *J* = 9.7 Hz, 1H), 4.99 (d, *J* = 10.1 Hz, 1H), 4.77 (d, *J* = 1.3 Hz, 1H), 4.73 (dt, *J* = 6.5, 4.9 Hz, 1H), 4.66 (s, 1H), 4.60 (d, *J* = 11.5 Hz, 1H), 4.41 (d, *J* = 11.5 Hz, 1H), 4.29–4.25 (m, 1H), 4.23 (t, *J* = 4.9 Hz, 2H), 4.07–3.98 (m, 1H), 3.96 (d, *J* = 3.3 Hz, 1H), 3.88 (t, *J* = 4.8 Hz, 2H), 3.79–3.70 (m, 3H), 3.70–3.66 (m, 2H), 3.64–3.61 (m, 2H), 3.61–3.55 (m, 16H), 3.52 (s, 3H), 3.49–3.44 (m, 2H), 3.29 (s, 3H), 2.97–2.84 (m, 2H), 2.78–2.62 (m, 3H), 2.56 (sept, *J* = 7.0 Hz, 1H), 2.52–2.47 (m, 1H), 2.44 (ddd, *J* = 13.9, 9.0, 4.5 Hz, 1H), 1.96–1.91 (m, 1H), 1.81 (s, 3H), 1.73 (s, 3H), 1.66 (s, 3H), 1.33 (d, *J* = 6.2 Hz, 3H), 1.30–1.12 (m, 16H), 1.09 (s, 3H), 0.82 (t, *J* = 7.4 Hz, 3H) ppm; **^{13}C NMR** (151 MHz, acetone-d_6) δ 176.8, 167.9, 167.8, 155.0, 153.4, 145.4, 143.4, 141.2, 136.9, 136.1, 133.8, 128.2, 126.3, 125.3, 124.0, 118.2, 115.9, 110.9, 101.8, 96.8, 93.3, 81.6, 78.2, 77.5, 75.7, 73.8, 73.7, 72.9, 72.8, 72.6, 72.4, 71.35, 71.25, 71.21, 71.19, 71.16, 71.1, 71.0, 70.9, 70.6, 70.2, 67.7, 63.4, 61.7, 58.8, 42.0, 37.3, 34.8, 28.7, 28.4, 26.5, 25.9, 20.7, 19.4, 19.2, 18.6, 18.1, 17.5, 15.2, 14.5, 13.8, 11.2 ppm; **HRMS** ESI+ (MeOH), calculated for $C_{65}H_{100}Cl_2O_{24}Na$ $[M+Na]^+$: 1357.58738, found: 1357.58787.

7b

Specific Rotation $[\alpha]_D^{24°C}$ = −35.9 (β = 0.93 g/100 mL, $CHCl_3$); **FT-IR** $\tilde{\nu}$ (neat) 3458, 2975, 2934, 2875, 1736, 1703, 1641, 1568, 1454, 1383, 1368, 1351, 1315, 1278, 1249, 1199, 1099, 1070, 1027, 949, 904, 862, 791, 772, 745, 714 cm^{-1}; **^{1}H NMR** (500 MHz, acetone-d_6) δ 7.22 (d, *J* = 11.2 Hz, 1H), 6.63 (dddd, *J* = 14.7, 11.5, 2.1, 1.0 Hz, 1H), 5.95 (ddd, *J* = 14.6, 9.5, 4.6 Hz, 1H), 5.83 (s, 1H), 5.66–5.58 (m, 1H), 5.20 (dt, *J* = 10.6, 1.6 Hz, 1H), 5.03 (t, *J* = 9.7 Hz, 1H), 4.99 (d, *J* = 10.1 Hz, 1H), 4.76 (d, *J* = 1.2 Hz, 1H), 4.72 (q, *J* = 5.3 Hz, 1H), 4.63 (d, *J* = 0.8 Hz, 1H), 4.59 (d, *J* = 11.5 Hz, 1H), 4.40 (d, *J* = 11.5 Hz, 1H), 4.29–4.22 (m, 4H), 4.13 (dt, *J* = 10.0, 4.7 Hz, 1H), 4.06–3.99 (m, 2H), 3.95 (s, 1H), 3.89 (t, *J* = 4.9 Hz, 2H), 3.88–3.87 (m, 1H), 3.84 (s, br, 1H), 3.81 (t, *J* = 4.9 Hz, 2H), 3.75–3.71 (m, 3H), 3.71–3.66 (m, 3H), 3.66–3.54 (m, 36H), 3.53 (s, 3H), 3.49–3.44 (m, 4H), 3.28 (s, 6H), 2.93–2.60 (m,

5H), 2.56 (sept, *J* = 7.0 Hz, 1H), 2.53–2.47 (m, 1H), 2.43 (ddd, *J* = 13.9, 9.1, 4.4 Hz, 1H), 1.98–1.89 (m, 1H), 1.81 (d, *J* = 1.3 Hz, 3H), 1.72 (d, *J* = 1.4 Hz, 3H), 1.65 (dd, *J* = 1.4, 0.7 Hz, 3H), 1.37 (d, *J* = 6.2 Hz, 3H), 1.29–1.21 (m, 1H), 1.19–1.12 (m, 15H), 1.09 (s, 3H), 0.82 (t, *J* = 7.5 Hz, 3H) ppm; **^{13}C NMR** (151 MHz, acetone-d_6) δ 176.8, 167.9, 166.5, 154.4, 152.4, 145.3, 143.3, 139.9, 136.9, 136.1, 133.8, 128.3, 128.2, 126.4, 125.7, 125.4, 124.0, 122.0, 101.8, 96.8, 93.3, 82.0, 78.2, 77.5, 75.7, 75.0, 73.9, 73.8, 72.9, 72.8, 72.7, 72.5, 71.5, 71.4, 71.33, 71.29, 71.26, 71.1, 70.9, 70.8, 70.6, 70.2, 67.8, 63.4, 61.8, 58.84, 58.83, 42.1, 37.3, 34.8, 28.7, 28.4, 26.5, 25.6, 20.7, 19.4, 19.2, 18.6, 18.4, 17.5, 15.2, 14.5, 13.8, 11.2 ppm; **HRMS** ESI+ (MeOH), calculated for $C_{78}H_{126}Cl_2O_{30}Na$ $[M+Na]^+$: 1635.76032, found: 1635.75986.

SuFEx-Fidaxomicin (8)

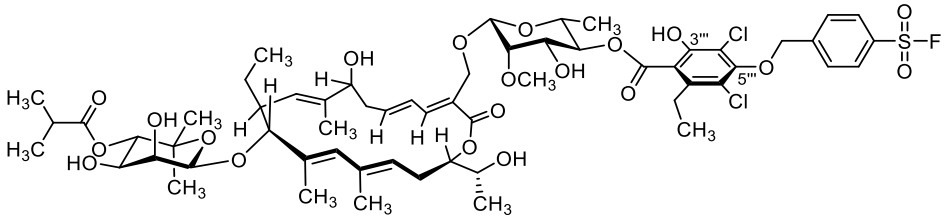

8a

Chemical Formula: $C_{59}H_{79}Cl_2FO_{20}S$

Exact Mass: 1228.4246

Molecular Weight: 1230.2194

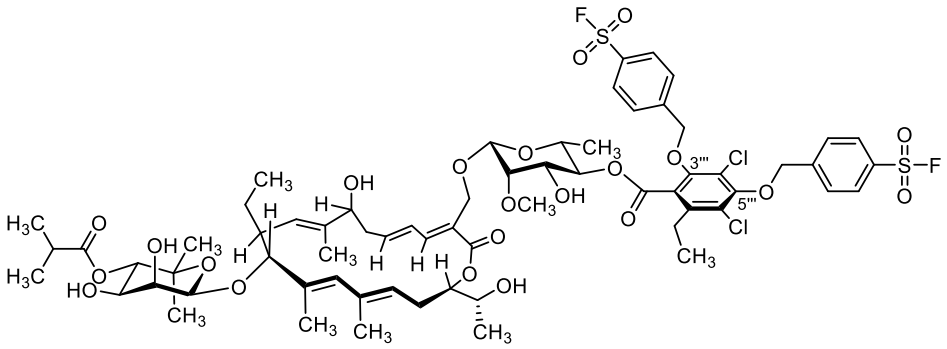

8b

Chemical Formula: $C_{66}H_{84}Cl_2F_2O_{22}S_2$

Exact Mass: 1400.4241

Molecular Weight: 1402.3928

An oven-dried microwave tube under an atmosphere of argon was charged with fidaxomicin (**1**, 52.0 mg, 49.1 µmol, 1.0 equiv.) and 4-(bromomethyl)benzene sulfonyl fluoride (22.0 mg, 86.9 µmol, 1.8 equiv.). The solids were dissolved in dry DMF (1.5 mL) and K_2CO_3 (27.0 mg, 0.195 mmol, 4.0 equiv.) was added. The reaction mixture was stirred at 45 °C. After 2 hours, the reaction mixture was diluted with Et_2O (15 mL) and quenched with a saturated aqueous solution of NH_4Cl (15 mL). The layers were separated and the aqueous phase extracted with Et_2O (4 x 15 mL). The organic phase was washed with a saturated aqueous solution of NH_4Cl (2 x 50 mL). The combined organic phases were dried over anhydrous $MgSO_4$. After filtration of the drying agent, the solvent was evaporated under reduced pressure. The crude product was subjected to preparative RP-HPLC [Gemini NX C18, 5 µ, 110 Å, 250 mm x 21.2 mm; solvent A: H_2O +0.1 % HCOOH, solvent B: MeCN+0.1 % HCOOH; 20 mL/min; LC time program (min – % B): 4.0 min – 60 %, 35.0 min – 85 %, 45.1 min – 100 %; λ = 270 nm] to give the monosubstitution product

8a (t_R = 22.53–23.56 min, 11.0 mg, 8.95 µmol, 16 %) and the disubstitution product **8b** (t_R = 32.39–34.17 min, 32.0 mg, 22.8 µmol, 47 %) as colourless solids.

8a

Specific Rotation $[\alpha]_D^{24°C}$ = −23.3 (β = 0.54 g/100 mL, $CHCl_3$); **FT-IR** $\tilde{\nu}$ (film) 3476, 2976, 2935, 2878, 2154, 2081, 1737, 1703, 1642, 1601, 1583, 1554, 1455, 1416, 1387, 1371, 1345, 1296, 1245, 1214, 1145, 1095, 1070, 1027, 900, 779 cm^{-1}; **^{1}H NMR** (500 MHz, acetone-d_6) δ 8.20 (d, *J* = 8.2 Hz, 2H), 8.04 (d, *J* = 8.2, 2H), 7.23 (d, *J* = 11.5 Hz, 1H), 6.63 (dddd, *J* = 14.7, 11.5, 2.0, 1.0 Hz, 1H), 5.96 (ddd, *J* = 14.5, 9.5, 4.6 Hz, 1H), 5.83 (s, 1H), 5.67–5.59 (m, 1H), 5.32 (s, 2H), 5.21 (dt, *J* = 10.4, 1.5 Hz, 1H), 5.08 (t, *J* = 9.8 Hz, 1H), 5.00 (d, *J* = 10.1 Hz, 1H), 4.77 (d, *J* = 1.2 Hz, 1H), 4.73 (dt, *J* = 6.4, 4.8 Hz, 1H), 4.68 (d, *J* = 0.8 Hz, 1H), 4.61 (d, *J* = 11.5 Hz, 1H), 4.41 (d, *J* = 11.5 Hz, 1H), 4.27 (m, 1H), 4.09–3.98 (m, 2H), 3.97–3.94 (m, 1H), 3.81 (d, *J* = 3.6 Hz, 1H), 3.78 (dd, *J* = 9.9, 3.4 Hz, 1H), 3.76–3.69 (m, 3H), 3.64–3.61 (m, 1H), 3.60–3.55 (m, 1H), 3.52 (s, 3H), 3.25 (d, *J* = 9.4 Hz, 1H), 2.99–2.86 (m, 2H), 2.81–2.69 (m, 2H), 2.67–2.60 (m, 1H), 2.56 (sept, *J* = 7.1 Hz, 1H), 2.53–2.40 (m, 2H), 1.99–1.88 (m, 1H), 1.81 (d, *J* = 1.3 Hz, 3H), 1.73 (d, *J* = 1.3 Hz, 3H), 1.66 (d, *J* = 1.2 Hz, 3H), 1.34 (d, *J* = 6.1 Hz, 1H), 1.29–1.23 (m, 1H), 1.21 (t, *J* = 7.4 Hz, 1H), 1.18 (d, *J* = 5.7 Hz, 1H), 1.16–1.12 (m, 9H), 1.09 (s, 3H), 0.83 (t, *J* = 7.5 Hz, 3H) ppm; **^{13}C NMR** (125 MHz, acetone-d_6) δ 176.8, 167.8, 167.5, 154.01, 152.9, 146.6, 145.4, 143.4, 141.5, 136.9, 136.12, 136.10, 133.8, 133.0 (d, $^2J_{C-F}$ = 24.6 Hz), 129.9, 129.5, 128.2, 126.3, 125.3, 124.0, 121.1, 119.0, 116.0, 101.9, 96.8, 93.3, 81.6, 78.2, 77.6, 75.70, 75.67, 73.9, 73.8, 72.9, 72.8, 72.4, 70.6, 70.2, 67.7, 63.4, 61.7, 42.0, 37.3, 34.8, 28.7, 28.4, 26.5, 25.9, 20.7, 19.4, 19.2, 18.6, 18.1, 17.5, 15.2, 14.5, 13.8, 11.2 ppm; **^{19}F NMR** (377 MHz, acetone-d_6) δ 64.87 (s) ppm; **HRMS** ESI+ (MeOH), calculated for $C_{59}H_{79}Cl_2FO_{20}SNa$ $[M+Na]^+$: 1251.41497, found: 1251.41380.

8b

Specific Rotation $[\alpha]_D^{22°C}$ = −41.6 (β = 0.45 g/100 mL, $CHCl_3$); **FT-IR** $\tilde{\nu}$ (film) 3474, 2976, 2935, 2878, 2098, 1734, 1703, 1642, 1602, 1569, 1469, 1454, 1409, 1384, 1368, 1330, 1316, 1298, 1250, 1213, 1185, 1137, 1107, 1096, 1068, 1024, 951, 901, 859, 818, 772, 735, 701, 671, 633, 587, 566, 538, 499, 461 cm^{-1}; **^{1}H NMR** (500 MHz, acetone-d_6) δ 8.20 (d, *J* = 6.3 Hz, 2H), 8.19 (d, *J* = 6.3 Hz, 2H), 8.05 (d, *J* = 8.2 Hz, 2H), 7.96 (d, *J* = 8.2 Hz, 2H), 7.21 (d, *J* = 11.4 Hz, 1H), 6.64–6.54 (m, 1H), 5.94 (ddd, *J* = 14.5, 9.5, 4.6 Hz, 1H), 5.82 (s, 1H), 5.66–5.57 (m, 1H), 5.40–5.34 (m, 3H), 5.26 (d, *J* = 12.1 Hz, 1H), 5.20 (dt, *J* = 10.6, 1.6 Hz, 1H), 5.02 (t, *J* = 9.7 Hz, 1 H), 4.99 (d, *J* = 10.1 Hz, 1 H), 4.77 (d, *J* = 1.2 Hz, 1H), 4.74–4.69 (m, 1H), 4.62 (s, 1 H), 4.56 (d, *J* = 11.4 Hz, 1H), 4.36 (d, *J* = 11.4 Hz, 1H), 4.27 (m, 1H), 4.07–3.97 (m, 2H), 3.98–3.88 (m, 2H), 3.81 (s, 1H), 3.77–3.64 (m, 4H), 3.55 (d, *J* = 3.4 Hz, 1H), 3.51 (s, 3H), 3.50–3.44 (m, 1H), 3.31–3.22 (m, 1 H), 2.98–2.85 (m, 2H), 2.81–2.69 (m, 2H), 2.67–2.60 (m, 1H), 2.56 (sept, *J* = 7.0 Hz, 1H), 2.52–2.37 (m, 2H), 1.99–1.89 (m, 1H), 1.80 (d, *J* = 1.2 Hz, 3H), 1.72 (d, *J* = 1.3 Hz, 3H), 1.65 (d, *J* = 1.2 Hz, 3H), 1.29–1.23 (m, 1H), 1.21 (t, *J* = 7.4 Hz, 3H), 1.17 (d, *J* = 5.8 Hz, 3H), 1.16–1.12 (m, 6 H), 1.15 (s, 3 H), 1.09 (s, 3H), 0.82 (t, *J* = 7.4 Hz, 3H) ppm; **^{13}C NMR** (126 MHz, acetone-d_6) (126 MHz, Acetone) δ 176.8, 167.9, 166.3, 153.6, 151.6, 146.4, 146.3, 145.3, 143.3, 140.6, 136.9, 136.1, 133.8, 133.1 (d, $^2J_{C-F}$ = 24.4 Hz), 133.0 (d, $^2J_{C-F}$ = 24.4 Hz), 130.05, 129.98, 129.6, 129.5, 129.1, 128.2, 126.6, 126.4, 125.4, 123.9, 122.4, 101.9, 96.7,

93.3, 81.8, 78.2, 77.7, 75.9, 75.7, 74.2, 73.8, 72.9, 72.8, 72.3, 70.5, 70.2, 67.7, 63.4, 61.7, 42.0, 37.2, 34.8, 28.7, 28.4, 26.5, 25.7, 20.7, 19.4, 19.2, 18.6, 18.1, 17.4, 15.2, 14.4, 13.8, 11.2 ppm; **^{19}F NMR** (377 MHz, acetone-d_6) δ 64.93 (s), 64.88 (s) ppm; **HRMS** ESI+ (MeOH), calculated for $C_{66}H_{88}Cl_2F_2O_{22}S_2N$ $[M+NH_4]^+$: 1418.45790, found: 1418.45885.

Tetrazine-Fidaxomicin (9b)

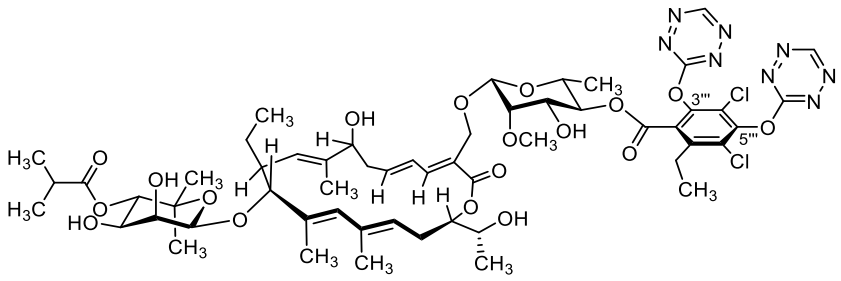

8b

Chemical Formula: $C_{56}H_{874}Cl_2N_8O_{18}$

Exact Mass: 1216.4498

Molecular Weight: 1218.1460

This compound was prepared according to a literature procedure.[6]

3-Azidopropan-1-ol[7]

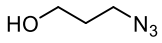

Chemical Formula: $C_3H_7N_3O$
Exact Mass: 101.0589
Molecular Weight: 101.1090

3-Azidopropan-1-ol was synthesized following a literature procedure.[7] In a 500 mL round-bottom flask, 3-bromopropan-1-ol (12.4 g, 89.2 mmol, 1.0 equiv.) was dissolved in acetone (200 mL). A solution of NaN_3 (29.0 g, 466 mmol, 5.2 equiv.) in H_2O (120 mL) was added while stirring. A catalytic amount of KI (2.0 mg, 12 µmol) was added. This solution was stirred at room temperature for 48 hours. After extraction with Et_2O (3 x 80 mL), the combined organic layers were dried over K_2CO_3. The drying agent was filtered off and the solvent was evaporated *in vacuo* to give 3-azidopropan-1-ol as a highly viscous colourless oil (8.09 g, 80.0 mmol, 90 %).

R_f (pentane/Et_2O 1:1) = 0.41; **FT-IR** (film) $\tilde{\nu}$ = 3352, 2949, 2878, 2513, 2090 (-N3), 1641, 1457, 1427, 1371, 1343, 1299, 1258, 1184, 1048, 957, 901, 861, 771, 638, 557, 509 cm^{-1}; **^{1}H NMR** (400 MHz, $CDCl_3$) δ 3.76 (t, *J* = 6.0 Hz, 2H), 3.46 (t, *J* = 6.6 Hz, 2H), 1.84 (quint, *J* = 6.3 Hz, 2H) ppm; **^{13}C NMR** (101 MHz, $CDCl_3$) δ 60.1, 48.7, 31.6 ppm; **HRMS** ESI(+) (MeOH) calculated for $C_3H_7N_3ONa$ $[M+Na]^+$: 124.04813, found: 124.04790.

3-Azidopropyl 4-nitrobenzenesulfonate[8]

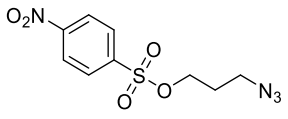

Chemical Formula: $C_9H_{10}N_4O_5S$
Exact Mass: 286.0372
Molecular Weight: 286.2620

3-Azidopropyl 4-nitrobenzenesulfonate was synthesized in analogy to a nosylation procedure reported in literature.[8] In a flame-dried 250 mL three-necked round-bottom flask, 3-azidopropan-1-ol (2.50 g, 24.7 mmol, 1.0 equiv.) was dissolved in dry THF (30 mL). DMAP (453 mg, 3.70 mmol, 0.15 equiv.) and NEt_3 (6.95 mL, 45.5 mmol, 1.8 equiv.) were added. The reaction mixture was cooled to 0 °C and a solution of nosyl chloride (11.0 g, 49.5 mmol, 2.0 equiv.) in THF (100 mL, dry) was added slowly *via* a dropping funnel. As large amounts of precipitate had formed, another

portion of dry THF (50 mL) was added. The reaction mixture was stirred at room temperature for 48 hours. The mixture was diluted with CH_2Cl_2 (700 mL), washed with a saturated aqueous solution of NaCl (3 x 200 mL), dried over anhydrous $MgSO_4$, filtered and concentrated *in vacuo*. After purification by flash column chromatography (SiO_2, pentane/CH_2Cl_2 1:3) the product (4.7 g, 16.5 mmol, 67 %) was obtained as a slightly yellow amorphous solid.

R_f (pentane/Et_2O 1:1) = 0.59; **FT-IR** (film) $\tilde{\nu}$ = 2978, 2099 (-N_3), 1609, 1531, 1479, 1455, 1423, 1403, 1391, 1373, 1349, 1316, 1295, 1227, 1201, 1186, 1171, 1096, 1065, 1017, 930, 904, 874, 855, 826, 761, 746, 732, 682, 608, 569, 528 cm^{-1}; **^{1}H NMR** (400 MHz, $CDCl_3$) δ 8.45–8.39 (m, 2H), 8.15–8.10 (m, 2H), 4.23 (t, *J* = 6.0 Hz, 2H), 3.42 (t, *J* = 6.4 Hz, 2H), 1.95 (quint, *J* = 6.1 Hz, 1H) ppm; **^{13}C NMR** (101 MHz, $CDCl_3$) δ 151.0, 141.6, 129.4, 124.7, 68.3, 47.2, 28.6 ppm; **HRMS** ESI(+) (MeOH) calculated for $C_9H_{10}N_4O_5S$ $[M]^{+\cdot}$: 286.03774, found: 286.03739.

Mono(azidopropyl)fidaxomicin (10a) and Bis(azidopropyl)fidaxomicin (10b)

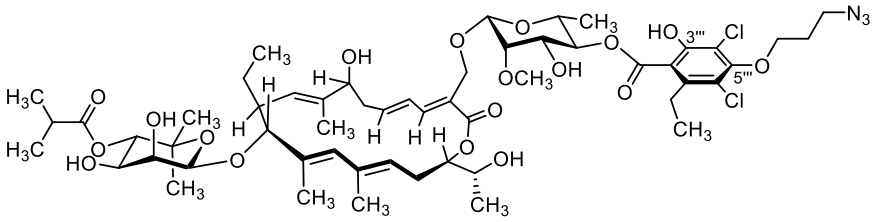

10a

Chemical Formula: $C_{55}H_{79}Cl_2N_3O_{18}$

Exact Mass: 1139.4736

Molecular Weight: 1141.1400

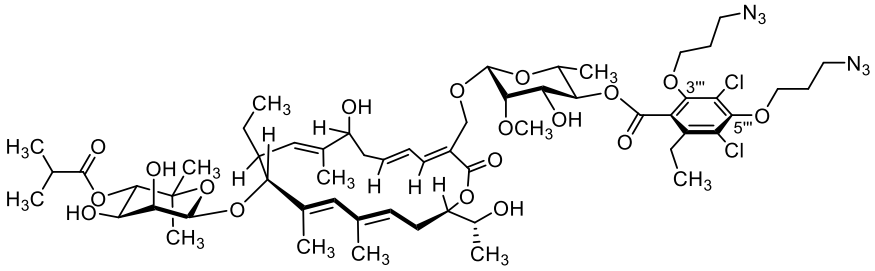

10b

Chemical Formula: $C_{58}H_{84}Cl_2N_6O_{18}$

Exact Mass: 1222.5219

Molecular Weight: 1224.2340

Fidaxomicin (**1**, 101 mg, 95.8 µmol, 1.0 equiv.) was weighed into a flame-dried 5 mL Schlenk tube under nitrogen atmosphere and dissolved in dry DMF (1.0 mL). 3-Azidopropyl 4-nitrobenzenesulfonate (40.9 mg, 0.143 mmol, 1.5 equiv.) and K_2CO_3 (60.8 mg, 0.440 mmol, 4.0 equiv.) were added followed by another portion of dry DMF (1 mL). The reaction mixture was stirred at 45 °C for 3 hours. The reaction mixture was diluted with EtOAc (10 mL), washed with a saturated aqueous solution of NH_4Cl (5 x 10 mL) and dried over anhydrous $MgSO_4$. After filtration of the drying agent, the solvent was evaporated under reduced pressure to give a yellow oil. The crude product was purified by preparative RP-HPLC [Gemini NX C18, 10 µ, 110 Å, 250 mm x 21.2 mm; solvent A: H_2O+0.1 % HCOOH, solvent B: MeCN+0.1 % HCOOH; 20 mL/min; LC time program (min – % B): 0.0 – 60 %, 3.0 – 60 %, 30.0 – 85 %; λ = 270 nm) to afford the desired products after lyophilization (monosubstituted product **10a**: t_R = 19.3 min, 20.4 mg, 17.9 µmol, 19 %; disubstituted product **10b**: t_R = 26.9 min, 33.7 mg, 27.5 µmol, 29 %).

10a

Specific Rotation $[\alpha]_D^{29°C}$ = −48.9 (β = 0.90 g/100 mL, MeOH); **FT-IR** $\tilde{\nu}$ (film) 3445, 2978, 2935, 2876, 2099 (-N_3), 1739, 1697, 1641, 1582, 1471, 1449, 1417, 1387, 1369, 1349, 1299, 1246, 1199, 1146, 1114, 1068, 1025, 948, 903, 855, 800, 767, 745, 713, 504 cm^{-1}; **^{1}H NMR** (500 MHz, acetone-d_6) δ 7.23 (d, *J* = 11.4 Hz, 1H), 6.63 (dd, *J* = 15.3, 11.9 Hz, 1H), 5.96 (ddd, *J* = 14.9, 9.6, 4.7 Hz, 1H), 5.83 (s, 1H), 5.62 (t, *J* = 8.3 Hz, 1H), 5.21 (d, *J* = 10.5 Hz, 1H), 5.07 (t, *J* = 9.8 Hz, 1H), 4.99 (d, *J* = 10.1 Hz, 1H), 4.77 (d, *J* = 1.0 Hz, 1H), 4.75–4.70 (m, 1H), 4.68–4.66 (m, 1H), 4.60 (d, *J* = 11.5 Hz, 1H), 4.41 (d, *J* = 11.5 Hz, 1H), 4.28–4.25 (m, 1H), 4.16 (t, *J* = 6.0 Hz, 2H), 4.13–4.06 (m, 1H), 4.06–3.97 (m, 1H), 3.97–3.94 (m, 1H), 3.90–3.80 (m, 1H), 3.76 (dd, *J* = 9.9, 3.4 Hz, 1H), 3.75–3.71 (m, 2H), 3.69 (t, *J* = 6.7 Hz, 2H), 3.59–3.54 (m, 1H), 3.60–3.55 (m, 1H), 3.52 (s, 3H), 3.38–3.25 (s, br, 1H), 2.96–2.81 (m, 2H), 2.79–2.71 (m, 1H), 2.71–2.66 (m, 1H), 2.67–2.60 (m, 1H), 2.56 (sept, *J* = 7.0 Hz, 1H), 2.53–2.46 (m, 1H), 2.44 (ddd, *J* = 14.0, 9.1, 4.4 Hz, 1H), 2.12 (quint, *J* = 6.4 Hz, 2H), 2.09 (s, br, 1H), 1.98–1.90 (m, 1H), 1.81 (d, *J* = 1.4 Hz, 3H), 1.73 (d, *J* = 1.4 Hz, 3H), 1.65 (d, *J* = 1.3 Hz, 3H), 1.33 (d, *J* = 6.2 Hz, 3H), 1.30–1.22 (m, 1H), 1.19 (t, *J* = 7.4 Hz, 3H), 1.17 (d, *J* = 6.2 Hz, 3H), 1.15 (d, *J* = 7.0 Hz, 3H), 1.15 (s, 3H), 1.13 (d, *J* = 7.0 Hz, 3H), 1.09 (s, 3H), 0.82 (t, *J* = 7.5 Hz, 3H) ppm; **^{13}C NMR** (126 MHz, acetone-d_6) δ 176.8, 167.8, 167.7, 154.7, 153.1, 145.4, 143.4, 141.5, 136.9, 136.13, 136.11, 133.8, 128.2, 126.4, 125.3, 124.0, 121.0, 118.3, 115.9, 101.8, 96.8, 93.3, 81.6, 78.2, 77.5, 75.7, 73.8, 72.9, 72.8, 72.4, 71.1, 70.6, 70.2, 67.7, 63.4, 61.7, 48.9, 42.0, 37.3, 34.8, 32.1, 28.7, 28.4, 26.5, 25.9, 20.7, 19.4, 19.2, 18.6, 18.1, 17.5, 15.2, 14.5, 13.8, 11.2 ppm; **HRMS** ESI+ (MeOH), calculated for $C_{55}H_{79}Cl_2N_3O_{18}Na$ $[M+Na]^+$: 1162.46279, found: 1162.46327.

10b

Specific Rotation $[\alpha]_D^{29°C}$ = −44.5 (β = 0.70 g/100 mL, MeOH); **FT-IR** $\tilde{\nu}$ (film) 3474, 2976, 2935, 2876, 2098 (-N_3), 1738, 1692, 1641, 1569, 1470, 1412, 1381, 1298, 1248, 1198, 1137, 1117, 1067, 1023, 950, 901, 855, 798, 754, 712, 667, 505 cm^{-1}; **^{1}H NMR** (500 MHz, acetone-d_6) δ 7.22 (d, *J* = 11.4 Hz, 1H), 6.62 (dd, *J* = 15.4, 11.9 Hz, 1H), 5.95 (ddd, *J* = 14.7, 9.5, 4.6 Hz, 1H), 5.83 (s, 1H), 5.62 (t, *J* = 8.2 Hz, 1H), 5.21 (d, *J* = 10.6 Hz, 1H), 5.03 (t, *J* = 9.7 Hz, 1H), 4.99 (d, *J* = 10.1 Hz, 1H), 4.77 (s, 1H), 4.75–4.69 (m, 1H), 4.65 (s, 1H), 4.60 (d, *J* = 11.4 Hz, 1H), 4.40 (d, *J* = 11.4 Hz, 1H), 4.29–4.24 (m, 1H), 4.24–4.20 (m, 1H), 4.19–4.13 (m, 2H), 4.12–4.06 (m, 1H), 4.06–3.98 (m, 2H), 3.95 (d, *J* = 3.2 Hz, 1H), 3.87 (d, *J* = 10.1 Hz, 1H), 3.81 (s, br, 1H), 3.77–3.64 (m, 6H), 3.59 (t, *J* = 6.8 Hz, 2H), 3.57–3.53 (m, 2H), 3.53 (s, 3H), 3.26 (s, br, 1H), 2.96–2.73 (m, 2H), 2.84–2.70 (m, 1H), 2.71–2.66 (m, 1H), 2.67–2.59 (m, 1H), 2.56 (sept, *J* = 7.1 Hz, 1H), 2.53–2.46 (m, 1H), 2.46–2.40 (m, 1H), 2.13 (quint, *J* = 6.3 Hz, 2H), 2.07 (m, 2H), 1.97–1.89 (m, 1H), 1.81 (s, 3H), 1.73 (s, 3H), 1.65 (s, 3H), 1.36 (d, *J* = 6.4 Hz, 3H), 1.30–1.20 (m, 1H), 1.19–1.12 (m, 15H), 1.09 (s, 3H), 0.82 (t, *J* = 7.4 Hz, 3H) ppm; **^{13}C NMR** (126 MHz, acetone-d_6) δ 176.8, 167.9, 166.4, 154.0, 152.2, 145.3, 143.3, 140.1, 136.9, 136.1, 133.8, 128.5, 128.2, 126.4, 125.8, 125.4, 124.0, 122.1, 101.9, 96.8, 93.3, 81.9, 78.2, 77.6, 75.7, 73.8, 73.1, 72.9, 72.8, 72.4, 71.3, 70.6, 70.2, 67.7, 63.4, 61.8, 48.84, 48.77, 42.0, 37.3, 34.8, 28.7, 28.4, 26.5, 25.6, 20.7, 19.4, 19.2, 18.6, 18.3, 17.5, 15.2, 14.4, 13.8, 11.2 ppm; **HRMS** ESI+ (MeOH), calculated for $C_{58}H_{84}Cl_2N_6O_{18}Na$ $[M+Na]^+$: 1245.51114, found: 1245.50954.

Monotriazole (11a) and Bistriazole with Ethynylaniline (11b)

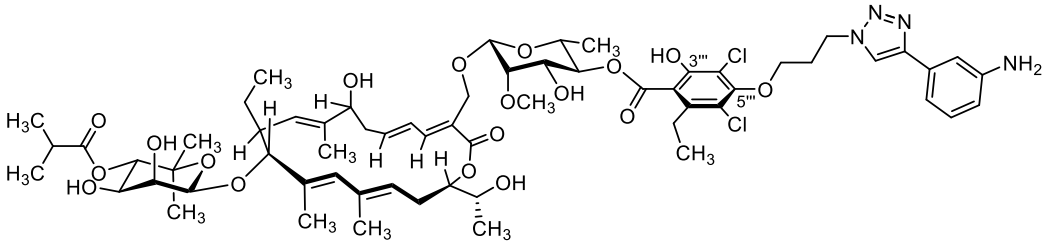

11a

Chemical Formula: $C_{63}H_{86}Cl_2N_4O_{18}$

Exact Mass: 1256.5314

Molecular Weight: 1258.2910

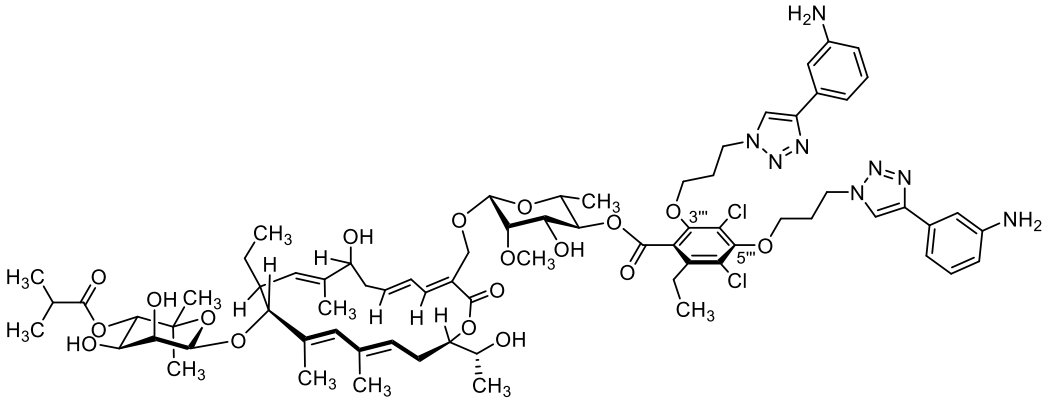

11b

Chemical Formula: $C_{74}H_{98}Cl_2N_8O_{18}$

Exact Mass: 1456.6376

Molecular Weight: 1458.5360

A flame-dried Schlenk tube under an atmosphere of argon was charged with fidaxomicin (70.0 mg, 66.2 µmol, 1.0 equiv.). 3-Azidopropyl 4-nitrobenzenesulfonate (23.0 mg, 80.3 µmol, 1.2 equiv.) was added. The flask was evacuated and flushed with argon several times. The two solids were dissolved in dry DMF (1.0 mL) and solid K_2CO_3 (37.0 mg, 0.268 mmol, 4.0 equiv.) was added followed by another portion of dry DMF (1.5 mL). The reaction mixture was stirred at 40 °C. After 2 hours, the reaction temperature was raised to 45 °C. After 4.5 hours, the reaction mixture was diluted with EtOAc (15 mL) and a saturated aqueous solution of NH_4Cl (20 mL) was added. The aqueous phase was extracted with EtOAc (15 mL). The combined organic phases were washed with a

saturated aqueous solution of NH_4Cl (3 x 15 mL) and dried over anhydrous $MgSO_4$. After filtration of the drying agent, the solvent was evaporated under reduced pressure to afford the crude azides **10a** and **10b**.

The dinuclear CuAAC catalyst (9.6 mg, 13.6 µmol) of Straub *et al.*[9] was weighed into an oven-dried Schlenk flask under an atmosphere of argon. The crude mixture from the preceding reaction containing fidaxomicin as well as mono(azidopropyl)- and bis(azidopropyl)fidaxomicin was dissolved in dry CH_2Cl_2 (2.0 mL) and added to the catalyst. Glacial acetic acid (100 %, 11 µL, 0.195 mmol) and 3-ethynylaniline (22 µL, 0.195 mmol; distilled prior to use at 110 °C oil bath temperature and 3 mbar) were dissolved in dry CH_2Cl_2 (0.8 mL) and added to the reaction mixture, which turned bright yellow upon addition of the alkyne solution. After 4 hours, the reaction mixture was diluted with dry CH_2Cl_2 (10 mL), washed with a saturated aqueous solution of NaCl (3 x 10 mL) and dried over anhydrous $MgSO_4$. After filtration of the drying agent, the solvent was removed *in vacuo*. The product mixture was separated by preparative RP-HPLC [Gemini NX C18, 5 µ, 110 Å, 250 mm x 21.2 mm; solvent A: H_2O +0.1 % HCOOH, solvent B: MeCN+0.1 % HCOOH; 20 mL/min; LC time program (min – % B): 5.0 min – 40 %, 36.0 min – 65 %, 39.0 min – 80 %, 39.1 min – 100 %; λ = 270 nm] to give the monotriazole product **11a** (t_R = 22.6–25.8 min, 18.0 mg, 14.5 µmol, 22 % over two steps) and the bistriazole **11b** (t_R = 26.5–28.8 min, 19.0 mg, 12.8 µmol, 19 % over two steps) as well as recovered fidaxomicin starting material (t_R = 31.2 min, 12.1 mg, 11.4 µmol, 17 %) as colourless solids.

11a

Specific Rotation $[\alpha]_D^{25°C}$= −42.1 (β = 0.53 g/100 mL, $CHCl_3$); **FT-IR** $\tilde{\nu}$ (film) 3364, 2976, 2934, 2875, 1734, 1699, 1640, 1591, 1456, 1417, 1387, 1370, 1243, 1200, 1145, 1111, 1067, 1025, 900, 872, 783, 745, 693 cm^{-1}; **^{1}H NMR** (400 MHz, CD_2Cl_2) δ 7.87 (s, 1H), 7.26–7.09 (m, 4H), 6.65 (ddd, *J* = 7.8, 2.4, 1.2 Hz, 1H), 6.58 (ddd, *J* = 15.0, 11.4, 1.6 Hz, 1H), 5.93–5.78 (m, 1H), 5.85 (s, 1H), 5.48 (t, *J* = 8.2 Hz, 1H), 5.06 (t, *J* = 9.6 Hz, 1H), 5.00–4.95 (m, 1H), 4.89 (d, *J* = 10.0 Hz, 1H), 4.73 (t, *J* = 7.0 Hz, 2H), 4.77–4.67 (m, 1H), 4.65 (d, *J* = 1.3 Hz, 1H), 4.63 (d, *J* = 11.5 Hz, 1H), 4.59 (d, *J* = 0.9 Hz, 1H), 4.39 (d, *J* = 11.4 Hz, 1H), 4.12 (t, *J* = 5.7 Hz, 2H), 4.04–3.99 (m, 1H), 3.97 (dd, *J* = 3.4, 1.2 Hz, 1H), 3.71–3.60 (m, 4H), 3.58 (s, 3H), 3.51 (dq, *J* = 9.6, 6.2 Hz, 1H), 3.00 (qd, *J* = 7.3, 1.5 Hz, 2H), 2.78–2.64 (m, 3H), 2.58 (sept, *J* = 7.0 Hz, 1H), 2.56–2.42 (m, 3H), 2.34–2.25 (m, 1H), 1.94–1.84 (m, 1H), 1.89 (s, 3H), 1.79 (d, *J* = 1.2 Hz, 3H), 1.67 (s, 3H), 1.31 (d, *J* = 6.2 Hz, 3H), 1.27–1.19 (m, 1H), 1.21 (t, *J* = 7.4 Hz, 3H), 1.19–1.13 (m, 9H), 1.10 (s, 3H), 1.09 (s, 3H), 0.83 (t, *J* = 7.4 Hz, 3H) ppm; **^{13}C NMR** (126 MHz, CD_2Cl_2) δ 177.6, 169.5, 169.0, 156.0, 155.7, 148.1, 147.7, 144.7, 143.2, 141.8, 137.4, 136.6, 135.2, 134.5, 132.3, 130.3, 129.1, 128.0, 125.5, 123.6, 121.7, 120.9, 116.2, 115.8, 115.2, 113.6, 112.4, 102.0, 95.5, 93.0, 80.7, 79.8, 77.5, 75.3, 73.8, 73.1, 72.3, 72.2, 70.5, 70.3, 69.3, 63.7, 62.2, 47.7, 42.2, 37.3, 34.8, 31.4, 29.0, 28.4, 26.4, 26.3, 19.4, 19.2, 18.9, 18.6, 18.0, 17.4, 15.6, 14.4, 14.0, 11.3 ppm; **HRMS** ESI− (MeOH), calculated for $C_{63}H_{85}Cl_2N_4O_{18}$ $[M-H]^-$: 1255.52414, found: 1255.52560.

11b

Specific Rotation $[\alpha]_D^{29^\circ C}$ = −11.2 (β = 0.10 g/100 mL, MeOH); **FT-IR** $\tilde{\nu}$ (film) 3364, 2976, 2934, 2875, 1734, 1699, 1640, 1591, 1456, 1417, 1387, 1370, 1243, 1200, 1145, 1111, 1067, 1025, 900, 872, 783, 745, 693 cm^{-1}; **^{1}H NMR** (500 MHz, CD_2Cl_2) δ 7.85 (s, 1H), 7.85 (s, 1H), 7.24–7.22 (m, 1H), 7.22–7.21 (m, 1H), 7.21–7.16 (m, 2H), 7.16–7.10 (m, 3H), 6.67–6.62 (m, 2H), 6.61–6.55 (m, 1H), 5.91–5.79 (m, 2H), 5.84 (s, 1H), 5.51–5.45 (m, 1H), 5.00–4.94 (m, 2H), 4.89 (d, *J* = 10.0 Hz, 1H), 4.73–4.68 (m, 3H), 4.64 (d, *J* = 1.2 Hz, 1H), 4.62–4.56 (m, 3H), 4.53 (s, 1H), 4.38 (d, *J* = 11.4 Hz, 1H), 4.23 (s, br, 1H), 4.15–4.06 (m, 3H), 4.03–3.93 (m, 3H), 3.67–3.53 (m, 7H), 3.44–3.38 (m, 1H), 2.86–2.61 (m, 5H), 2.58 (sept, *J* = 6.8 Hz, 1H), 2.54–2.36 (m, 5H), 2.32–2.25 (m, 1H), 1.89 (s, 3H), 1.78 (s, 3H), 1.66 (s, 3H), 1.34 (d, *J* = 6.1 Hz, 3H), 1.33–1.13 (m, 13H), 1.10 (s, 3H), 1.09 (s, 3H), 0.82 (t, *J* = 7.5 Hz, 3H) ppm; **^{13}C NMR** (126 MHz, CD_2Cl_2) δ 177.5, 169.0, 166.5, 153.6, 151.7, 148.14, 148.10, 147.91, 147.88, 144.7, 141.8, 140.0, 137.4, 136.6, 135.1, 134.5, 132.29, 132.27, 130.3, 129.2, 128.1, 127.8, 125.9, 125.6, 123.6, 121.7, 120.9, 120.8, 116.11, 116.09, 115.19, 115.17, 112.42, 112.35, 101.8, 95.5, 93.0, 81.0, 79.7, 77.3, 75.3, 73.8, 73.1, 72.4, 72.3, 72.2, 70.6, 70.5, 70.3, 69.3, 63.6, 62.2, 47.7, 47.6, 42.3, 37.3, 34.7, 31.3, 31.1, 28.9, 28.4, 26.3, 25.7, 19.4, 19.2, 18.9, 18.6, 18.1, 17.4, 15.6, 14.3, 14.0, 11.3 ppm; **HRMS** ESI+ (MeOH), calculated for $C_{74}H_{99}Cl_2N_8O_{18}$ $[M+H]^+$: 1457.64489, found: 1457.64631.

Monotriazole with PEG5-acid (12a)

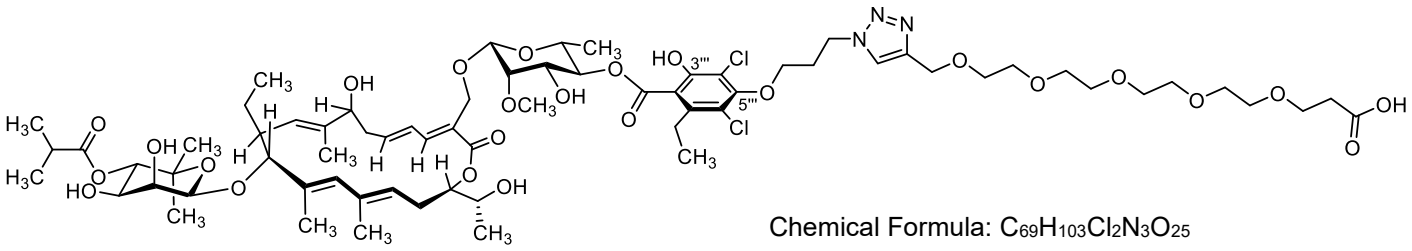

Chemical Formula: $C_{69}H_{103}Cl_2N_3O_{25}$

Exact Mass: 1443.6258

Molecular Weight: 1445.4790

A flame-dried 5 mL flask was charged with a solution of alkyne-PEG5-acid (8.8 mg, 29 µmol, 1.5 equiv.) in a solvent mixture of *t*-BuOH/H_2O (1:1, degassed by freeze-pump-thaw cycling, 1.5 mL). 3-Azidopropylfidaxomicin **10a** (22.0 mg, 19.3 µmol, 1.0 equiv.) as well as solid Cu(I)OAc (2.4 mg, 19 µmol, 1.0 equiv.) were added. The mixture was stirred at room temperature under an atmosphere of argon for 14 hours. It was diluted with CH_2Cl_2 and washed with a saturated aqueous solution of NaCl (3x). The combined organic phases were dried over anhydrous $MgSO_4$. After filtration of the drying agent, the solvent was evaporated under reduced pressure. The product was purified by preparative RP-HPLC (Gemini NX C18, 5 µ, 110 Å, 250 mm x 21.2 mm; solvents: H_2O+0.1 % HCOOH; MeCN+0.1 % HCOOH; 20 mL/min; LC time program (min – % B): 0.0 – 5 %, 10.0 – 5 %, 12.0 – 55 %, 50.0 – 65 %, 51.0 – 100 %; λ = 270 nm; t_R = 20.8 min) to afford **12a** after lyophilization (8.60 mg, 5.950 µmol, 31 %).

Specific Rotation $[\alpha]_D^{26°C}$ = −57.9 (β = 0.25 g/100 mL, MeOH); **FT-IR** (film) $\tilde{\nu}$ = 3441, 2975, 2934, 2875, 1735, 1704, 1642, 1580, 1452, 1417, 1386, 1370, 1349, 1297, 1243, 1199, 1111, 1092, 1071, 1027, 903, 768 cm^{-1}; **^{1}H NMR** (500 MHz, CD_2Cl_2) δ 7.73 (s, 1H), 7.15 (d, *J* = 11.5 Hz, 1H), 6.58 (dd, *J* = 14.8, 11.5 Hz, 1H), 5.94–5.76 (m, 1H), 5.85 (s, 1H), 5.48 (t, *J* = 8.2 Hz, 1H), 5.05 (t, *J* = 9.6 Hz, 1H), 4.98 (d, *J* = 10.6 Hz, 1H), 4.89 (d, *J* = 10.0 Hz, 1H), 4.74–4.54 (m, 7H), 4.39 (d, *J* = 11.5 Hz, 1H), 4.24 (s, br, 1H), 4.09 (t, *J* = 5.7 Hz, 2H), 4.04–3.99 (m, 1H), 3.98–3.95 (m, 1H), 3.73 (t, *J* = 5.9 Hz, 2H), 3.69–3.49 (m, 24H), 3.58 (s, 3H), 2.99 (q, *J* = 7.2 Hz, 2H), 2.78–2.64 (m, 3H), 2.63–2.44 (m, 5H), 2.33–2.25 (m, 1H), 1.99–1.83 (m, 1H), 1.89 (s, 3H), 1.79 (s, 3H), 1.67 (s, 3H), 1.32 (d, *J* = 6.1 Hz, 3H), 1.24–1.14 (m, 1H), 1.21 (t, *J* = 7.4 Hz, 3H), 1.20–1.13 (m, 9H), 1.10 (s, 3H), 1.09 (s, 3H), 0.83 (t, *J* = 7.4 Hz, 3H) ppm; **^{13}C NMR** (126 MHz, CD_2Cl_2) δ 177.5, 173.4, 169.5, 169.0, 155.9, 155.5, 145.3, 144.7, 143.1, 141.8, 137.4, 136.6, 135.2, 134.5, 129.1, 128.1, 125.5, 124.0, 123.5, 121.6, 115.8, 113.7, 101.9, 95.5, 93.0, 80.7, 79.8, 77.4, 75.3, 73.7, 73.1, 72.23, 72.16, 71.1, 71.03, 71.01, 70.90, 70.89, 70.88, 70.6, 70.5, 70.4, 70.3, 70.1, 69.3, 67.1, 64.7, 63.7, 62.2, 47.8, 42.3, 37.3, 34.7, 31.3, 29.0, 28.4, 26.4, 26.3, 19.4, 19.2, 18.8, 18.6, 18.0, 17.3, 15.6, 14.3, 14.0, 11.3 ppm; **^{1}H NMR** (500 MHz, CD_3OD) δ 8.07 (s, 1H), 7.21 (d, *J* = 11.4 Hz, 1H), 6.64–6.54 (m, 1H), 5.95 (ddd, *J* = 14.6, 9.4, 4.8 Hz, 1H), 5.83 (s, 1H), 5.56 (t, *J* = 8.2 Hz, 1H), 5.13 (dt, *J* = 10.5, 1.6 Hz, 1H), 5.05 (t, *J* = 9.8 Hz, 1H), 5.02 (d, *J* = 10.2 Hz, 1H), 4.75–4.69 (m, 4H), 4.66 (s, 2H), 4.63–4.59 (m, 2H), 4.42 (d, *J* = 11.5 Hz, 1H), 4.24–4.20 (br m, 1H), 4.07 (t, *J* = 5.8 Hz, 2H), 4.02 (p, *J* = 6.4 Hz, 1H), 3.92 (dd, *J* = 3.2, 1.1 Hz, 1H), 3.75–3.57 (m, 21H), 3.56 (s, 3H), 3.55 (d, *J* = 3.5 Hz, 1H), 3.53–3.48 (m, 1H), 2.82 (qd, *J* = 7.5, 1.6 Hz, 2H), 2.71 (tt, *J* =

13.9, 5.0 Hz, 3H), 2.59 (sept, *J* = 7.1 Hz, 1H), 2.55–2.39 (m, 6H), 2.03–1.97 (m, 1H), 1.81 (s, 3H), 1.76 (s, 3H), 1.66 (s, 3H), 1.38 (d, *J* = 6.2 Hz, 3H), 1.32–1.23 (m, 1H), 1.20–1.11 (m, 18H), 0.87 (t, *J* = 7.4 Hz, 3H) ppm; **^{13}C NMR** (126 MHz, CD_3OD) δ 178.4, 176.0, 169.1, 168.2, 154.2, 152.3, 146.2, 146.1, 143.7, 140.9, 137.04, 136.97, 136.4, 134.6, 128.5, 126.9, 125.7, 124.6, 121.1, 120.9, 116.0, 102.3, 97.2, 94.3, 82.5, 78.6, 76.9, 75.9, 74.5, 73.5, 73.2, 72.8, 71.6, 71.53, 71.49, 71.4, 71.3, 71.0, 70.7, 70.5, 68.3, 68.1, 65.0, 63.9, 62.2, 48.5, 42.5, 37.3, 36.2, 35.4, 31.8, 28.7, 38.3, 26.9, 26.1, 20.3, 19.5, 19.1, 18.7, 18.0, 17.5, 15.4, 14.6, 13.9, 11.3 ppm; **HRMS** ESI− (MeOH), calculated for $C_{69}H_{102}Cl_2N_3O_{25}$ $[M-H]^-$: 1442.61849, found: 1442.61987.

Monotriazole with Piperidin-4-amine Substituent (13a)

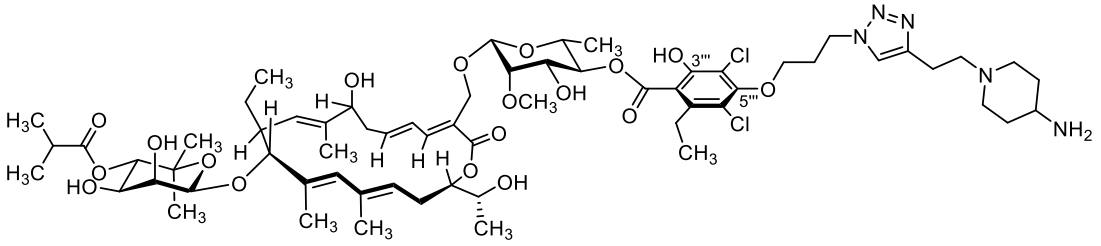

13a

Chemical Formula: $C_{64}H_{95}Cl_2N_5O_{18}$

Exact Mass: 1291.6049

Molecular Weight: 1293.3810

In an oven-dried Schlenk-tube, Cu(I)OAc (1.2 mg, 9.7 µmol, 0.5 equiv.) was added to a solution of fidaxomicin-monoazide **10a** (22.0 mg, 19.3 µmol, 1.0 equiv.) and 1-(but-3-yn-1-yl)piperidine-4-amine dihydrochloride (8.7 mg, 39 µmol, 1.3 equiv.) in *t*-BuOH/H_2O (1:1, 2.0 mL, degassed by freeze-pump-thaw cycling). This mixture was stirred at room temperature for 30 hours under argon atmosphere. The solvent was evaporated under reduced pressure and the obtained solid was dissolved in MeOH/H_2O (7:3) and filtered over an SPE-C18 cartridge. The product was further purified by RP-HPLC [Gemini NX-C18, 5µm, 110 Å, 250 mm x 21.2 mm; solvent A: H_2O+0.1% HCOOH, solvent B: MeCN+0.1% HCOOH; 20 mL/min; LC time program (min – %B): 0.0 – 5 %, 30.0 – 95 %, 31.0 – 100%] to afford, after lyophilization, **12a** (t_R = 17.2 min, 14.2 mg, 11.0 µmol, 57 %) as a colourless solid.

Specific Rotation $[\alpha]_D^{26^\circ C}$ = +84.0 (β = 0.19 g/100 mL, MeOH); **FTIR** (film) $\tilde{\nu}$ = 3378, 2974, 2933, 1708, 1598, 1411, 1381, 1245, 1210, 1115, 1068, 1029, 902 cm^{-1}; **^{1}H NMR** (500 MHz, CD_3OD) δ 7.81 (s, 1H), 7.12 (d, *J* = 11.3 Hz, 1H), 6.54–6.45 (m, 1H), 5.85 (ddd, *J* = 14.7, 9.5, 4.8 Hz, 1H), 5.74 (s, 1H), 5.47 (t, *J* = 8.2 Hz, 1H), 5.03 (d, *J* = 10.6 Hz, 1H), 4.97–4.90 (m, 2H), 4.64–4.58 (m, 4H), 4.52–4.46 (m, 2H), 4.33 (d, *J* = 11.6 Hz, 1H), 4.13 (m, br, 1H), 3.96–3.86 (m, 3H), 3.83 (d, *J* = 3.2 Hz, 1H), 3.65–3.59 (m, 3H), 3.48 (d, *J* = 3.6 Hz, 1H), 3.46 (s, 3H), 3.44–3.38 (m, 1H), 2.92–2.86 (m, 2H), 2.80 (t, *J* = 7.0 Hz, 2H), 2.70–2.54 (m, 6H), 2.50 (quint, *J* = 7.1 Hz, 1H), 2.43–2.29 (m, 4H), 1.91–1.83 (m, 2H), 1.93–1.86 (m, 1H), 1.83–1.75 (m, 2H), 1.72 (s, 3H), 1.67 (s, 3H), 1.56 (s, 3H), 1.55–1.44 (m, 2H), 1.27 (d, *J* = 6.1 Hz, 3H), 1.22–1.12 (m, 1H), 1.10–1.02 (m, 18H), 0.77 (t, *J* = 7.4 Hz, 3H) ppm; **^{13}C NMR** (126 MHz, CD_3OD) δ 178.4, 169.1, 168.5, 154.2, 153.4, 146.7, 146.2, 143.7, 140.5, 137.04, 136.96, 136.4, 134.6, 128.5, 126.9, 125.7, 124.6, 124.1, 120.3, 116.1, 102.2, 97.2, 94.3, 82.3, 78.6, 77.1, 75.9, 74.5, 73.5, 73.2, 73.0, 71.6, 70.9, 70.5, 68.3, 63.9, 62.2, 58.3, 52.3, 49.6, 48.3, 42.5, 37.3, 35.4, 31.7, 30.8, 28.7, 28.3, 26.9, 26.1, 23.9, 20.3, 19.5, 19.1, 18.7, 18.0, 17.5, 15.4, 14.5, 13.9, 11.3 ppm; **HRMS** ESI+ (MeOH), calculated for $C_{64}H_{96}Cl_2N_5O_{18}$ $[M+H]^+$: 1292.61219, found: 1292.61307.

Ditriazole with Piperidin-4-amine Substituent (13b)

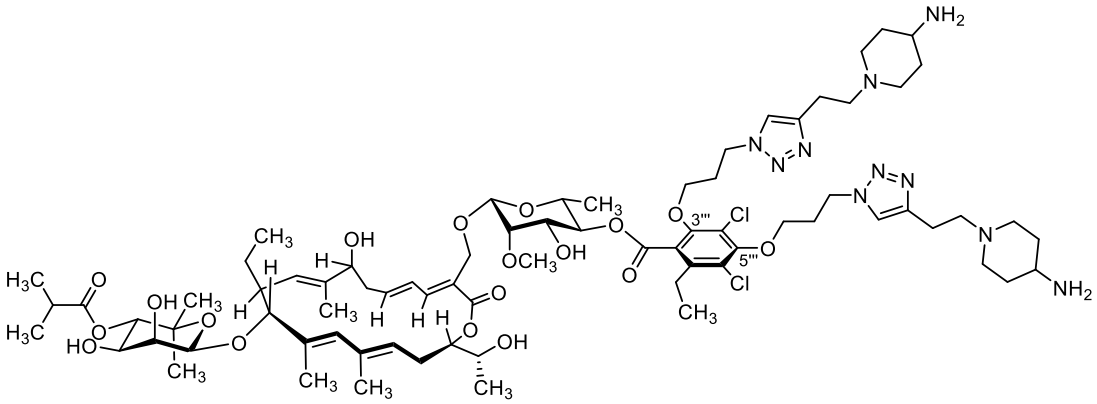

13b

Chemical Formula: $C_{76}H_{116}Cl_2N_{10}O_{18}$

Exact Mass: 1526.7846

Molecular Weight: 1528.7160

An oven-dried Schlenk tube was charged with a solution of bis(3-azidopropyl)fidaxomicin **10b** (15.2 mg, 12.4 µmol, 1.0 equiv.) and 1-(but-3-yn-1-yl)piperidine-4-amine dihydrochloride (7.0 mg, 31 µmol, 2.5 equiv.) in *t*-BuOH/H_2O (1:1, 1.4 mL, degassed by freeze-pump-thaw cycling). Cu(I)OAc (0.5 mg, 3.7 µmol, 0.3 equiv.) was added and the reaction mixture stirred at room temperature for 24 hours under an atmosphere of argon. The solvent was evaporated under reduced pressure and the obtained solid was dissolved in MeOH/H_2O (3:2) and filtered over an SPE-C18 cartridge. The product was purified by preparative RP-HPLC [Gemini NX C18, 5 µ, 110 Å, 250 mm x 21.2 mm; solvent A: H_2O+0.1 % HCOOH, solvent B: MeCN+0.1 % HCOOH; 20 mL/min; LC time program (min – % B): 0.0 – 5 %, 5.0 – 5 %, 30.0 – 95 %, 31.0 – 100 %] to afford, after lyophilization, **13b** as a colourless solid (t_R=15.0 min, 8.2 mg, 5.0 µmol, 43 %).

Specific Rotation $[\alpha]_D^{26°C}$ = +8.6 (β = 0.38 g/100 mL, MeOH); **FT-IR** (film) $\tilde{\nu}$ = 3359, 3143, 2970, 2935, 1733, 1704, 1638, 1591, 1469, 1457, 1434, 1413, 1382, 1372, 1348, 1316, 1249, 1199, 1132, 1112, 1091, 1068, 1028, 902, 793 cm^{-1}; **^{1}H NMR** (500 MHz, CD_3OD) δ 8.57 (s, br, 1H), 7.88 (s, 1H), 7.87 (s, 1H), 7.21 (d, *J* = 11.4 Hz, 1H), 6.62–6.53 (m, 1H), 5.95 (ddd, *J* = 14.5, 9.3, 4.8 Hz, 1H), 5.82 (s, 1H), 5.57 (t, *J* = 8.3 Hz, 1H), 5.13 (d, *J* = 10.5 Hz, 1H), 5.05 (t, *J* = 9.8 Hz, 1H), 5.01 (d, *J* = 10.3 Hz, 1H), 4.74–4.66 (m, 4H), 4.63–4.56 (m, 4H), 4.42 (d, *J* = 11.5 Hz, 1H), 4.24–4.21 (m, br, 1H), 4.17–3.98 (m, 5H), 3.92 (d, *J* = 3.3 Hz, 1H), 3.75–3.66 (m, 3H), 3.56 (s, 3H), 3.54 (d, *J* = 3.5 Hz, 1H), 3.53–3.46 (m, 1H), 3.11–3.02 (m, 6H), 2.96–2.89 (m, 4H), 2.83 (sept, *J* = 6.8 Hz, 2H), 2.76–2.65 (m, 7H), 2.59 (quint, *J* = 7.0 Hz, 1H), 2.52–2.32 (m, 6H), 2.23–2.11 (m, 4H), 1.99 (d, *J* = 12.3 Hz, 5H), 1.81 (s, 3H), 1.75 (s, 3H), 1.65 (s, 3H), 1.70–1.58 (m, 4H), 1.35 (d, *J* = 6.2 Hz, 3H), 1.31–1.22 (m, 1H), 1.20–1.10 (m, 18H), 0.87 (d, *J* =

7.2 Hz, 3H); **^{13}C NMR** (126 MHz, CD_3OD) δ 178.4, 169.1, 167.1, 154.4, 146.8, 146.2, 145.5, 143.8, 140.7, 136.9, 136.4, 134.6, 128.7, 128.4, 126.8, 126.3, 125.6, 124.6, 123.9, 122.3, 102.1, 97.2, 94.3, 82.7, 78.6, 77.3, 75.9, 74.6, 73.5, 73.2, 73.0, 72.8, 71.4, 71.39, 71.35, 70.5, 68.2, 63.9, 62.3, 58.6, 58.5, 52.5, 48.3, 48.2, 42.5, 37.3, 35.4, 31.8, 31.6, 30.7, 28.7, 28.4, 26.9, 26.0, 24.05, 24.01, 20.3, 19.5, 19.1, 18.7, 18.4, 17.5, 15.4, 14.5, 13.9, 11.3 ppm; **HRMS** ESI+ (MeOH), calculated for $C_{76}H_{118}Cl_2N_{10}O_{18}$ $[M+2H]^{2+}$: 764.39959, found: 764.39950.

Bromoacetylciprofloxacin (14)

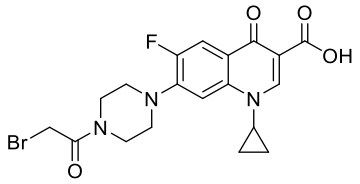

Chemical Formula: $C_{19}H_{19}BrFN_3O_4$
Exact Mass: 451.0543
Molecular Weight: 452.2804

In a flame-dried flask, ciprofloxacin (250 mg, 0.754 mmol, 1.0 equiv.) was dissolved in dry THF (0.5 mL). Dry pyridine (61 µL, 0.75 mmol, 1.0 equiv.) and bromoacetylbromide (65 µL, 0.75 mmol, 1.0 equiv.) were added. The orange mixture was stirred at room temperature for 18 hours. Upon addition of ice to the reaction mixture, the product precipitated. The yellow solid was filtered and washed with H_2O (3x). The filtrate was extracted with CH_2Cl_2 (3x) and dried over anhydrous $MgSO_4$. After filtration of the drying agent, the solvent was evaporated under reduced pressure. The two portions of the crude product, *i.e.* the yellow material obtained by filtration and by extraction with CH_2Cl_2, were combined and purified by flash column chromatography (SiO_2, CH_2Cl_2/MeOH 95:5) to afford bromoacetylciprofloxacin **14** as a yellow solid (186 mg, 0.411 mmol, 55 %).

R_f (CH_2Cl_2/MeOH 95:5) = 0.22; **FT-IR** (film) $\tilde{\nu}$ = 1742, 1731, 1652, 1624, 1533, 1495, 1452, 1380, 1339, 1299, 1272, 1250, 1213, 1140, 1105, 1089, 1051, 1024, 976, 954, 917, 885, 848, 831, 804, 779, 745, 715, 703, 666, 638, 623, 612, 552, 528, 496, 474 cm^{-1}; **^{1}H NMR** (500 MHz, $CDCl_3$) δ 14.86 (s, 1H), 8.80 (s, 1H), 8.09 (d, *J* = 12.8 Hz, 1H), 7.39 (d, *J* = 7.0 Hz, 1H), 3.93 (s, 2H), 3.91–3.87 (m, 2H), 3.72–3.67 (m, 2H), 3.54 (tt, *J* = 7.3, 4.0 Hz, 1H), 3.45–3.40 (m, 2H), 3.35–3.30 (m, 2H), 1.44–1.38 (m, 2H), 1.24–1.20 (m, 2H) ppm; **^{13}C NMR** (126 MHz, $CDCl_3$) δ 177.3 (d, $^4J_{C\text{-}F}$ = 2.6 Hz), 167.0, 165.5, 153.8 (d, $^1J_{C\text{-}F}$ = 251.2 Hz), 147.9, 145.3 (d, $^2J_{C\text{-}F}$ = 10.7 Hz), 139.1, 120.9 (d, $^3J_{C\text{-}F}$ = 8.1 Hz), 113.1 (d, $^2J_{C\text{-}F}$ = 23.3 Hz), 108.6, 105.4 (d, $^3J_{C\text{-}F}$ = 2.7 Hz), 50.1 (d, $^4J_{C\text{-}F}$ = 5.7 Hz), 49.4 (d, $^4J_{C\text{-}F}$ = 3.1 Hz), 46.7, 41.8, 35.5, 25.6, 8.5 ppm; **^{19}F NMR** (376 MHz, $CDCl_3$) δ −121.32 (dd, *J* = 12.7, 7.1 Hz) ppm; **HRMS** ESI+ (MeOH) calculated for $C_{19}H_{20}BrFN_3O_4$ $[M+H]^+$: 452.06157, found: 452.06162.

Fidaxomicin-Ciprofloxacin Hybrid (15)

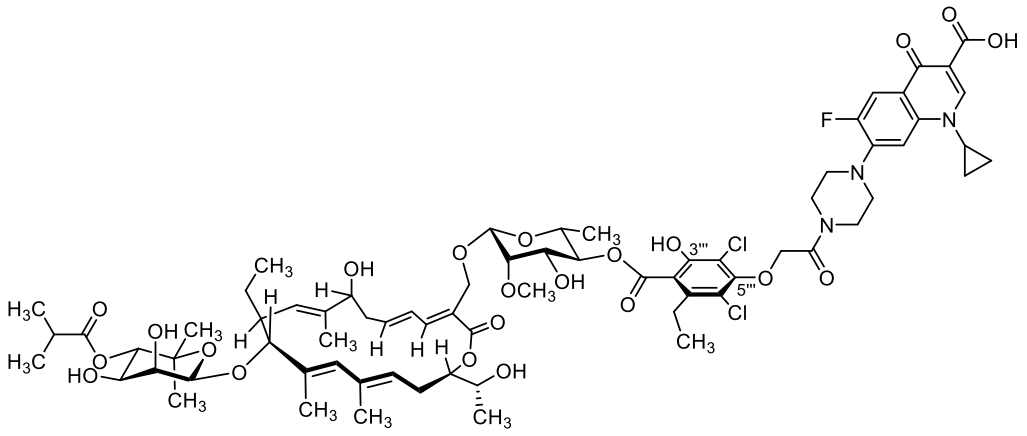

15a

Chemical Formula: $C_{71}H_{92}Cl_2FN_3O_{22}$

Exact Mass: 1427.5534

Molecular Weight: 1429.4144

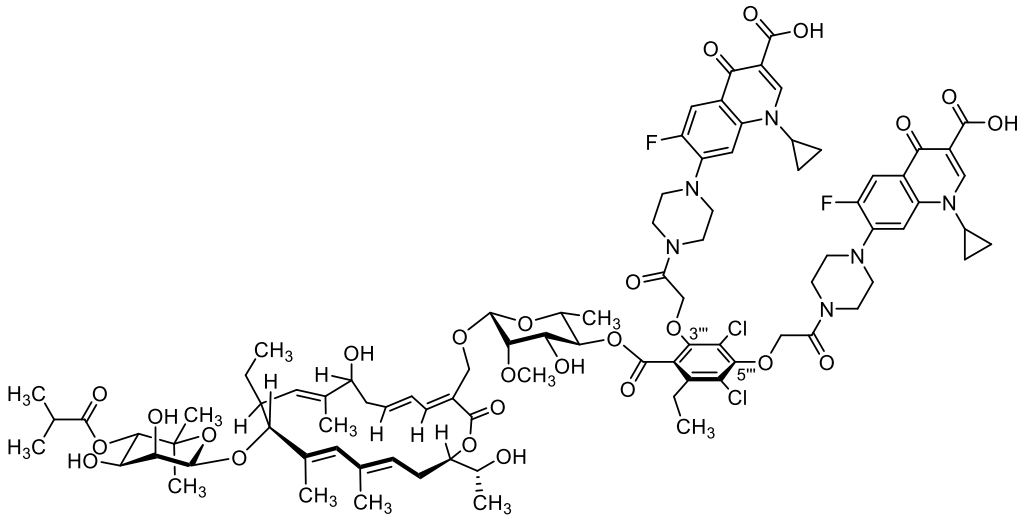

15b

Chemical Formula: $C_{90}H_{110}Cl_2F_2N_6O_{26}$

Exact Mass: 1798.6815

Molecular Weight: 1800.7828

An oven-dried 5 mL flask was charged with fidaxomicin (**1**, 20.0 mg, 18.9 µmol, 1.0 equiv.), K_2CO_3 (10.4 mg, 75.6 µmol, 4.0 equiv.) and bromoacetyl ciprofloxacin (**14**, 11.1 mg, 24.6 µmol, 1.3 equiv.) under an atmosphere of argon. The solids were dissolved in dry DMF (0.8 mL). The milky yellow mixture was stirred at 45 °C for 4 hours. The reaction mixture was filtered over Celite and washed with MeOH/MeCN (1:1). The crude product was purified by RP-HPLC [Gemini NX C18, 5 µ, 110 Å, 250 mm x 21.2 mm, solvent A: H_2O+0.1 % HCOOH, solvent B: MeCN+0.1 % HCOOH; 20 mL/min; LC time program (min – % B): 0.0 min – 5 %, 10.0 min – 5 %, 12 min – 60 %, 60 min – 70 %) to afford the two products as colourless solids after lyophilization (**15a**: t_R = 24.1 min, 10.0 mg, 7.00 µmol, 37 %; **15b**: t_R = 25.6 min, 6.60 mg, 3.67 µmol, 20 %).

15a

Specific Rotation $[\alpha]_D^{23^\circ C}$ = −5.3 (β = 0.19 g/100 mL, MeOH); **FT-IR** (film) $\tilde{\nu}$ = 3433, 2974, 2934, 1725, 1627, 1470, 1385, 1302, 1257, 1213, 1146, 1070, 1029, 896, 745 cm^{-1}; **^{1}H NMR** (500 MHz, acetone-d_6) δ 14.93 (s, 1H), 8.73 (s, 1H), 7.96 (d, *J* = 13.2 Hz, 1H), 7.78 (d, *J* = 7.3 Hz, 1H), 7.23 (d, *J* = 11.3 Hz, 1H), 6.67–6.59 (m, 1H), 5.96 (ddd, *J* = 14.6, 9.5, 4.6 Hz, 1H), 5.83 (s, 1H), 5.62 (t, *J* = 8.3 Hz, 1H), 5.21 (dt, *J* = 10.6, 1.6 Hz, 1H), 5.06 (t, *J* = 9.7 Hz, 1H), 4.99 (d, *J* = 10.1 Hz, 1H), 4.83 (s, 1H), 4.77 (d, *J* = 1.3 Hz, 1H), 4.73 (dt, *J* = 6.5, 5.0 Hz, 1H), 4.66 (d, *J* = 0.8 Hz, 1H), 4.60 (d, *J* = 11.5 Hz, 1H), 4.41 (d, *J* = 11.4 Hz, 1H), 4.27 (s, br, 1H), 4.06–3.97 (m, 3H), 3.95 (d, *J* = 2.7 Hz, 1H), 3.94–3.82 (m, 4H), 3.75 (dd, *J* = 9.9, 3.3 Hz, 1H), 3.78–3.70 (m, 3H), 3.61–3.55 (m, 2H), 3.55–3.49 (m, 2H), 3.52 (s, 3H), 3.49–3.42 (m, 2H), 2.96–2.80 (m, 2H), 2.78–2.60 (m, 3H), 2.56 (sept, *J* = 7.0 Hz, 1H), 2.53–2.40 (m, 2H), 1.99–1.89 (m, 1H), 1.81 (d, *J* = 1.4 Hz, 3H), 1.73–1.72 (m, 3H), 1.65 (dd, *J* = 1.3, 0.6 Hz, 3H), 1.50–1.45 (m, 2H), 1.35–1.31 (m, 5H), 1.21–1.12 (m, 15H), 1.09 (s, 3H), 0.82 (t, *J* = 7.3 Hz, 3H) ppm; **^{13}C NMR** (126 MHz, acetone-d_6) δ 178.0 (d, $^4J_{C\text{-}F}$ = 2.6 Hz), 176.8, 167.8, 167.6, 166.7, 165.8, 154.5 (d, $^1J_{C\text{-}F}$ = 249.2 Hz), 154.3, 153.0, 149.0, 146.3 (d, $^2J_{C\text{-}F}$ = 10.4 Hz), 145.4, 143.4, 141.4, 140.4, 136.9, 136.13, 136.10, 133.8, 128.2, 126.4, 125.3, 124.0, 120.8 (d, $^3J_{C\text{-}F}$ = 7.1 Hz), 118.8, 115.8, 112.2 (d, $^2J_{C\text{-}F}$ = 23.4 Hz), 108.7, 107.6 (d, $^3J_{C\text{-}F}$ = 3.2 Hz), 101.9, 96.8, 93.3, 81.6, 78.2, 77.6, 75.7, 73.8, 72.9, 72.8, 72.4 (two peaks), 70.6, 70.2, 67.7, 63.4, 61.7, 51.1, 50.4, 45.9, 42.2, 42.0, 37.3, 36.6, 34.8, 28.7, 28.4, 26.5, 25.9, 20.7, 19.4, 19.2, 18.6, 18.1, 17.5, 15.2, 14.5, 13.8, 11.2, 8.5 ppm; **HRMS** ESI− (MeOH), calculated for $C_{71}H_{91}Cl_2FN_3O_{22}$ $[M-H]^-$: 1426.54608, found: 1426.54661.

15b

FT-IR (film) $\tilde{\nu}$ = 3456, 2976, 2934, 1728, 1628, 1493, 1467, 1403, 1386, 1336, 1302, 1257, 1113, 1069, 1028, 1007, 889, 834 cm^{-1}; **^{1}H NMR** (500 MHz, acetone-d_6) δ 14.91 (s, 1H), 14.90 (s, 1H), 8.72 (s, 2H), 7.95 (d, *J* = 13.1 Hz, 2H), 7.85–7.68 (m, 2H), 7.22 (d, *J* = 11.4 Hz, 1H), 6.60 (dd, *J* = 14.8, 11.7 Hz, 1H), 5.95 (ddd, *J* = 14.6, 9.6, 4.5 Hz, 1H), 5.81 (s, 1H), 5.61 (t, *J* = 8.0 Hz, 1H), 5.21 (d, *J* = 10.6 Hz, 1H), 5.03 (t, *J* = 9.7 Hz, 1H), 4.99 (d, *J* = 10.2 Hz, 1H), 4.88 (s, 2H), 4.87 (s, 2H), 4.76 (s, 1H), 4.70 (q, *J* = 5.4 Hz, 1H), 4.60 (s, 1H), 4.56 (d, *J* = 11.5 Hz, 1H), 4.38 (d, *J* = 11.5 Hz, 1H), 4.27 (s, br, 1H), 4.11–3.67 (m, 15H), 3.61–3.51 (m, 6H), 3.51 (s, 3H), 3.51–3.41 (m, 4H), 2.91–2.80 (m, 2H), 2.74–2.60 (m, 3H), 2.56 (sept, *J* = 7.0 Hz, 1H), 2.50 (ddd, *J* = 14.7, 10.6, 5.3 Hz, 1H), 2.41 (ddd, *J* = 13.8, 9.2, 4.5 Hz, 1H), 1.96–1.90 (m, 1H), 1.80 (s, 3H), 1.71 (s, 3H), 1.64 (s, 3H), 1.51–1.44 (m, 4H), 1.36–1.30 (m, 4H), 1.34 (d, *J* = 6.2 Hz, 3H), 1.29–1.23 (m, 1H), 1.21–1.11 (m, 12H), 1.19 (t, *J* = 7.3 Hz, 3H), 1.08 (s, 3H), 0.82 (t,

J = 7.4 Hz, 3H) ppm; **^{13}C NMR** (126 MHz, acetone-d_6) δ 177.97–177.91, 176.8, 167.8, 166.70, 166.65, 166.2, 165.9, 165.7, 154.3 (d, $^{1}J_{C\text{-}F}$ = 249.2 Hz), 153.8, 151.7, 149.0, 146.3 (d, $^{2}J_{C\text{-}F}$ = 10.8 Hz), 145.6, 143.6, 140.5, 140.4, 136.8, 136.1, 133.7, 128.6, 128.0, 126.3, 126.2, 125.1, 124.0, 122.0, 120.8 (d, $^{3}J_{C\text{-}F}$ = 7.2 Hz), 112.23 (d, $^{2}J_{C\text{-}F}$ = 23.0 Hz), 112.21 (d, $^{2}J_{C\text{-}F}$ = 23.1 Hz), 108.6, 107.61, 107.56, 101.5, 96.7, 93.2, 81.9, 78.2, 77.9, 75.7, 73.8, 73.2, 72.9, 72.8, 72.5, 72.4, 70.8, 70.1, 67.7, 63.2, 61.7, 51.0, 50.4, 45.9, 45.5, 42.24, 42.16, 42.0, 37.4, 36.62, 36.59, 34.8, 28.7, 28.3, 26.5, 25.7, 20.7, 19.4, 19.2, 18.7, 18.6, 17.5, 15.2, 14.4, 13.8, 11.2, 8.54, 8.50 ppm; **HRMS** ESI+ (MeOH), calculated for $C_{90}H_{112}Cl_2F_2N_6O_{26}$ $[M+2H]^{2+}$: 900.34802, found: 900.34890.

23-Azido-3,6,9,12,15,18,21-heptaoxatricosyl 4-Nitrobenzenesulfonate (16)

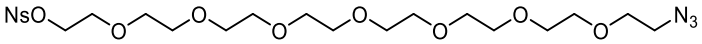

Chemical Formula: $C_{22}H_{36}N_4O_{12}S$
Exact Mass: 580.2050
Molecular Weight: 580.6060

In a flame-dried 10 mL Schlenk tube, *O*-(2-azidoethyl)heptaethylene glycol (215 mg, 0.545 mmol, 1.0 equiv.) was dissolved in dry CH_2Cl_2 (2.0 mL). Et_3N (150 µL, 109 mg, 1.08 mmol, 2.0 equiv.) and DMAP (15.0 mg, 0.122 mmol, 0.23 equiv.) were added and the flask was cooled in an ice bath. Nosyl chloride (241 mg, 1.08 mmol, 2.0 equiv.) in CH_2Cl_2 (1.0 mL) was added by syringe together with another portion of CH_2Cl_2 (1.0 mL). The reaction mixture was stirred at 0 °C for five minutes and then allowed to warm to room temperature. After stirring at room temperature for 22 hours, the reaction mixture was poured on a saturated aqueous solution of NH_4Cl (20 mL) and the phases were separated. The aqueous phase was extracted with CH_2Cl_2 (3 x 15 mL). The combined organic phases were dried over anhydrous $MgSO_4$. After filtration of the drying agent and evaporation of the solvent, the crude product **16** was purified by preparative RP-HPLC [Gemini NX C18, 10 µ, 110 Å, 250 mm x 21.2 mm; solvent A: H_2O+0.1 % HCOOH, solvent B: MeCN+0.1 % HCOOH; 20 mL/min; LC time program (min – % B): 4.0 min – 45 %, 36.0 min – 80 %, 46.0 min – 100 %; λ = 270 nm] to afford the desired product **16** (t_R = 12.2 min, 168 mg, 0.289 mmol, 53 %) after lyophilization.

FT-IR (film) $\tilde{\nu}$ = 2869, 2101 (N_3), 1609, 1531, 1452, 1403, 1350, 1307, 1291, 1250, 1185, 1094, 1034, 1007, 921, 855, 788, 746, 734, 685, 638, 614, 577, 556, 504, 464 cm^{-1}; **^{1}H NMR** (500.30 MHz, $CDCl_3$) δ 8.40 (d, *J* = 8.6 Hz, 2H), 8.14 (d, *J* = 8.6 Hz, 2H), 4.30 (t, *J* = 4.5 Hz, 2H), 3.71 (t, *J* = 4.6 Hz, 2H), 3.69–3.58 (m, 26H), 3.39 (t, *J* = 5.1 Hz, 2H) ppm; **^{13}C NMR** (125.81 MHz, $CDCl_3$) δ =150.9, 142.1, 129.5, 124.5, 70.87, 70.85, 70.81, 70.77, 70.72, 70.70, 70.67, 70.2, 68.7, 50.9 ppm; **HRMS** ESI+ (MeOH) calculated for $C_{22}H_{40}N_5O_{12}S$ $[M+NH_4]^+$: 598.23887, found: 598.23907.

Fiadxomicin-OEG-Azide (17)

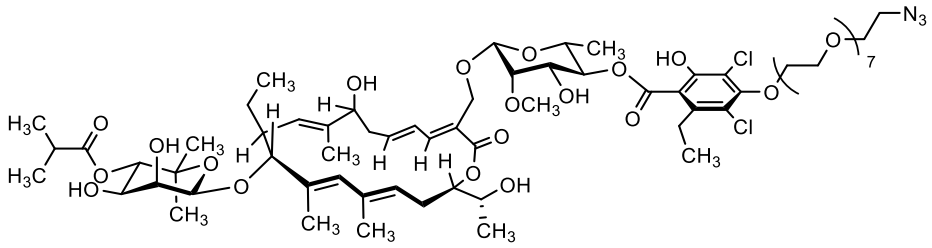

Chemical Formula: $C_{68}H_{105}Cl_2N_3O_{25}$

Exact Mass: 1433.6414

Molecular Weight: 1435.4840

A flame-dried Schlenk tube under an atmosphere of argon was charged with fidaxomicin (**1**, 84.0 mg, 79.4 µmol, 1.0 equiv.) and a solution of 23-azido-3,6,9,12,15,18,21-heptaoxatricosyl 4-nitrobenzenesulfonate (**16**, 68.6 mg, 0.118 mmol, 1.5 equiv.) in dry DMF (1 mL) was added by microliter syringe. K_2CO_3 (44.5 mg, 0.322 mmol, 4.1 equiv.) was added and washed down with dry DMF (1.0 mL). The reaction mixture was stirred for 21.75 hours at 45 °C. The reaction mixture was diluted with EtOAc (15 mL) and quenched with a saturated aqueous solution of NH_4Cl (15 mL). The layers were separated and the aqueous phase extracted with EtOAc (2 x 15 mL). The combined organic phases were dried over anhydrous $MgSO_4$. After filtration of the drying agent, the solvent was evaporated under reduced pressure. The crude product was subjected to preparative HPLC [Gemini NX C18, 5 µ, 110 Å, 250 mm x 21.2 mm; solvent A: H_2O+0.1 % HCOOH, solvent B: MeCN+0.1 % HCOOH; 20 mL/min; LC time program (min – % B): 4.0 min – 60 %, 35.0 min – 85 %, 45.1 min – 100 %; λ = 270 nm] to afford the desired product **17** as a red solid after lyophilization (t_R = 17.6 min, 39.9 mg, 0.289 mmol, 35 %).

Specific Rotation $[\alpha]_D^{22°C}$ = −42.9 (β = 0.92 g/100 mL, $CHCl_3$); **FT-IR** (neat) $\tilde{\nu}$ = 3455, 2972, 2932, 2875, 2104 (N_3), 1736, 1702, 1643, 1581, 1455, 1415, 1384, 1369, 1348, 1298, 1244, 1199, 1107, 1094, 1070, 1027, 949, 903, 860, 800, 769, 744 cm^{-1}; **^{1}H NMR** (500 MHz, acetone-d_6) δ 7.23 (d, *J* = 11.4 Hz, 1H), 6.69–6.56 (m, 1H), 5.96 (ddd, *J* = 14.7, 9.5, 4.6 Hz, 1H), 5.83 (s, 1H), 5.63 (t, *J* = 8.2 Hz, 1H), 5.25–5.18 (m, 1H), 5.07 (t, *J* = 9.7 Hz, 1H), 4.99 (d, *J* = 10.1 Hz, 1H), 4.77 (d, *J* = 1.2 Hz, 1H), 4.73 (q, *J* = 5.2 Hz, 1H), 4.67 (d, *J* = 0.8 Hz, 1H), 4.60 (d, *J* = 11.4 Hz, 1H), 4.41 (d, *J* = 11.5 Hz, 1H), 4.27 (s, 1H), 4.26–4.20 (m, 2H), 4.08–3.93 (m, 2H), 3.88 (dd, *J* = 5.6, 4.2 Hz, 2H), 3.82–3.55 (m, 31H), 3.52 (s, 3H), 3.39 (t, *J* = 5.0 Hz, 2H), 3.25 (d, *J* = 9.4 Hz, 1H), 3.03–2.60 (m, 5H), 2.56 (sept, *J* = 7.0 Hz, 1H), 2.53–2.39 (m, 2H), 1.99–1.88 (m, 1H), 1.81 (d, *J* = 1.3 Hz, 3H), 1.73 (s, 3H), 1.66 (d, *J* = 1.2 Hz, 3H), 1.33 (d, *J* = 6.2 Hz, 3H), 1.30–1.24 (m, 1H), 1.24–1.11 (m, 15H), 1.09 (s, 3H), 0.83 (t, *J* = 7.4 Hz, 3H) ppm; **^{13}C NMR** (126 MHz, acetone-d_6) δ 176.8, 168.0, 167.8, 155.1, 153.8, 145.4, 143.4, 141.1, 136.9, 136.12, 136.11, 133.8, 128.2, 126.4, 125.3, 124.0, 118.2, 116.0, 101.8, 96.8, 93.3, 81.6, 78.2, 77.5, 75.7, 73.8, 73.7, 72.9, 72.4, 71.4, 71.32, 71.30, 71.28, 71.26, 71.24, 71.20, 70.9, 70.7, 70.6, 70.1, 67.7, 63.4, 61.7, 51.4, 42.0, 37.3, 34.8, 28.7, 28.4, 26.5, 25.9, 20.7, 19.4, 19.2, 18.6, 18.2, 17.5, 15.6, 15.2, 14.6, 13.8, 11.2 ppm; **HRMS** ESI(+) (MeOH) calculated for $C_{68}H_{113}Cl_2N_5O_{25}$ $[M+2NH_4]^{2+}$: 734.85454, found: 734.85350.

1-Nitrosopiperazine

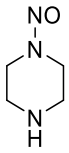

Chemical Formula: $C_4H_9N_3O$

Exact Mass: 115.0746

Molecular Weight: 115.1360

1-Nitrosopiperazine was synthesized following a literature procedure.[10] In a flame-dried 500 mL round-bottom flask piperazine (10.3 g, 120 mmol, 1.0 equiv.) was dissolved in 6 M aqueous HCl (72 mL) and cooled to −10 °C. A solution of $NaNO_2$ (8.26 g, 120 mmol, 1.0 equiv.) in H_2O (144 mL) was added dropwise by dropping funnel over 1 hour. After completion of the addition, the reaction mixture was adjusted to pH = 10 with 3 M NaOH (80 mL) and extracted with $CHCl_3$ (5 x 75 mL). The combined organic phases were dried over anhydrous $MgSO_4$, filtered and concentrated *in vacuo*. After purification by flash column chromatography (SiO_2, CH_2Cl_2/MeOH 92:8), the product (4.05 g, 35.6 mmol, 29 %) was obtained as a yellowish oil.

R_f (CH_2Cl_2/MeOH 92:8) = 0.24; **FT-IR** (neat) $\tilde{\nu}$ = 3315, 2957, 2925, 2828, 1651, 1448, 1418, 1347, 1314, 1279, 1208, 1173, 1137, 1100, 995, 894, 795, 670, 572, 476 cm^{-1}; **^{1}H NMR** (400 MHz, $CDCl_3$) δ 4.26–4.19 (m, 2H), 3.86–3.79 (m, 2H), 3.10–3.04 (m, 2H), 2.86–2.79 (m, 2H) ppm; **^{13}C NMR** (100 MHz, $CDCl_3$) δ 50.8, 46.3, 44.7, 40.6 ppm; **HRMS** ESI(+) (MeOH) calculated for $C_4H_{10}N_3O$ $[M+H]^+$: 116.0818, found: 116.0819.

1-Nitroso-4-propargylpiperazine

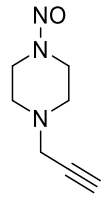

Chemical Formula: $C_7H_{11}N_3O$

Exact Mass: 153.0902

Molecular Weight: 153.1850

1-Nitroso-4-propargylpiperazine was synthesized following a literature procedure.[10] In a flame-dried 50 mL round-bottom flask, 1-nitrosopiperazine (1.53 g, 13.3 mmol, 1.0 equiv.) was dissolved in dry MeCN (36 mL). Propargyl bromide (1.45 mL, 13.3 mmol, 1.0 equiv.) and Et_3N (3.70 mL, 26.6 mmol, 2.0 equiv.) were added and the reaction mixture was heated under reflux conditions. Reaction control after 5 hours by TLC indicated only sluggish conversion. Therefore, another portion of propargyl bromide (400 mg, 2.68 mmol, 0.2 equiv.) was added and the reaction mixture was stirred for 16 hours under reflux conditions. The reaction mixture was concentrated *in vacuo*, dissolved in 10 % aqueous NaOH (100 mL) and extracted with CH_2Cl_2 (3 x 40 mL). The combined organic phases were dried over anhydrous $MgSO_4$, filtered and concentrated *in vacuo*. After purification by flash column chromatography (SiO_2, CH_2Cl_2/MeOH 96:4) the product (1.34 g, 8.74 mmol, 66 %) was obtained as a beige solid.

R_f (CH_2Cl_2/MeOH 96:4) = 0.5; **^{1}H NMR** (400 MHz, $CDCl_3$) δ 4.33–4.28 (m, 2H), 3.91–3.85 (m, 2H), 3.40 (d, *J* = 2.4 Hz, 2H), 2.82–2.76 (m, 2H), 2.57–2.51 (m, 2H), 2.28 (t, *J* = 2.4 Hz, 1H) ppm; **^{13}C NMR** (101 MHz, $CDCl_3$) δ 77.8, 74.1, 52.0, 50.5, 49.6, 46.8, 39.3 ppm; **HRMS** ESI+ (MeOH) calculated for $C_7H_{12}N_3O$ $[M+H]^+$: 154.0974, found: 154.0976.

1-Amino-4-propargylpiperazine

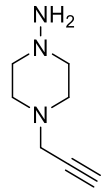

Chemical Formula: $C_7H_{13}N_3$
Exact Mass: 139.1109
Molecular Weight: 139.2020

1-Amino-4-propargylpiperazine was synthesized following a modified literature procedure.[10] In a flame-dried 250 mL round-bottom flask, $LiAlH_4$ (228 mg, 6.01 mmol, 2.0 equiv.) was suspended in dry Et_2O (80 mL) and was stirred vigorously. A solution of 1-nitroso-4-propargylpiperazine (460 mg, 3.00 mmol, 1.0 equiv.) in dry Et_2O (20 mL) was added and the reaction mixture was stirred under reflux conditions for 3 hours. The reaction mixture was cooled to 0 °C and a saturated aqueous solution of sodium potassium tartrate (100 mL) was added slowly. After completion of the addition, the mixture was vigorously stirred for 3 hours, filtered and extracted with CH_2Cl_2 (3 x 100 mL). The combined organic phases were dried over anhydrous $MgSO_4$, filtered and concentrated *in vacuo*. After purification by flash column chromatography (SiO_2, CH_2Cl_2/MeOH 10:1) the product (104 mg, 740 µmol, 25 %) was obtained as an colourless solid.

R_f (CH_2Cl_2/MeOH 10:1) = 0.15; **^{1}H NMR** (400 MHz, $CDCl_3$) δ 3.28 (d, *J* = 2.5 Hz, 2H), 2.82–2.49 (m, 8 H), 2.24 (t, *J* = 2.4 Hz, 1H) ppm; **^{13}C NMR** (101 MHz, $CDCl_3$) δ = 78.7, 73.4, 59.3, 51.7, 46.5 ppm; **^{1}H NMR** (500 MHz, CD_3OD) δ 3.35 (d, *J* = 2.5 Hz, 2H, overlain by solvent signal), 3.00–2.40 (m, br, 8H), 2.73 (t, *J* = 2.5 Hz, 1H) ppm; **^{13}C NMR** (126 MHz, CD_3OD) δ = 79.0, 75.2, 58.7, 52.2 ppm; **HRMS** ESI(+) (MeOH) calculated for $C_7H_{14}N_3$ $[M+H]^+$: 140.1182, found: 140.1182.

Alkinylated Rifampicin (18)

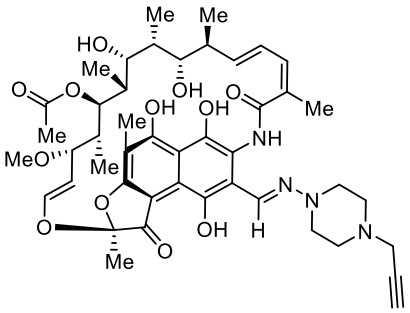

Chemical Formula: $C_{45}H_{58}N_4O_{12}$

Exact Mass: 846.4051

Molecular Weight: 846.9750

Alkinylated rifampicin was synthesized following a literature procedure.[10] In a flame-dried 5 mL Schlenk tube, 3-formylrifamycin SV (100 mg, 0.138 mmol, 1.0 equiv.) was dissolved in dry THF (2 mL) and 1-amino-4-propargylpiperazine (21.1 mg, 0.152 mmol, 1.1 equiv.) was added. Additional dry THF (2.0 mL) was added to the reaction mixture and it was stirred at room temperature for 15 minutes. The reaction mixture was diluted with CH_2Cl_2 (10 mL), washed with a saturated aqueous solution of NaCl (2 x 10 mL) and the combined organic phases were dried over anhydrous $MgSO_4$. After filtration of the drying agent and evaporation of the solvent, the product **18** (106 mg, 0.125 mmol, 91 %, containing slight impurities) was obtained as a bright red solid.

UV/VIS (MeCN, c = 2.5 x 10^{-5} mol L^{-1}, d = 1 cm) λ_{max} [nm] (log ε [L mol^{-1} cm^{-1}]) = 478 (4.20), 338 (4.44), 238 (4.58), λ_{min} [nm] (log ε [L mol^{-1} cm^{-1}]) = 396 (3.40), 292 (4.17), 214 (4.43); **FT-IR** (film) $\tilde{\nu}$ = 3476, 3302, 2973, 2939, 2884, 2829, 2106, 1715, 1646, 1565, 1522, 1452, 1420, 1374, 1330, 1283, 1249, 1216, 1182, 1146, 1083, 1049, 1021, 1001, 972, 945, 898, 853, 803, 755, 735, 665, 524 cm^{-1}; **^{1}H NMR** (400 MHz, $CDCl_3$) δ 13.52 (s, br, 1H), 13.24 (s, 1H), 13.21 (s, 1H), 12.02 (s, br, 1H), 8.29 (s, 1H), 6.63–6.52 (m, 1H), 6.39 (d, *J* = 11.0 Hz, 1H), 6.21 (d, *J* = 12.7 Hz, 1H), 5.94 (dd, *J* = 15.5 Hz, 5.0 Hz, 1H), 5.11 (dd, *J* = 12.6 Hz, 6.7 Hz, 1H), 4.94 (d, *J* = 10.5 Hz, 1H), 3.80–3.72 (m, 1H), 3.60 (d, *J* = 5.0 Hz, 1H), 3.48 (d, *J* = 6.8 Hz, 1H), 3.44 (s, 1H), 3.37 (d, *J* = 2.4 Hz, 2H), 3.25–3.15 (m, 2H), 3.14–3.06 (m, 2H), 3.04 (s, 3H), 3.04–2.99 (m, 1H), 2.80–2.65 (m, 4H, 2.43–2.32 (m, 1 H), 2.28 (t, *J* = 2.3 Hz, 1H), 2.23 (s, 3H), 2.08 (s, 3H), 2.06 (s, 3H), 1.80 (s, 3H), 1.76–1.66 (m, 1H), 1.61–1.50 (m, 1H, 1.41–1.31 (m, 1H), 1.02 (d, *J* = 7.0 Hz, 3H), 0.89 (d, *J* = 7.0 Hz, 3H), 0.60 (d, *J* = 6.8 Hz, 3H), −0.30 (d, *J* = 6.9 Hz, 3H); **^{13}C NMR** (126 MHz, $CDCl_3$) δ 195.7, 174.7, 172.3, 169.8, 169.4, 148.2, 142.94, 142.88, 138.7, 135.3, 134.7, 129.5, 123.3, 120.7, 118.8, 118.1, 113.1, 111.0, 109.0, 106.3, 104.8, 78.2, 77.0, 76.9, 74.6, 73.8, 70.7, 57.2, 50.7, 50.4, 46.8, 39.7, 38.7, 37.6, 33.5, 21.6, 20.9, 18.1, 11.0, 9.1, 8.6, 7.7 ppm; **HRMS** ESI+ (MeOH) calculated for $C_{45}H_{59}N_4O_{12}$ $[M+H]^+$: 847.41240, found: 847.41231.

Fidaxomicin-Rifampicin Hybrid (19)

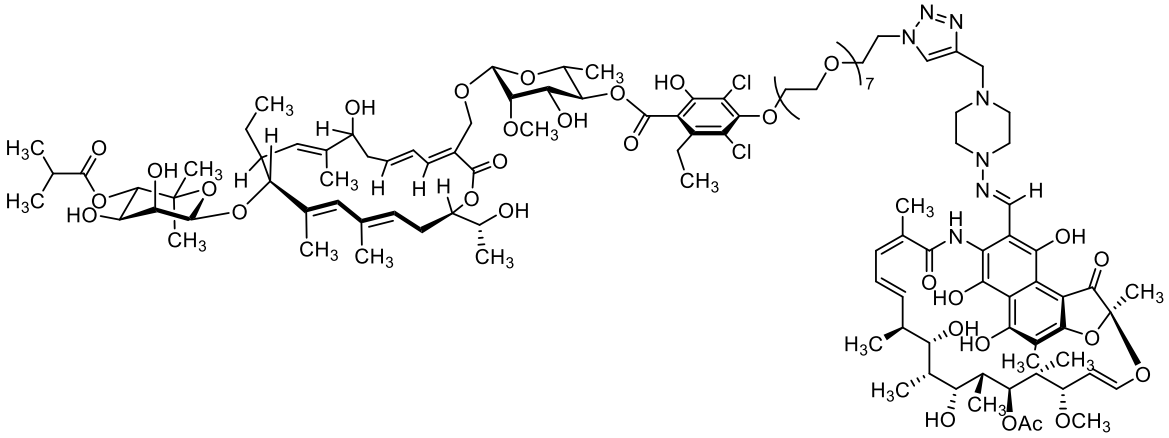

Chemical Formula: $C_{113}H_{163}Cl_2N_7O_{37}$

Exact Mass: 2280.0465

Molecular Weight: 2282.4590

A 10 mL flask containing fidaxomicin-OEG-azide (**16**, 20.9 mg, 14.6 µmol, 1.0 equiv.) was charged with rifampicin alkyne (**17**, 14.8 mg, 17.5 µmol, 1.2 equiv.) and the flask was evacuated and flushed with argon several times. The solids were dissolved in dry CH_2Cl_2 (0.7 mL). The CuAAC dicopper catalyst of Straub *et al*.[9] was added as a solid (2.4 mg, 3.4 µmol, 0.23 equiv.) and washed down with another portion of dry CH_2Cl_2 (0.1 mL). After 2.5 hours, another portion of dicopper catalyst (3.4 mg, 4.8 µmol, 0.33 equiv.) was added. After 3 hours, the reaction mixture was diluted with CH_2Cl_2 (5.0 mL) and poured on a saturated aqueous solution of NH_4Cl (5.0 mL). The phases were separated and the aqueous phase was extracted with CH_2Cl_2 (3 x 5.0 mL). The combined organic phases were dried over anhydrous $MgSO_4$. After filtration of the drying agent and evaporation of the solvent, the crude product was purified by preparative RP-HPLC [*Phenomenex Synergi Hydro-RP*, 10 µ, 80 Å, 250 mm x 21.2 mm, solvent A: H_2O+0.1 % HCOOH, solvent B: MeCN+0.1 % HCOOH; 20 mL/min; LC time program (min – % B): 0.0 min – 55 %, 4.00 – 55 %, 44.0 min – 70 %, 50.0 min – 85 %, 50.1 min – 100 %) to yield the bright red solid product **18** after lyophilisation (8.6 mg, 3.8 µmol, 26 %).

UV/VIS (MeCN, c = 1.8 x 10^{-5} mol L^{-1}, d = 1 cm) λ_{max} [nm] (log ε [L mol^{-1} cm^{-1}]) = 478 (4.26), 340 (4.52), 234 (4.95), λ_{min} [nm] (log ε [L mol^{-1} cm^{-1}]) = 398 (3.55), 306 (4.29); **FT-IR** (film) $\tilde{\nu}$ = 3448, 2975, 2933, 2878, 1731, 1707, 1643, 1565, 1453, 1415, 1375, 1330, 1295, 1242, 1141, 1087, 1056, 1024, 997, 947, 900, 844, 801, 770, 724 cm^{-1}; **^{1}H NMR** (500 MHz, acetone-d_6) δ 13.30 (s, br), 12.14 (s), 8.26 (s, 1H), 7.92 (s, 1H), 7.23 (d, *J* = 11.5 Hz, 1H), 6.72–6.46 (m, 3H), 6.31 (dd, *J* = 12.8, 1.0 Hz, 1H), 6.05–5.91 (m, 2H), 5.82 (s, 1H), 5.62 (t, *J* = 8.3 Hz, 1H), 5.21 (dt, *J* = 10.4, 1.6 Hz, 1H), 5.14–5.02 (m, 3H), 4.99 (d, *J* = 10.1 Hz, 1H), 4.79–4.75 (m, 1H), 4.73 (m, 1H), 4.66 (s, 1H), 4.60 (d, *J* = 11.4 Hz, 1H), 4.57 (t, *J* = 5.1 Hz, 2H), 4.41 (d, *J* = 11.5 Hz, 1H), 4.32–4.24 (m, 2H), 4.23 (t, *J* = 4.9 Hz, 2H),

4.08–3.98 (m, 2H), 3.98–3.93 (m, 2H), 3.91 (t, *J* = 5.1 Hz, 2H), 3.88 (t, *J* = 4.8 Hz, 2H), 3.88–3.84 (m, 1H), 3.76 (dd, *J* = 9.9, 3.3 Hz, 2H), 3.74–3.64 (m, 7H), 3.64–3.54 (m, 27H), 3.52 (s, 3H), 3.47 (d, *J* = 7.8 Hz, 1H), 3.24–3.18 (m, 2H), 3.16–3.09 (m, 2H), 2.98 (s, 3H), 2.95–2.60 (m, 19H), 2.56 (sept, *J* = 7.0 Hz, 1H), 2.53–2.48 (m, 1H), 2.44 (ddt, *J* = 18.7, 9.2, 4.5 Hz, 1H), 2.36–2.29 (m, 1H), 2.19 (s, 3H), 2.08 (s, 3H), 2.01 (s, 3H), 1.99 (d, *J* = 3.3 Hz, 2H), 1.80 (d, *J* = 1.3 Hz, 3H), 1.77 (s, 3H), 1.75–1.68 (m, 4H), 1.65 (d, *J* = 1.3 Hz, 3H), 1.53–1.44 (m, 1H), 1.33 (d, *J* = 6.1 Hz, 3H), 1.30–1.12 (m, 19H), 1.09 (s, 3H), 0.99 (d, *J* = 7.0 Hz, 3H), 0.93 (d, *J* = 7.1 Hz, 3H), 0.82 (t, *J* = 7.4 Hz, 3H), 0.63 (d, *J* = 7.0 Hz, 3H), -0.32 (d, *J* = 6.8 Hz, 3H) ppm; **^{13}C NMR** (151 MHz, acetone-d_6) δ 176.8, 175.0, 171.1, 170.7, 167.81, 167.77, 162.3, 155.1, 153.0, 148.5, 145.4, 144.3, 144.0, 143.4, 141.2, 136.9, 136.1, 135.8, 134.2, 133.8, 128.1, 126.3, 125.3, 124.9, 124.3, 124.0, 121.1, 120.6, 118.6, 118.2, 115.9, 113.4, 110.9, 110.1, 101.8, 96.7, 93.3, 81.6, 78.2, 77.53, 77.45, 77.40, 77.3, 75.7, 74.6, 73.8, 73.7, 72.9, 72.8, 72.4, 71.7, 71.4, 71.29, 71.29, 71.26, 71.24, 71.23, 71.21, 71.17, 71.06, 70.9, 70.6, 70.2, 70.1, 67.7, 63.4, 61.7, 56.8, 53.5, 52.2, 51.1, 50.7, 42.0, 41.2, 40.0, 39.0, 37.3, 34.8, 34.2, 28.7, 28.3, 26.5, 25.9, 22.0, 20.8, 20.72, 20.69, 19.4, 19.2, 18.6, 18.3, 18.2, 17.5, 15.2, 14.5, 13.8, 11.2, 9.5, 9.2, 7.7 ppm; **HRMS** ESI(+) (MeOH) calculated for $C_{113}H_{168}Cl_2N_8O_{37}$ $[M+NH_4+H]^{2+}$: 1149.54382, found: 1149.54424.

Homology Modeling, Molecular Docking, and Molecular Modeling

We used our in-house homology modeling suite TopModel[11–13] to build homology models of the *M. tuberculosis* RNA polymerases (RNAPs), based on the templates of RpoB from *T. thermophilus* (PDB ID: 1IW7) and RNAP from *E. coli* (PDB ID: 4KN7). We selected the ten best RNAP models of each organism with the highest differences in binding pocket RMSD for subsequent docking.

The structure of Fidaxomicin was built and energetically relaxed with Maestro[14] and subsequently docked into the respective ten homology models of the RNAPs using AutoDock3[15] as a docking engine with DrugScore potentials[16] for scoring as described in the given reference.[17] For defining the docking box, the fidaxomicin binding pocket as suggested in literature.[18] was used and extended by up to 16 Å. The final binding mode model was chosen as the one with a low docking energy from the largest cluster of structurally similar binding modes, as previously described.[19–21] Additionally, the number of addressed residues, known to lead to Fidaxomicin resistance when mutated, was taken into account. As the binding mode in model 10 from the *E. coli* template (docking energy -19.9 kcal mol^{-1}; 25% of all poses in the largest cluster) addressed the most relevant residues in RNAP, this binding mode was finally used to guide further syntheses.

To generate the Fidaxomicin-Rifampicin hybrid, we structurally aligned the X-ray crystal structure of Rifampicin-bound RNAP (PDB ID: 4KMU[22]) to our model 10 and modeled a linker between the predicted binding mode of Fidaxomicin and Rifampicin (Figure S1), applying preferred *gauche* conformations[23] for the torsions along the polyethylene glycol chain and taking into account an additional 1,2,3-triazol-4-yl-piperidyl linker.

The interaction diagram of Fidaxomicin was generated using PoseView[24,25] and modified manually to also include residues putatively interacting in a water-mediated manner.

Supporting Figures and Tables

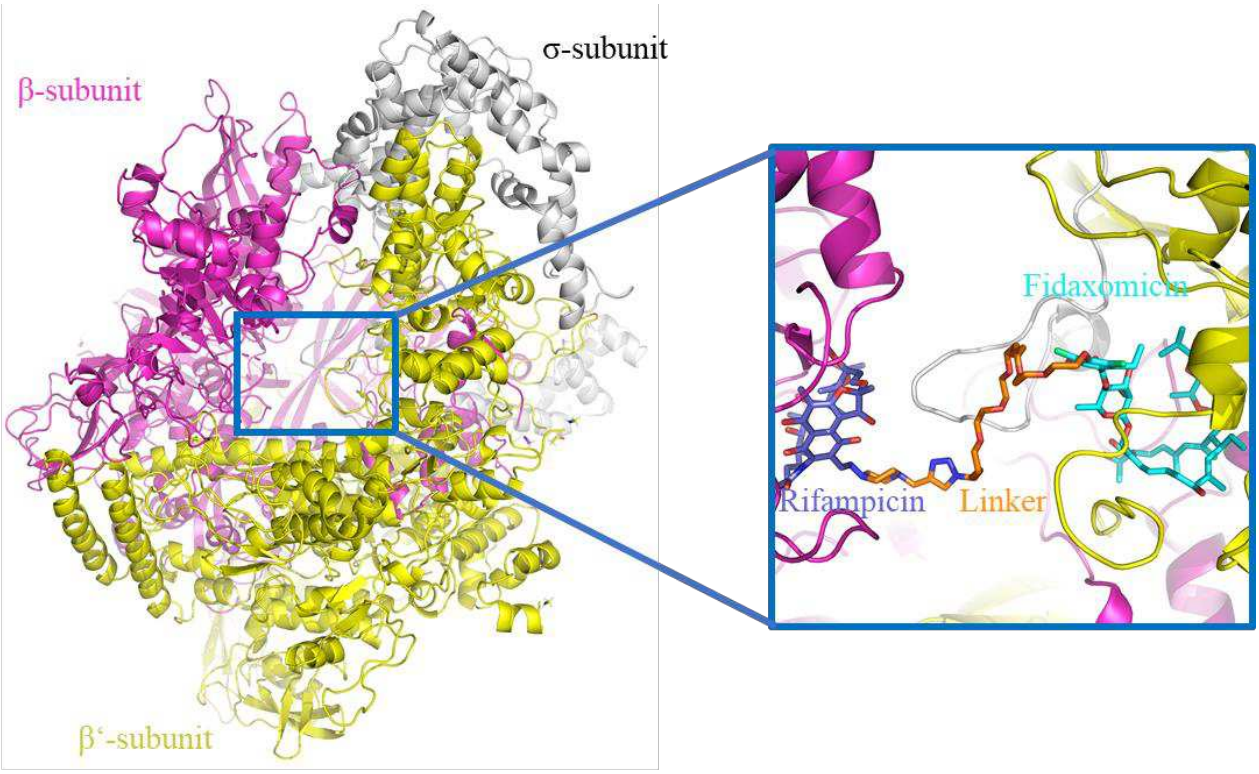

Figure S1. Binding mode prediction of the fidaxomicin(cyan)-rifampicin(navy)-hybrid in the homology model of *M. tuberculosis* RNAP (cartoon; white: σ-subunit; yellow: β'-subunit, magenta: β-subunit). Left: Overview of the RNAP is shown with the blue rectangle indicating the location of the zoomed-in (right) predicted binding region of the hybrid. The hybrid contains a predicted chain (orange) of polyethylene glycol with torsions in *gauche* conformation and a 1,2,3-triazol-4-yl-piperidyl linker. The position and orientation of rifampicin was determined by aligning a rifampicin-bound RNAP crystal structure (PDB ID: 4KMU[22]) onto our homology model.

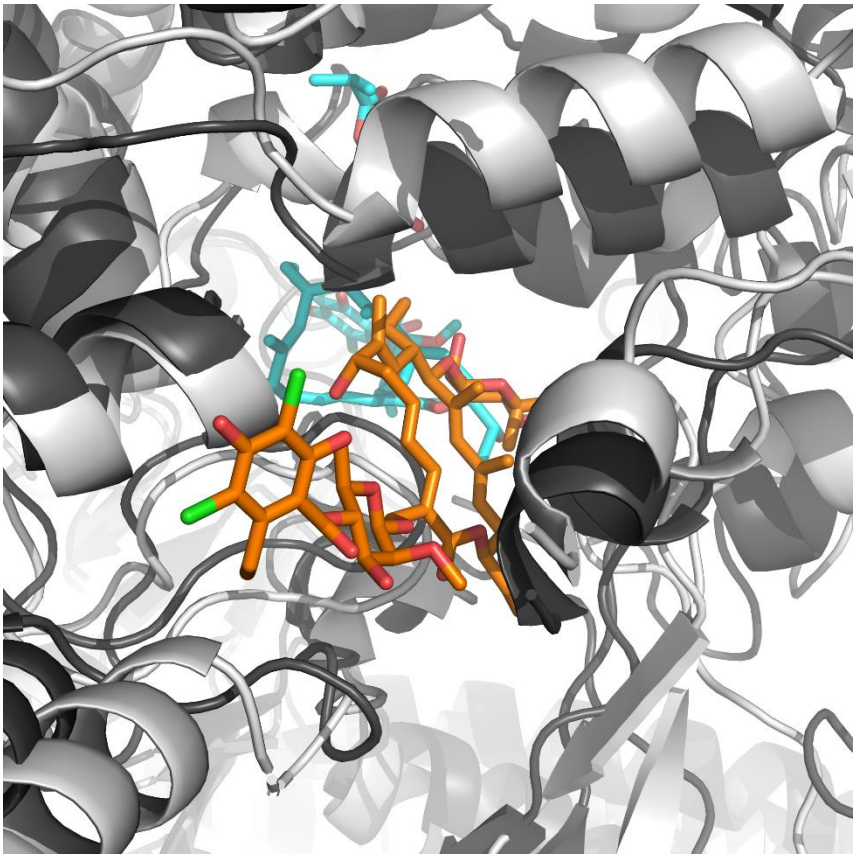

Figure S2. Comparison of the binding mode of Fidaxomicin in the structure of *M. tuberculosis* RNAP determined by cryo-EM (gray protein, orange ligand, PDB ID 6FBV[26]) or predicted by docking in a homology model (dark gray protein, blue ligand). In both binding modes, the binding sites of Fidaxomicin's macrocycle overlap, although the molecule's orientations differ. In the homology model, the binding site is narrower due to differently predicted loop conformations.

General Procedure for Determination of Aqueous Solubility by UHPLC Analysis

Determination of Aqueous Solubility

Calibration with Methanol Solutions

A standard stock solution of each analyte in MeOH at a concentration of 1.0 mg/mL was prepared. All analytes were completely soluble in MeOH. A standard stock solution of caffeine for use as internal standard (IS) in MeOH was prepared at a concentration of 1.0 mg/mL as well. These stock solutions were further diluted with MeOH to calibration standard samples at concentrations of 50, 100, 200, 300, 400, 500 µg/mL of analyte with each sample containing 50 µg/mL of caffeine as IS. These samples were analyzed by UHPLC [*Kinetex*® EVO C18; 1.7 µm; 100 Å, 50 mm x 2.1 mm; *Phenomenex*; solvent A: H_2O + 0.1 % HCOOH, solvent B: MeCN + 0.1 % HCOOH; 0.4 mL/min; 1.0 µL injection volume, LC time program (min – % B): 0.50 min – 5 %, 3.50 min – 95 %, 3.55 min – 100 %]. The peak area of the analyte signal was divided by the peak area of the IS. This peak ratio was plotted against the analyte's concentration to obtain a linear equation.

Determination of Aqueous Solubility

For reproducibility reasons, water solubility of the fidaxomicin derivatives was quantified in a pH = 7 phosphate buffered aqueous solution (Acros, CAS 7558-79-4). A stock solution of caffeine in phosphate buffer at a concentration of 1.0 mg/mL was prepared and diluted to a concentration of 50 µg/mL. To 1.0 mL of this caffeine solution, the analyte was added as a solid until a saturated solution was obtained. This solution was stirred for 5 hours at room temperature. The mixture was filtered over a 0.22 µm syringe filter and the obtained solution was analyzed by UHPLC. The concentration was then calculated from the linear equation obtained from the calibration. With most samples of fidaxomicin derivatives, two peaks for the analyte were detected, namely one for the original substance and one for its regioisomer formed (isobutyl ester migration to adjacent hydroxyl group). Depending on whether peak areas were added or the isomer peak was ignored, the calculated values for aqueous solubility differed from each other.

Antimicrobial Susceptibility Testing

General procedure for the determination of MIC values of *B. subtilis* and *S. aureus*

Organism	**Strain**
Bacillus subtilis	DSM3256
Staphylococcus aureus	ATCC29213

The strains of *Bacillus subtilis* and *Staphylococcus aureus* were grown overnight at 37 °C on MH II agar plates. (BD™ BBL™ Mueller Hinton II Agar, BD Diagnostics). MIC values were determined by broth dilution method according to the recommendations of the Clinical and Laboratory Standards Institute (CSLI; U.S.A.). The inoculum size was about $7.5x10^5$ colony forming units/well. The compounds were diluted in H_2O from 1.0 mg/mL stock solutions in 50 % methanol/H_2O in a 2-fold dilution series. The microtiter plates were incubated at 37 °C overnight. Afterwards, the MIC (lowest concentration of the compounds with no bacterial growth observed) was determined by visual inspection.

General procedure for the determination of MIC values of *M. tuberculosis*

MIC determination was essentially conducted as described recently.[27] Briefly, the Green-Fluorescent Protein (GFP) expressing recombinant *Mycobacterium tuberculosis* H37Rv *rpsL*[28] transformed with pOLYG-Pr-GFP[29] was grown in Middlebrook 7H9-OADC with 0.05 % Tween 80 until mid-log phase (optical density at 600 nm OD_{600} = 0.3 – 1.0), diluted to an OD_{600} of 0.04 and 20 µl of the suspension were added to an equal volume of 12-point two-fold serial dilutions of the compounds in 7H9-OADC-Tween in 384-well plates in triplicates. Compound concentrations were in the range of 62.5 to 0.031 µM. Fluorescence was measured immediately after inoculation (background) and after 10 days of incubation at 37 °C. Dose response curves were fitted with a 4-parameter log-normal model. P_{MIN} [-,-] and P_{MAX} [-, 120] are the minimum and the maximum, respectively, P_{Hill} [0,-] indicates the steepness, and EC_{50} [-,-] the log-back transformed Minimal Effective Concentration 50. The computational and statistical analysis was conducted with R (3.0.1 – 3.1.1; https://www.r-project.org/). Dose response curves were fitted with the ´drc´ package. The inhibitory potency I was calculated with the equation I = 100-[100●(S-P)/N-P)]. S is the sample's fluorescence while P and N derive from growth inhibition with the control drug (Kanamycin A) and solvent growth control measurements (DMSO 1.25 % vol./vol.), respectively. A fluorescence reduction of 90 % as compared to the no-drug control was reported as Minimal Inhibitory Concentration (MIC_{90}).

Table 1 Determined MIC values in [µg/mL]

Compound	*S. aureus*	*B. subtilis*	*M. tuberculosis*
1	8–16	8–16	0.25
2a	32–64	64–>64	4−8
2b	>64	>64	4−8
3a	32–64	>64	4−8
3b	>64	>64	16−32
4a	16	32	2
4b	32–64	8−16	0.5−1
fidaxomicin piperazine with alloc protecting group	16–32	>64	−
fidaxomicin dipiperazine with alloc protecting group	>64	>64	−
5a	>64	>64	1−2
6a	32	64–>64	8
6b	>64	>64	64
7a	>64	>64	16−32
7b	64	64	>64
8a	>64	>64	8−16
8b	>64	>64	2−4
9b	n.d	n.d	n.d
11a	>64	>64	>64
11b	64	>64	>64
12a	>64	>64	16
13a	>64	>64	4−8
13b	>64	8–16	16−32
15a	>64	32–>64	1−2
15b	>64	64	−
19	2−8	2–32	0.5
Rifampicin	0.008	0.25	0.004
Ciprofloxacin	−	−	1

General procedure for the determination of MIC values of *C. difficile*

MIC determination was carried out by Micromyx, LLC, 4717 Campus Drive, Kalamazoo, MI, USA 49008. Approximately 5 mg of each of 20 test compounds were provided. These were stored at -20°C until testing. On the day of the assay, the test articles were dissolved in 100% DMSO (dimethyl sulfoxide, Sigma; St. Louis, MO, Cat. No. 472301-500ML, Lot No. SHBH5551V) to a stock concentration of 3232 µg/mL. The concentration range tested for these test agents was 16 – 0.015 µg/mL. The comparator agents, metronidazole and clindamycin were supplied by Micromyx, as shown in the table below:

Comparator Drug	Supplier	Catalog No.	Lot No.	Solvent/Diluent	Testing Range (µg/mL)
Metronidazole	Sigma	M3761-100G	095K0693	DMSO/$_d$H2O	64 – 0.06
Clindamycin	Sigma	C5269-100MG	021M1533	$_d$H2O/ $_d$H2O	32 – 0.03

Test Organisms

Test organisms consisted of reference strains from the American Type Culture Collection (ATCC; Manassas, VA) and clinical isolates from the Micromyx repository (MMX; Kalamazoo, MI). Organisms were initially received at Micromyx and were streaked for isolation. Colonies were picked by sterile swab from the medium and suspended in the appropriate broth containing cryoprotectant. The suspensions were aliquoted into cryogenic vials and maintained at −80ºC.

Prior to testing, all isolates were streaked onto Brucella Agar supplemented with hemin, Vitamin K and 5% sheep blood (Becton Dickinson [BD]; Sparks, MD, Cat. No. 297716, Lot No. 8256909) and incubated anaerobically at 35-37°C for 44 – 48 hours.

Additionally, *Bacteroides fragilis* ATCC 25285 and *Clostridium difficile* ATCC 700057 were tested for purposes of quality control.

Test Medium

The medium employed for anaerobic testing in the broth microdilution MIC assay was Brucella Broth (BD, Cat. No. 211088, Lot No. 7128995), supplemented with hemin (Sigma, Lot No. SLBP5720V), Vitamin K (Sigma, Lot No. MKCG2075) and 5% laked horse blood (LHB, Cleveland Scientific; Bath, OH, Lot No. 474990).

Broth Microdilution Assay

The MIC assay method followed the procedure described by the CLSI[30,31] and employed automated liquid handlers (Multidrop 384, Labsystems, Helsinki, Finland; Biomek 2000 and Biomek FX, Beckman Coulter, Fullerton CA) to conduct serial dilutions and liquid transfers. The wells in columns 2 through 12 in a standard 96-well microdilution plate (Costar) were filled with 150 µL of the appropriate diluent (DMSO for the test agents; $_d$H2O for metronidazole and clindamycin). The drugs (300 µL at 101X the desired top concentration in the test plates) were dispensed into the appropriate well in column 1 of the mother plates. The Biomek 2000 was used to make serial 2-fold dilutions through column 11 in the “mother plate”. The wells of column 12 contained no drug and were the organism growth control wells.

The daughter plates for testing of all isolates were loaded with 190 µL per well of supplemented Brucella broth with 5% LHB using the Multidrop 384. The daughter plates were prepared on the Biomek FX instrument which transferred 2 µL of 101X drug solution from each well of a mother plate to the corresponding well of each daughter plate in a single step. The wells of the daughter plates ultimately contained 190 µL of medium, 2 µL of drug solution, and 10 µL of bacterial inoculum prepared in broth.

A standardized inoculum of each organism was prepared per CLSI methods.[30,31] For all bacteria, suspensions were prepared in supplemented Brucella broth supplemented with hemin and Vitamin K to equal the turbidity of a 0.5 McFarland standard. These suspensions were further diluted 1:10 in supplemented Brucella broth with 5% LHB. The inoculum was dispensed into sterile reservoirs (Beckman Coulter) and transferred by hand in the Bactron Anaerobe chamber so that inoculation took place from low to high drug concentration. A 10 µL aliquot of inoculum was delivered into each well. Inoculated daughter plates were stacked and placed in an anaerobic box with GasPak sachets (BD; Lot No. 6309689), covered with a lid on the top plate, and incubated at 35 – 37°C.

The microplates were viewed from the bottom using a plate viewer after 46 hours. For each mother plate, an un-inoculated solubility control plate was observed for evidence of drug precipitation. The MIC was read and recorded as the lowest concentration of drug that inhibited visible growth of the organism.

Table 2 Determination of MIC values against C. difficile in µg/mL

Compound	**MIC** in µg/mL									
	C. difficile ATCC 43255	*C. difficile ATCC 700057*	*C. difficile BAA-1805*	*C. difficile* BAA-1875	*C. difficile* ATCC 9689 (rt 001)	*C. difficile* 8260 (rt 017)	*C. difficile* 8282 (rt 017)	*C. difficile* 5680 (rt 027)	*C. difficile* 8264 (rt 027)	*C. difficile* 8290 (rt 078)
Metronidazole	0.25	0.25	1	0.25	0.25	0.12	0.25	0.5	2	0.25
Clindamycin	1	2	4	8	1	>32	>32	4	4	4
1	0.03	0.03	0.12	0.03	≤0.015	0.06	0.03	0.06	0.12	0.03
4a	>16	8	>16	8	2	16	8	>16	>16	16
4b	>16	16	>16	16	4	16	16	>16	>16	16
5a	0.5	0.25	0.5	0.5	0.03	0.03	0.06	0.5	0.5	0.25
9b	0.12	0.06	0.25	0.25	0.03	0.12	0.06	0.5	0.25	0.12
13a	4	2	8	2	0.5	4	1	8	8	4
13b	>16	>16	>16	>16	>16	>16	>16	>16	>16	>16
15a	0.03	0.06	0.12	0.06	≤0.015	0.03	0.03	0.12	0.12	0.12
15b	>16	>16	>16	>16	>16	>16	>16	>16	>16	>16
19	≤0.015	≤0.015	≤0.015	≤0.015	≤0.015	≤0.015	4	≤0.015	0.03	0.03
Rifampicin	≤0.015	≤0.015	≤0.015	≤0.015	≤0.015	>16	>16	≤0.015	≤0.015	≤0.015
Ciprofloxacin	>16	>16	>16	>16	16	>16	>16	>16	>16	>16

References

(1) Fulmer, G. R.; Miller, A. J. M.; Sherden, N. H.; Gottlieb, H. E.; Nudelman, A.; Stoltz, B. M.; Bercaw, J. E.; Goldberg, K. I. NMR Chemical Shifts of Trace Impurities: Common Laboratory Solvents, Organics, and Gases in Deuterated Solvents Relevant to the Organometallic Chemist. *Organometallics* **2010**, *29* (9), 2176–2179.

(2) An, H.; Wang, T.; Mohan, V.; Griffey, R. H.; Dan Cook, P. Solution Phase Combinatorial Chemistry. Discovery of 13- and 15-Membered Polyazapyridinocyclophane Libraries with Antibacterial Activity. *Tetrahedron* **1998**, *54* (16), 3999–4012.

(3) Smeenk, L. E. J.; Dailly, N.; Hiemstra, H.; Van Maarseveen, J. H.; Timmerman, P. Synthesis of Water-Soluble Scaffolds for Peptide Cyclization, Labeling, and Ligation. *Org. Lett.* **2012**, *14* (5), 1194–1197.

(4) Gobbo, P.; Gunawardene, P.; Luo, W.; Workentin, M. S. Synthesis of a Toolbox of Clickable Rhodamine B Derivatives. *Synlett* **2015**, *26* (9), 1169–1174.

(5) Brullo, C.; Massa, M.; Rocca, M.; Rotolo, C.; Guariento, S.; Rivera, D.; Ricciarelli, R.; Fedele, E.; Fossa, P.; Bruno, O. Synthesis, Biological Evaluation, and Molecular Modeling of New 3-(Cyclopentyloxy)-4-Methoxybenzaldehyde O-(2-(2,6-Dimethylmorpholino)-2- Oxoethyl) Oxime (GEBR-7b) Related Phosphodiesterase 4D (PDE4D) Inhibitors. *J. Med. Chem.* **2014**, *57* (16), 7061–7072.

(6) Schnell, S. D.; Hoff, L. V.; Panchagnula, A.; Wurzenberger, M. H. H.; Klapötke, T. M.; Sieber, S.; Linden, A.; Gademann, K. 3-Bromotetrazine: Labelling of Macromolecules via Monosubstituted Bifunctional s-Tetrazines. *Chem. Sci.* **2020**, *11* (11), 3042–3047.

(7) Gann, A. W.; Amoroso, J. W.; Einck, V. J.; Rice, W. P.; Chambers, J. J.; Schnarr, N. A. A Photoinduced, Benzyne Click Reaction. *Org. Lett.* **2014**, *16* (7), 2003–2005.

(8) Bucher, J.; Wurm, T.; Nalivela, K. S.; Rudolph, M.; Rominger, F.; Hashmi, A. S. K. Cyclization of Gold Acetylides: Synthesis of Vinyl Sulfonates via Gold Vinylidene Complexes. *Angew. Chem. Int. Ed.* **2014**, *53* (15), 3854–3858.

(9) Berg, R.; Straub, J.; Schreiner, E.; Mader, S.; Rominger, F.; Straub, B. F. Highly Active Dinuclear Copper Catalysts for Homogeneous Azide-Alkyne Cycloadditions. *Adv. Synth. Catal.* **2012**, *354* (18), 3445–3450.

(10) Cochrane, S. A.; Li, X.; He, S.; Yu, M.; Wu, M.; Vederas, J. C. Synthesis of Tridecaptin-Antibiotic Conjugates with in Vivo Activity against Gram-Negative Bacteria. *J. Med. Chem.* **2015**, *58* (24), 9779–9785.

(11) Widderich, N.; Pittelkow, M.; Höppner, A.; Mulnaes, D.; Buckel, W.; Gohlke, H.; Smits, S. H. J.; Bremer, E. Molecular Dynamics Simulations and Structure-Guided Mutagenesis Provide Insight into the Architecture of the Catalytic Core of the Ectoine Hydroxylase. *J. Mol. Biol.* **2014**, *426* (3), 586–600.

(12) Milić, D.; Dick, M.; Mulnaes, D.; Pfleger, C.; Kinnen, A.; Gohlke, H.; Groth, G. Recognition Motif and Mechanism of Ripening Inhibitory Peptides in Plant Hormone Receptor ETR1. *Sci. Rep.* **2018**, *8* (1), 3890.

(13) Gohlke, H.; Hergert, U.; Meyer, T.; Mulnaes, D.; Grieshaber, M. K.; Smits, S. H. J.; Schmitt, L. Binding Region of Alanopine Dehydrogenase Predicted by Unbiased Molecular Dynamics Simulations of Ligand Diffusion. *J. Chem. Inf. Model.* **2013**, *53* (10), 2493–2498.

(14) Maestro.Pdf. *Maestro* **2014**, version 9.9.013; Schrödinger, LLC: New York, NY.

(15) Goodsell, D. S.; Morris, G. M.; Olson, A. J. Automated Docking of Flexible Ligands: Applications of AutoDock. *J. Mol. Recognit.* **1996**, *9* (1), 1–5.

(16) Gohlke, H.; Hendlich, M.; Klebe, G. Knowledge-Based Scoring Function to Predict Protein-Ligand Interactions. *J. Mol. Biol.* **2000**, *295* (2), 337–356.

(17) Sotriffer, C. A.; Gohlke, H.; Klebe, G. Docking into Knowledge-Based Potential Fields: A Comparative Evaluation of DrugScore. *J. Med. Chem.* **2002**, *45* (10), 1967–1970.

(18) Artsimovitch, I.; Seddon, J.; Sears, P. Fidaxomicin Is an Inhibitor of the Initiation of Bacterial RNA Synthesis. *Clin. Infect. Dis.* **2012**, *55*, 127–131.

(19) Diedrich, D.; Hamacher, A.; Gertzen, C. G. W.; Alves Avelar, L. A.; Reiss, G. J.; Kurz, T.; Gohlke, H.; Kassack, M. U.; Hansen, F. K. Rational Design and Diversity-Oriented Synthesis of Peptoid-Based Selective HDAC6 Inhibitors. *Chem. Commun.* **2016**, *52* (15), 3219–3222.

(20) Stenzel, K.; Hamacher, A.; Hansen, F. K.; Gertzen, C. G. W.; Senger, J.; Marquardt, V.; Marek, L.; Marek, M.; Romier, C.; Remke, M.; Jung, M.; Gohlke, H.; Kassack, M. U.; Kurz, T. Alkoxyurea-Based Histone Deacetylase Inhibitors Increase Cisplatin Potency in Chemoresistant Cancer Cell Lines. *J. Med. Chem.* **2017**, *60* (13), 5334–5348.

(21) Krieger, V.; Hamacher, A.; Gertzen, C. G. W.; Senger, J.; Zwinderman, M. R. H.; Marek, M.; Romier, C.; Dekker, F. J.; Kurz, T.; Jung, M.; Gohlke, H.; Kassack, M. U.; Hansen, F. K. Design, Multicomponent Synthesis, and Anticancer Activity of a Focused Histone Deacetylase (HDAC) Inhibitor Library with Peptoid-Based Cap Groups. *J. Med. Chem.* **2017**, *60* (13), 5493–5506.

(22) Molodtsov, V.; Nawarathne, I. N.; Scharf, N. T.; Kirchhoff, P. D.; Showalter, H. D. H.; Garcia, G. A.; Murakami, K. S. X-Ray Crystal Structures of the Escherichia Coli RNA Polymerase in Complex with Benzoxazinorifamycins. *J. Med. Chem.* **2013**, *56* (11), 4758–4763.

(23) Liu, K. J.; Parsons, J. L. Solvent Effects on the Preferred Conformation of Poly (Ethylene Glycols). *Macromolecules* **1969**, *2* (5), 529–533.

(24) Stierand, K.; Maaß, P. C.; Rarey, M. Molecular Complexes at a Glance: Automated Generation of Two-Dimensional Complex Diagrams. *Bioinformatics* **2006**, *22* (14), 1710–1716.

(25) Fricker, P. C.; Gastreich, M.; Rarey, M. Automated Drawing of Structural Molecular Formulas under Constraints. *J. Chem. Inf. Comput. Sci.* **2004**, *44* (3), 1065–1078.

(26) Lin, W.; Das, K.; Degen, D.; Zhang, C.; Ebright, R. H.; Lin, W.; Das, K.; Degen, D.; Mazumder, A.; Duchi, D.; Wang, D.; Ebright, Y. W. Structural Basis of Transcription Inhibition by Fidaxomicin (Lipiarmycin A3). *Mol. Cell* **2018**, *70*, 60–71.

(27) Dal Molin, M.; Selchow, P.; Schäfle, D.; Tschumi, A.; Ryckmans, T.; Laage-Witt, S.; Sander, P. Identification of Novel Scaffolds Targeting Mycobacterium Tuberculosis. *J. Mol. Med.* **2019**, *97*, 1601–1613.

(28) Raynaud, C.; Papavinasasundaram, K. G.; Speight, R. A.; Springer, B.; Sander, P.; Böttger, E. C.; Colston, M. J.; Draper, P. The Functions of OmpATb, a Pore-Forming Protein of Mycobacterium Tuberculosis. *Mol. Microbiol.* **2002**, *46* (1), 191–201.

(29) Matt, U.; Selchow, P.; Dal Molin, M.; Strommer, S.; Sharif, O.; Schilcher, K.; Andreoni, F.; Stenzinger, A.; Zinkernagel, A. S.; Zeitlinger, M.; Sander, P.; Nemeth, J. Chloroquine Enhances the Antimycobacterial Activity of Isoniazid and Pyrazinamide by Reversing Inflammation-Induced Macrophage Efflux. *Int. J. Antimicrob. Agents* **2017**, *50* (1), 55–62.

(30) Clinical and Laboratory Standards Institute (CLSI). *Performance Standards for Antimicrobial Susceptibility Testing: 29th Edition*; 2019.

(31) Clinical and Laboratory Standards Institute (CLSI). *Methods for Antimicrobial Susceptibility Testing of Anaerobic Bacteria: Ninth Edition*; 2018; Vol. 9.

Fidaxomicin Acetamide (2a)

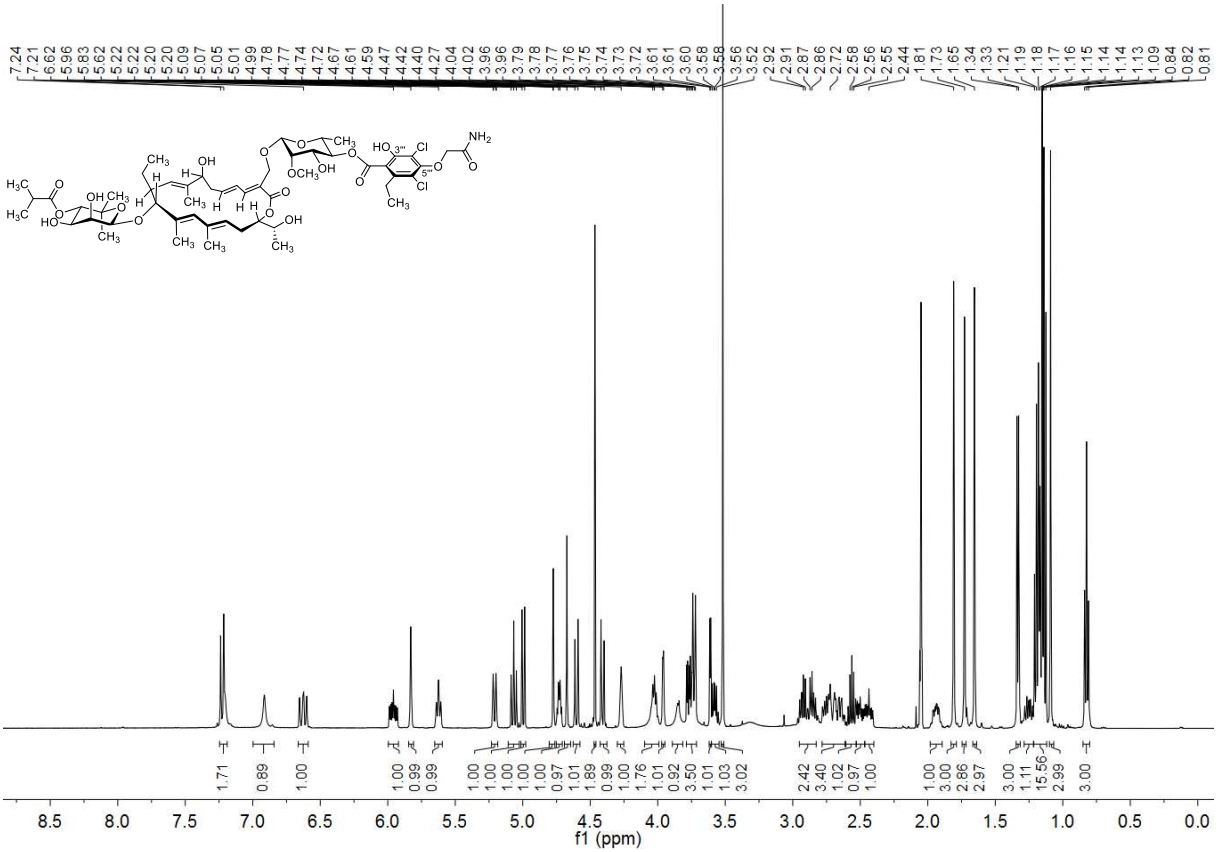

^{1}H NMR (400.13 MHz, 300 K, acetone-d_6)

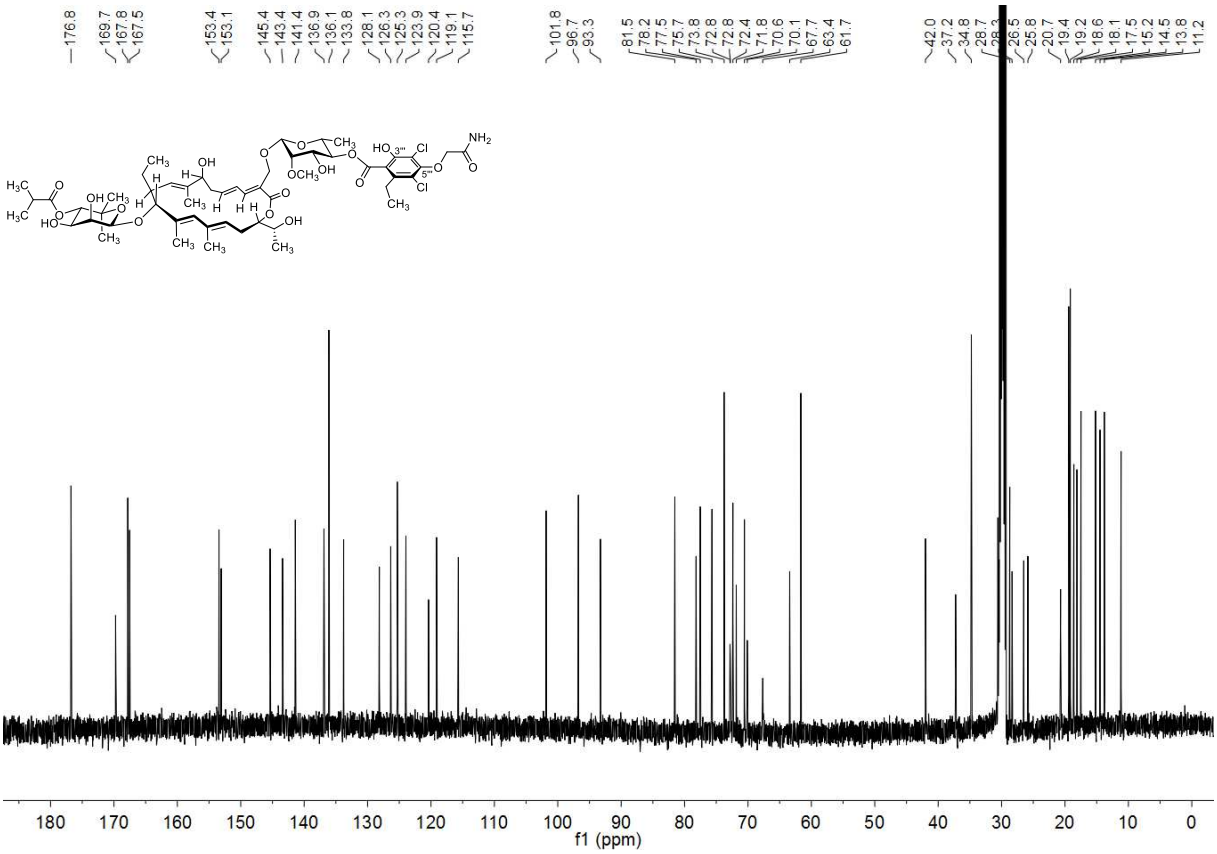

^{13}C NMR (125.81 MHz, 298 K, acetone-d_6)

Fidaxomicin Bis(acetamide) (2b)

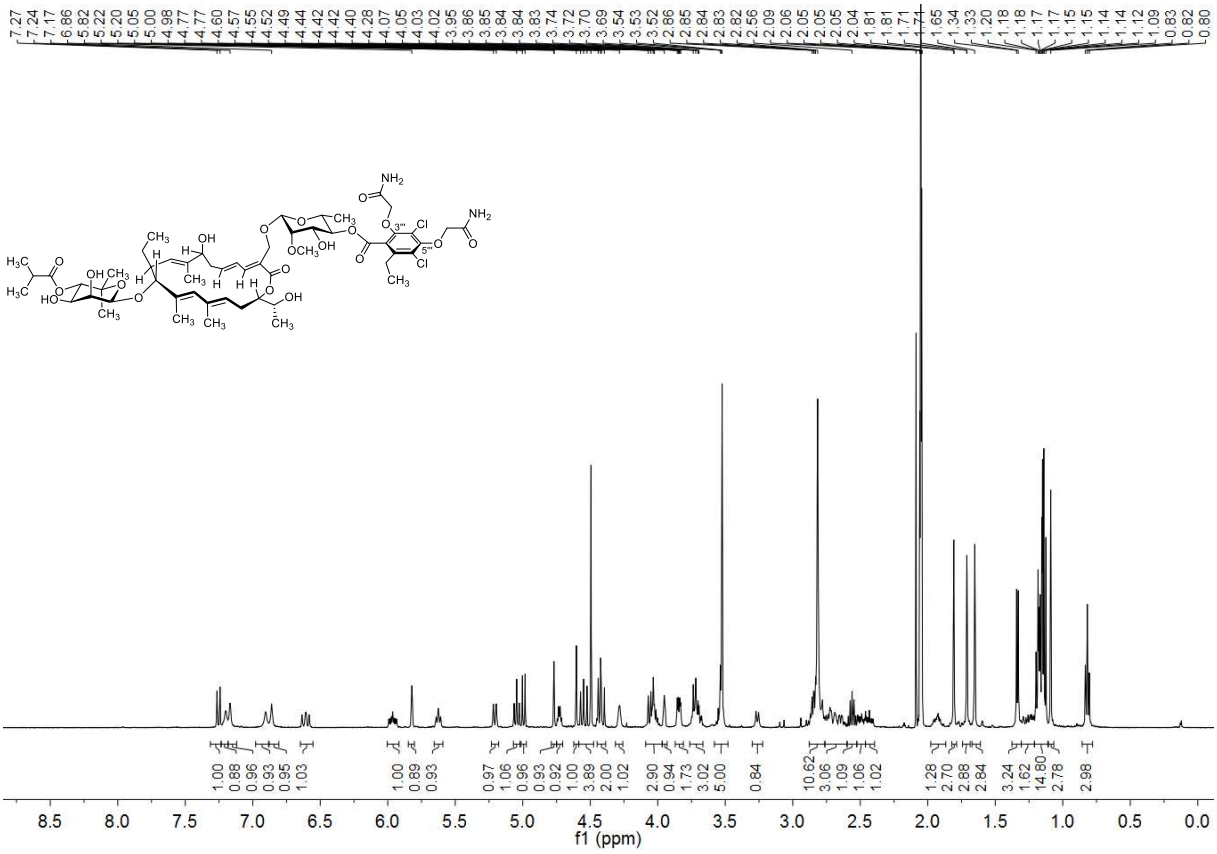

^{1}H NMR (500.25 MHz, 298 K, acetone-d_6)

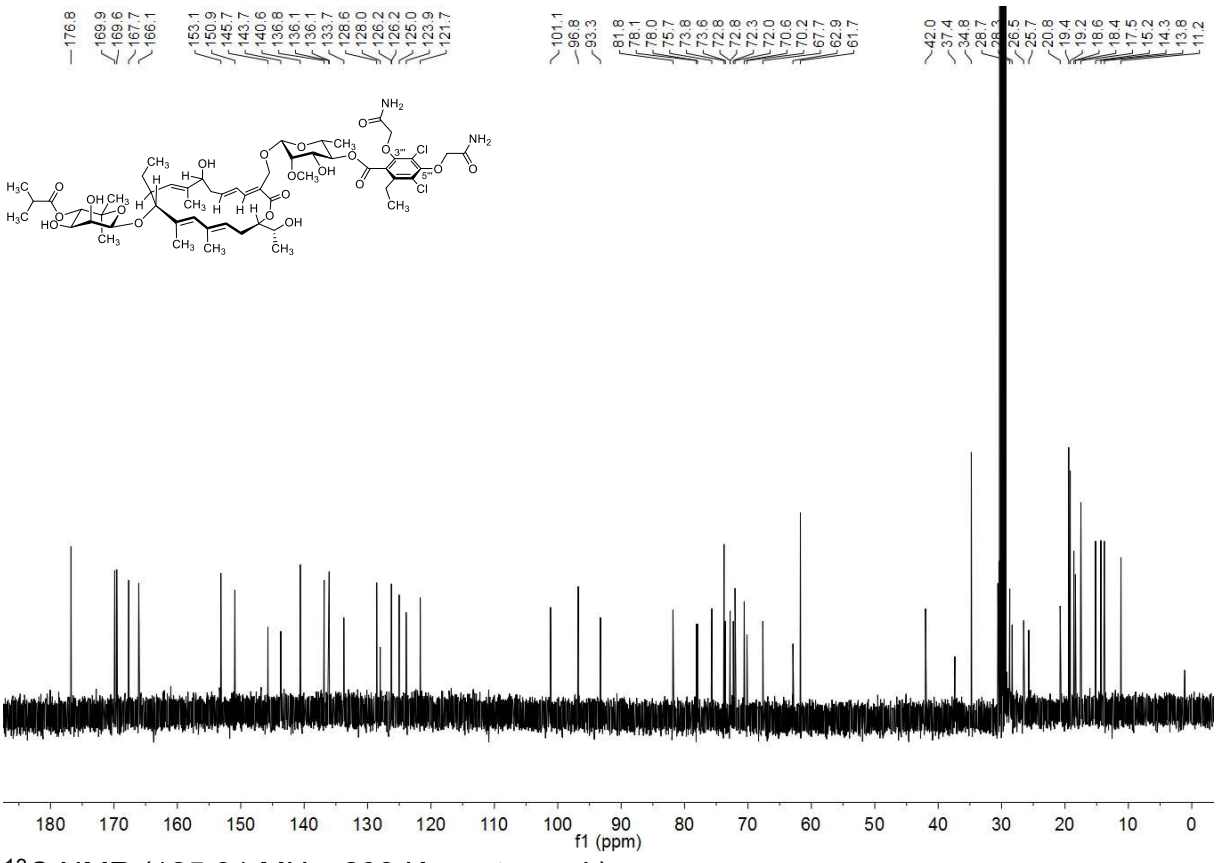

^{13}C NMR (125.81 MHz, 298 K, acetone-d_6)

Fidaxomicin Dimethylacetamide (3a)

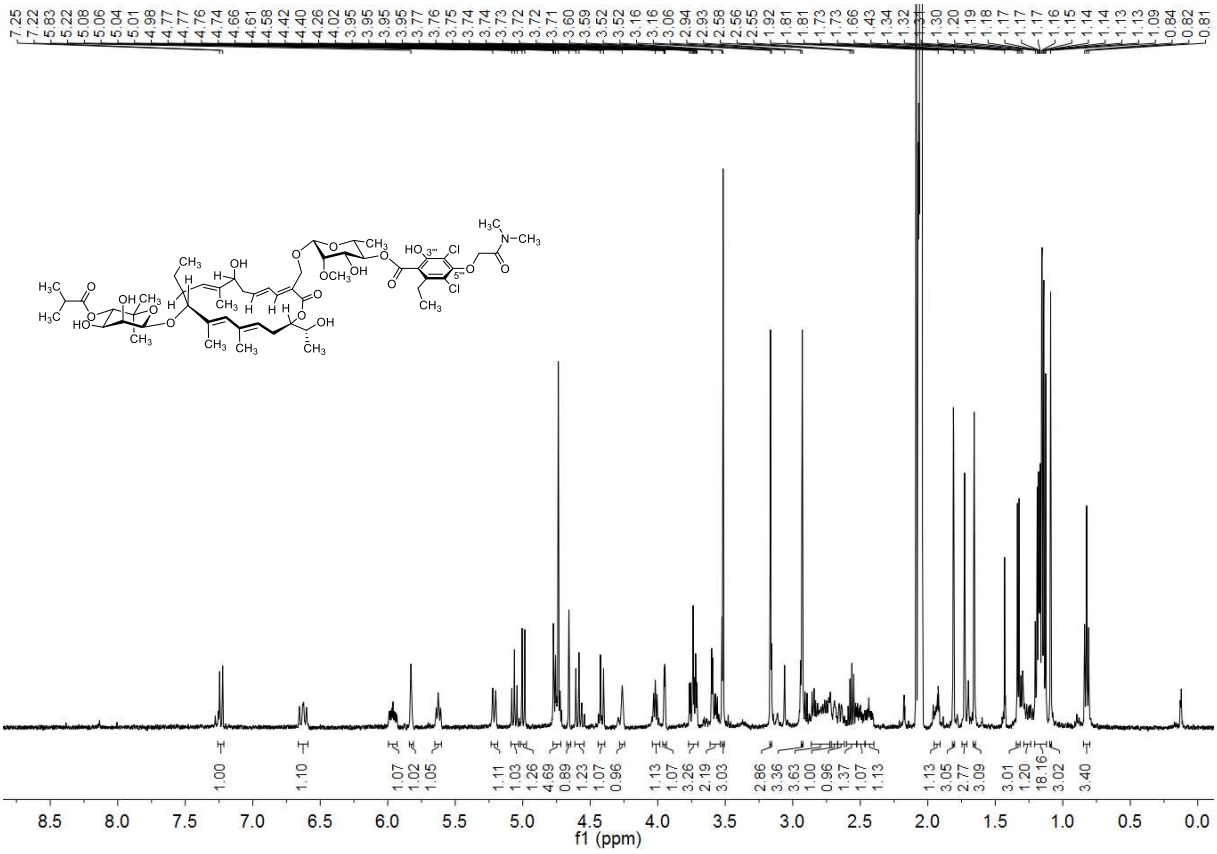

^{1}H NMR (500.25 MHz, 298 K, acetone-d_6)

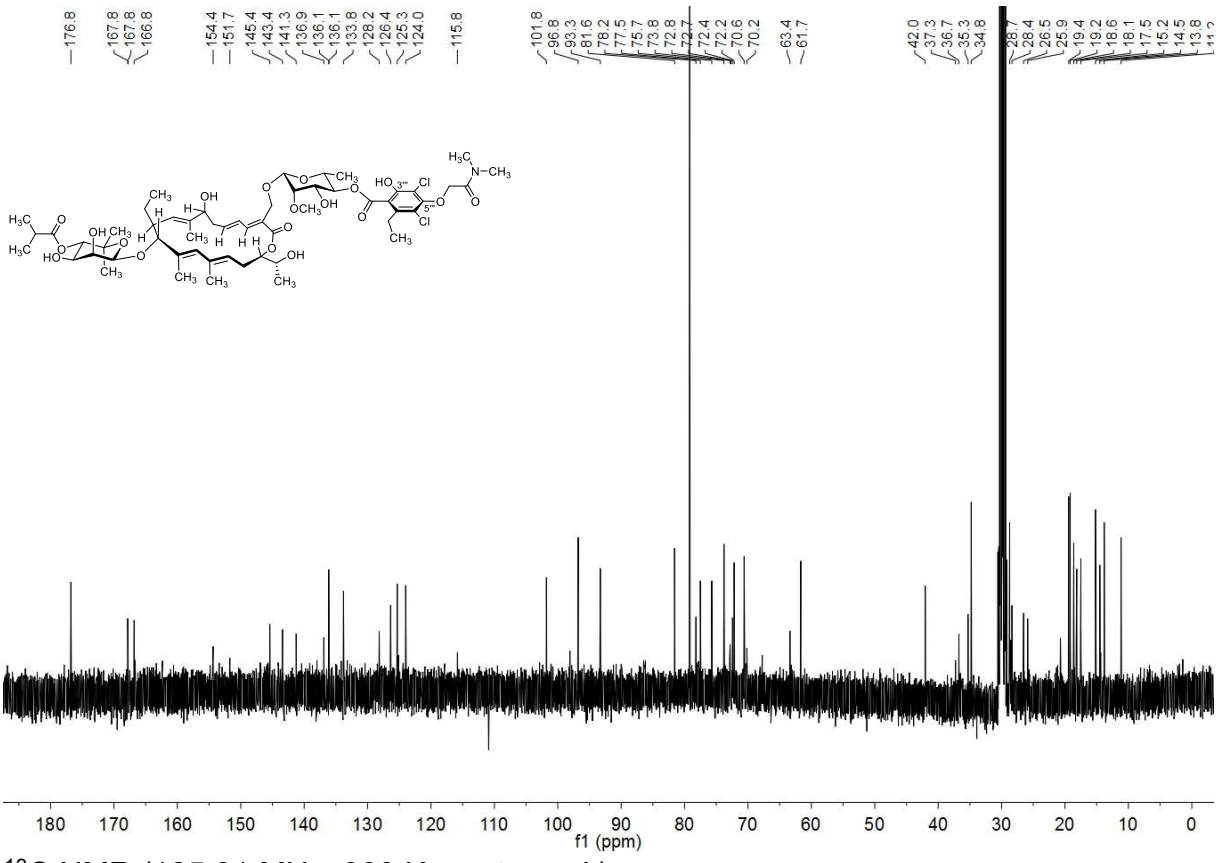

^{13}C NMR (125.81 MHz, 300 K, acetone-d_6)

Fidaxomicin Bis(dimethylacetamide) (3b)

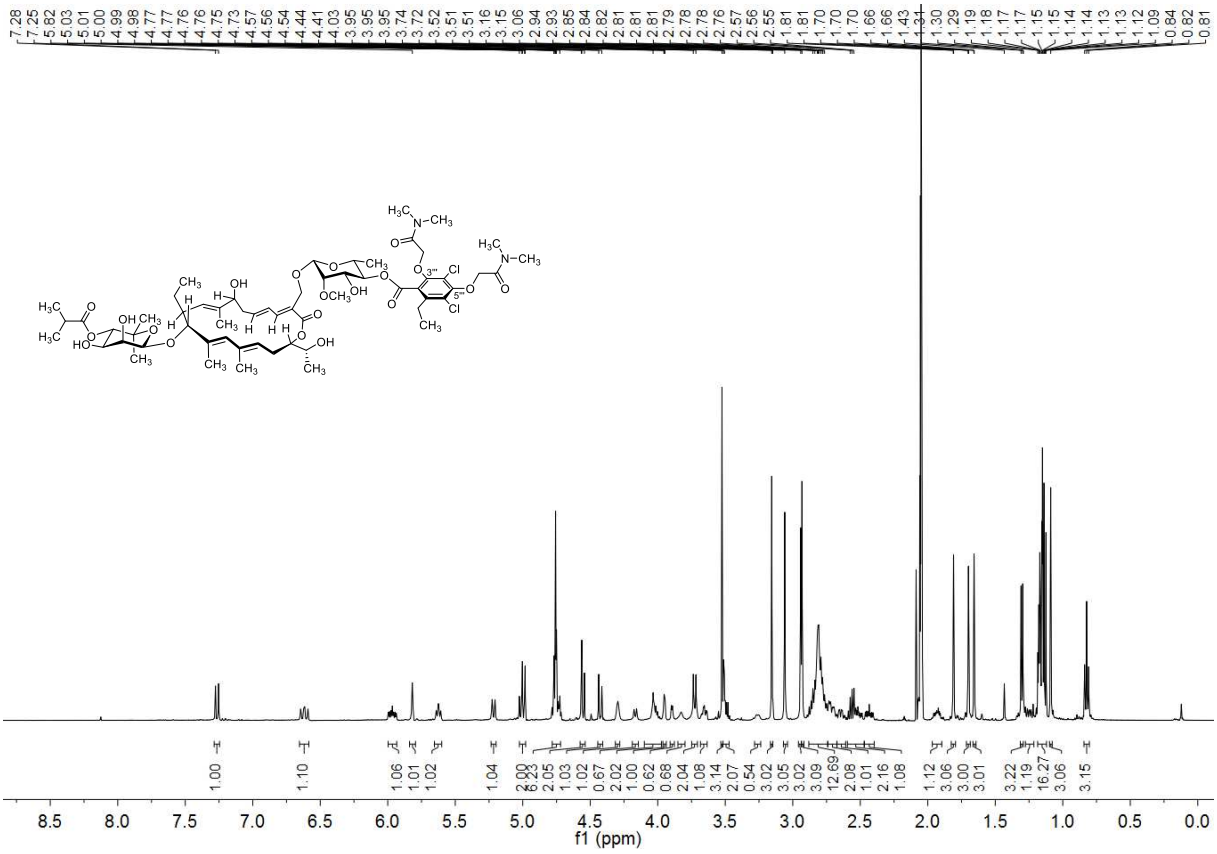

^{1}H NMR (500.13 MHz, 299 K, acetone-d_6)

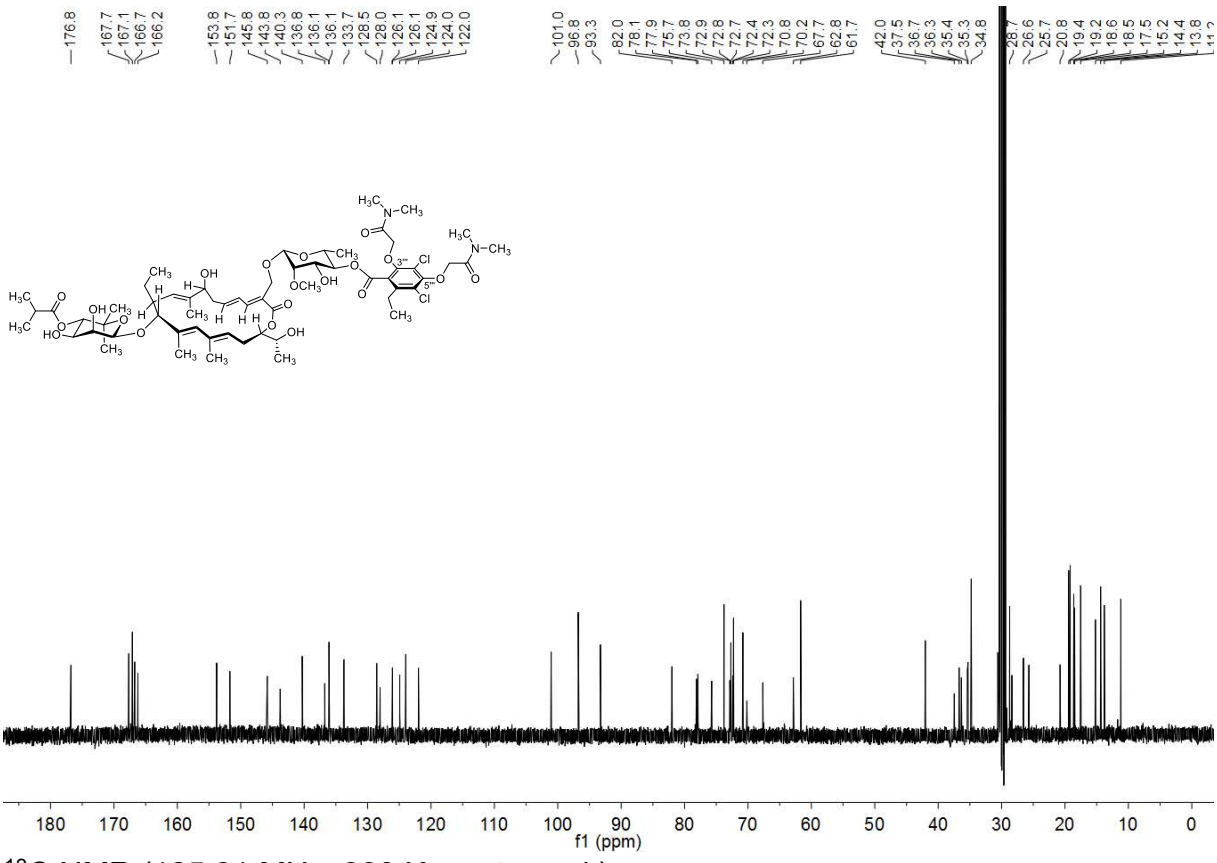

^{13}C NMR (125.81 MHz, 300 K, acetone-d_6)

Fidaxomicin Ethylacetate (4a)

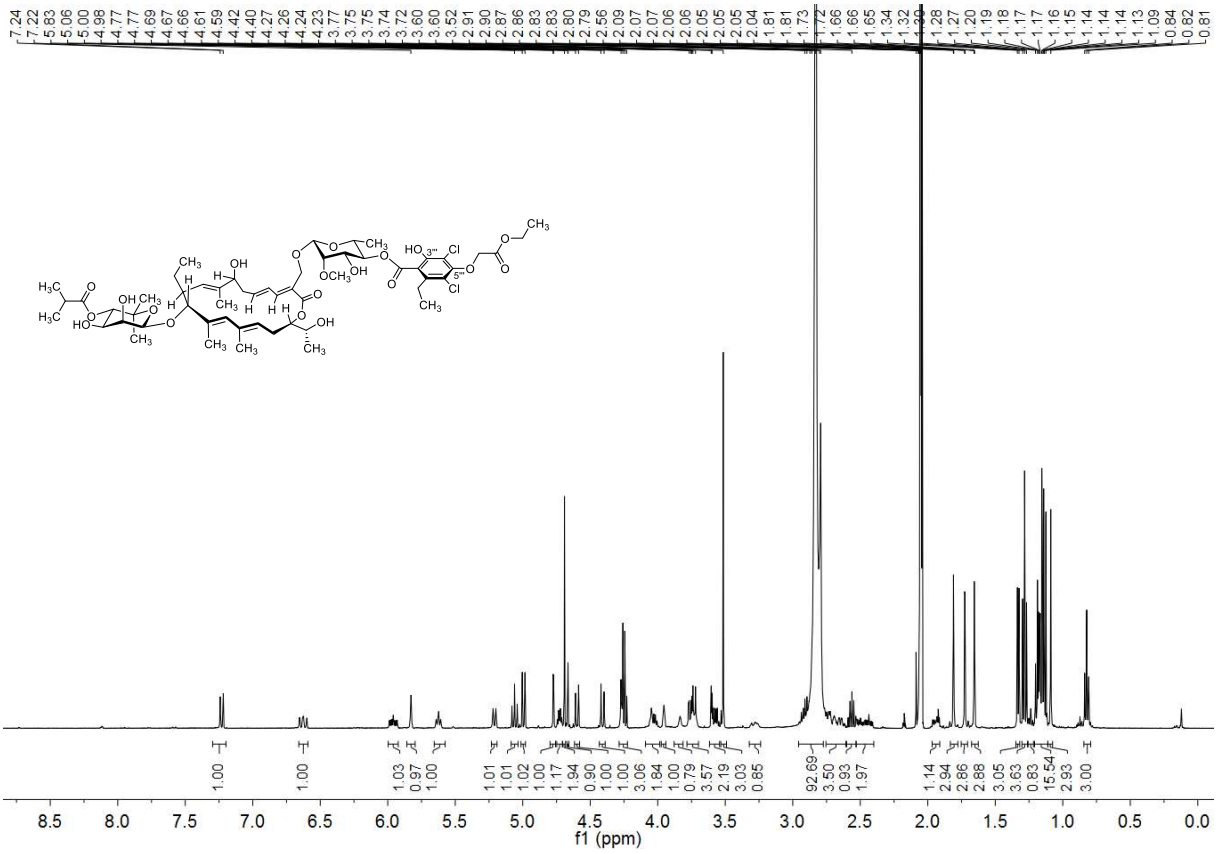

^{1}H NMR (500.13 MHz, 298 K, acetone-d_6)

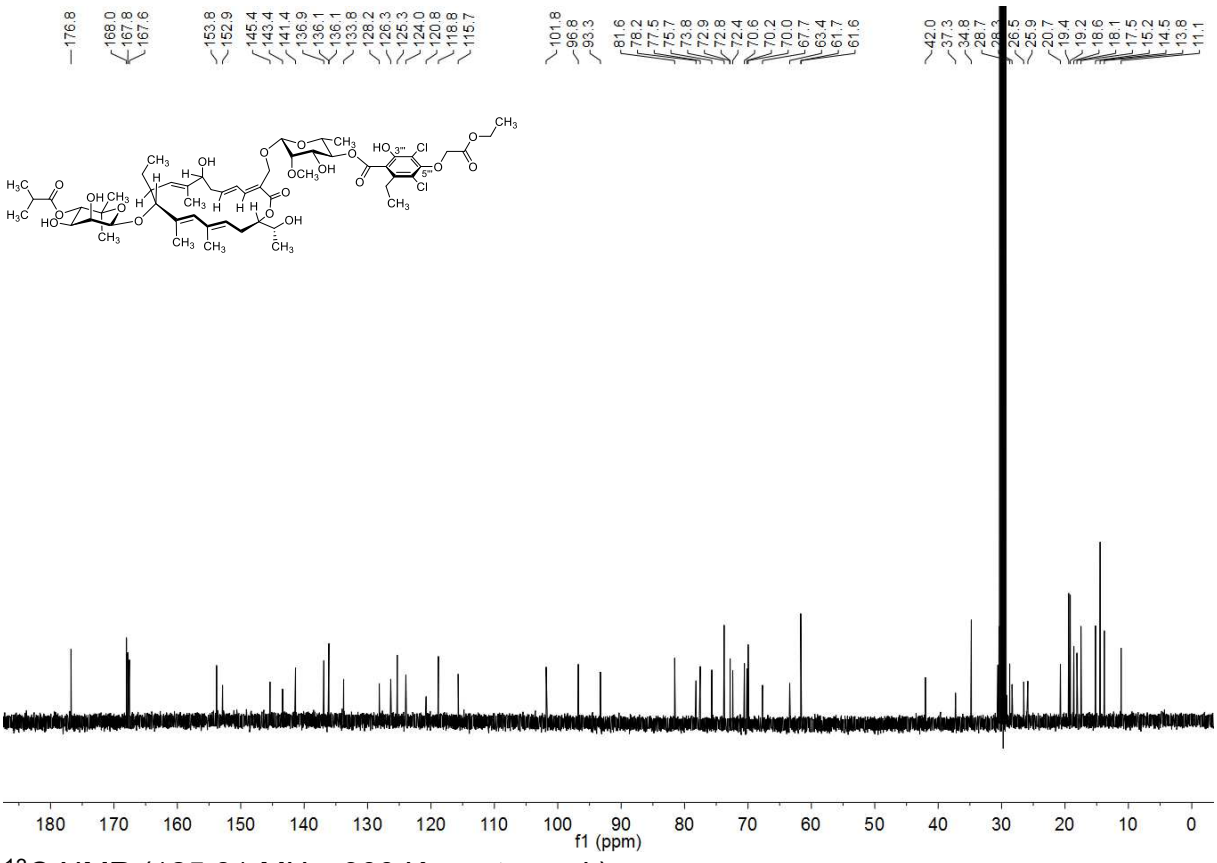

^{13}C NMR (125.81 MHz, 300 K, acetone-d_6)

Fidaxomicin Bis(ethylacetate) (4b)

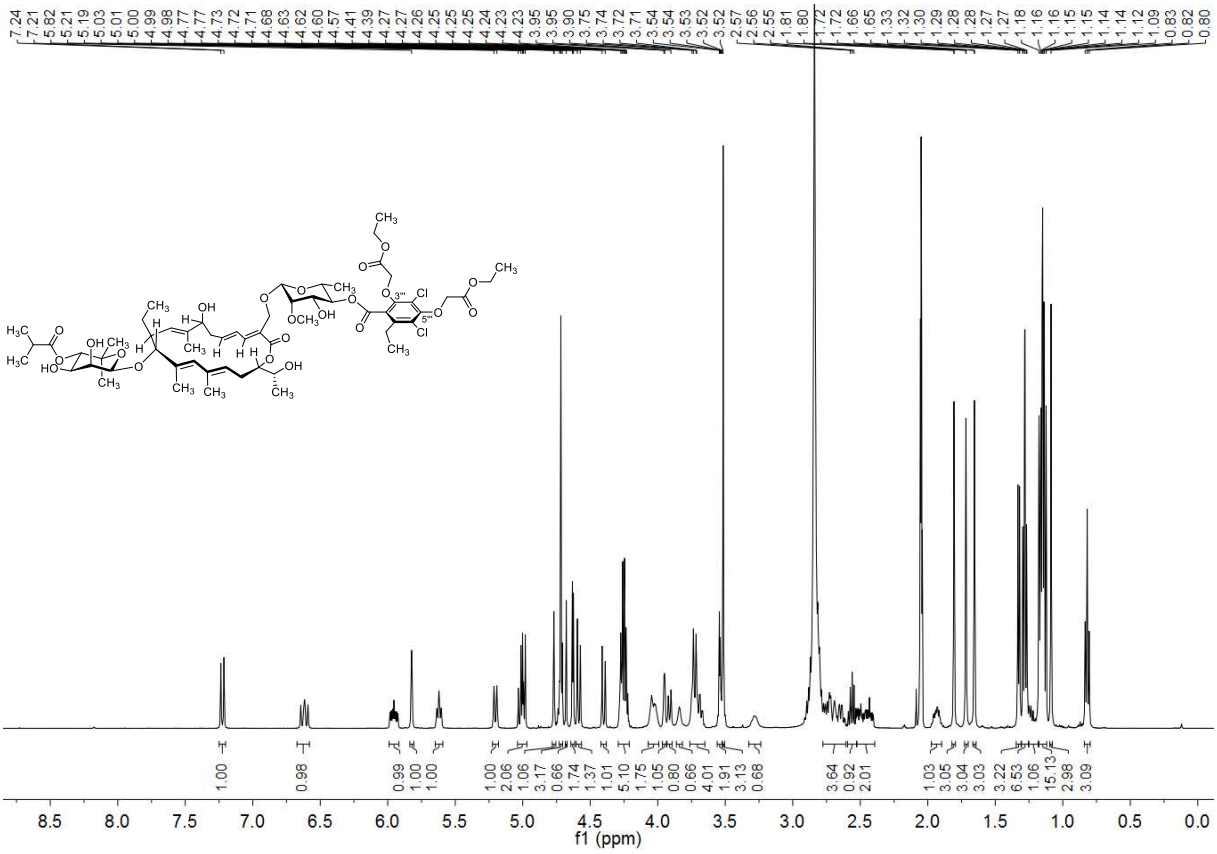

^{1}H NMR (500.13 MHz, 298 K, acetone-d_6)

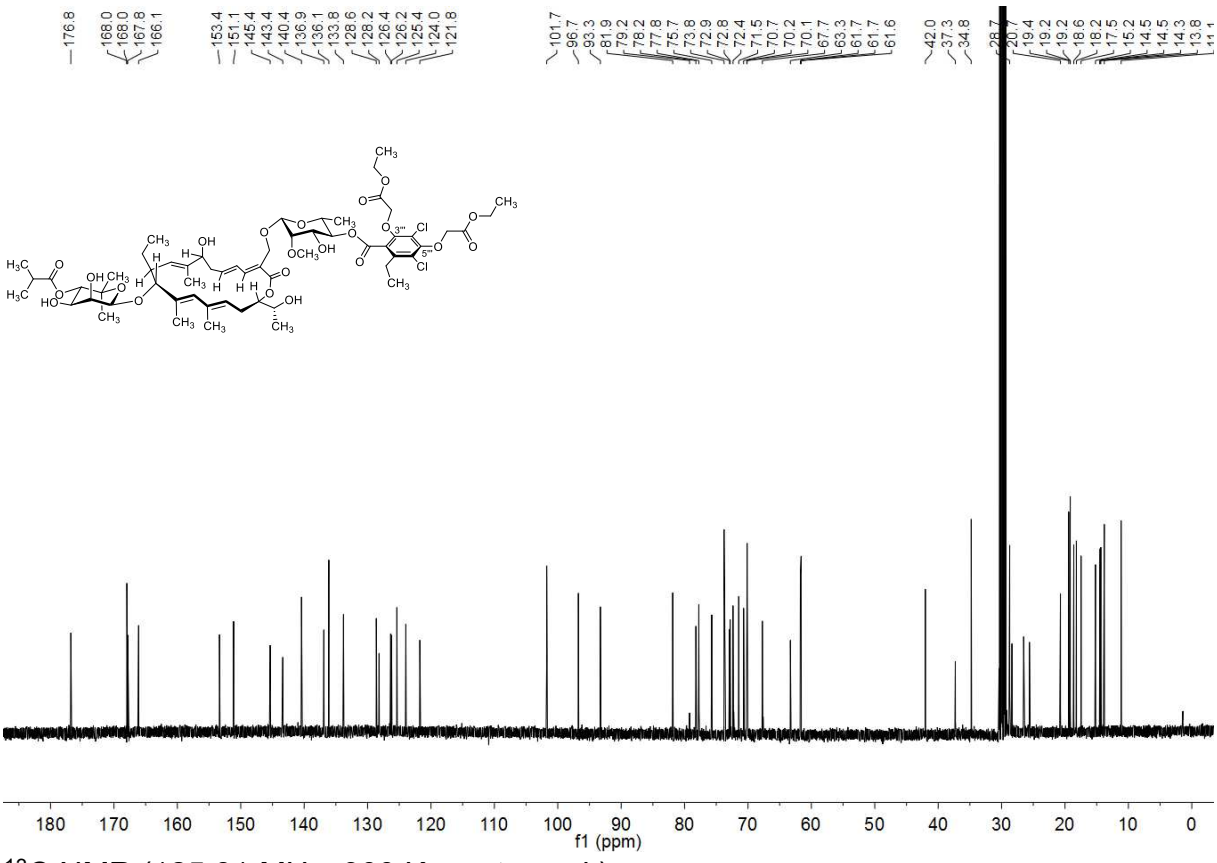

^{13}C NMR (125.81 MHz, 300 K, acetone-d_6)

Allyl 4-(2-chloroacetyl)piperazine-1-carboxylate

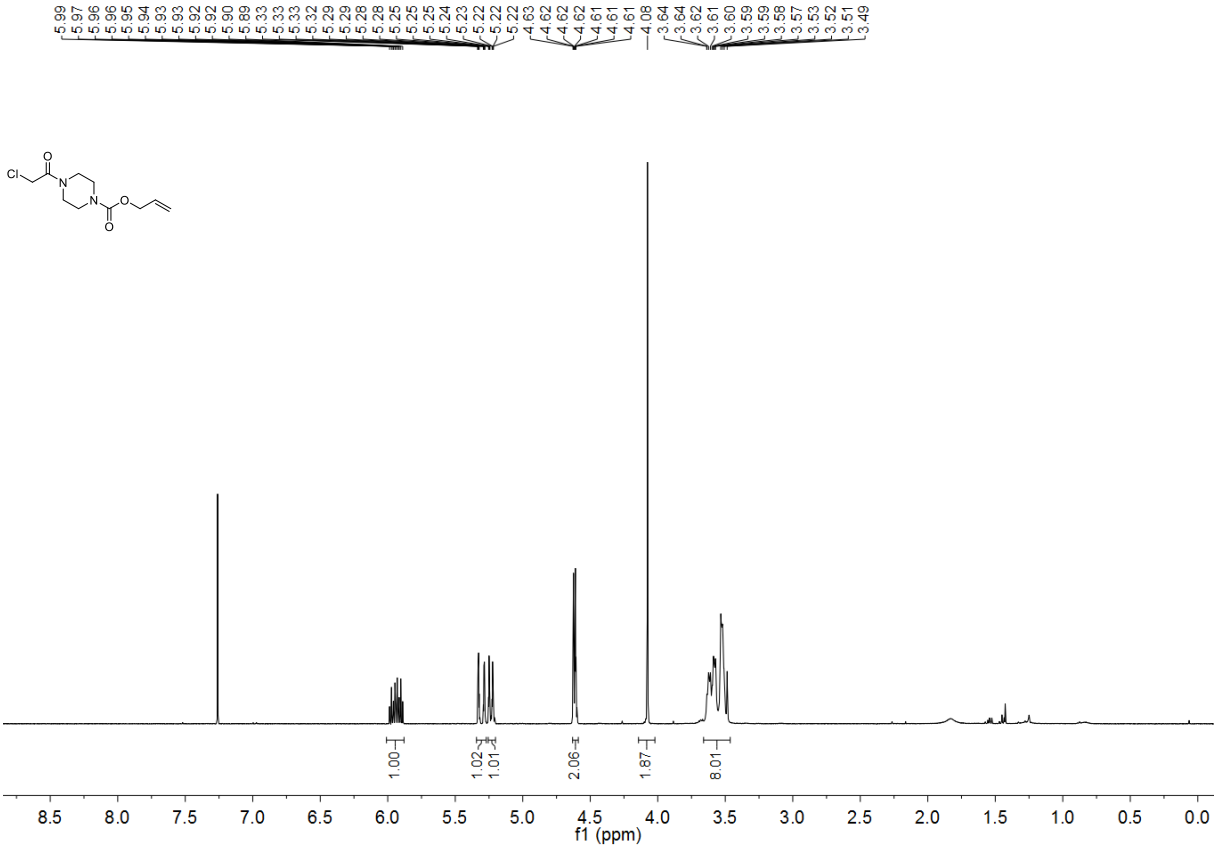

^{1}H NMR (400.13 MHz, 300 K, $CDCl_3$)

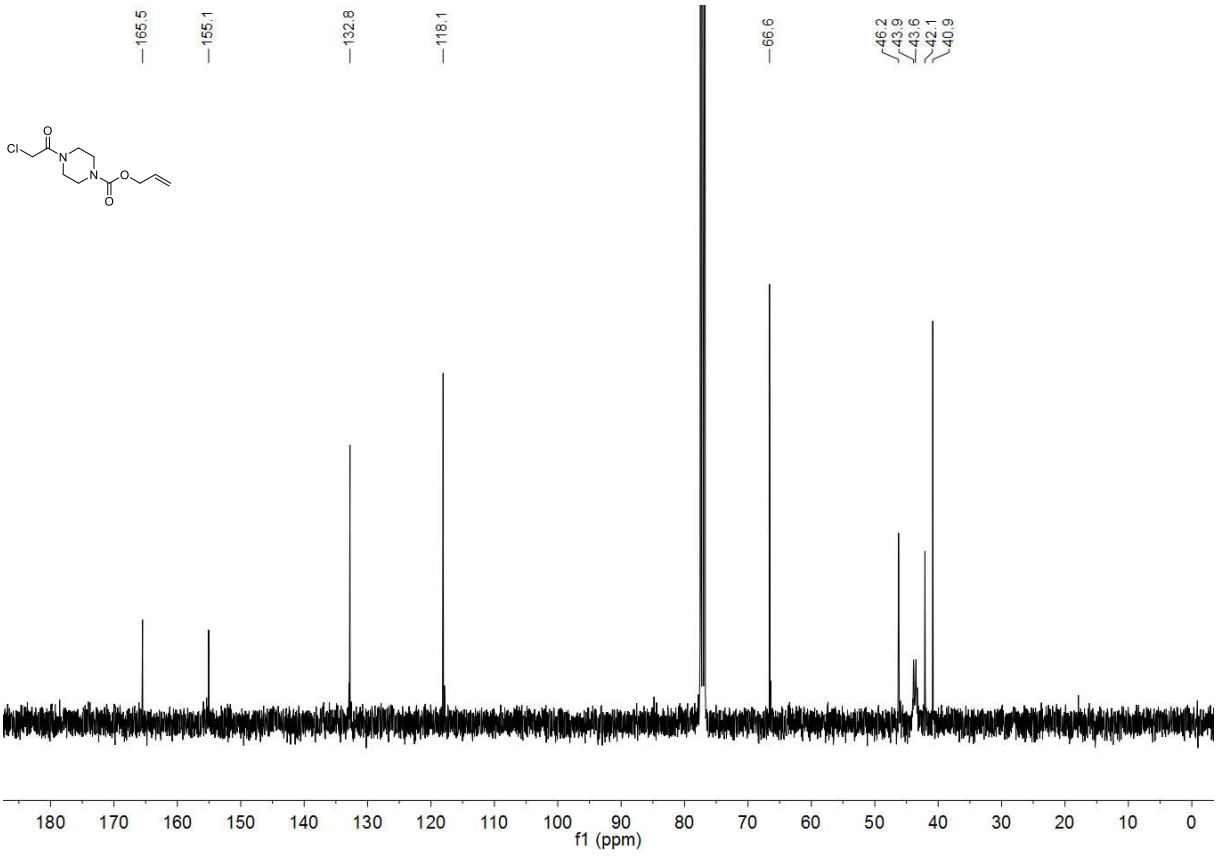

^{13}C NMR (100.62 MHz, 300 K, $CDCl_3$)

Allyl 4-(2-iodoacetyl)piperazine-1-carboxylate

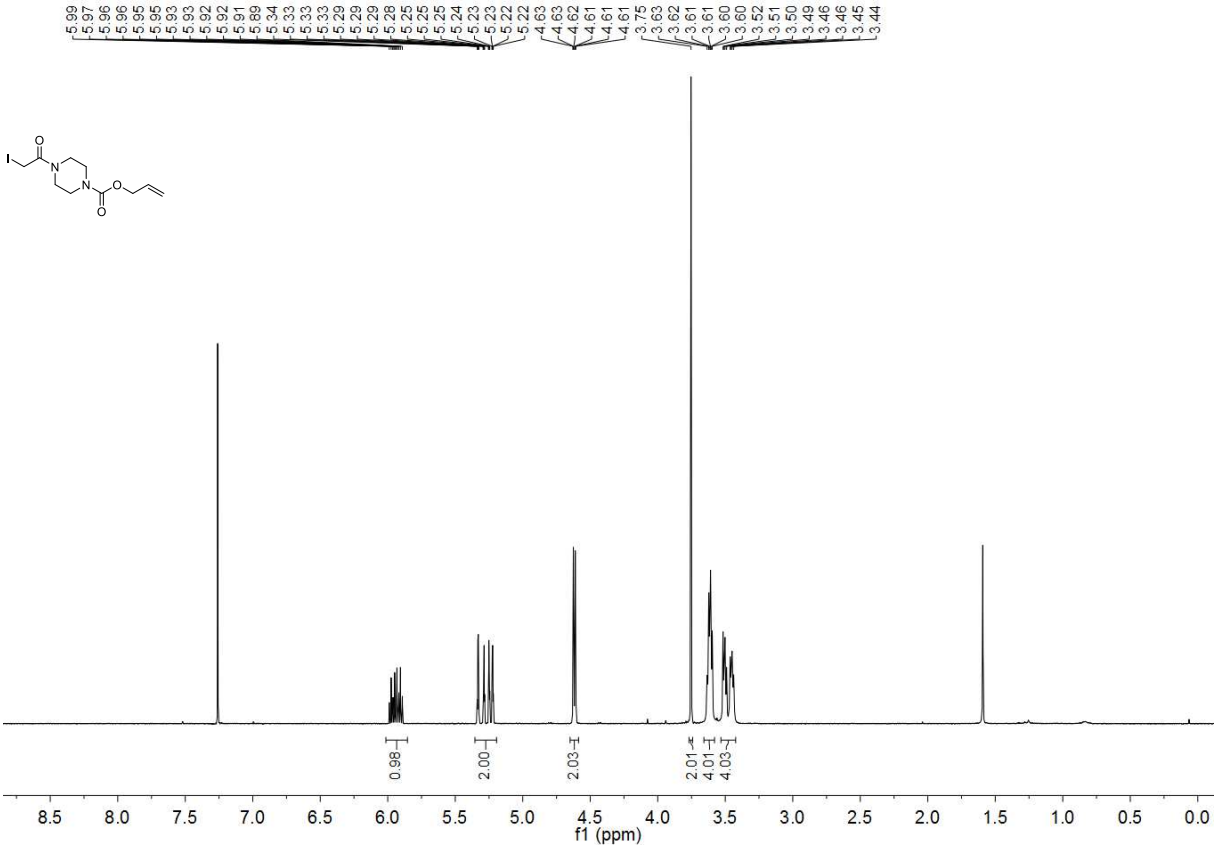

^{1}H NMR (400.13 MHz, 300 K, $CDCl_3$)

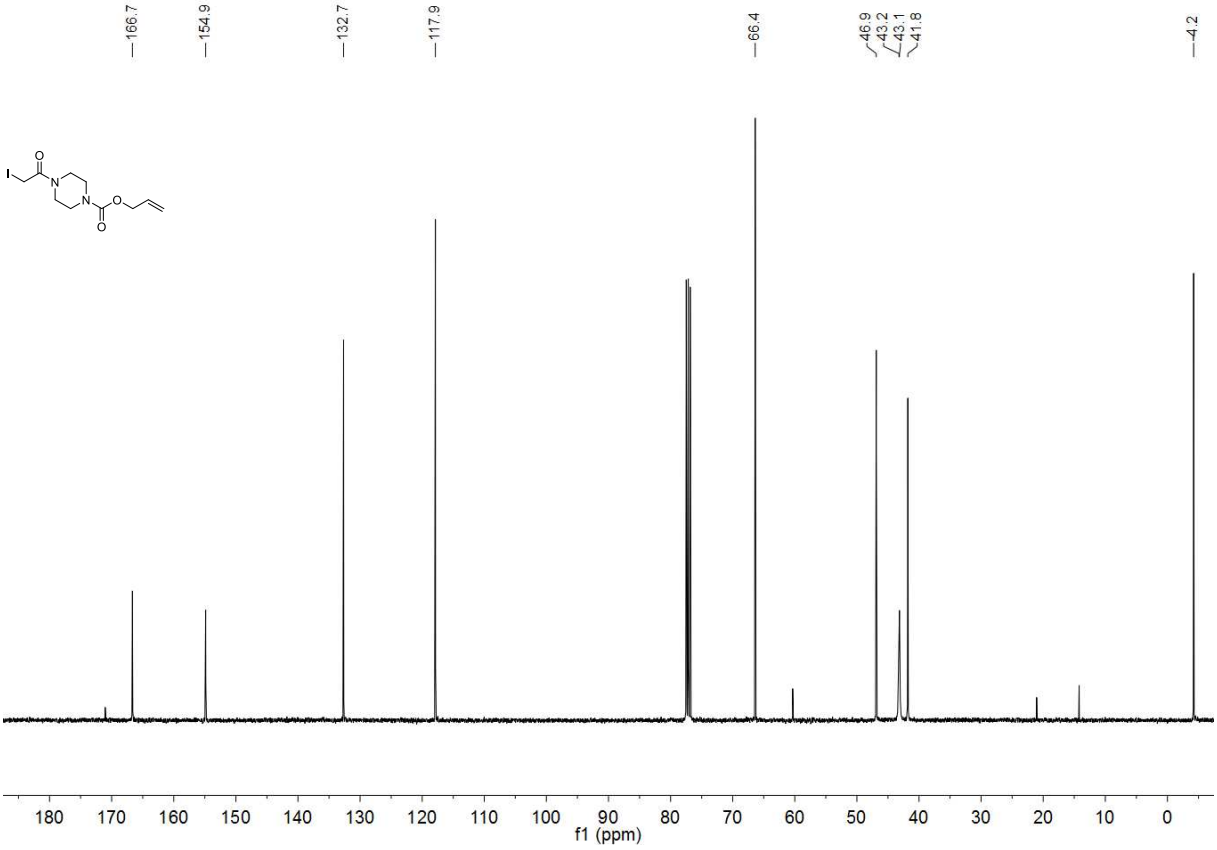

^{13}C NMR (100.62 MHz, 300 K, $CDCl_3$)

Fidaxomicin Piperazine with alloc Protecting Group

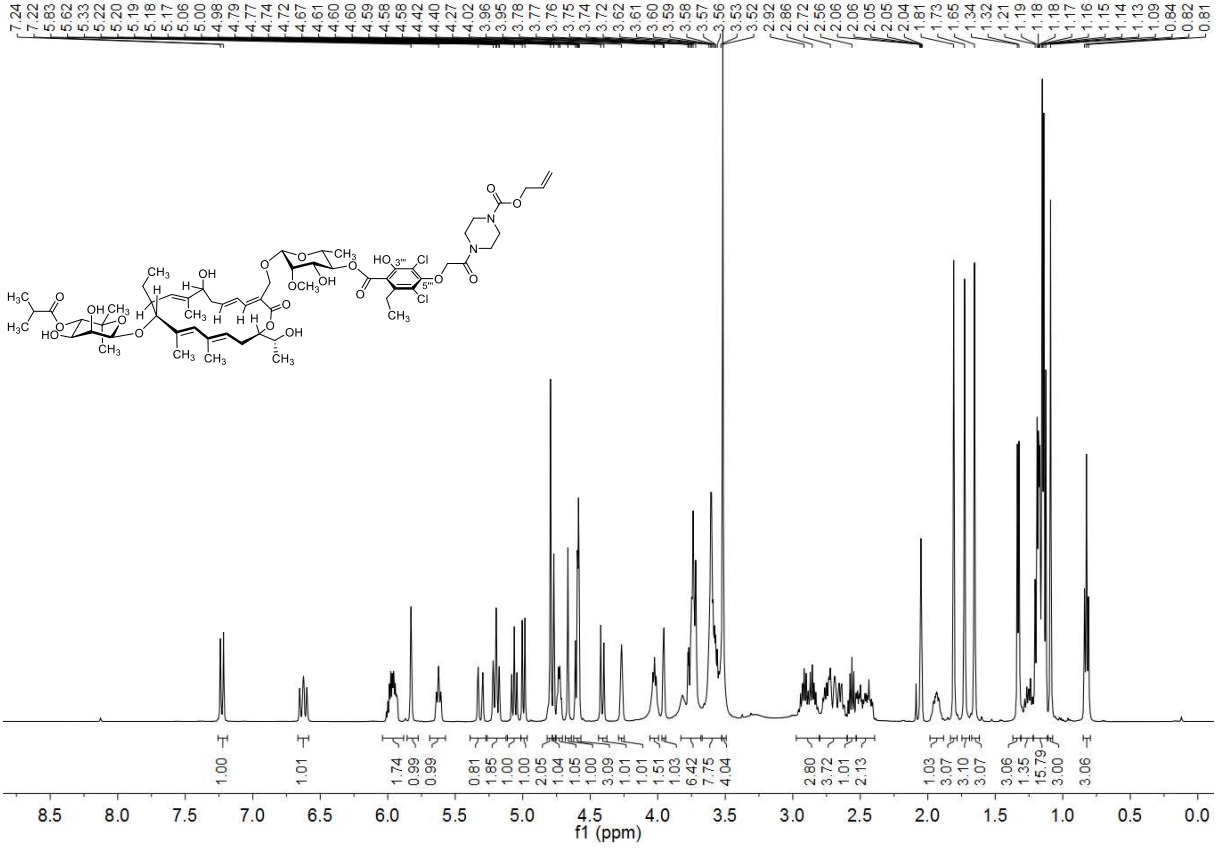

^{1}H NMR (500.13 MHz, 300 K, acetone-d_6)

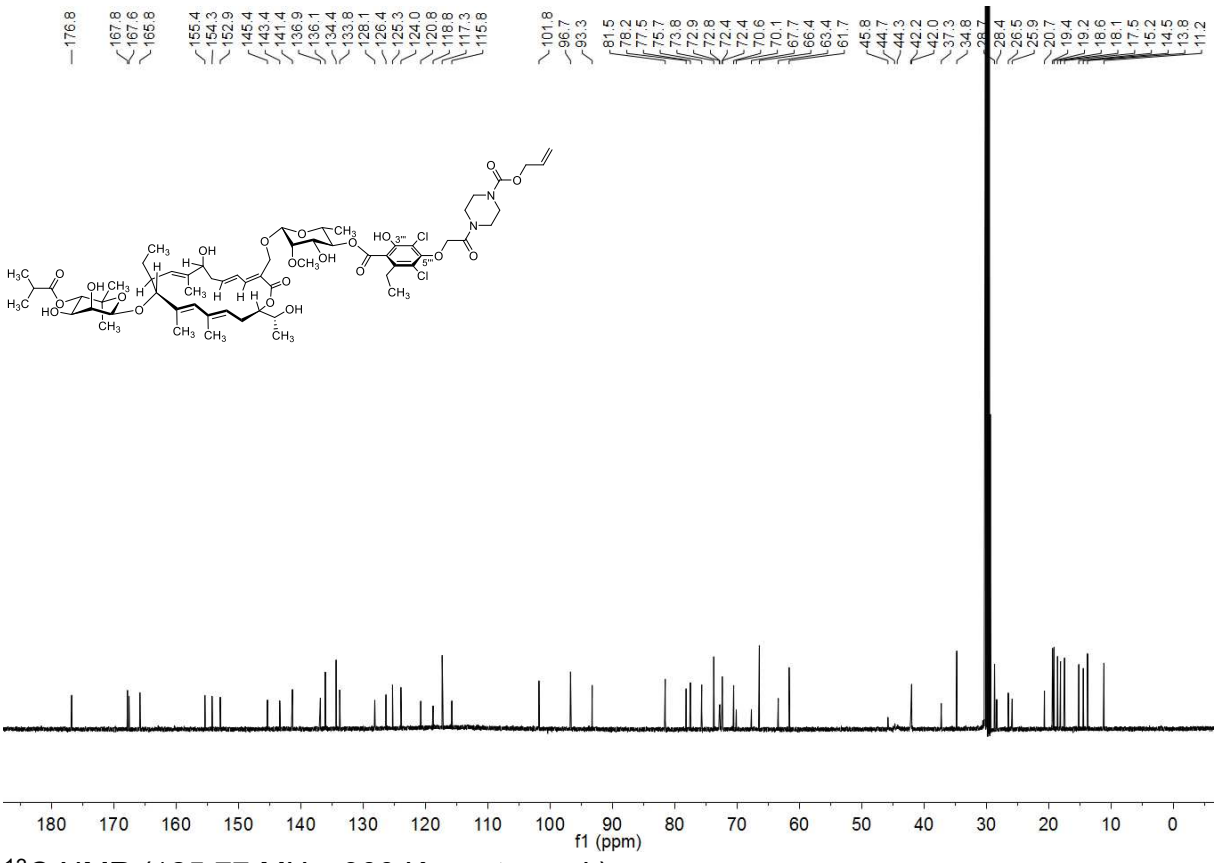

^{13}C NMR (125.77 MHz, 300 K, acetone-d_6)

Fidaxomicin Di(piperazine) with alloc Protecting Group

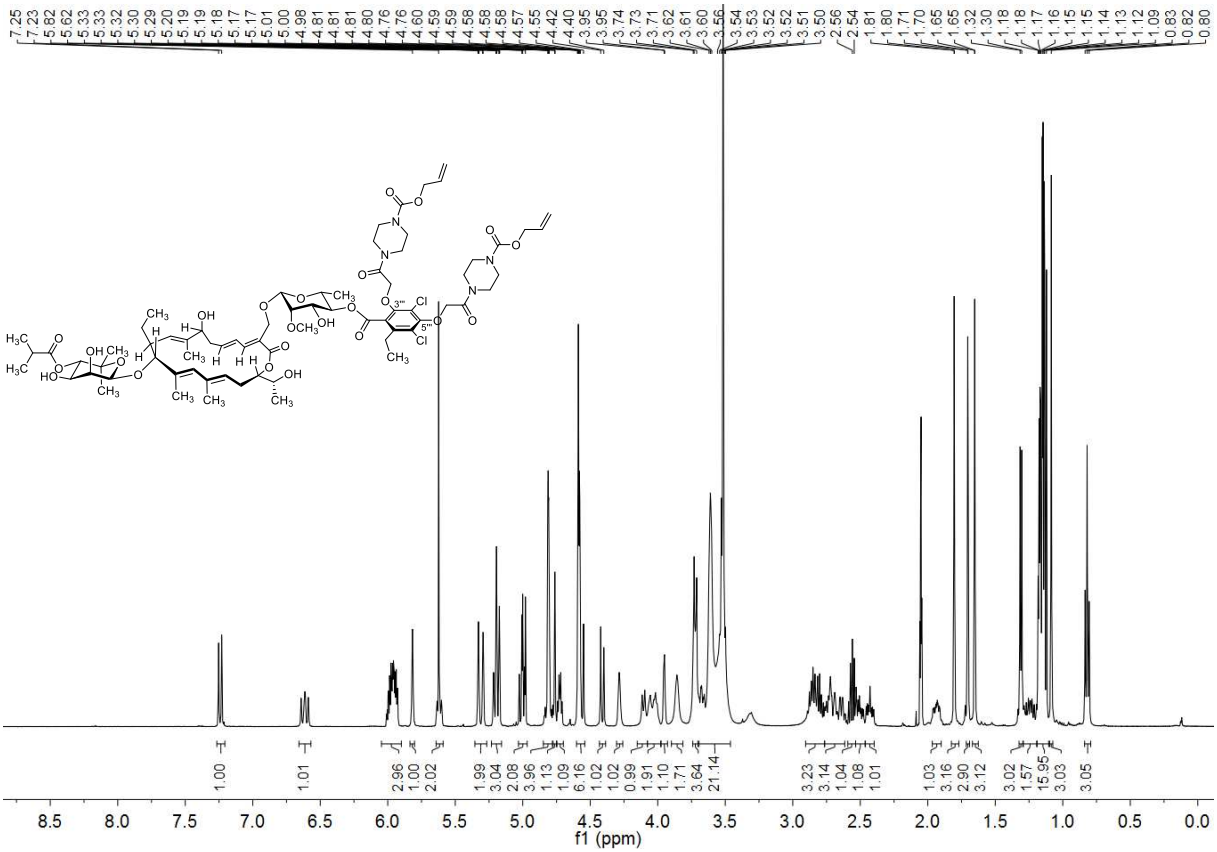

^{1}H NMR (500.25 MHz, 295 K, acetone-d_6)

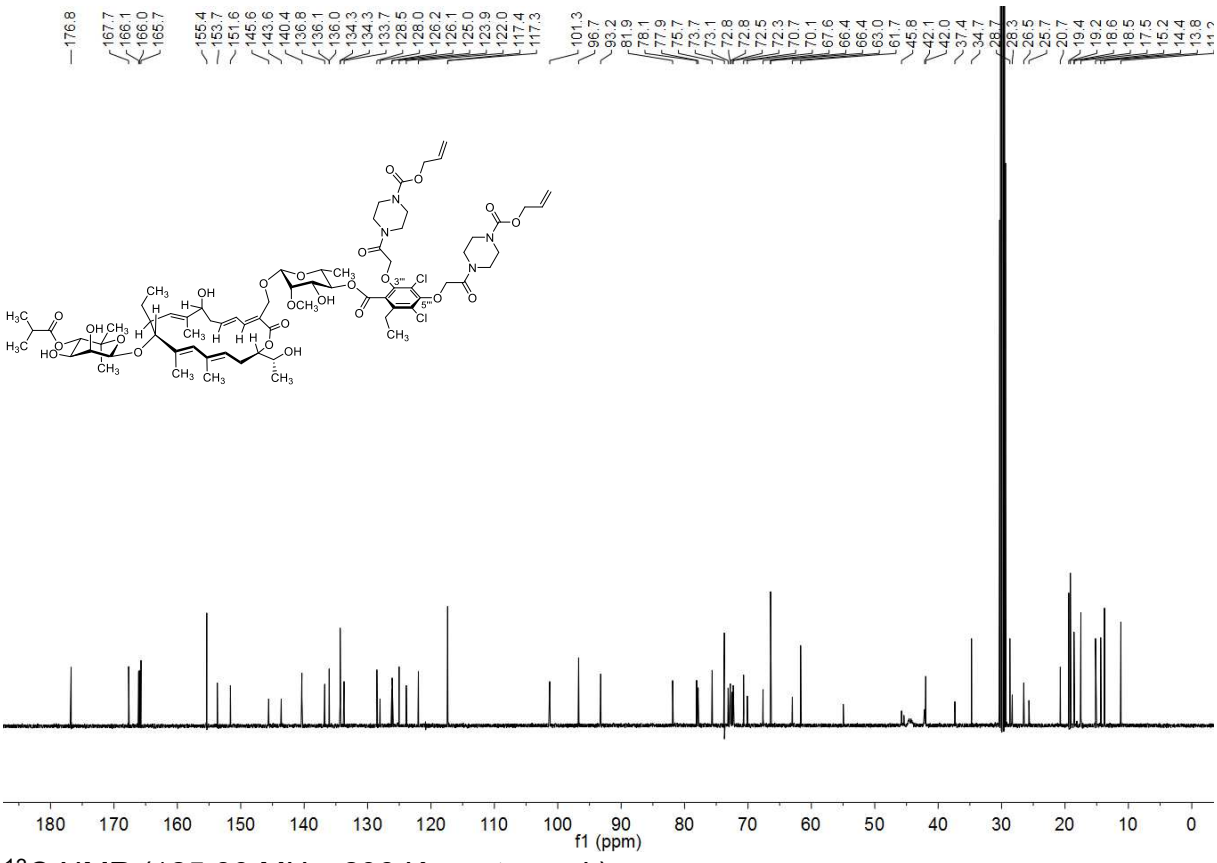

^{13}C NMR (125.80 MHz, 296 K, acetone-d_6)

Fidaxomicin Piperazine (5a)

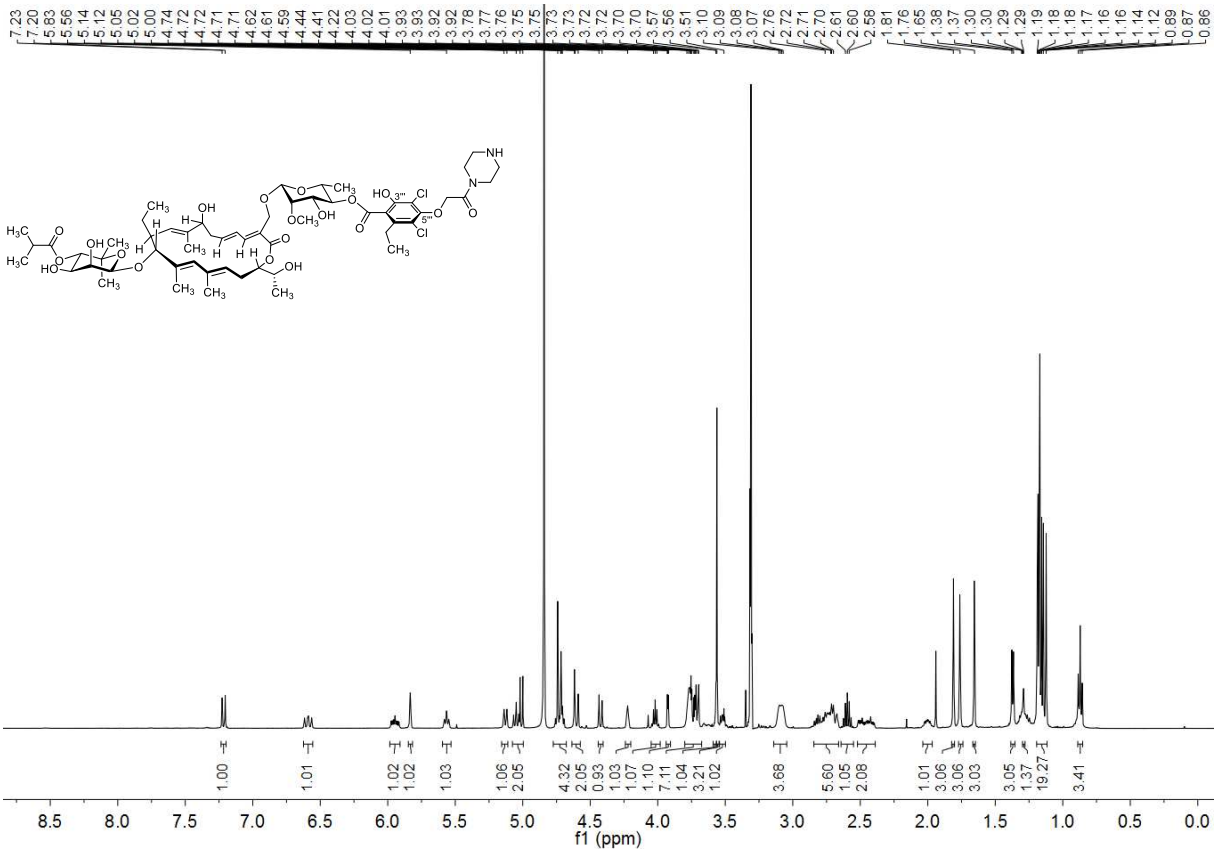

^{1}H NMR (500.13 MHz, 300 K, D$_3$COD)

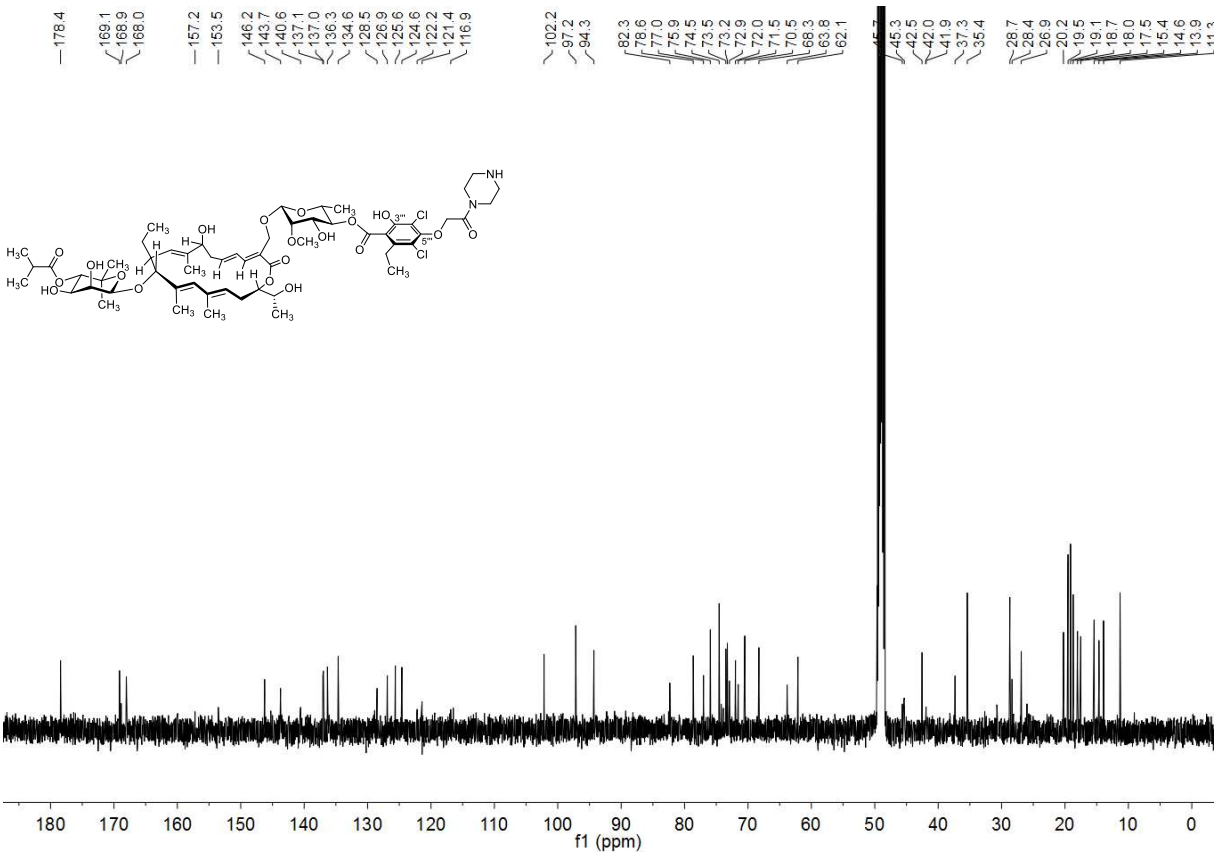

^{13}C NMR (125.80 MHz, 300 K, D$_3$COD)

Fidaxomicin Dipiperazine (5b)

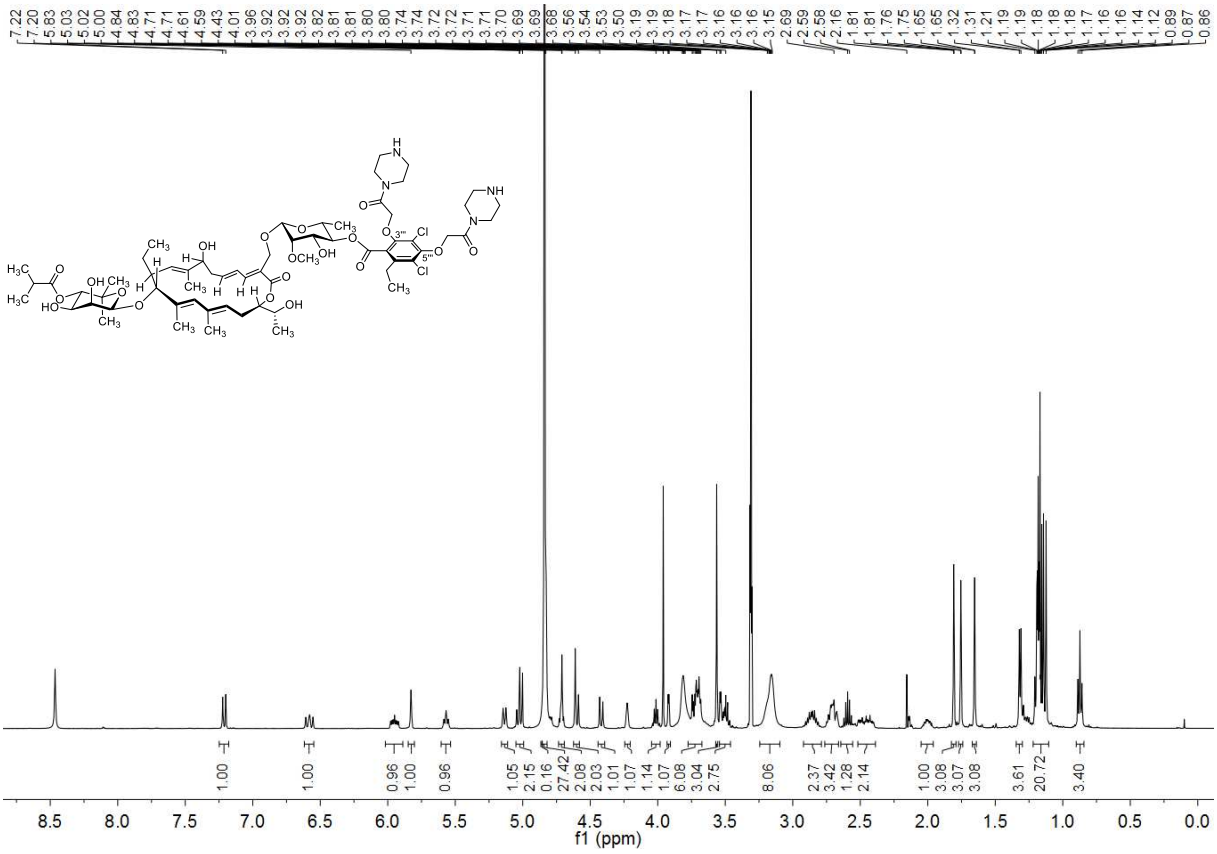

^{1}H NMR (500.13 MHz, 300 K, D$_3$COD)

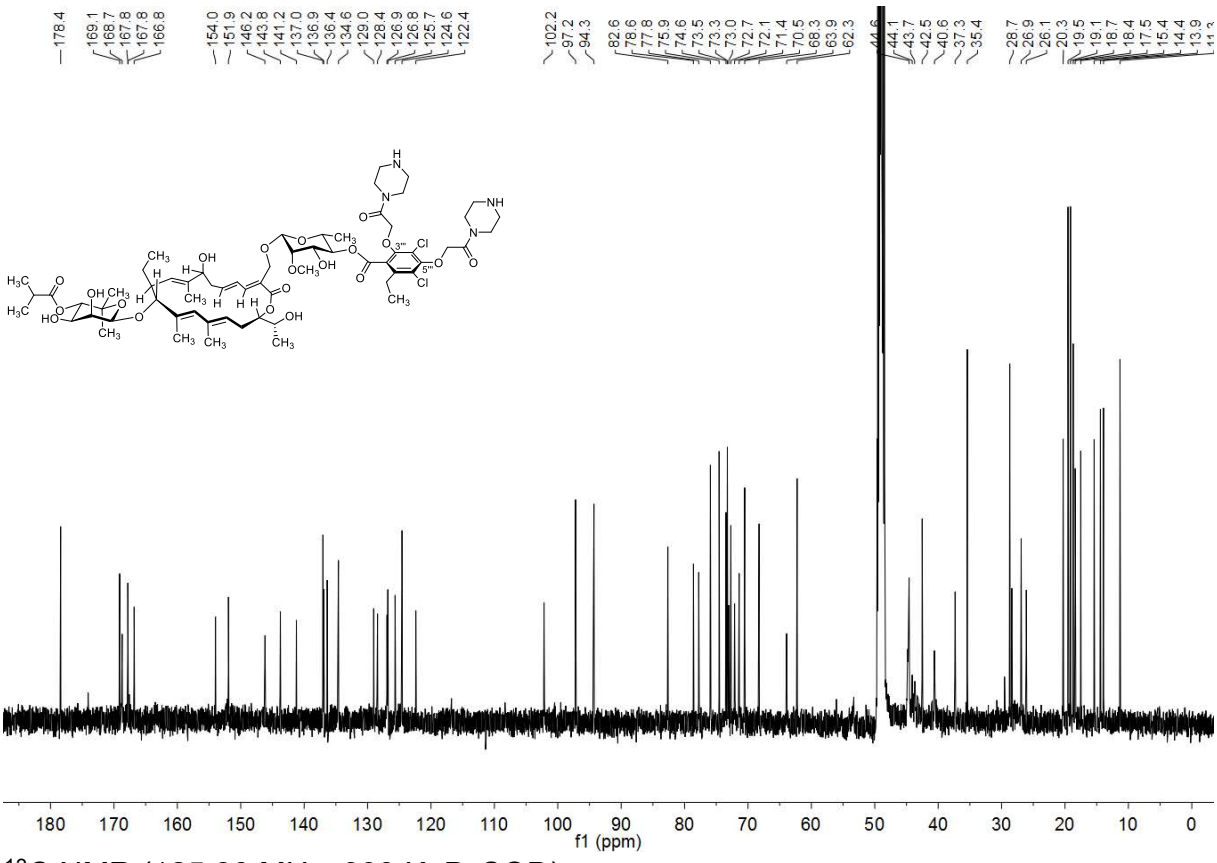

^{13}C NMR (125.80 MHz, 300 K, D$_3$COD)

1-(4-Hydroxypiperidin-1-yl)-2-iodoethan-1-one

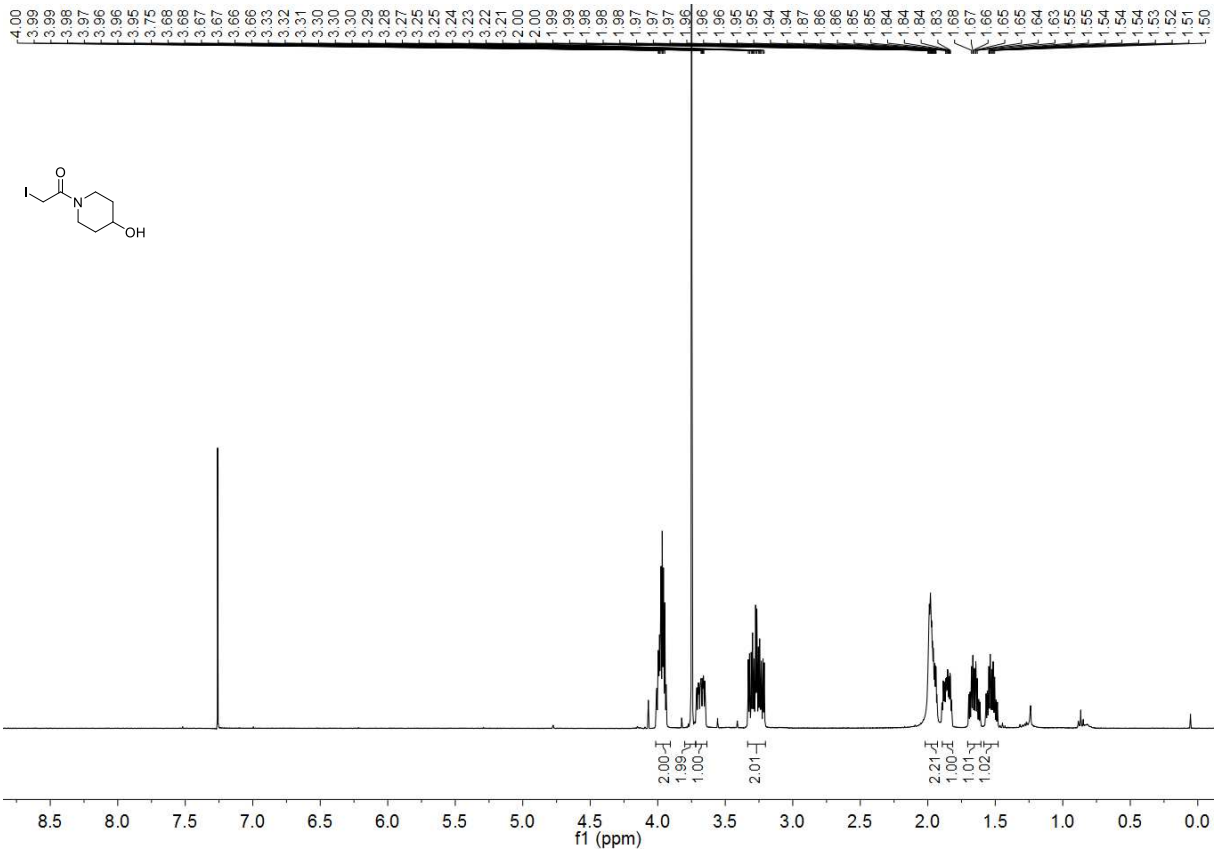

^{1}H NMR (400.13 MHz, 297 K, $CDCl_3$)

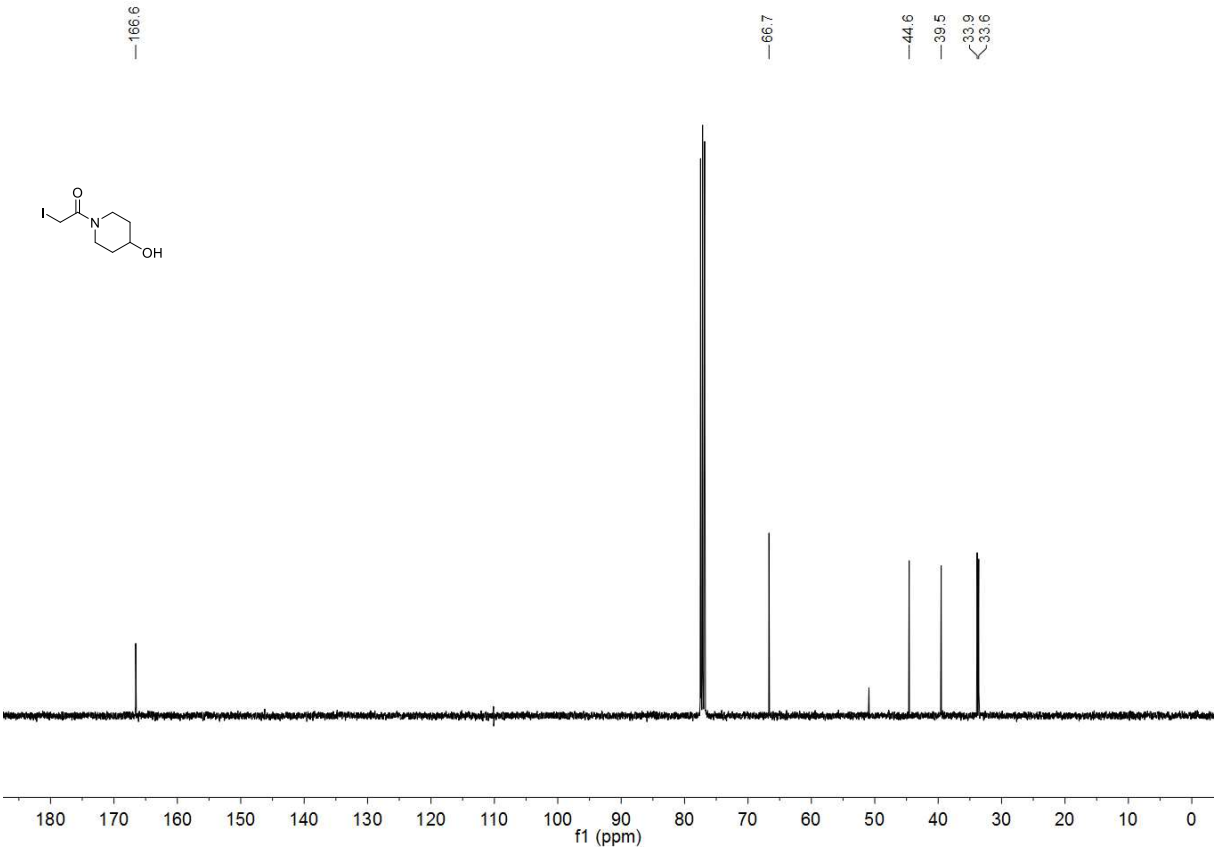

^{13}C NMR (100.62 MHz, 300 K, $CDCl_3$)

Fidaxomicin Piperidin-4-ol (6a)

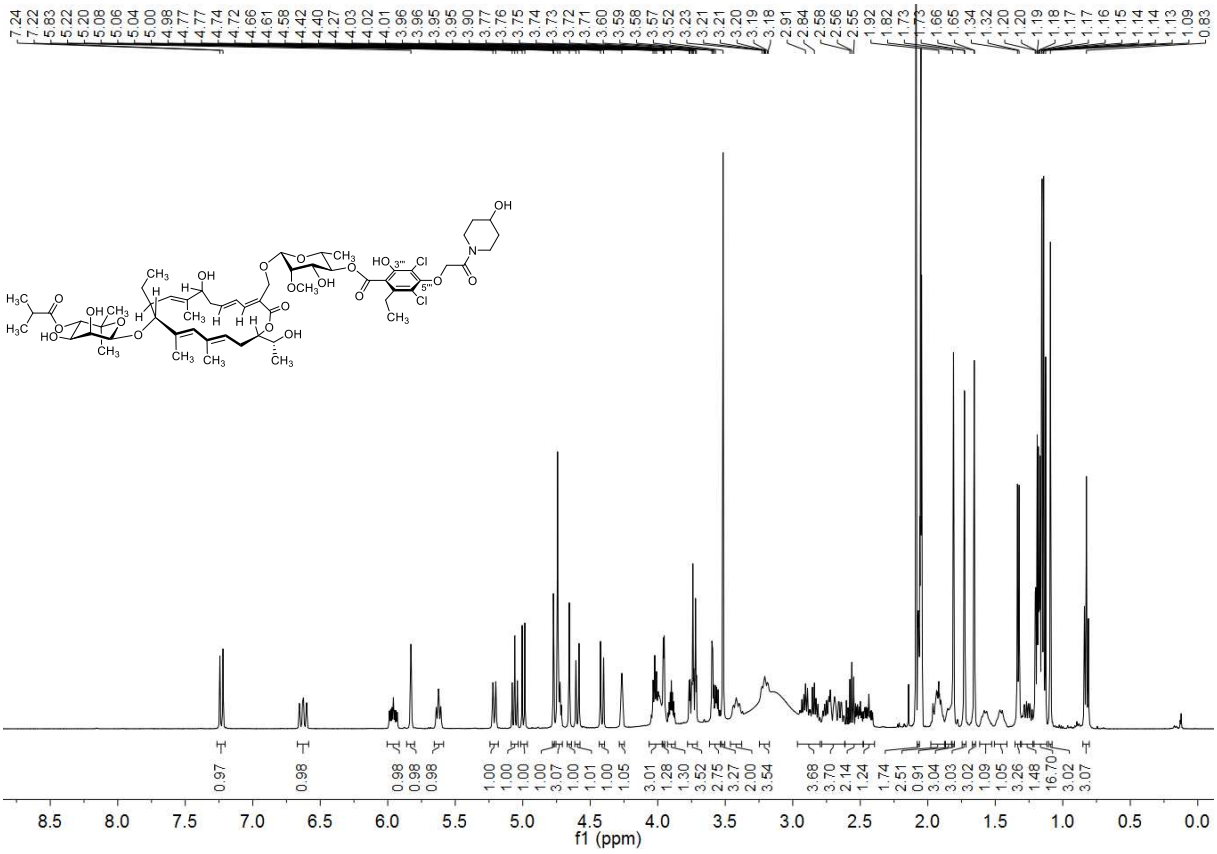

^{1}H NMR (500.13 MHz, 300 K, acetone-d_6)

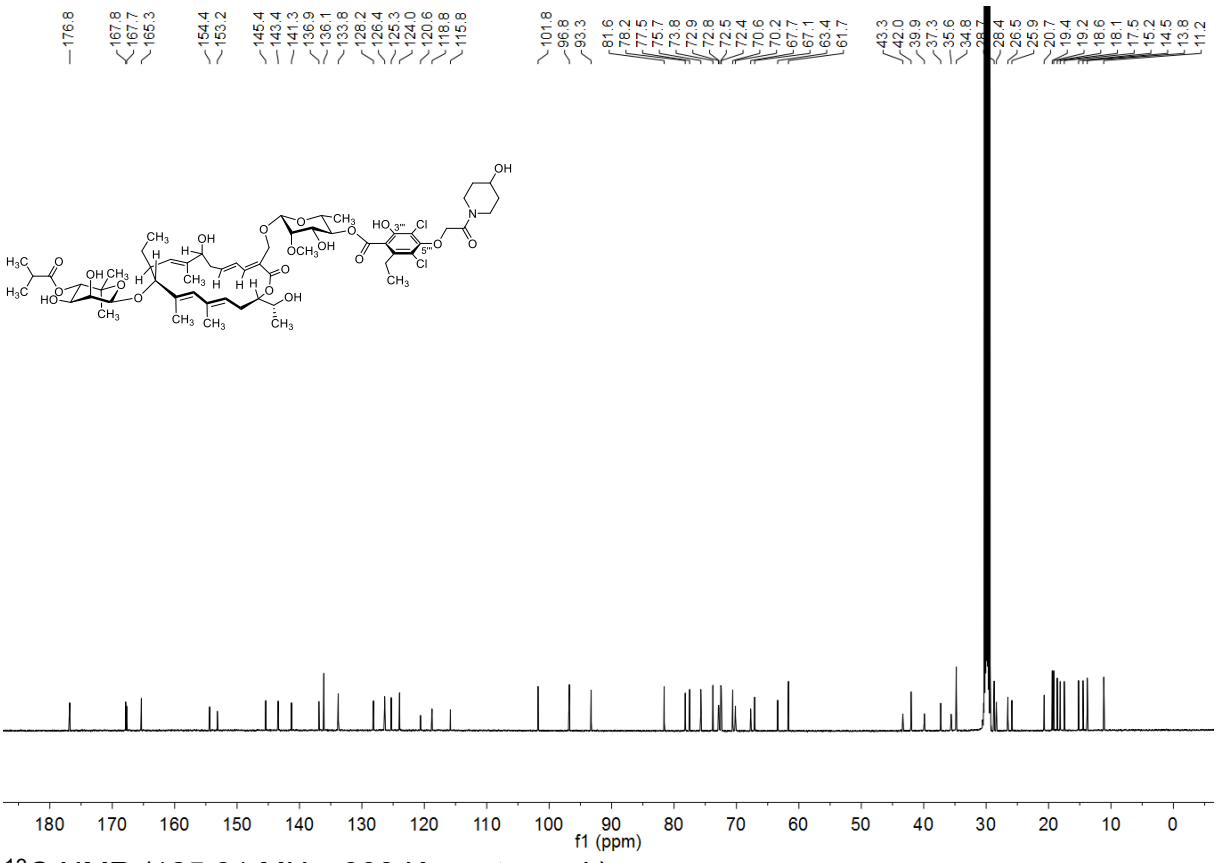

^{13}C NMR (125.81 MHz, 300 K, acetone-d_6)

Fidaxomicin Di(piperidin-4-ol) (6b)

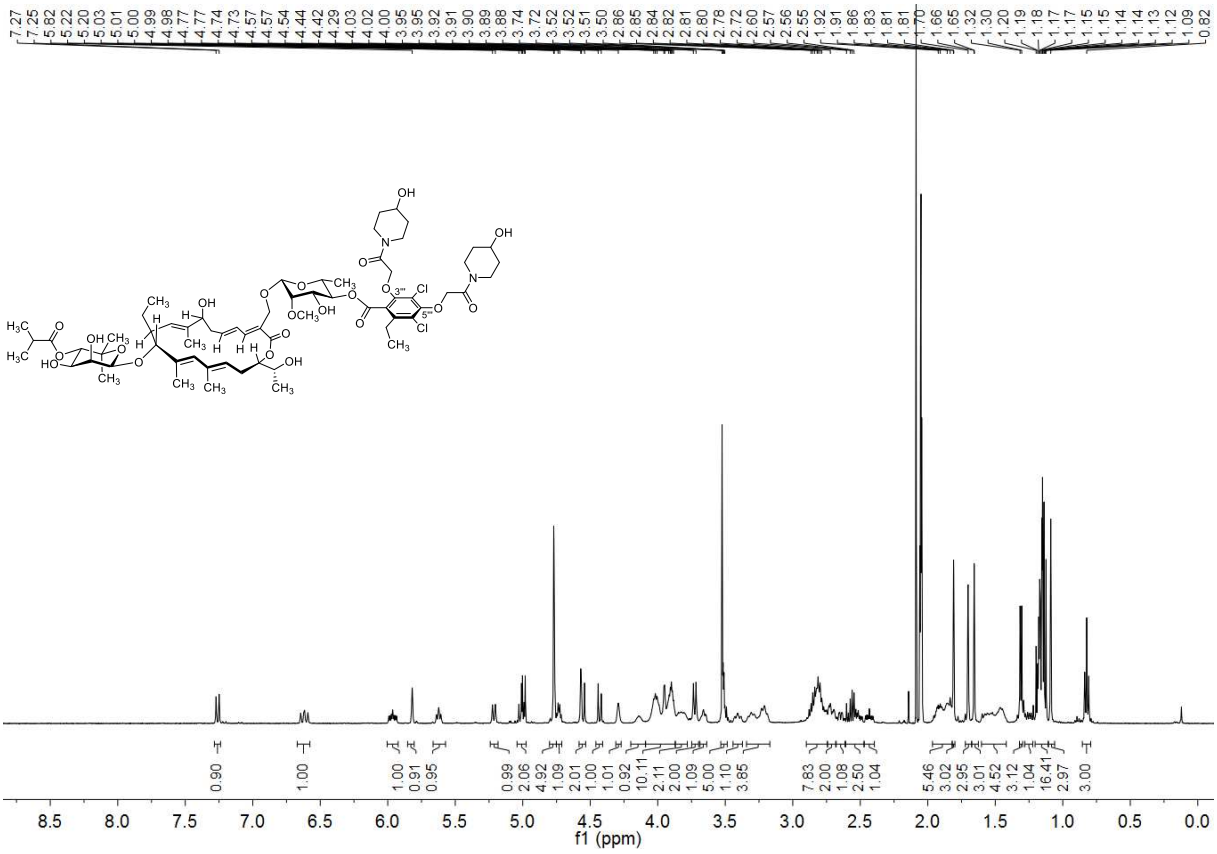

^{1}H NMR (500.25 MHz, 298 K, acetone-d_6)

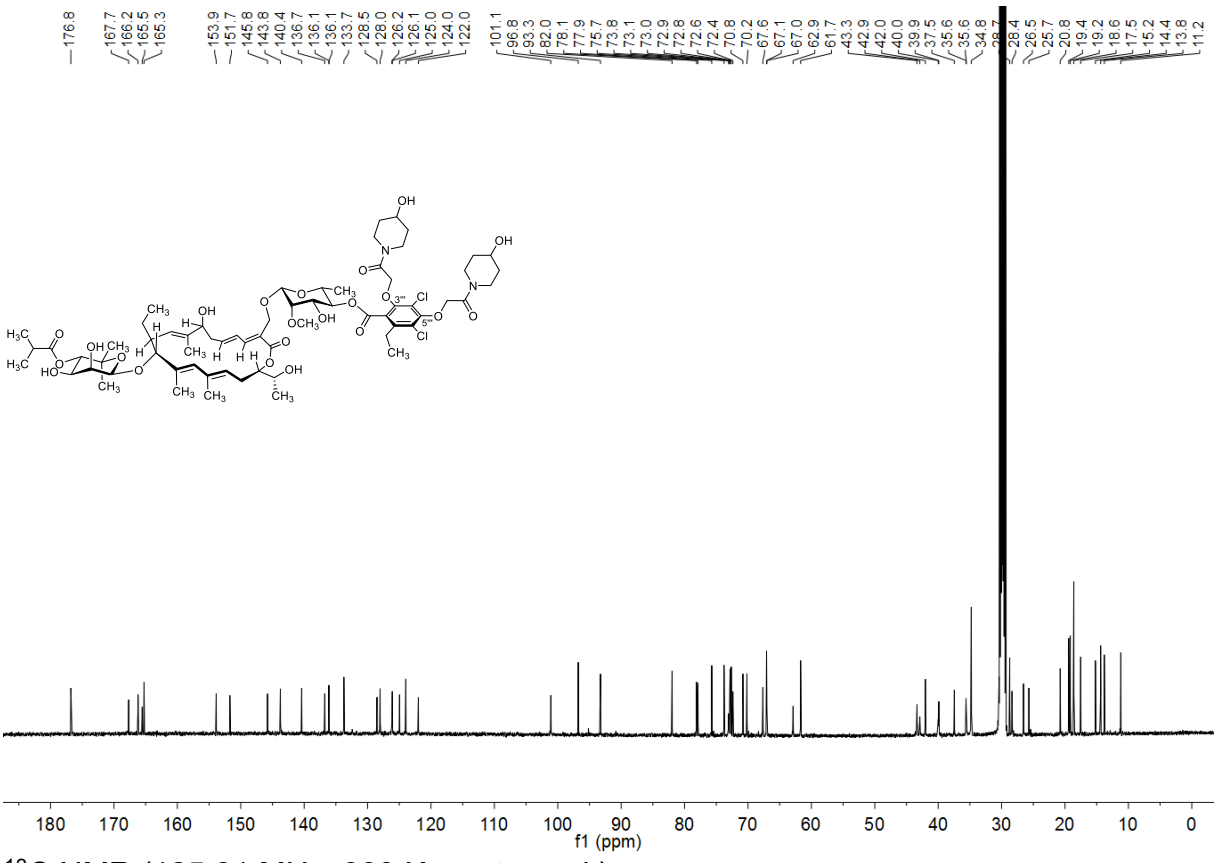

^{13}C NMR (125.81 MHz, 300 K, acetone-d_6)

2,5,8,11,14,17-Hexaoxanonadecan-19-yl 4-nitrobenzenesulfonate

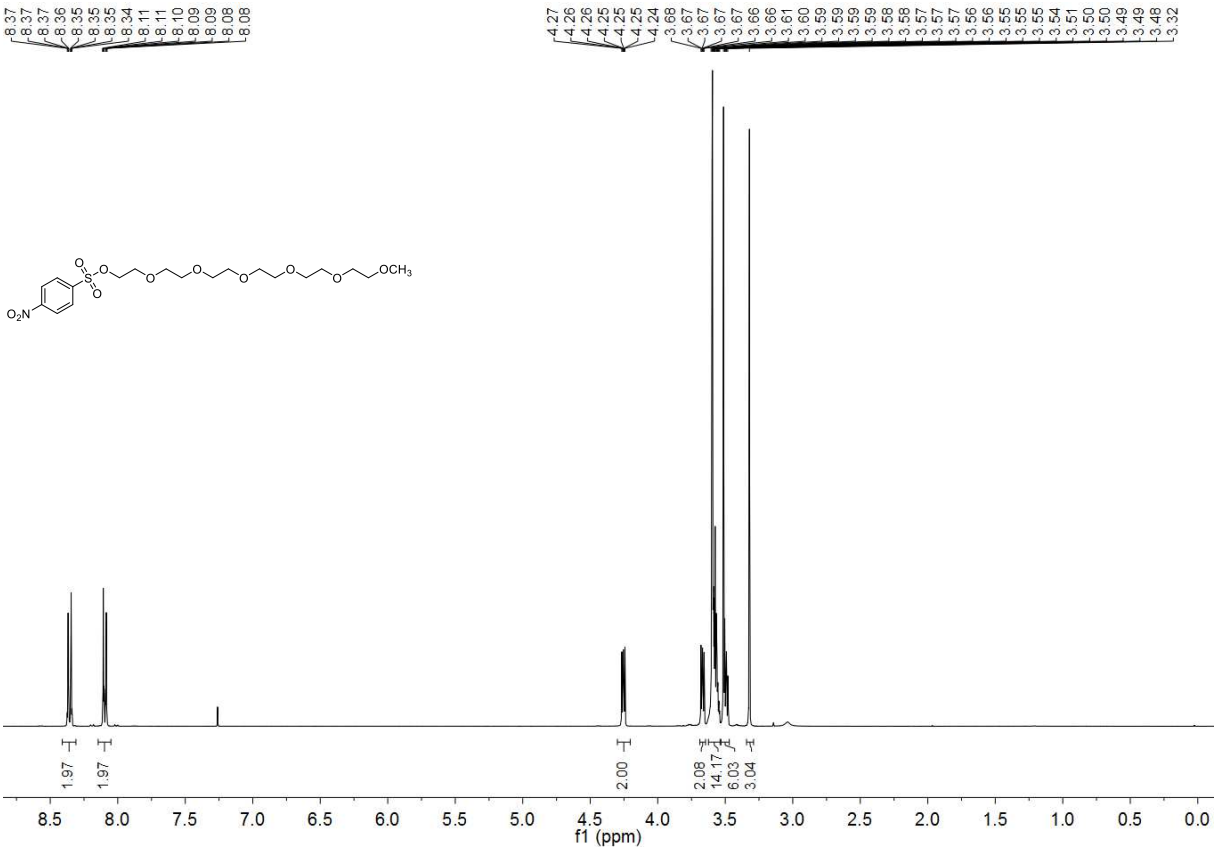

^{1}H NMR (400.13 MHz, 300 K, $CDCl_3$)

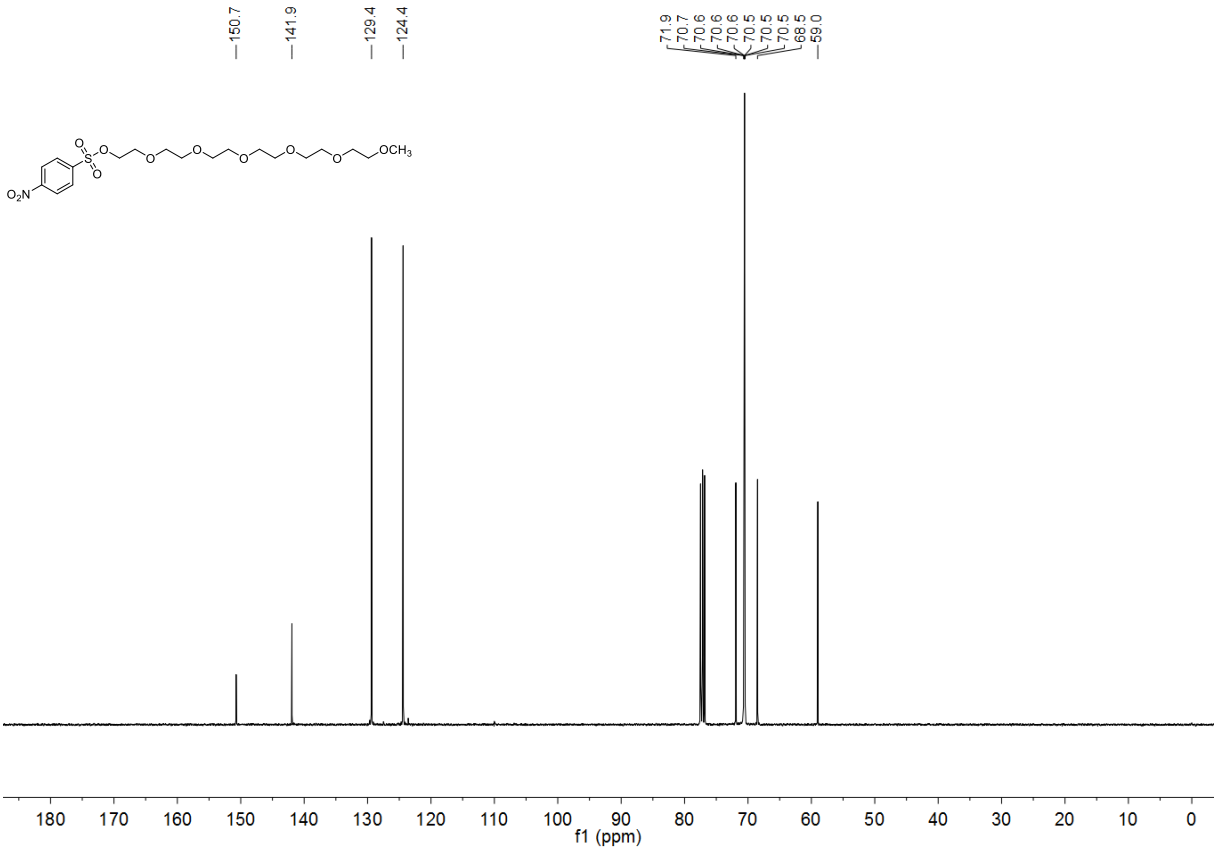

^{13}C NMR (100.62 MHz, 300 K, $CDCl_3$)

HEG-fidaxomicin (7a)

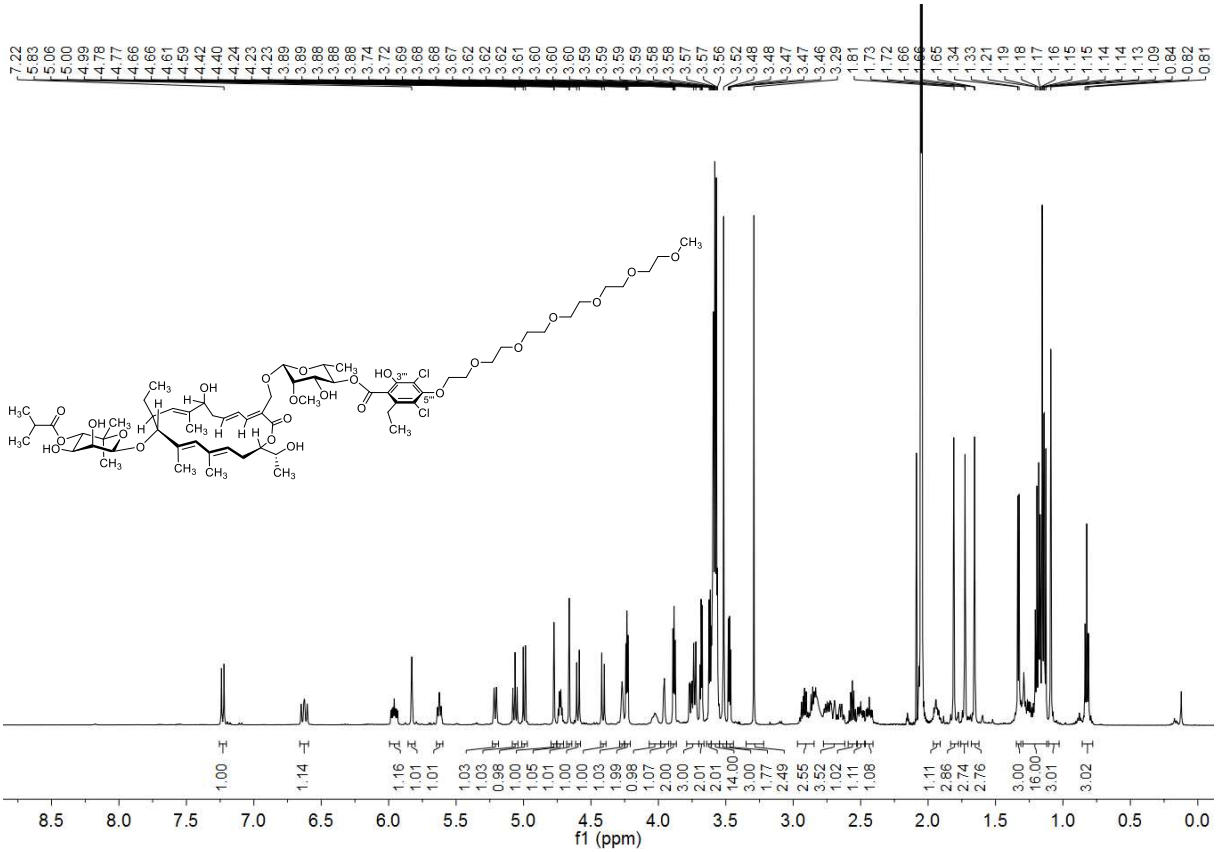

^{1}H NMR (600.23 MHz, 298 K, acetone-d_6, water suppression by presaturation)

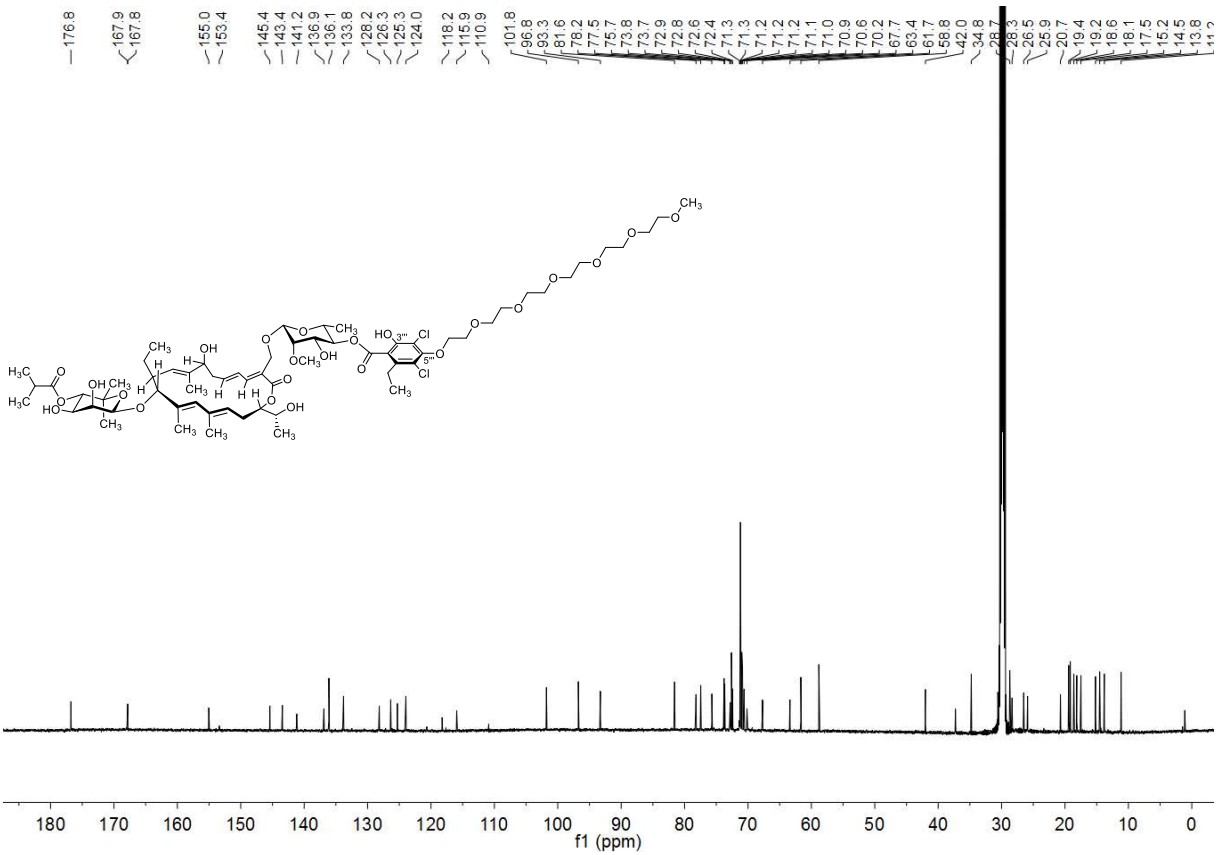

^{13}C NMR (150.94 MHz, 298 K, acetone-d_6)

Bis(HEG)-fidaxomicin (7b)

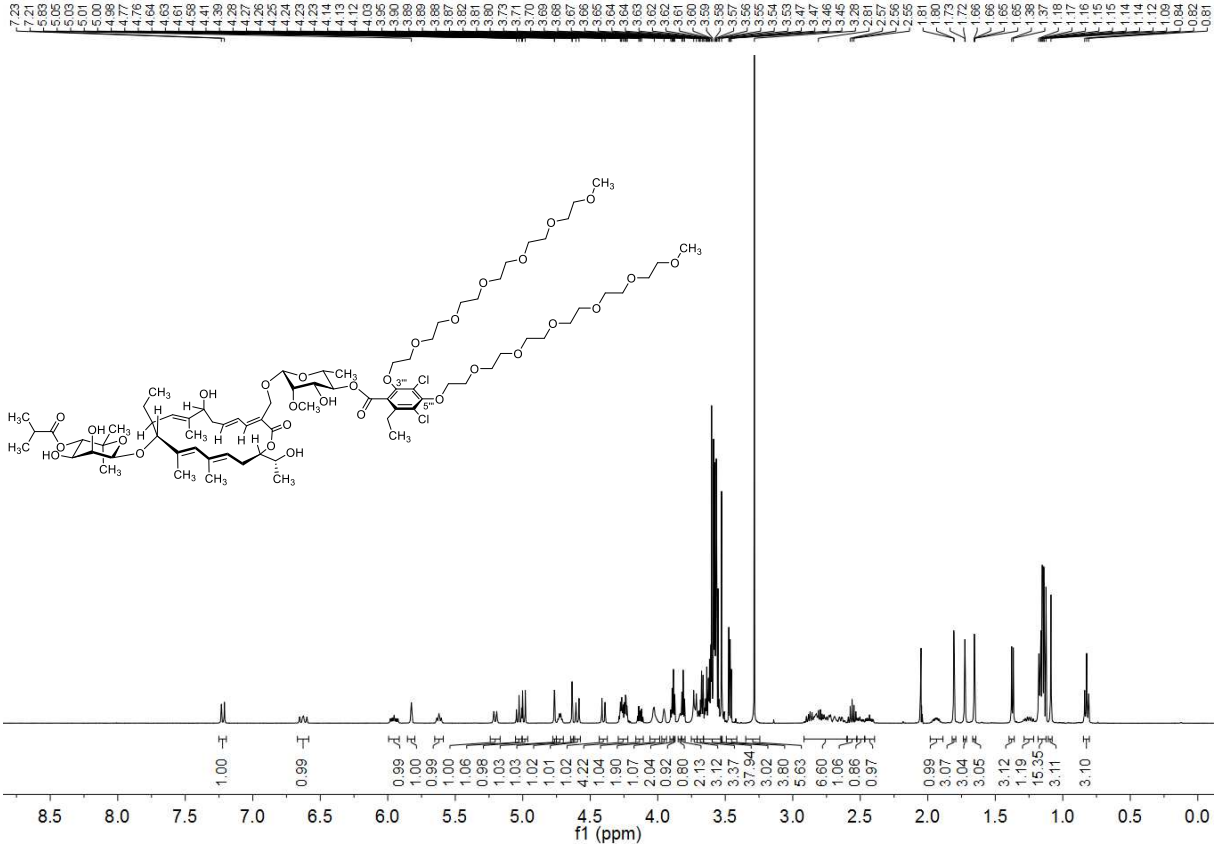

^{1}H NMR (500.13 MHz, 298 K, acetone-d_6)

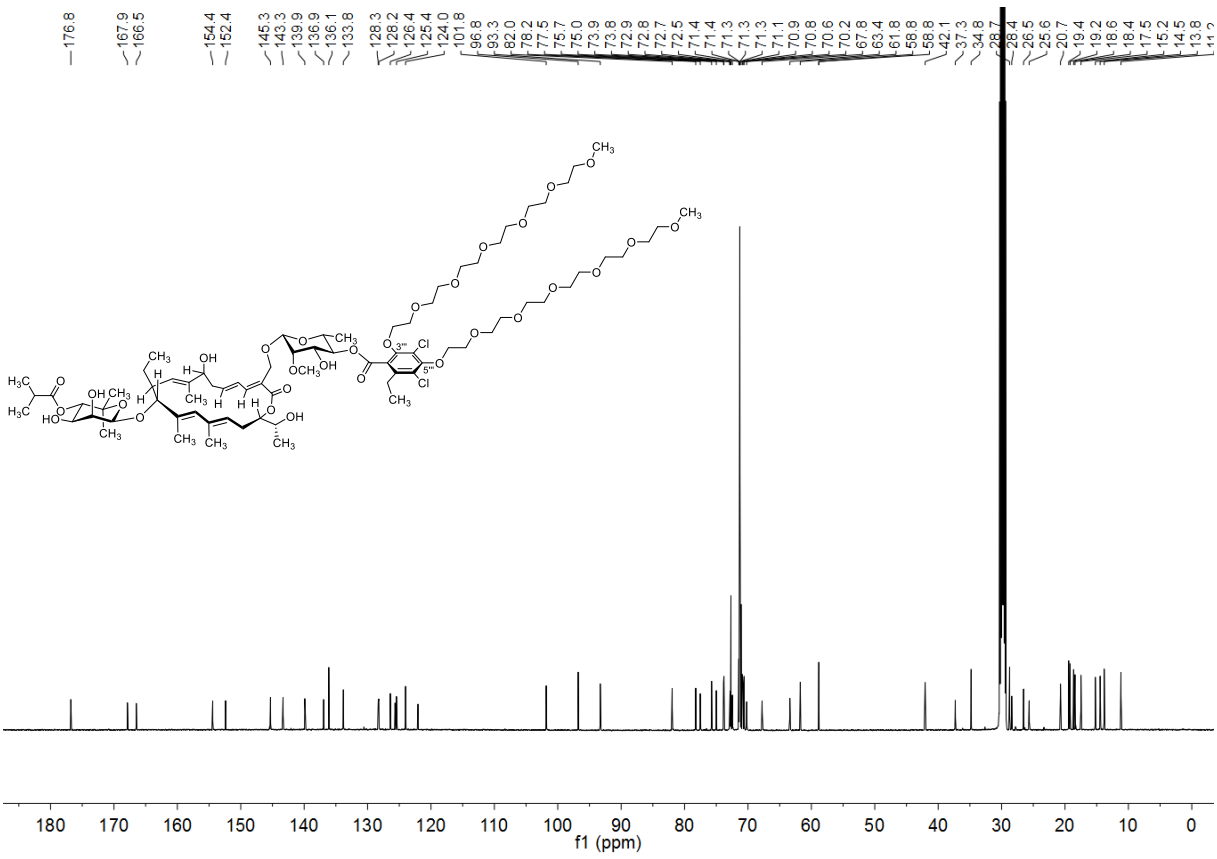

^{13}C NMR (125.81 MHz, 303 K, acetone-d_6)

SuFEx1-Fidaxomicin (8a)

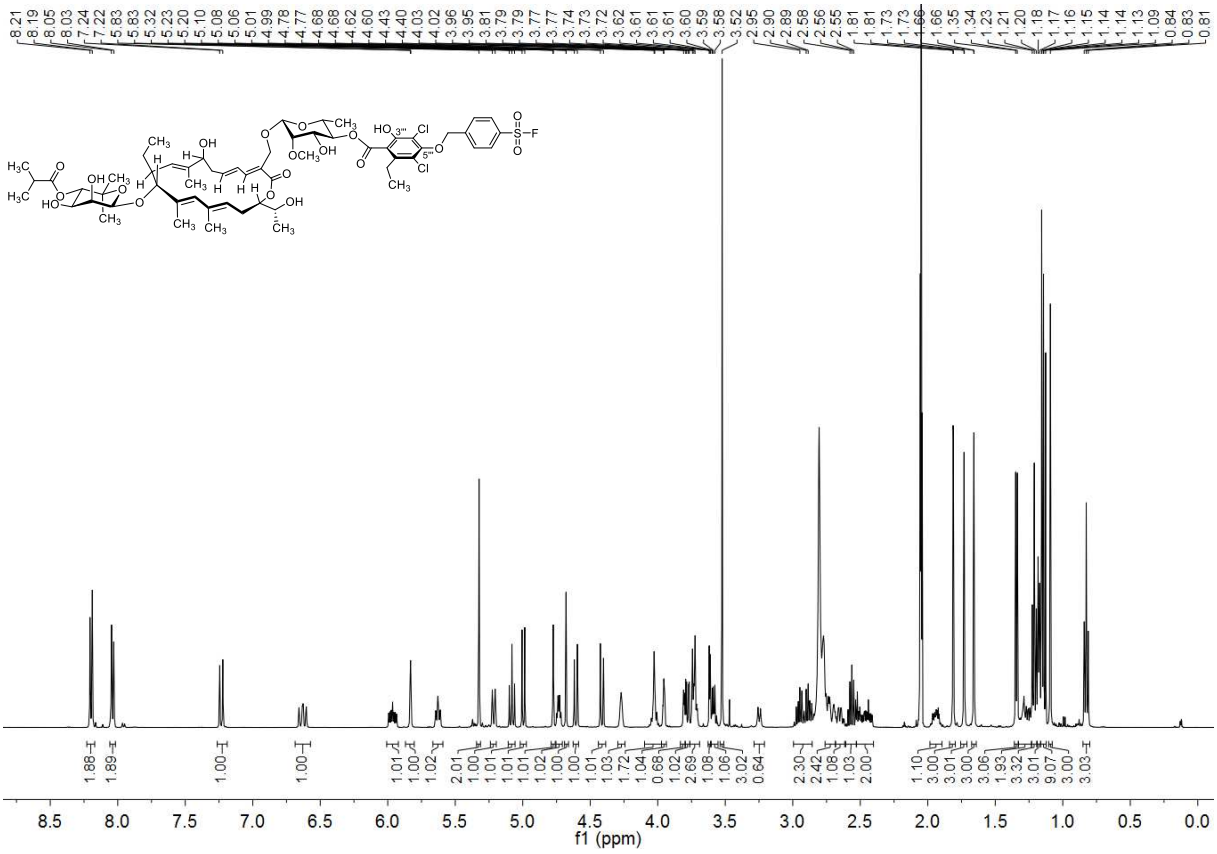

^{1}H NMR (500.13 MHz, 300 K, acetone-d_6)

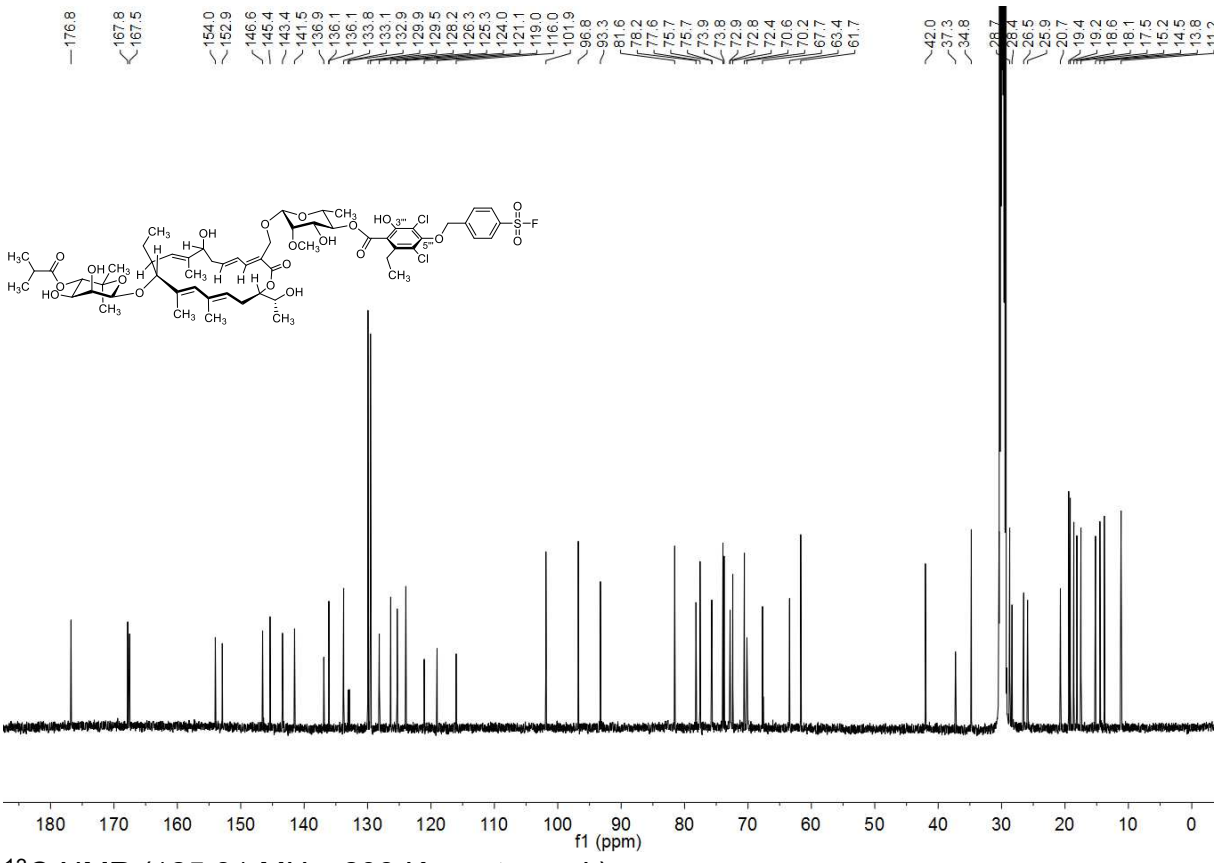

^{13}C NMR (125.81 MHz, 298 K, acetone-d_6)

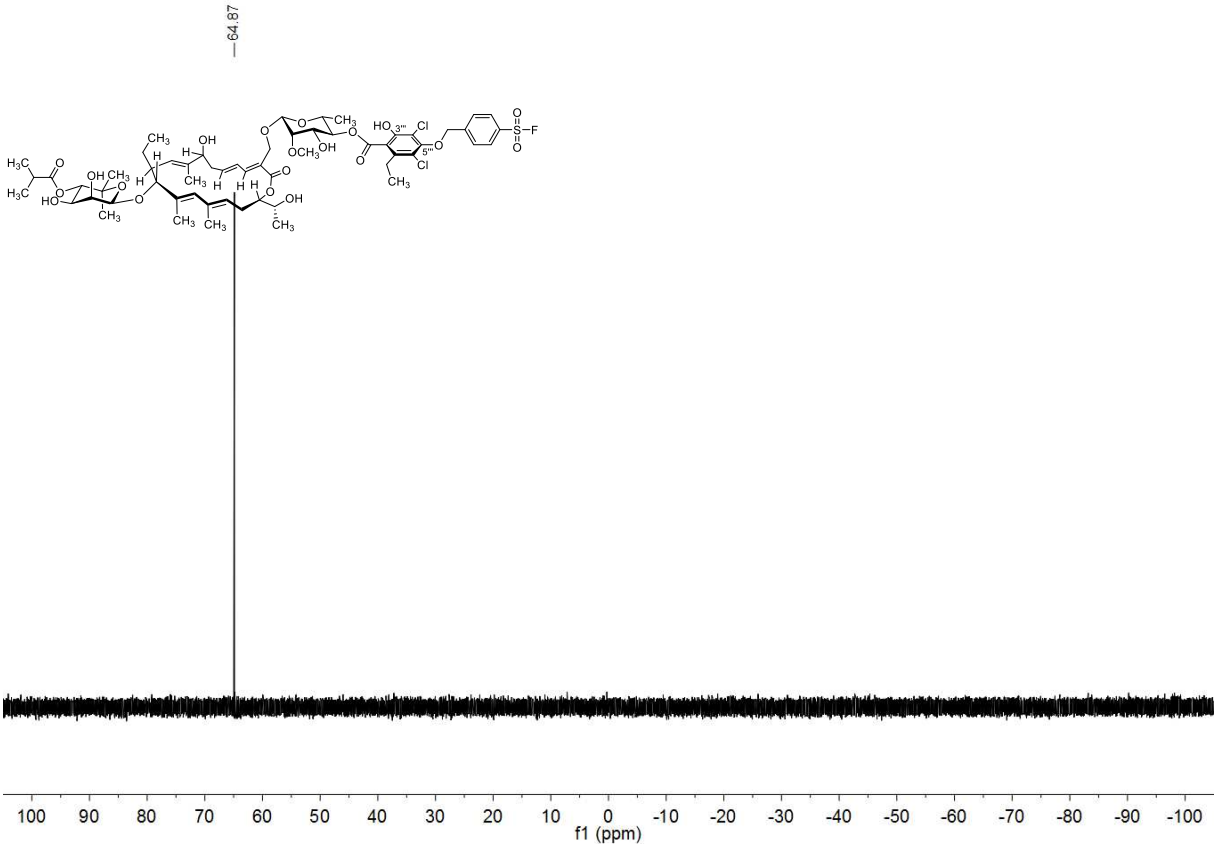

^{19}F NMR (376.5 MHz, 300 K, acetone-d_6)

SuFEx2-Fidaxomicin (8b)

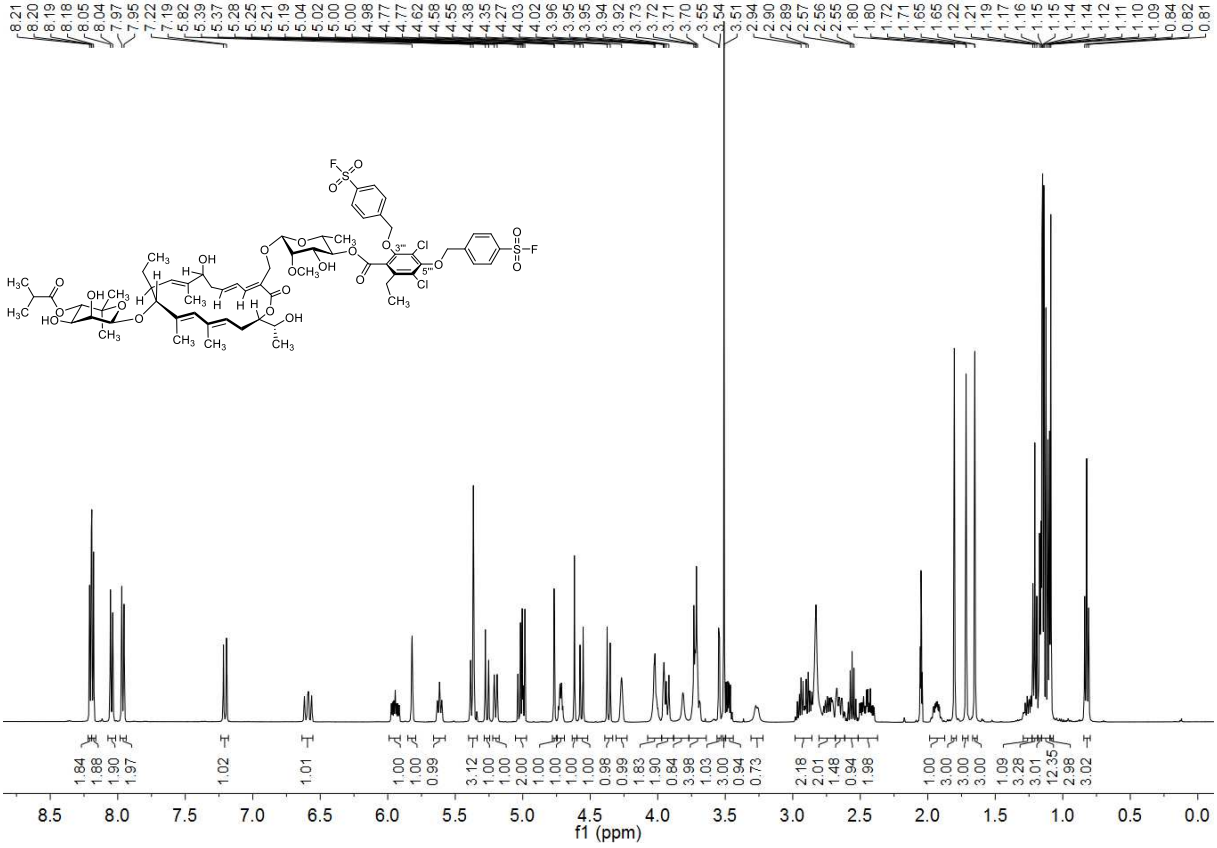

^{1}H NMR (500.13 MHz, 300 K, acetone-d_6)

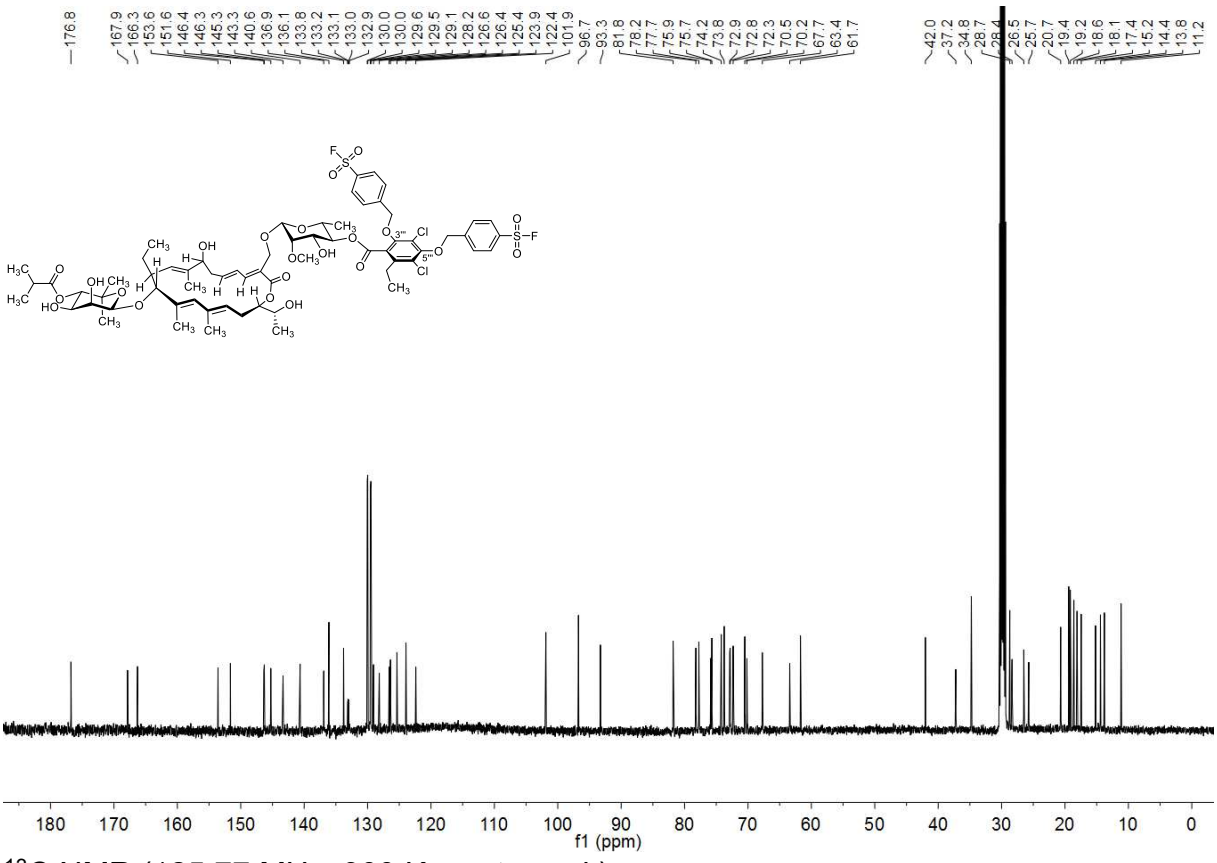

^{13}C NMR (125.77 MHz, 300 K, acetone-d_6)

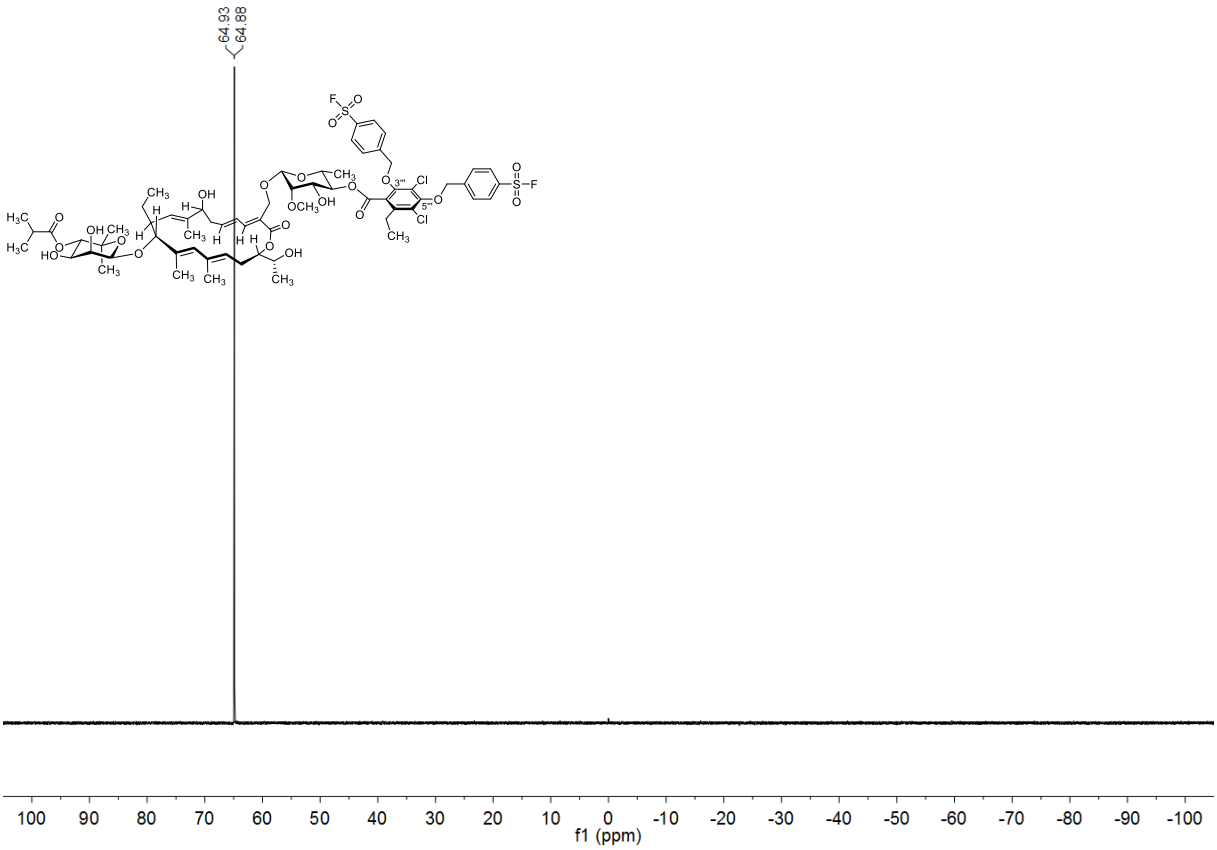

^{19}F NMR (376.50 MHz, 300 K, acetone-d_6)

3-Azidopropan-1-ol

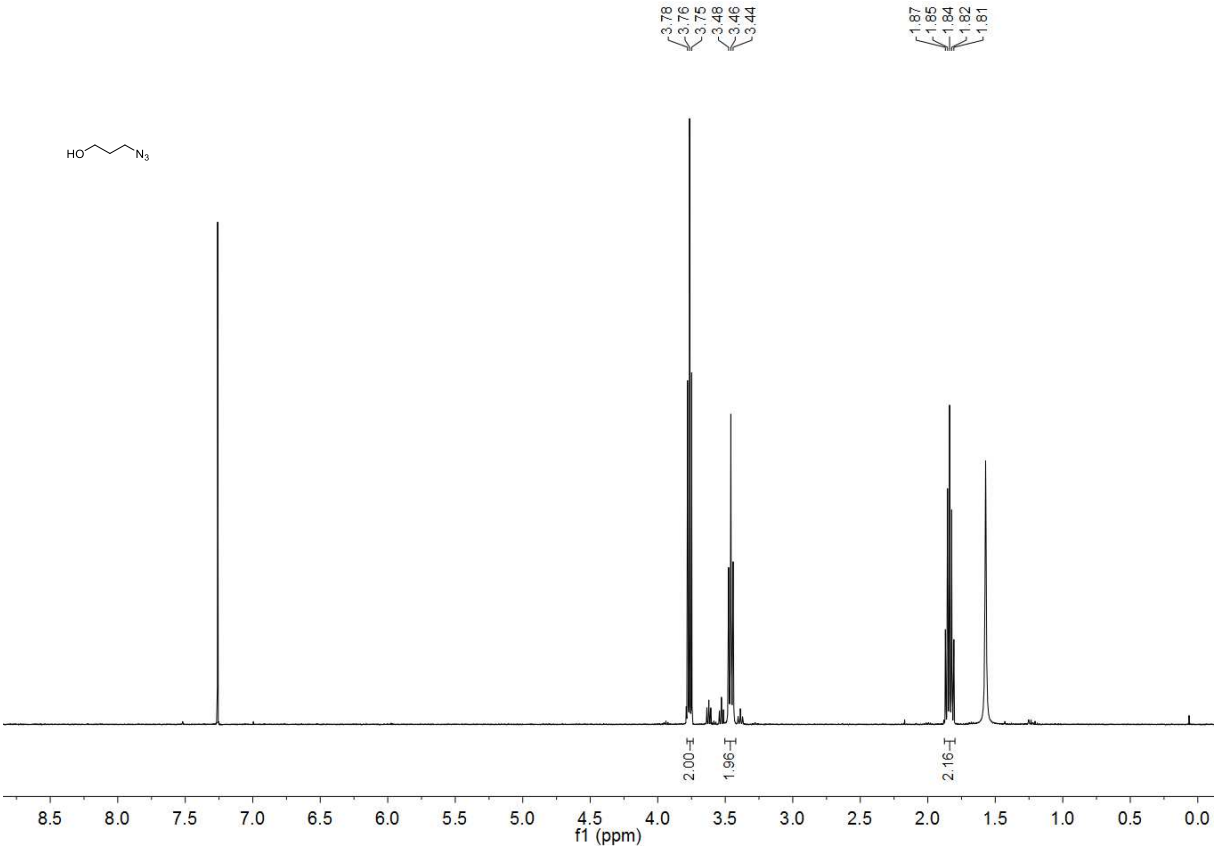

^{1}H NMR (400.13 MHz, 294 K, acetone-d_6)

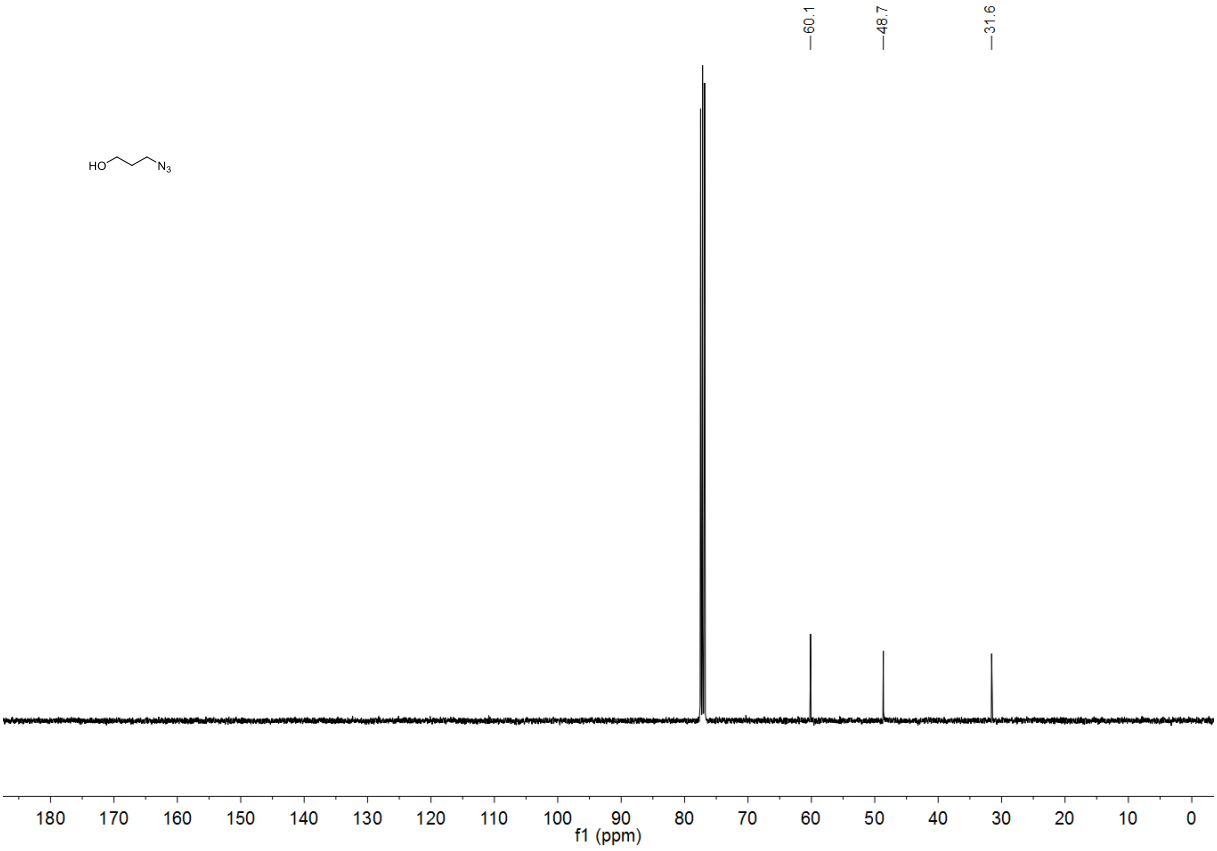

^{13}C NMR (100.62 MHz, 294 K, acetone-d_6)

3-Azidopropyl 4-nitrobenzenesulfonate

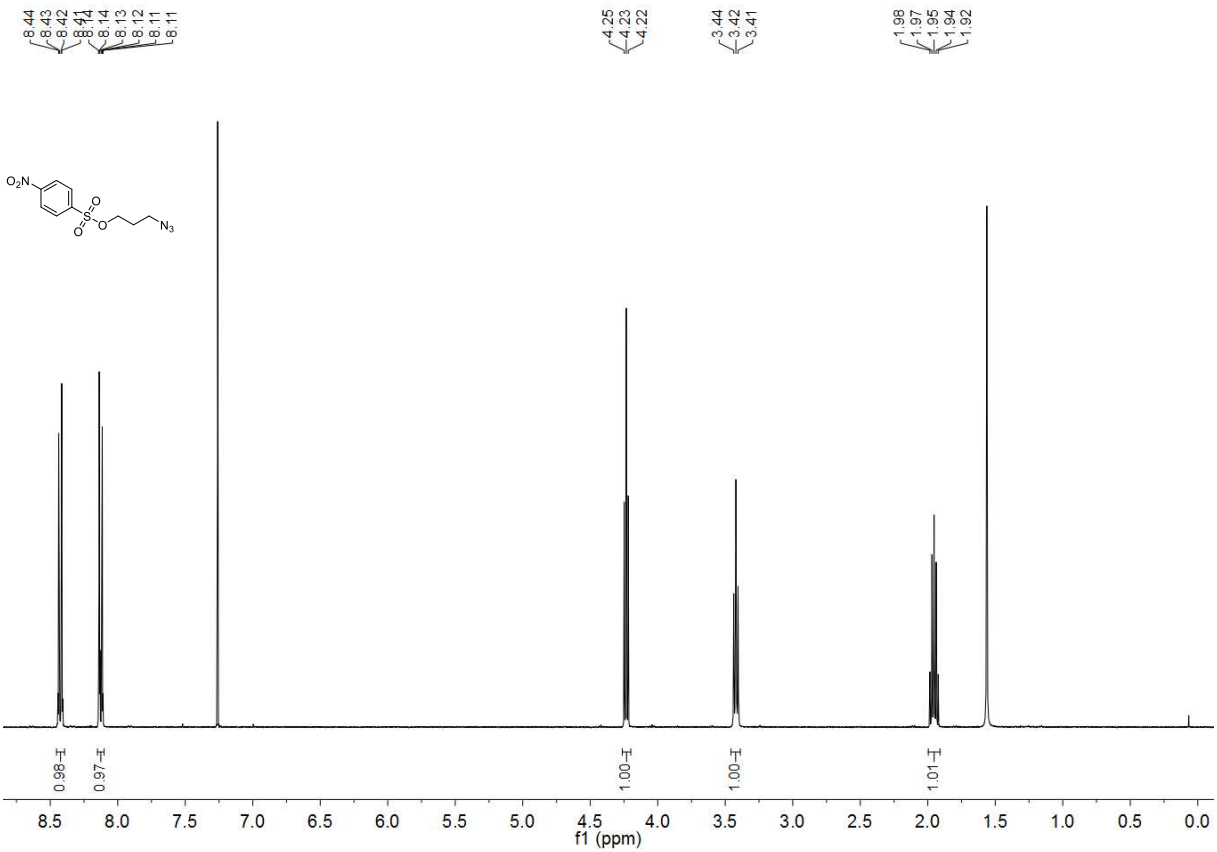

^{1}H NMR (400.13 MHz, 297 K, acetone-d_6)

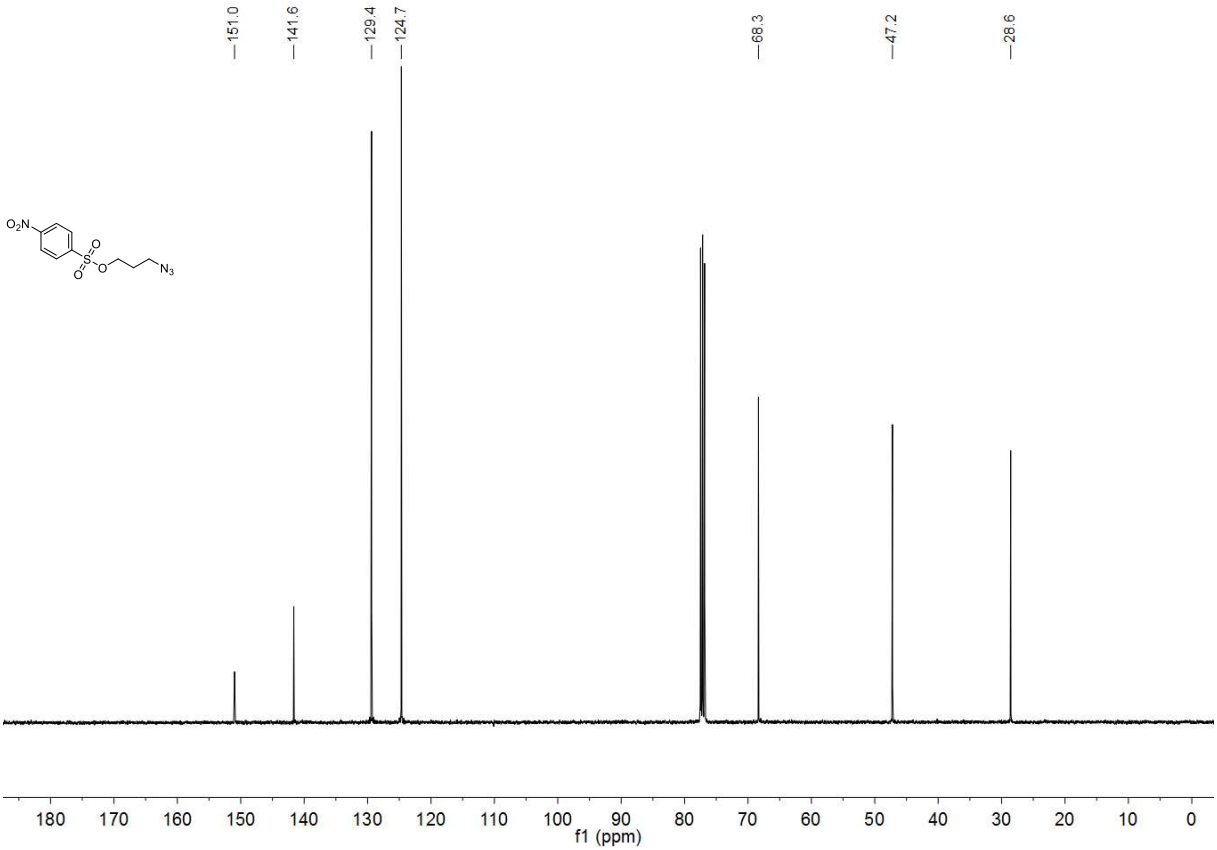

^{13}C NMR (100.62 MHz, 298 K, acetone-d_6)

Mono(azidopropyl)fidaxomicin (10a)

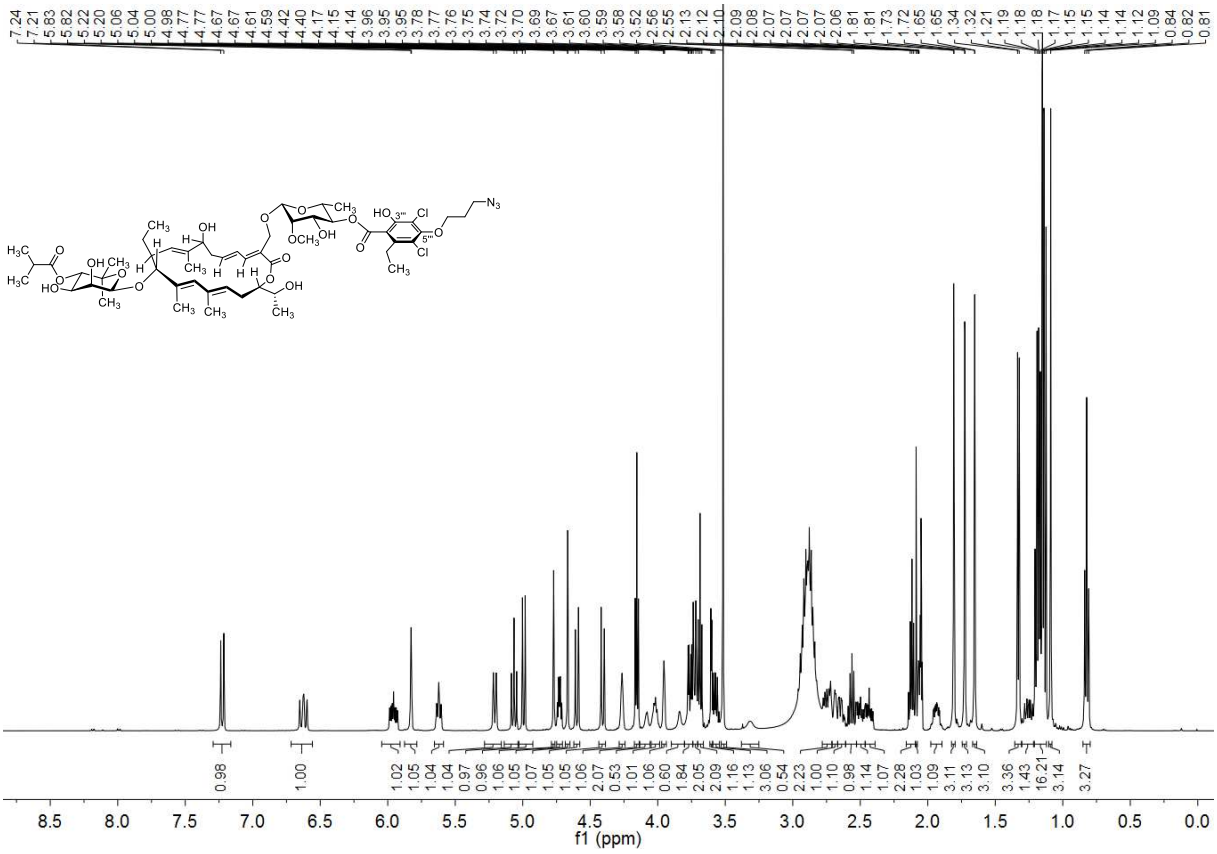

^{1}H NMR (500.13 MHz, 300 K, acetone-d_6)

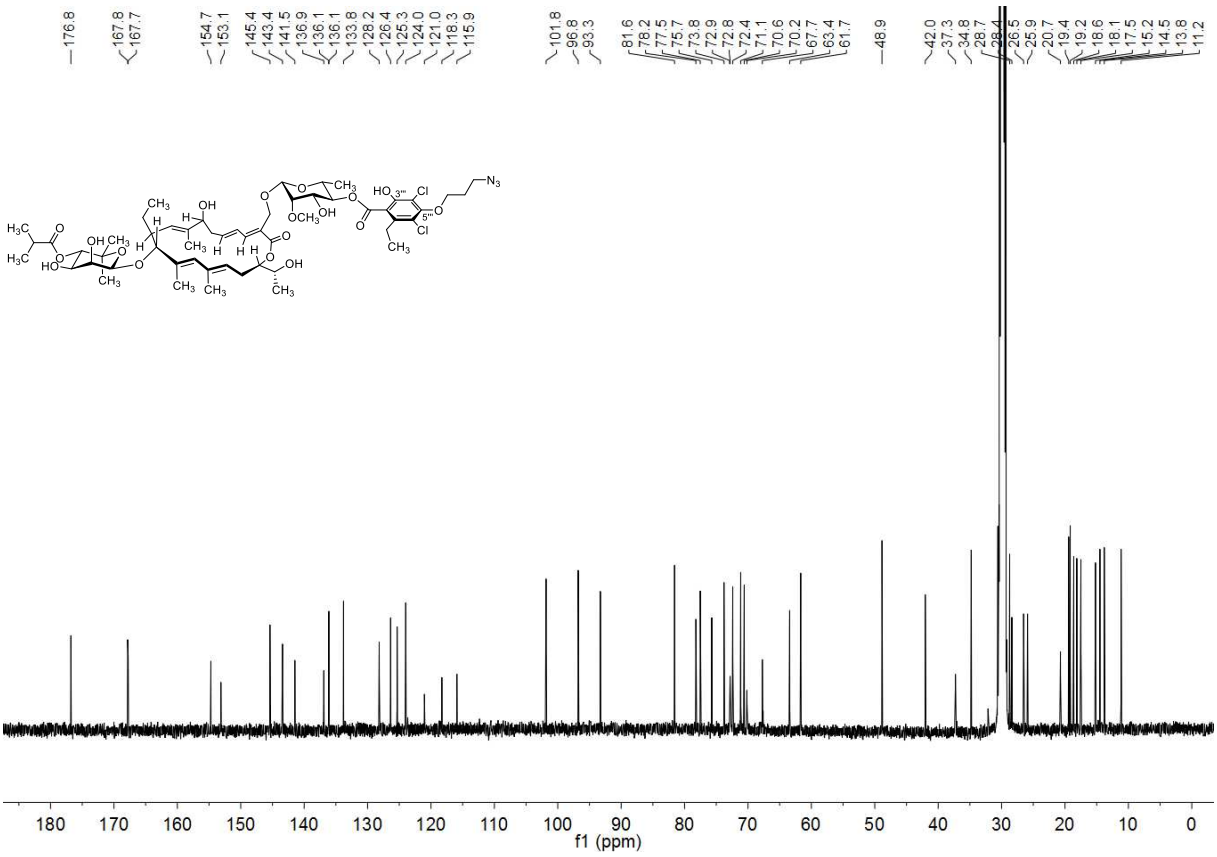

^{13}C NMR (125.81 MHz, 300 K, acetone-d_6)

Bis(azidopropyl)fidaxomicin (10b)

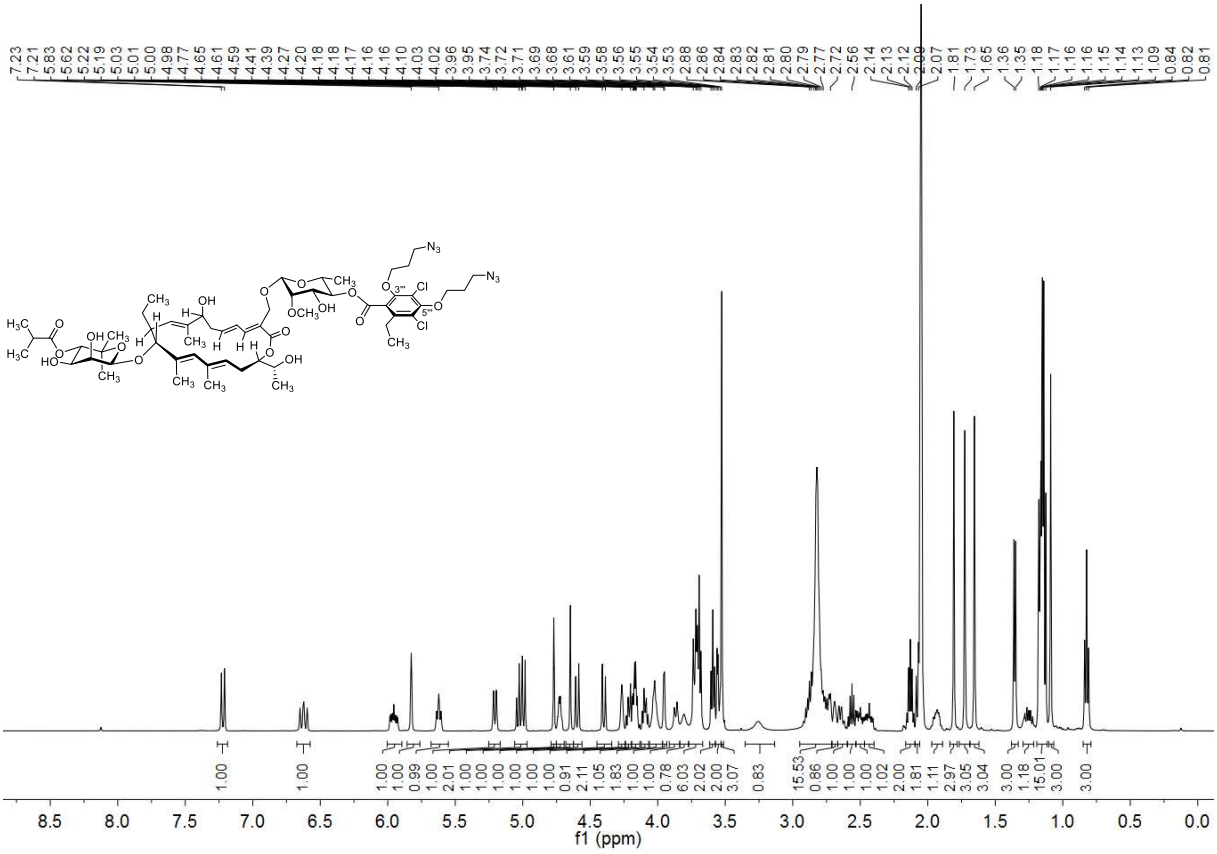

^{1}H NMR (500.30 MHz, 300 K, acetone-d_6)

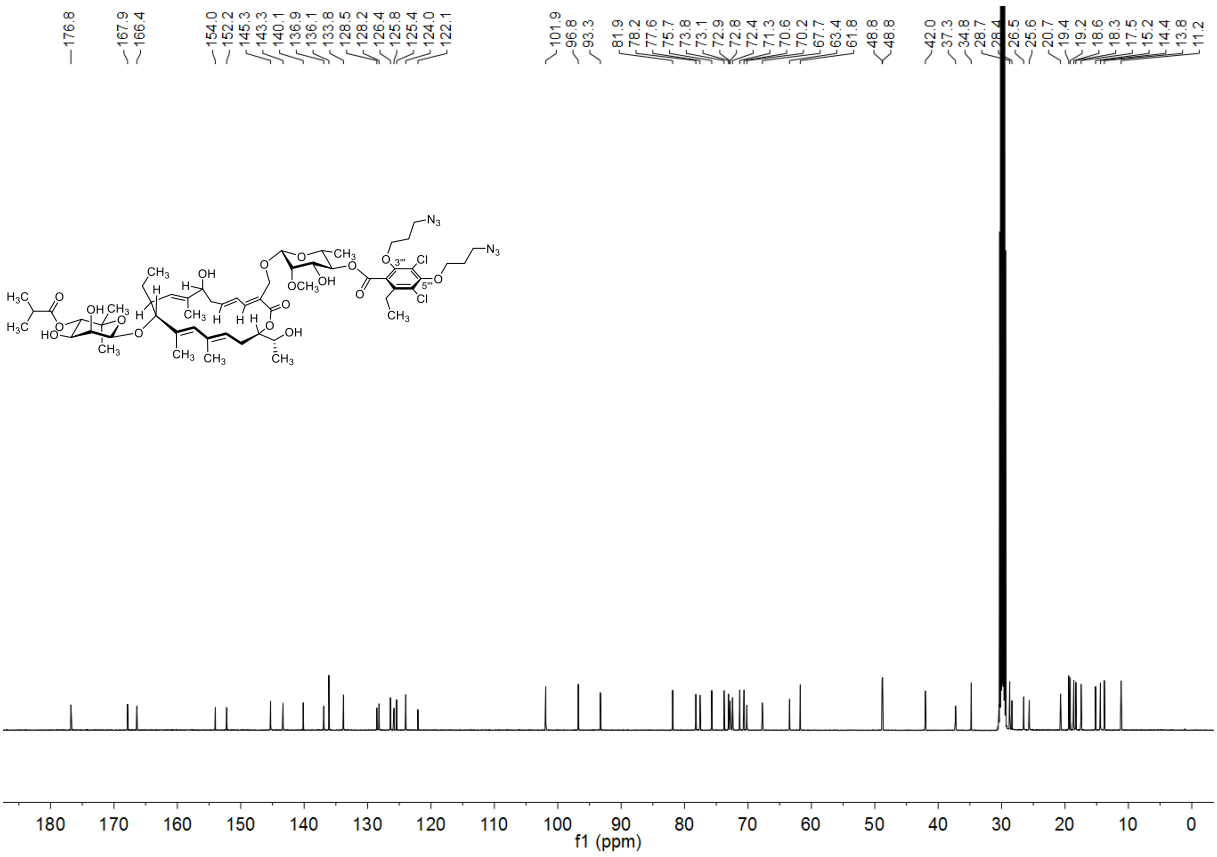

^{13}C NMR (125.81 MHz, 300 K, acetone-d_6)

Monotriazole with 3-Ethynylaniline (11a)

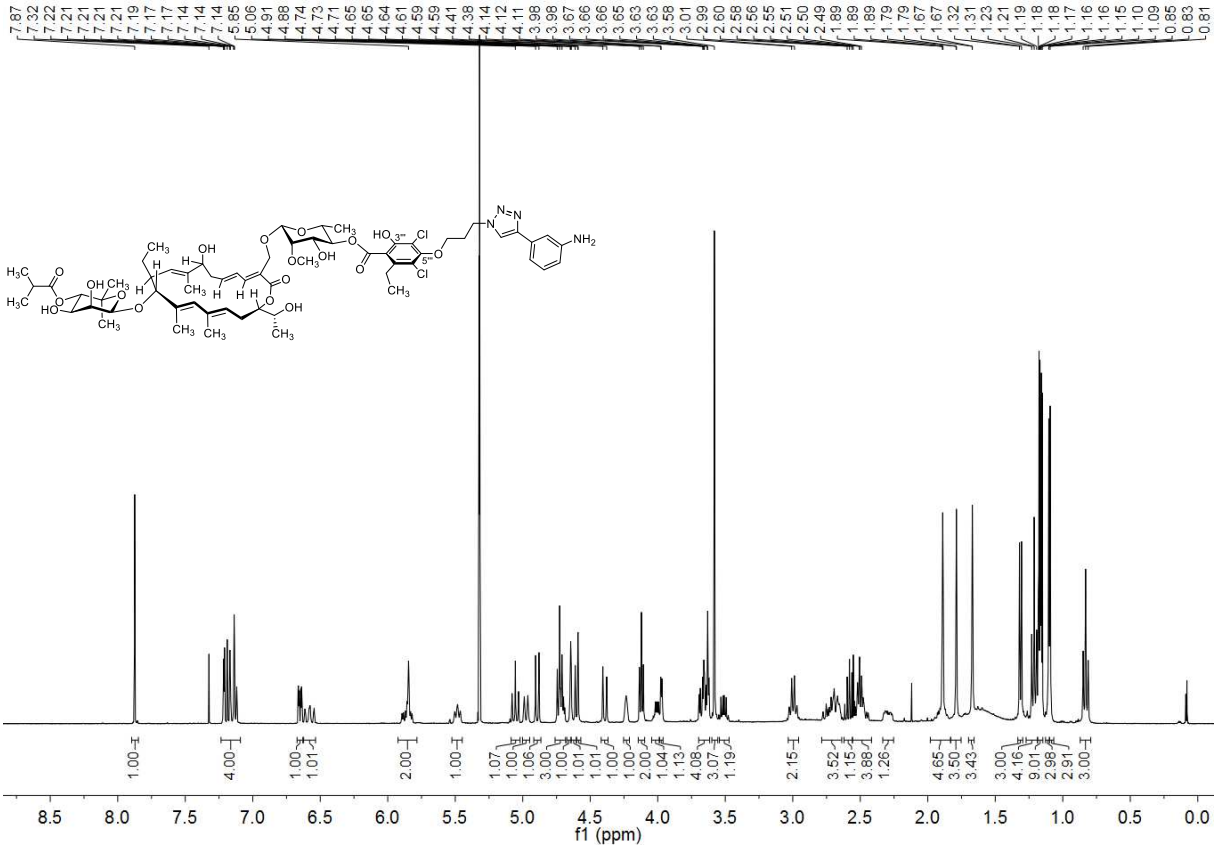

^{1}H NMR (400.23 MHz, 298 K, CD_2Cl_2)

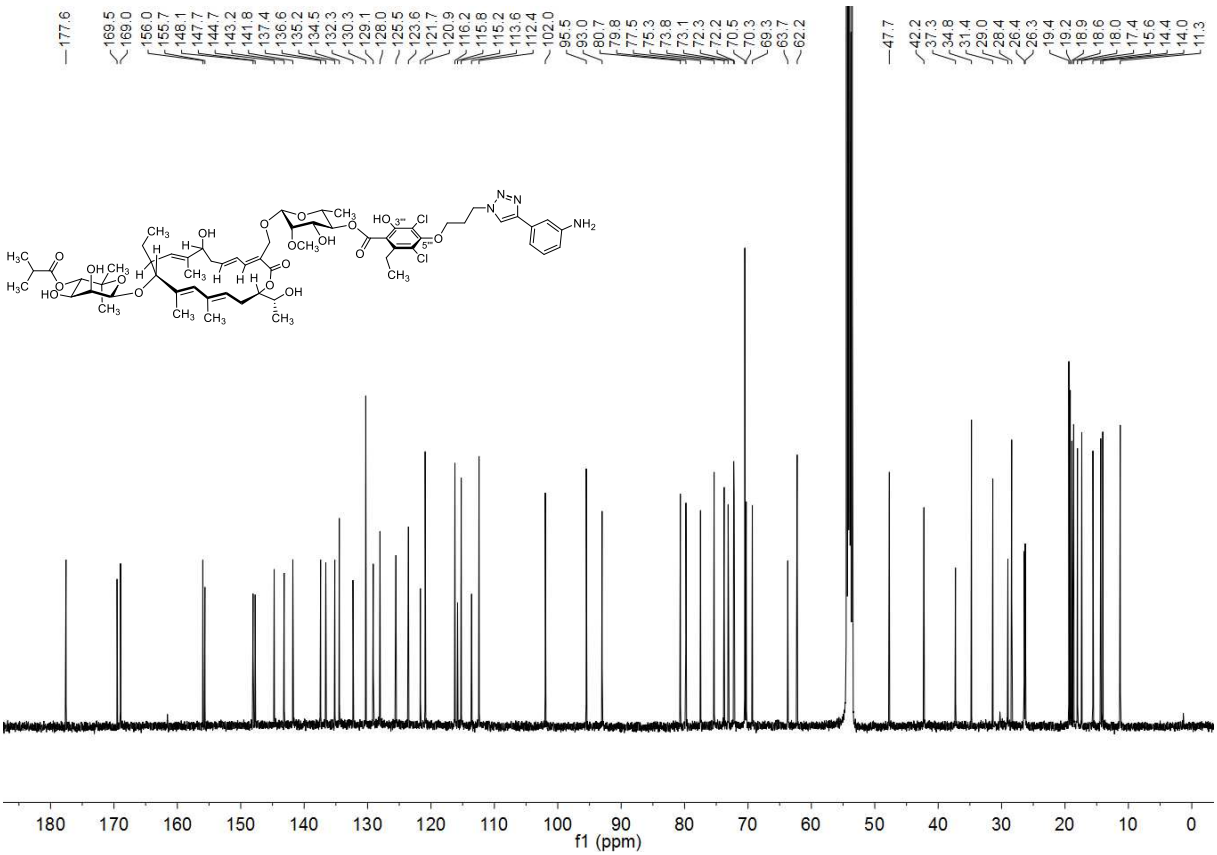

^{13}C NMR (125.81 MHz, 300 K, CD_2Cl_2)

Bistriazole with 3-Ethynylaniline (11b)

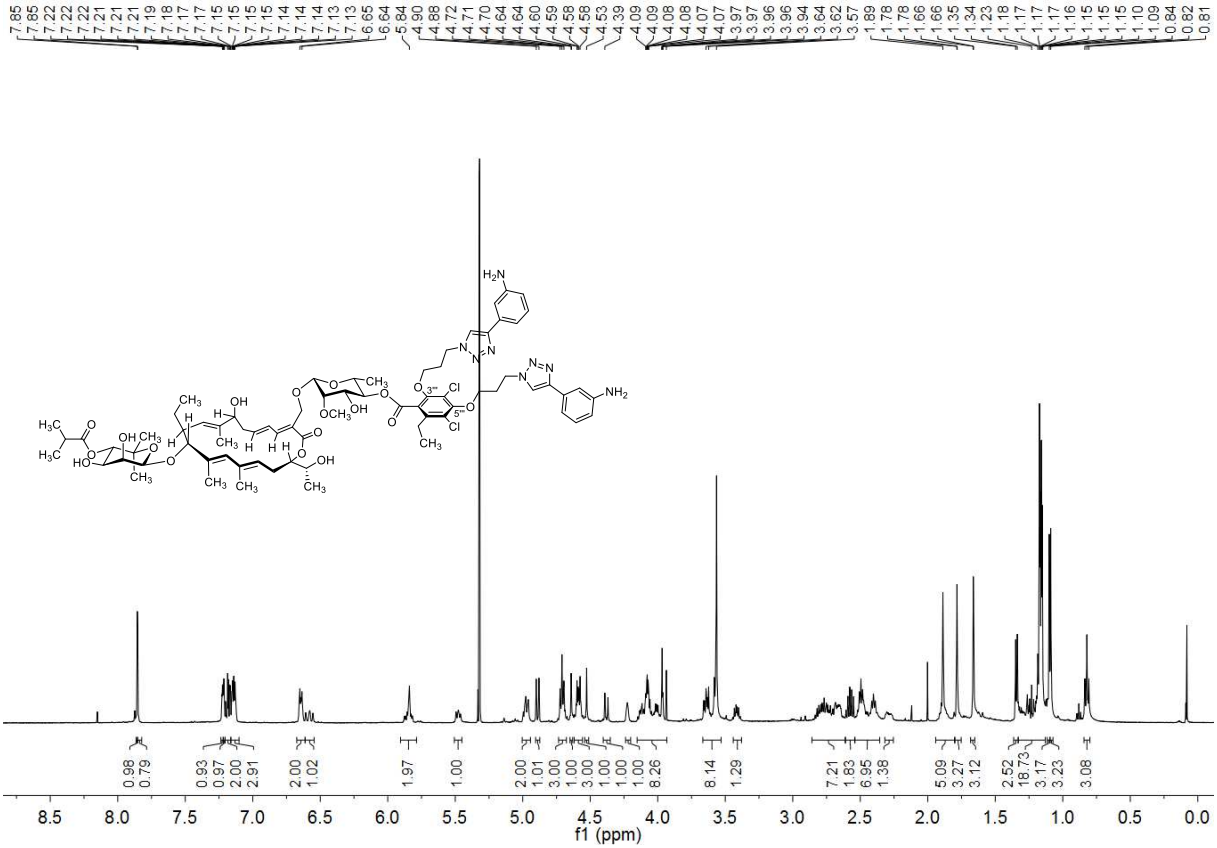

^{1}H NMR (500.25 MHz, 298 K, CD_2Cl_2)

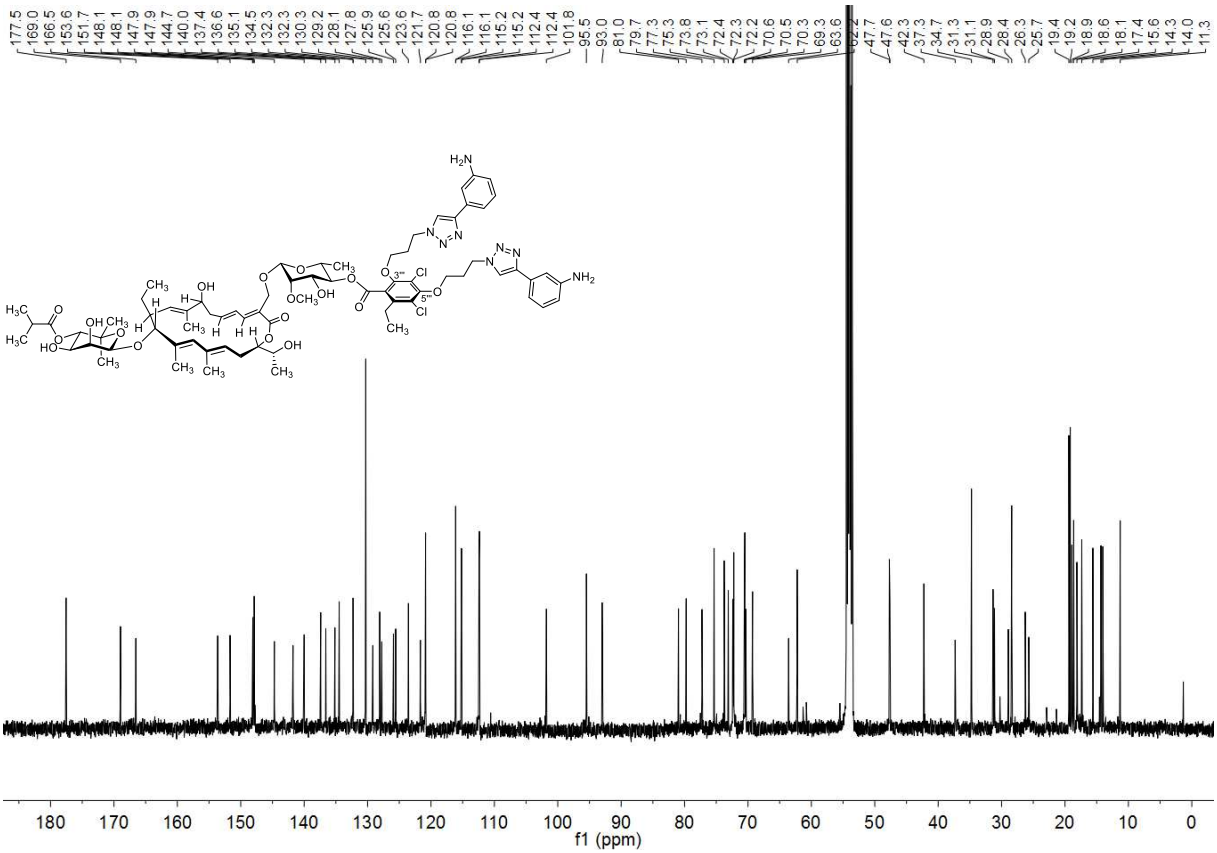

^{13}C NMR (125.81 MHz, 300 K, CD_2Cl_2)

Monotriazole with PEG5-acid (12)

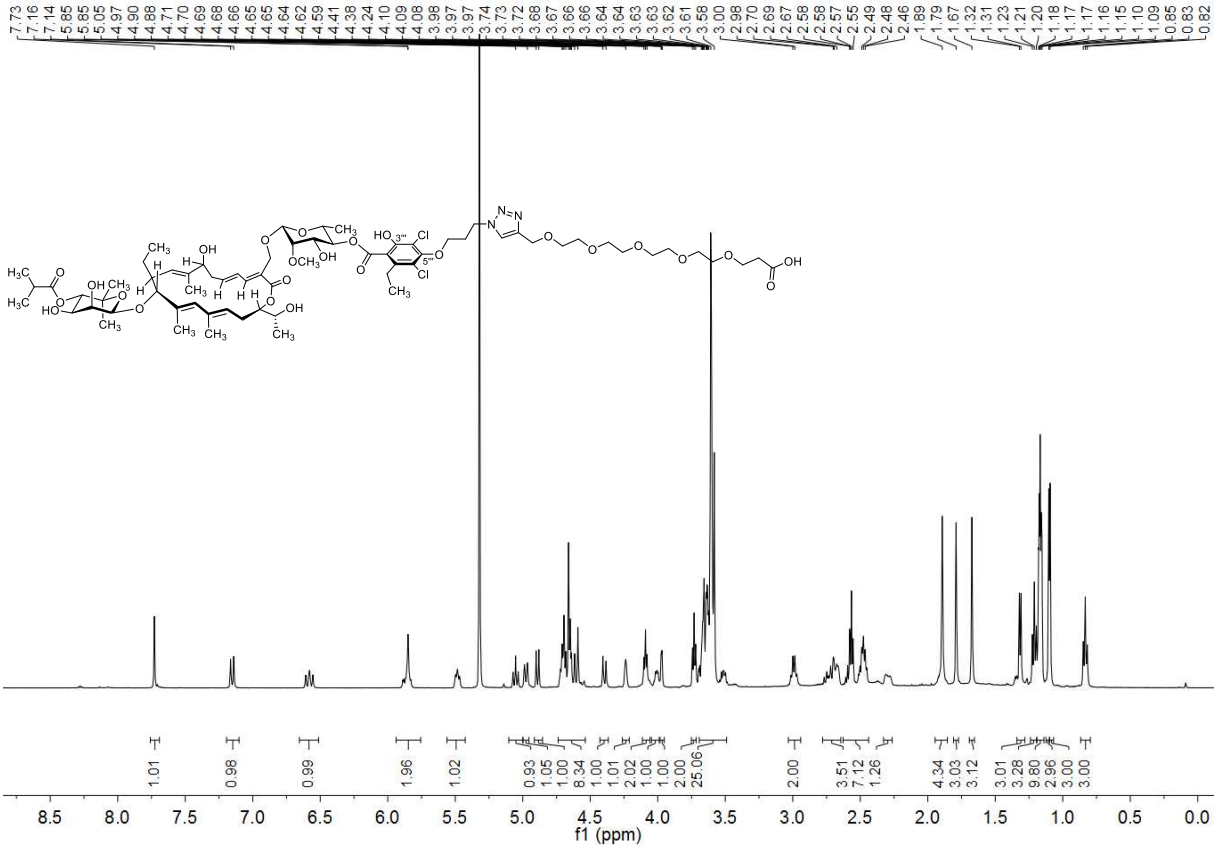

^{1}H NMR (500.30 MHz, 298 K, CD_2Cl_2)

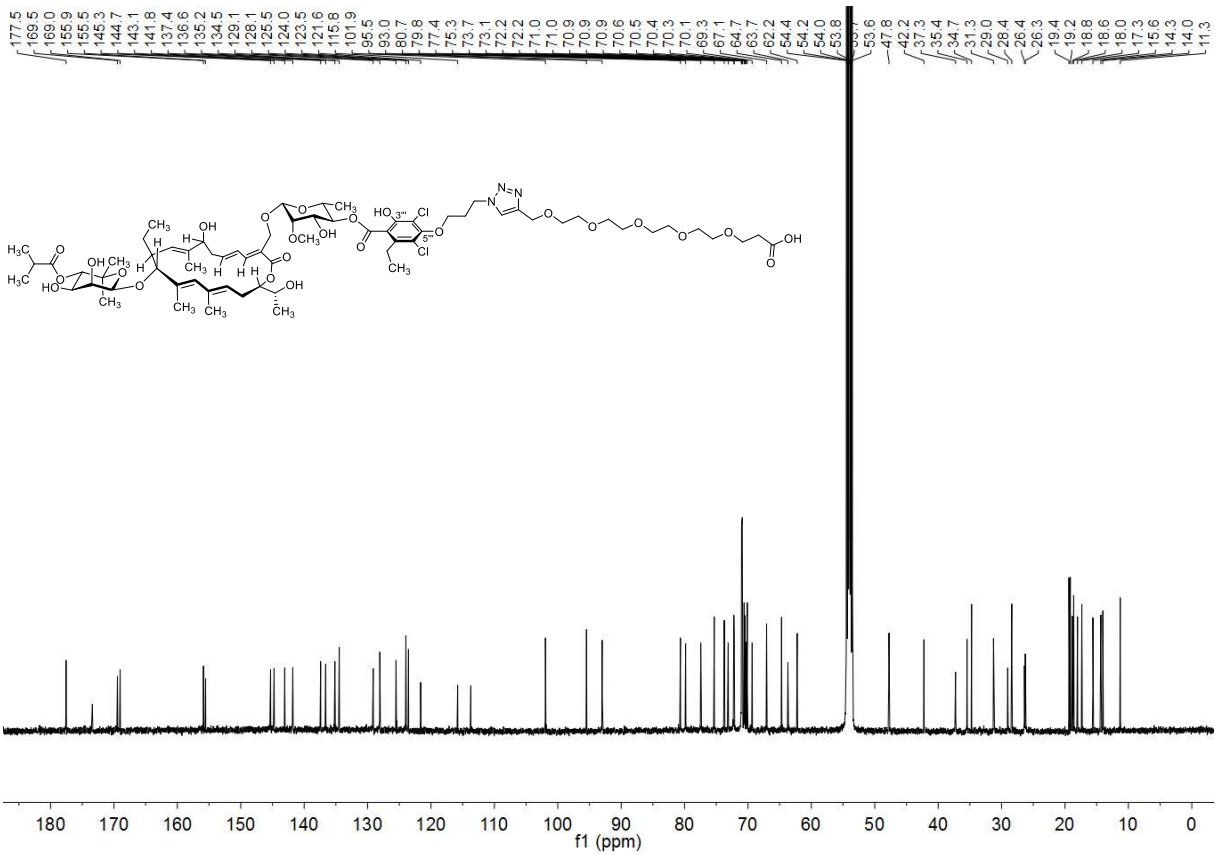

^{13}C NMR (125.81 MHz, 298 K, CD_2Cl_2)

Monotriazole with Piperidin-4-amine Substituent (13a)

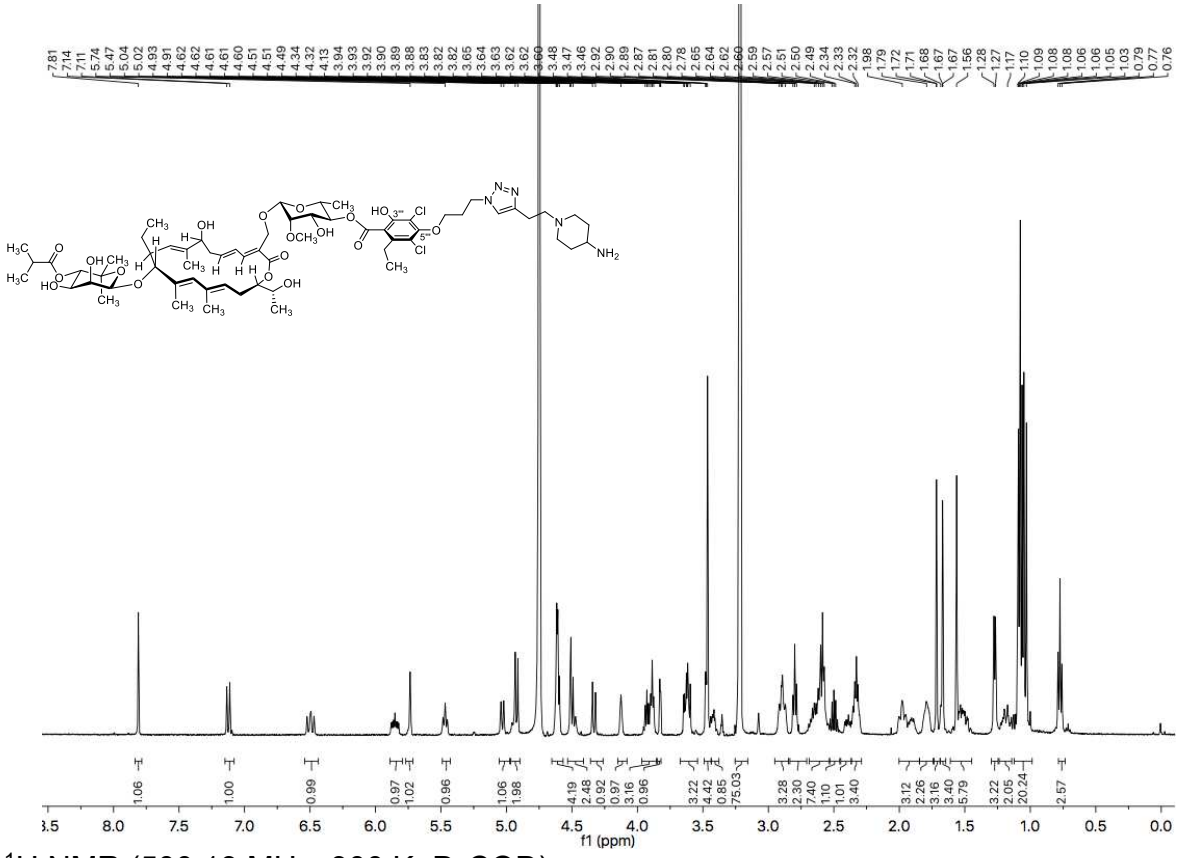

^{1}H NMR (500.13 MHz, 300 K, D_3COD)

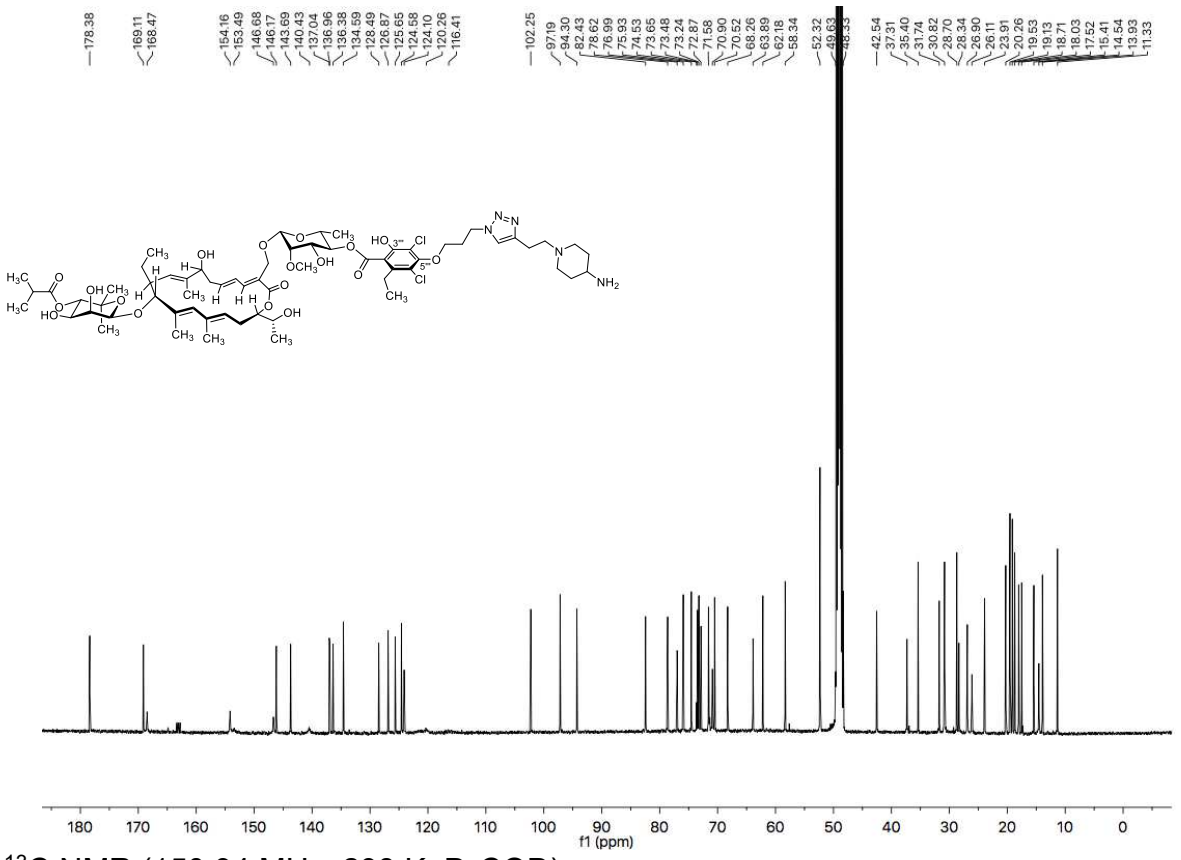

^{13}C NMR (150.94 MHz, 298 K, D_3COD)

Ditriazole with Piperidin-4-amine Substituent (13b)

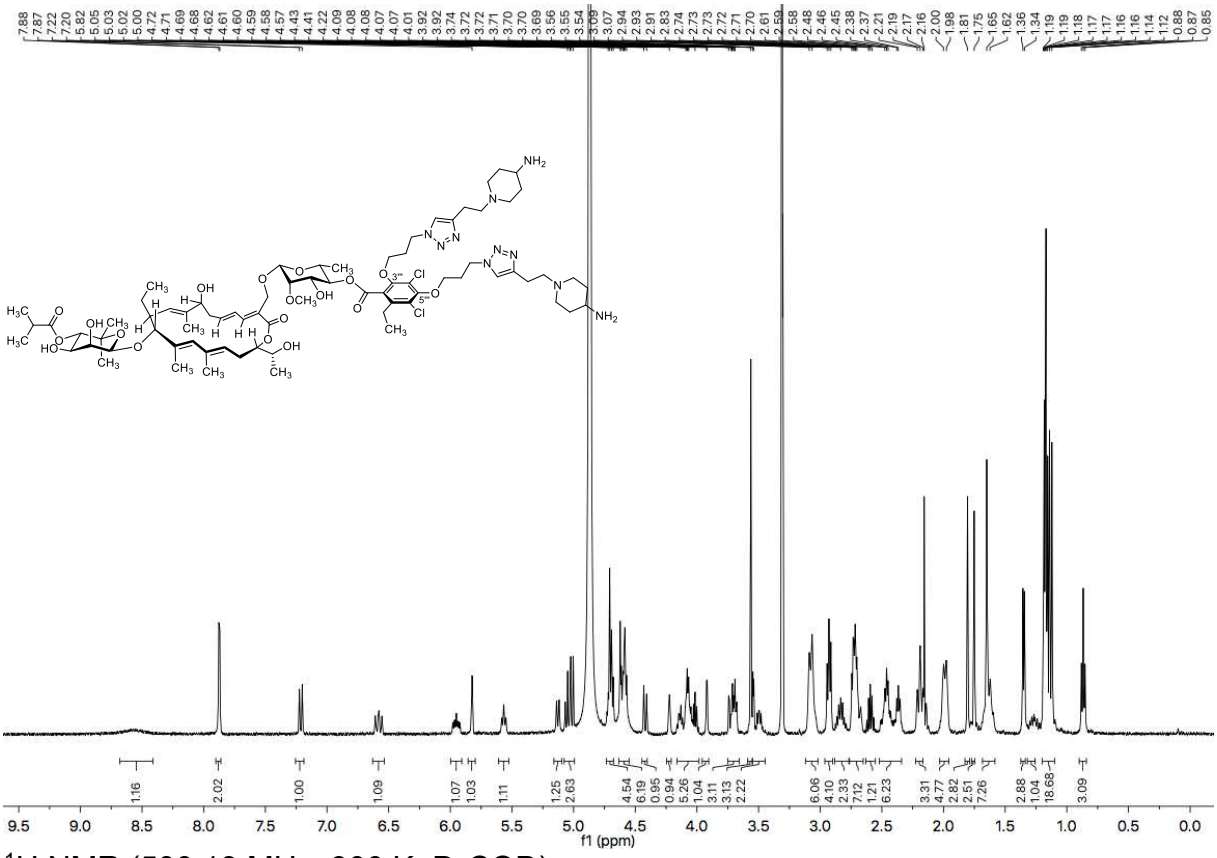

^{1}H NMR (500.13 MHz, 300 K, D_3COD)

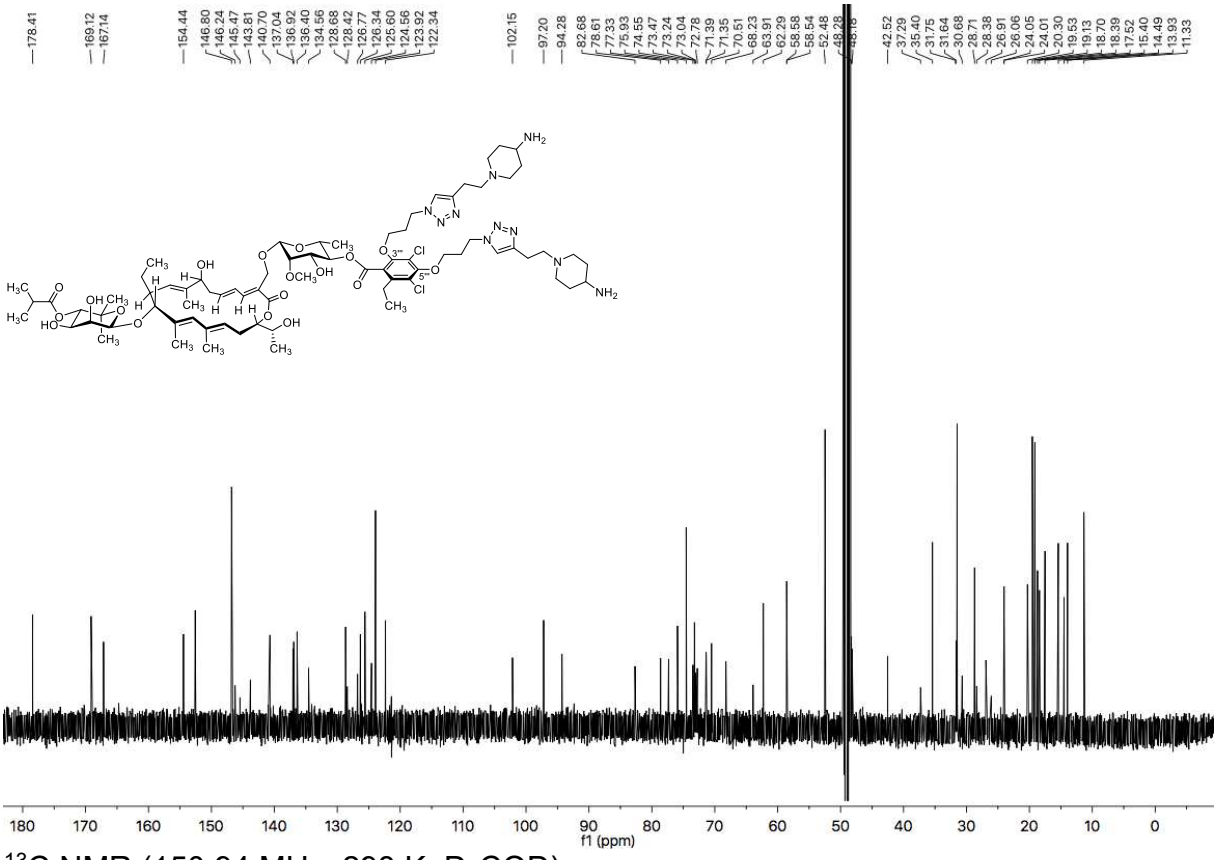

^{13}C NMR (150.94 MHz, 298 K, D_3COD)

6-Fluoro-7-[4-(2-bromoacetyl)piperazin-1-yl]-4-oxo-1,4-dihydroquinoline-3-carboxylic acid (14)

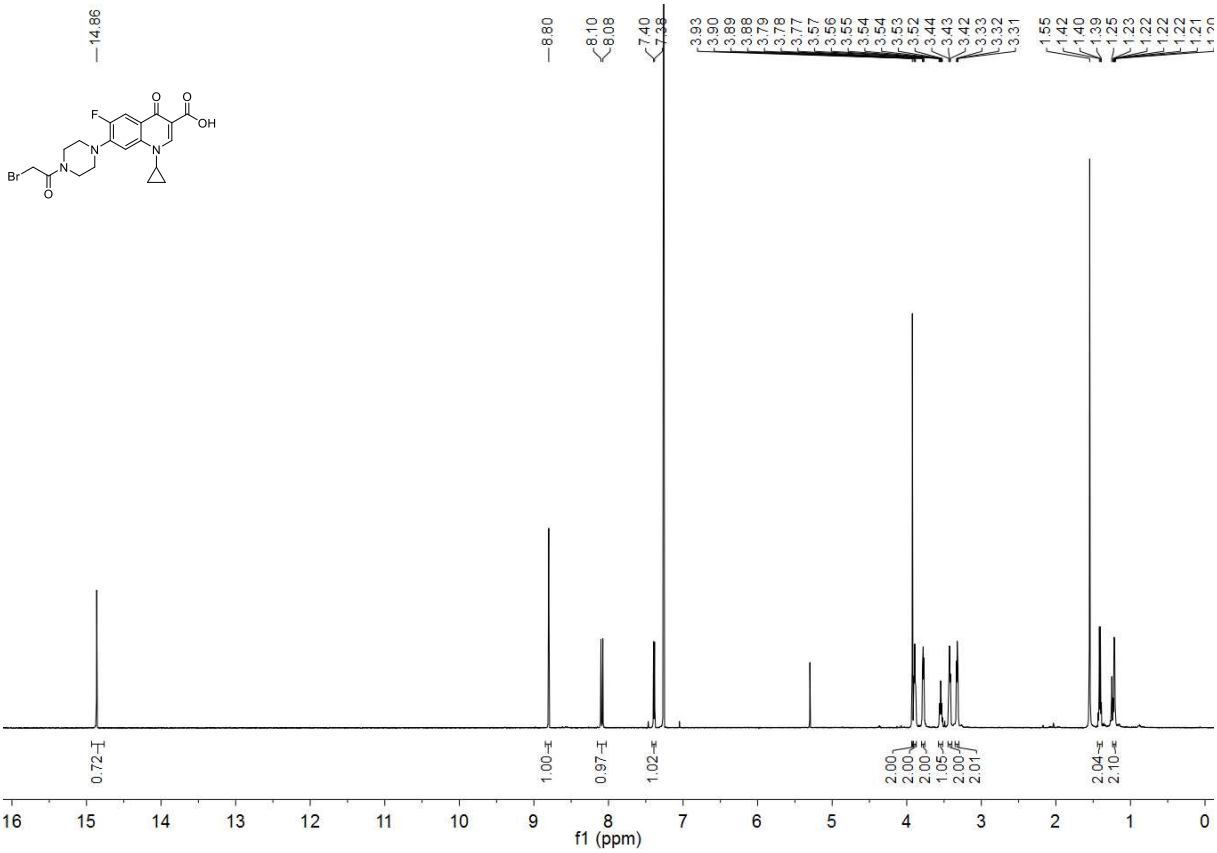

^{1}H NMR (500.13 MHz, 298 K, $CDCl_3$)

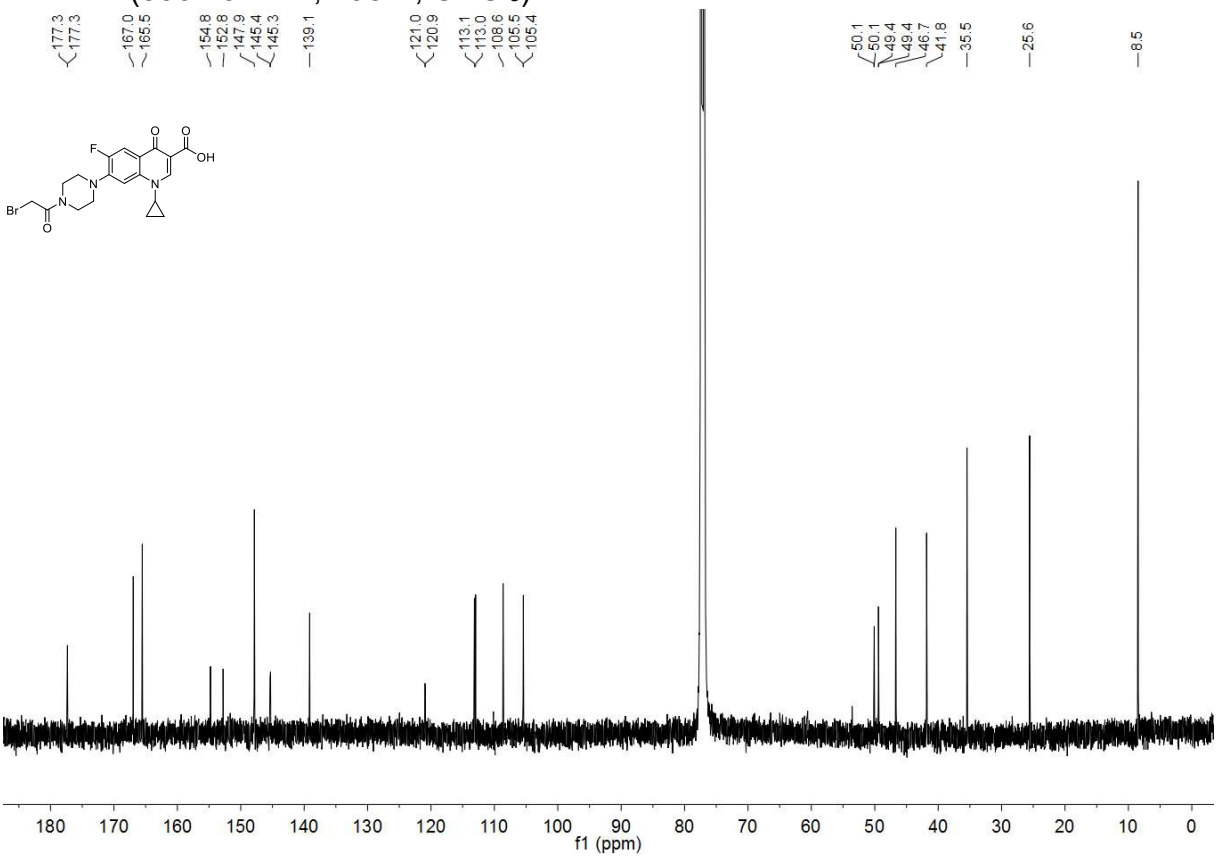

^{13}C NMR (125.81 MHz, 298 K, $CDCl_3$)

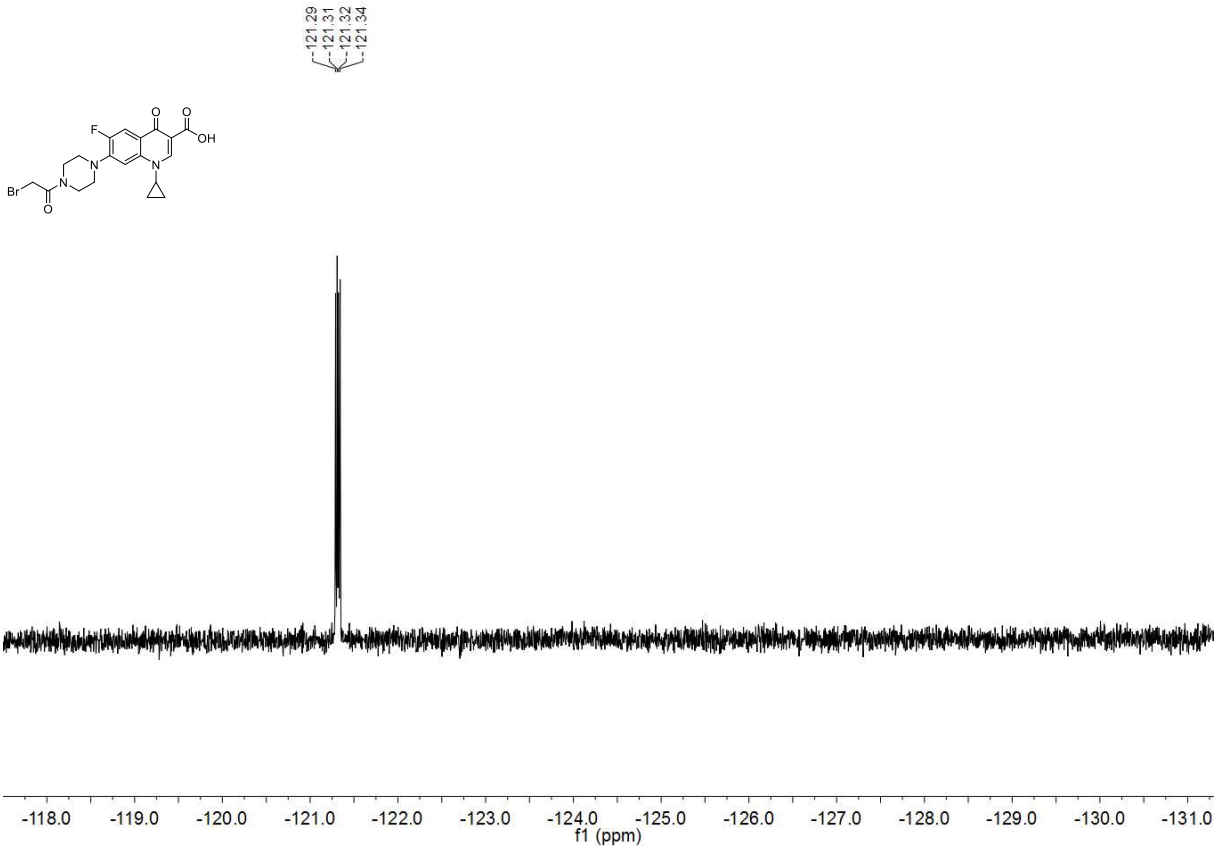

^{19}F NMR (376.46 MHz, 298 K, $CDCl_3$)

Fidaxomicin-Ciprofloxacin (15a)

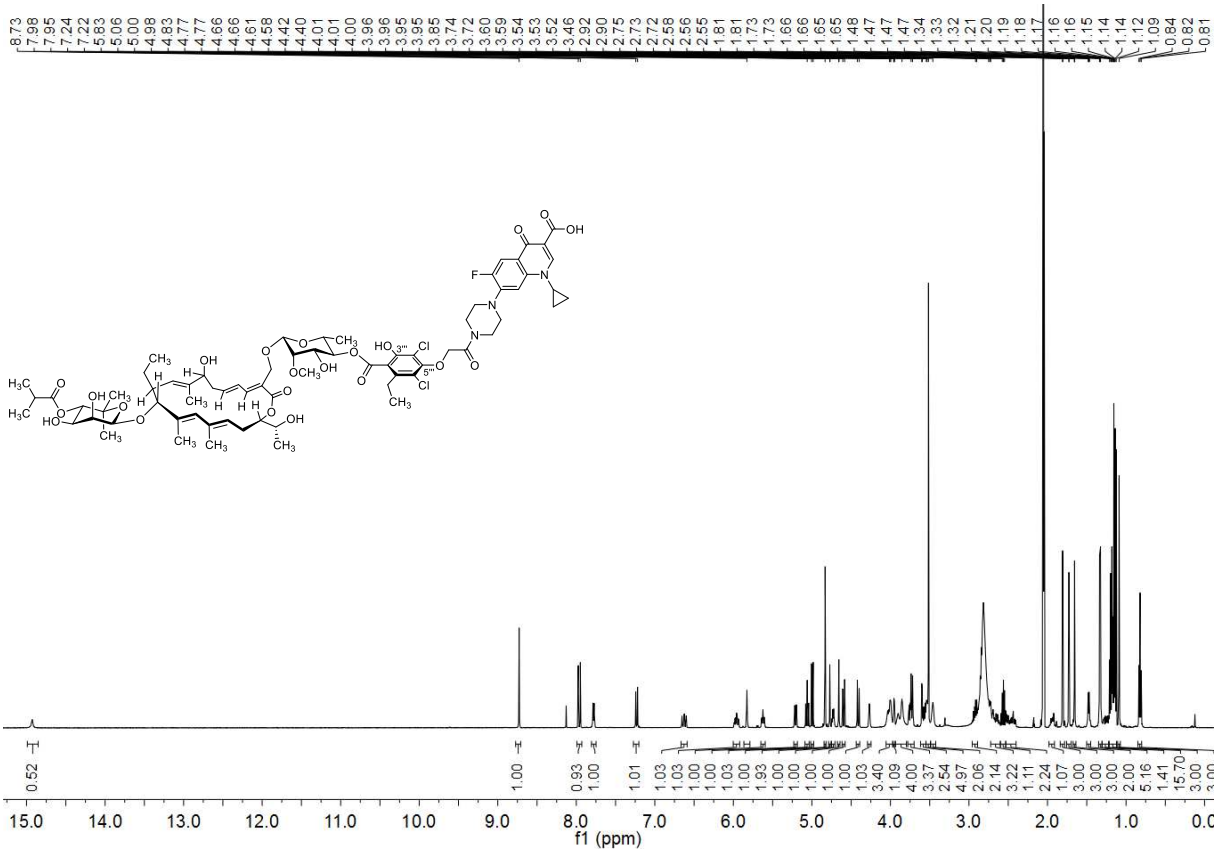

^{1}H NMR (500.13 MHz, 298 K, acetone-d_6)

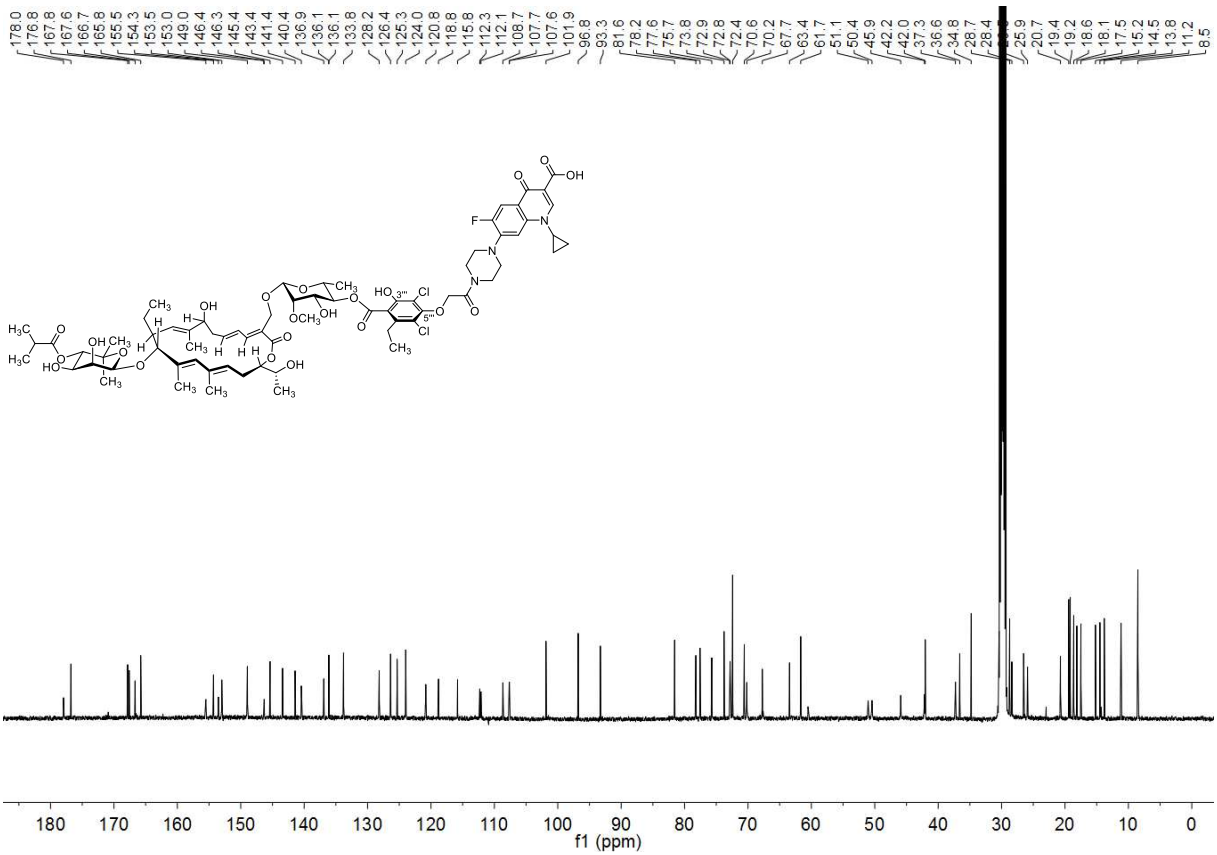

^{13}C NMR (125.81 MHz, 300 K, acetone-d_6)

Fidaxomicin-Bis(ciprofloxacin) (15b)

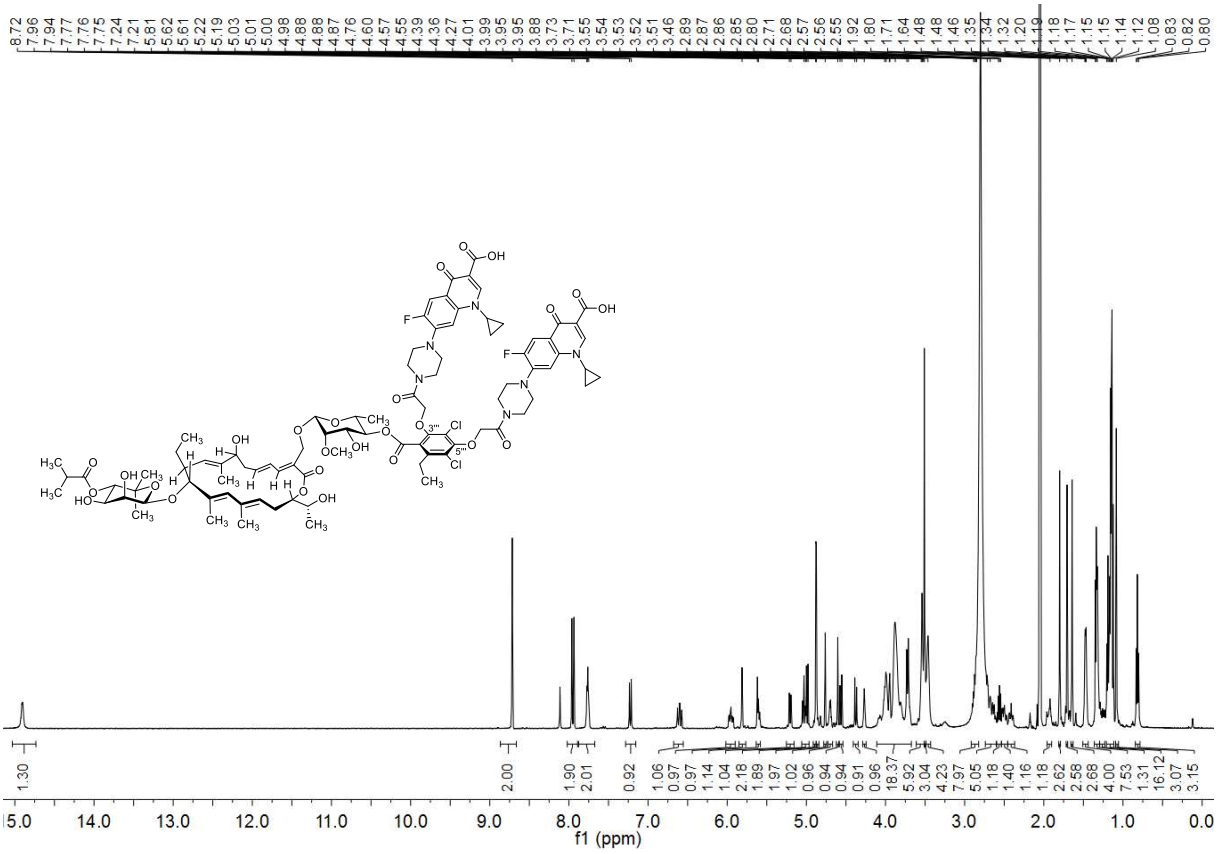

^{1}H NMR (500.13 MHz, 300 K, acetone-d_6)

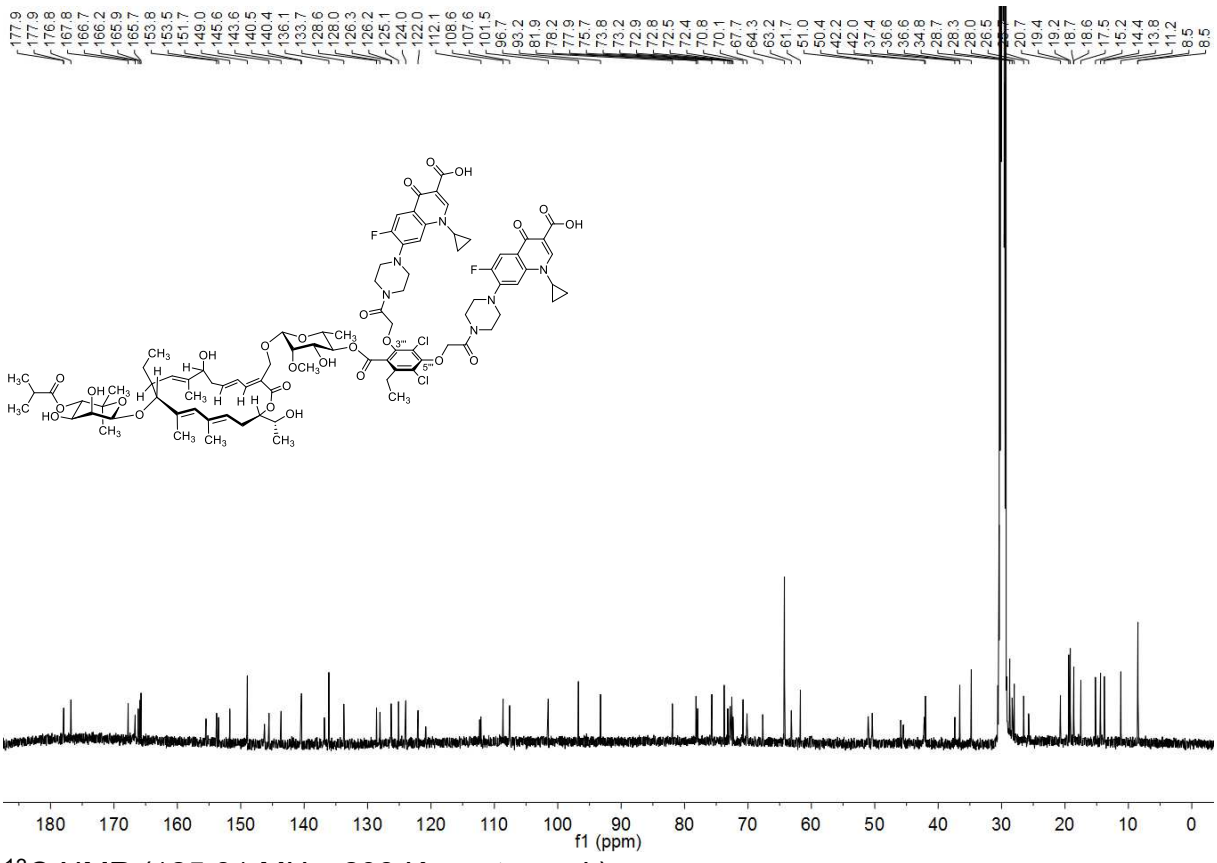

^{13}C NMR (125.81 MHz, 298 K, acetone-d_6)

23-Azido-3,6,9,12,15,18,21-heptaoxatricosyl 4-nitrobenzenesulfonate (16)

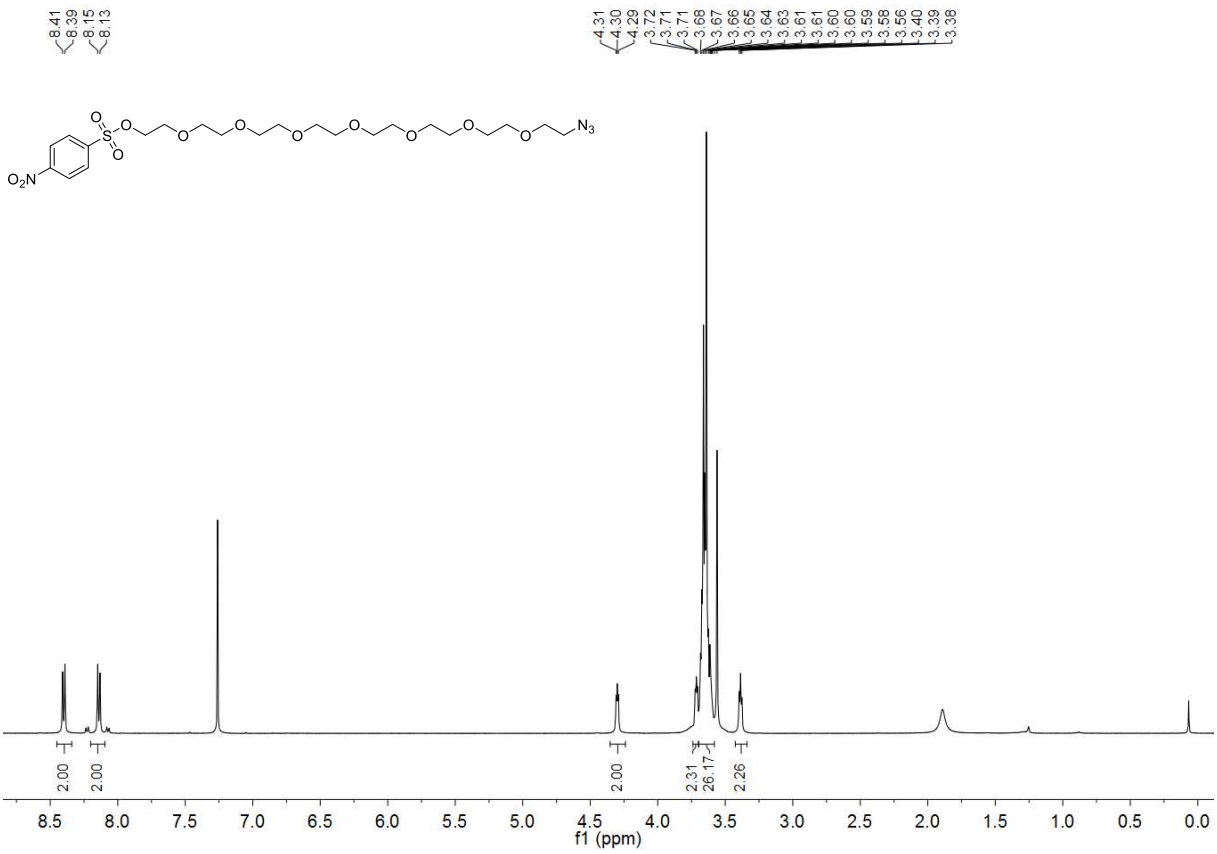

^{1}H NMR (500.30 MHz, 300 K, $CDCl_3$)

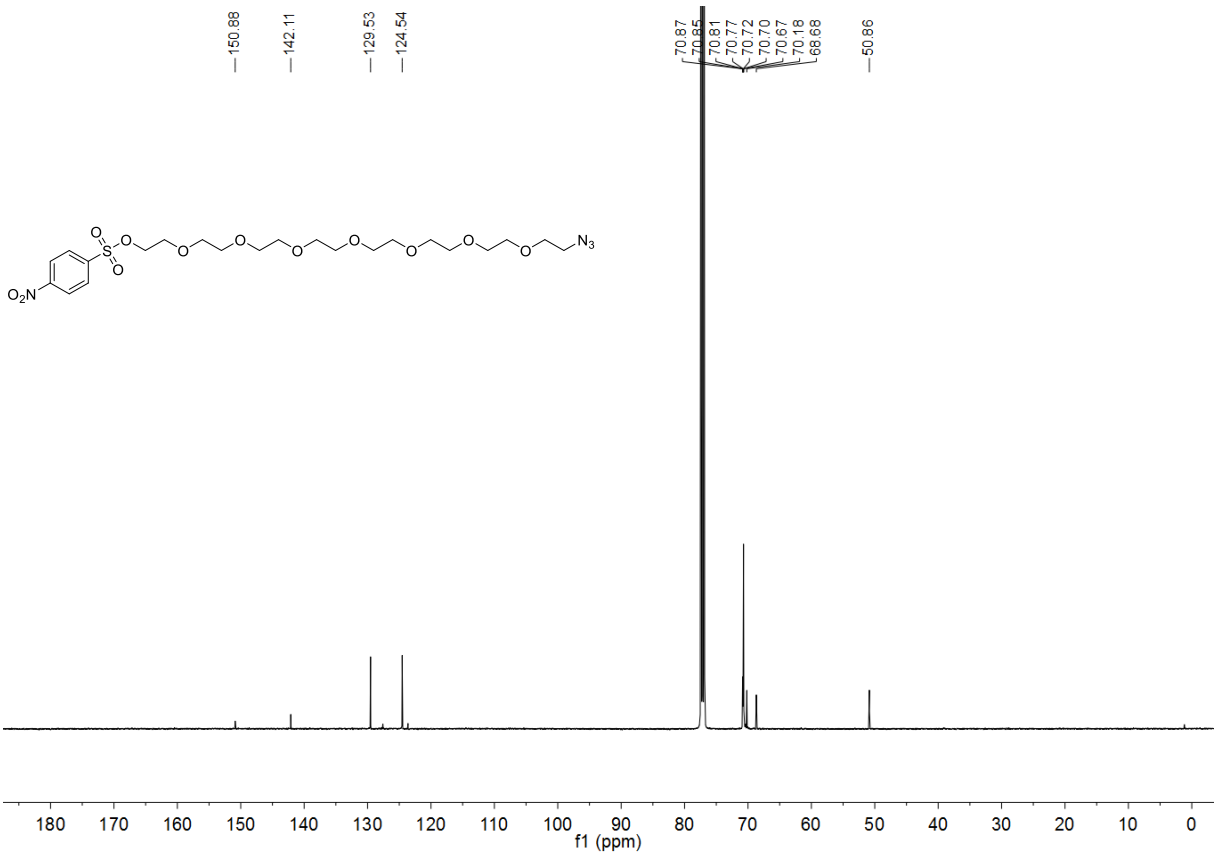

^{13}C NMR (125.81 MHz, 300 K, $CDCl_3$)

Fidaxomicin-OEG-azide (17)

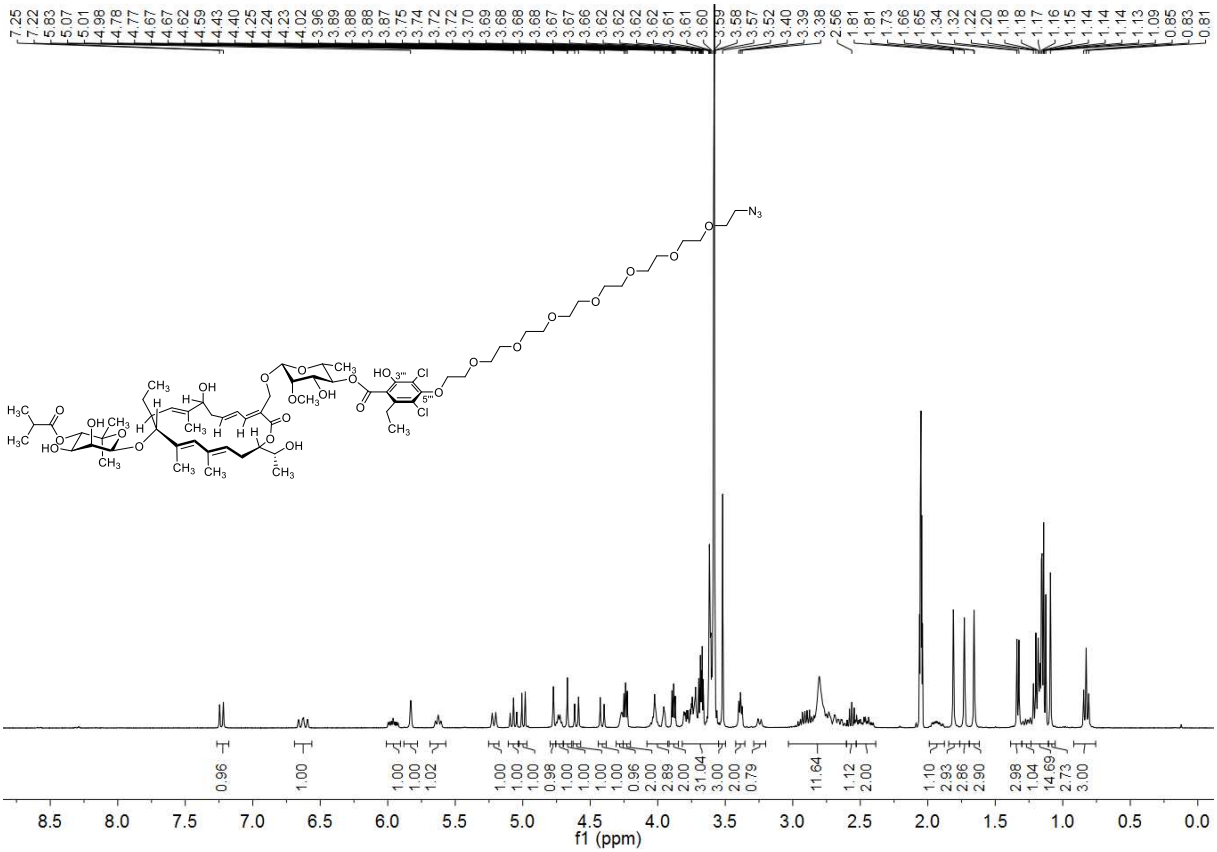

^{1}H NMR (400.23 MHz, 300 K, acetone-d_6)

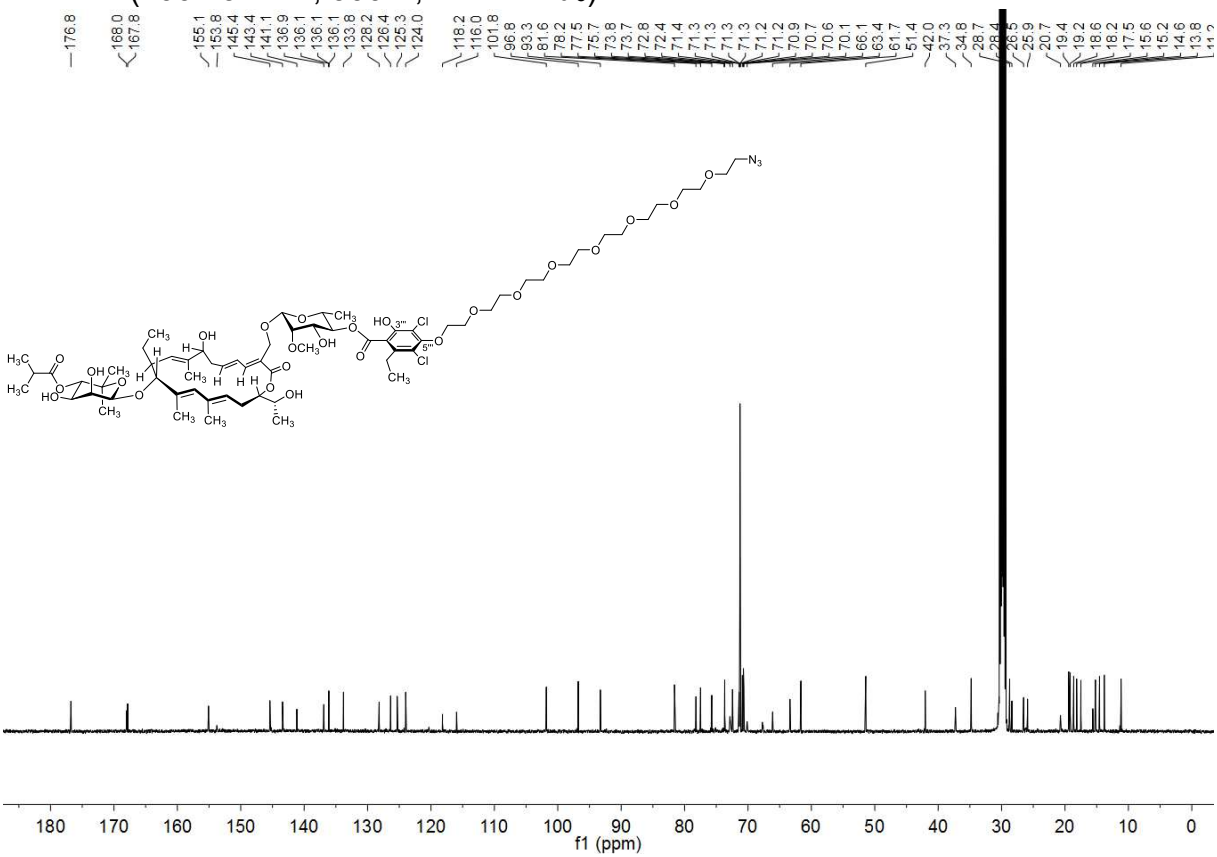

^{13}C NMR (125.81 MHz, 300 K, acetone-d_6)

1-Nitrosopiperazine

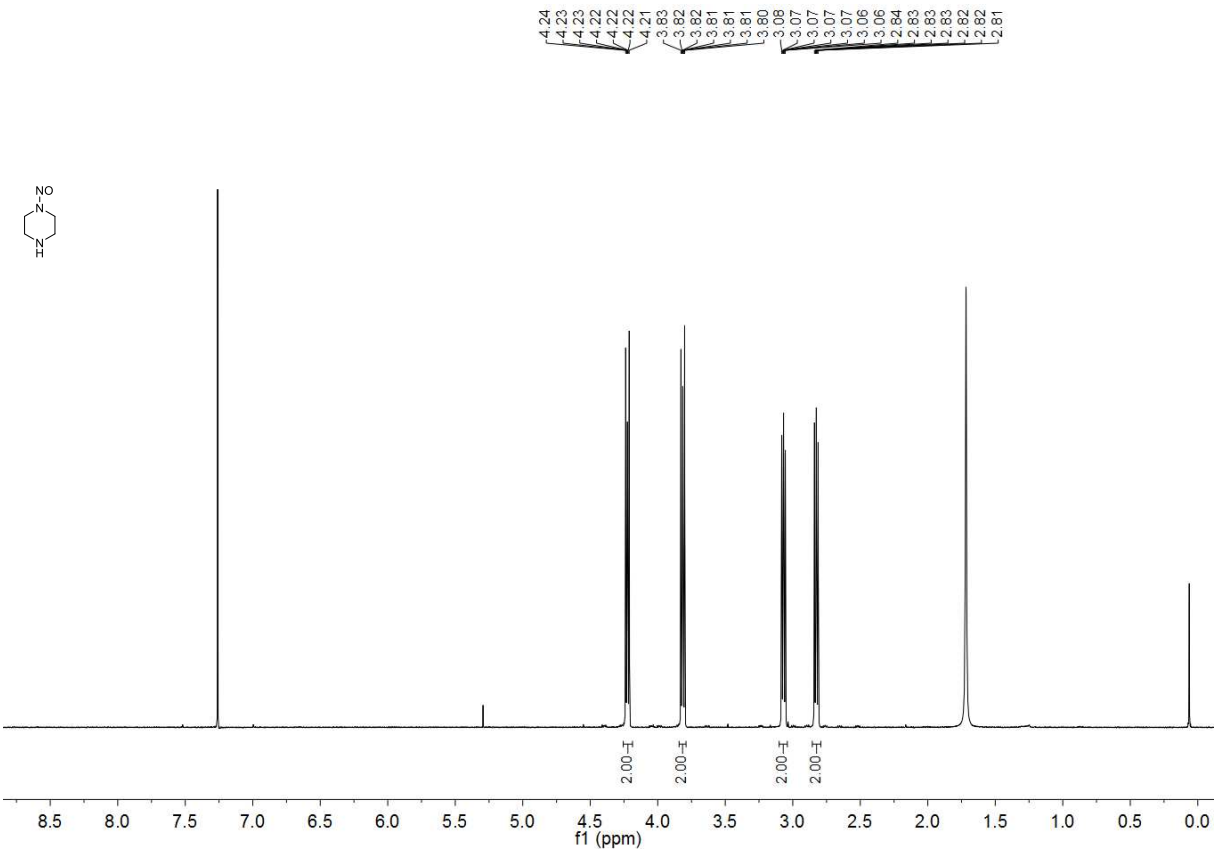

^{1}H NMR (400.13 MHz, 300 K, $CDCl_3$)

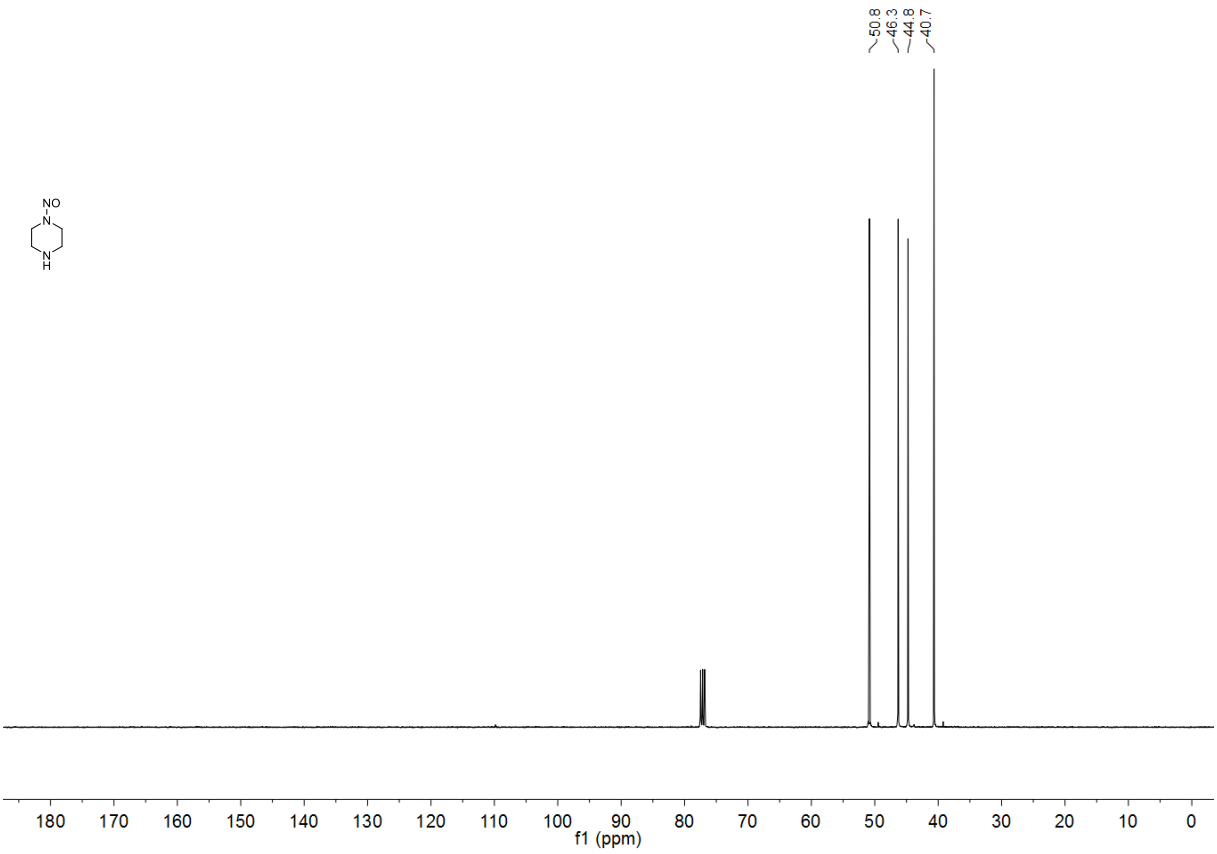

^{13}C NMR (100.62 MHz, 298 K, $CDCl_3$)

1-Nitroso-4-propargylpiperazine

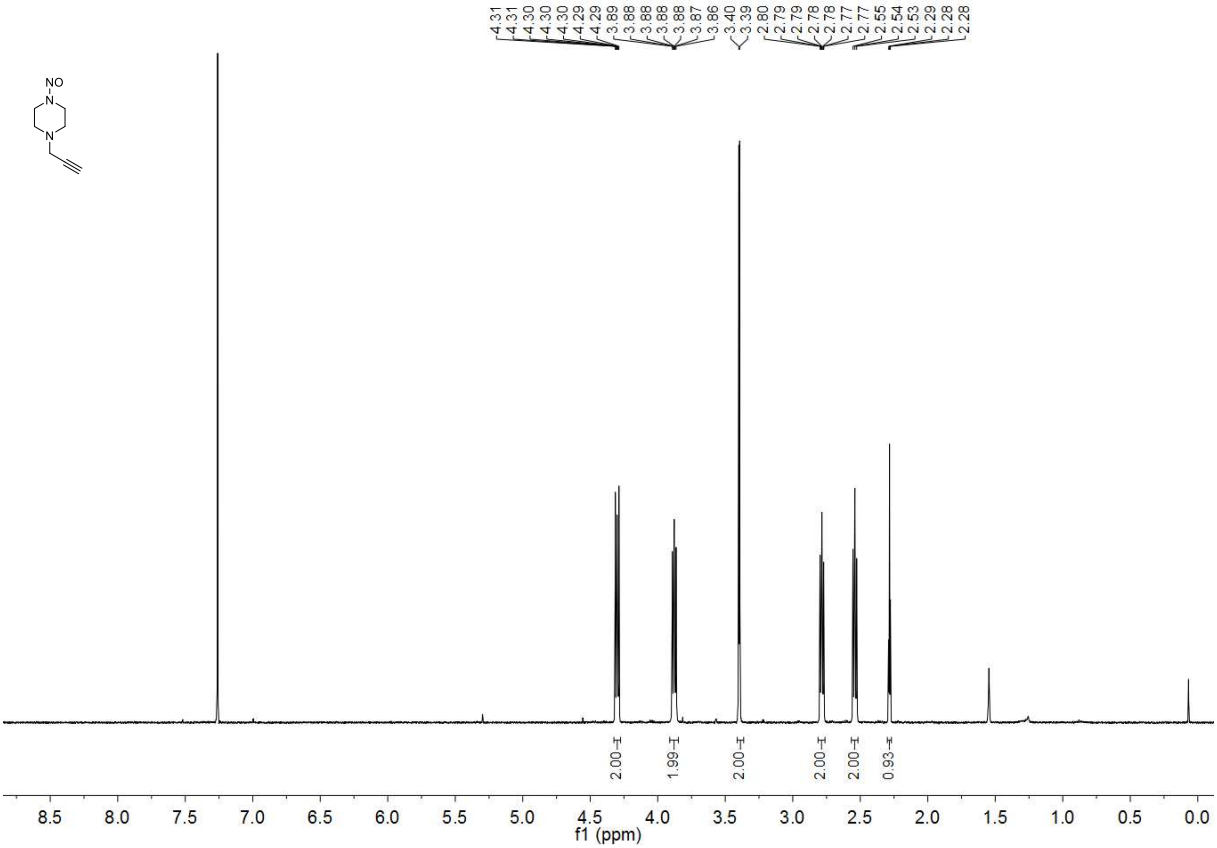

^{1}H NMR (400.13 MHz, 300 K, $CDCl_3$)

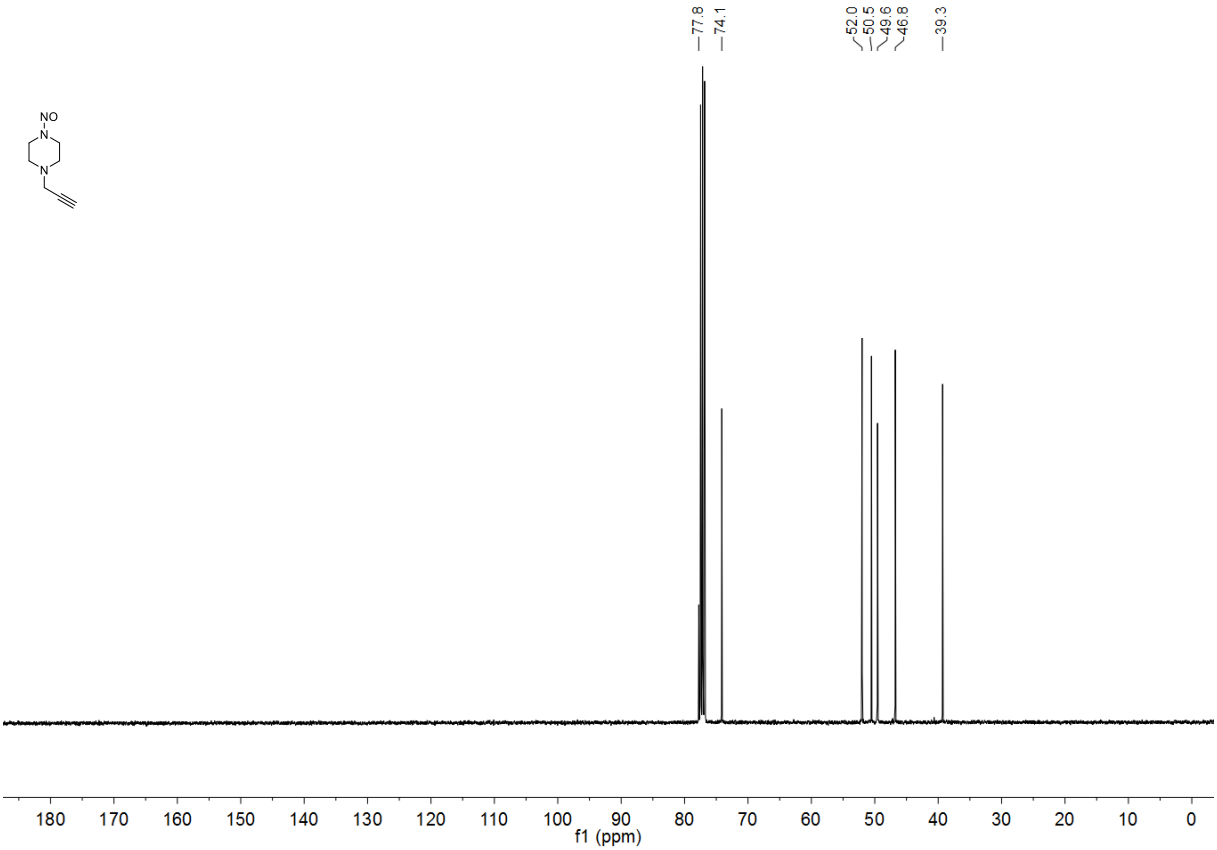

^{13}C NMR (100.62 MHz, 298 K, $CDCl_3$)

1-Amino-4-propargylpiperazine

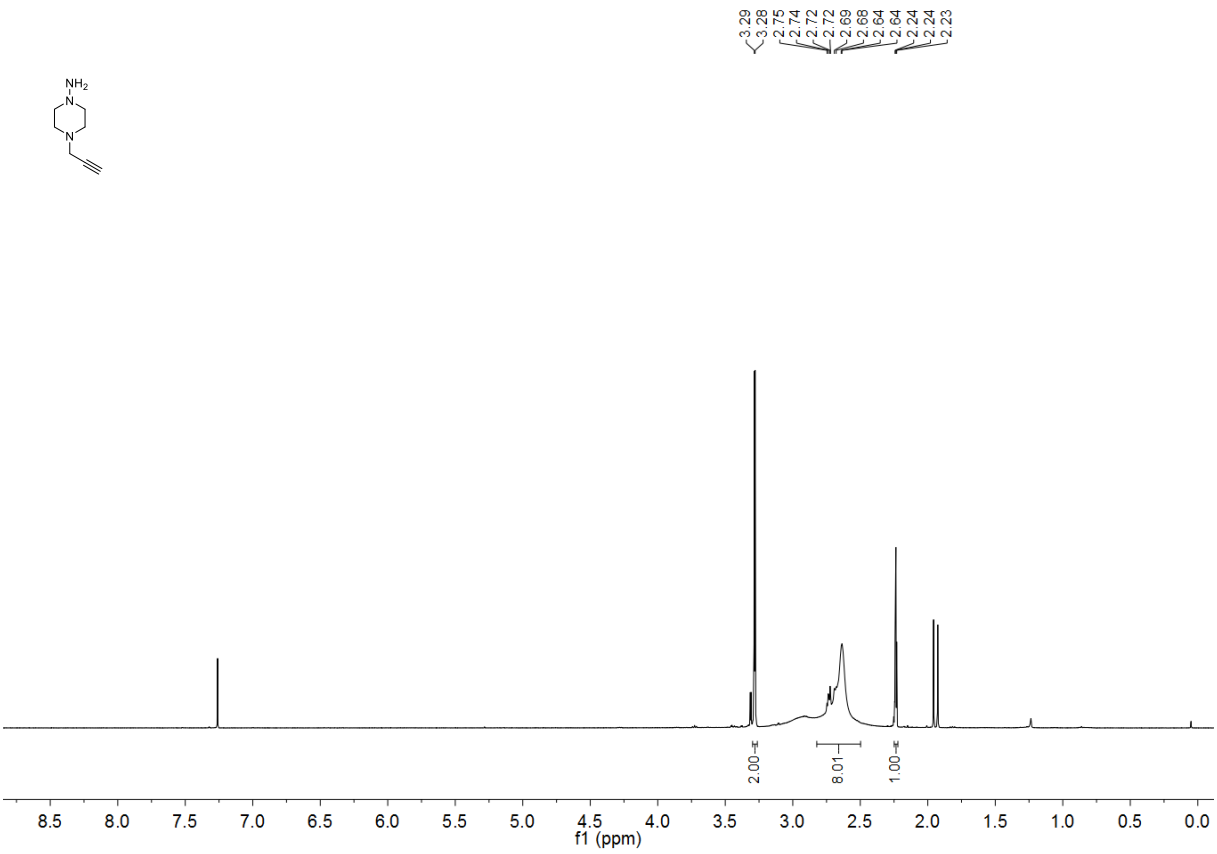

^{1}H NMR (400.13 MHz, 300 K, $CDCl_3$)

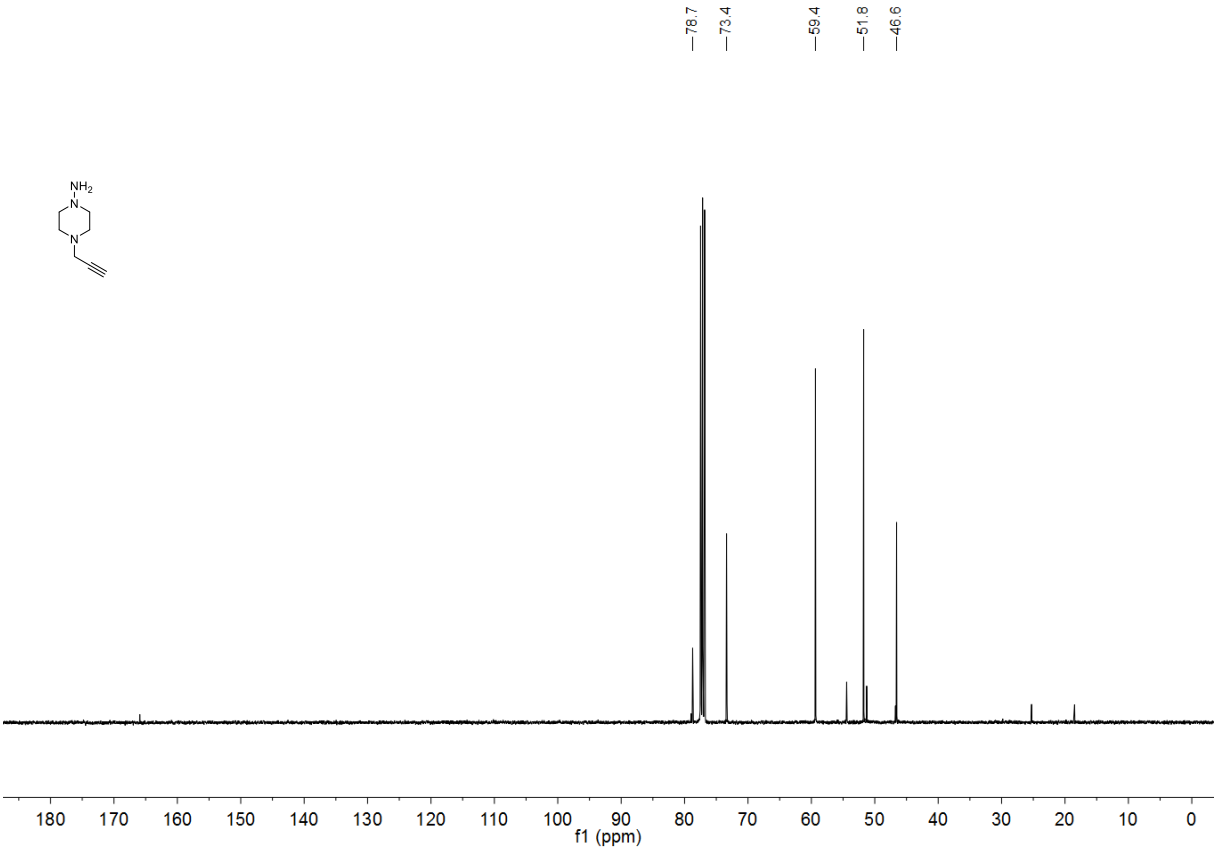

^{13}C NMR (100.62 MHz, 300 K, $CDCl_3$)

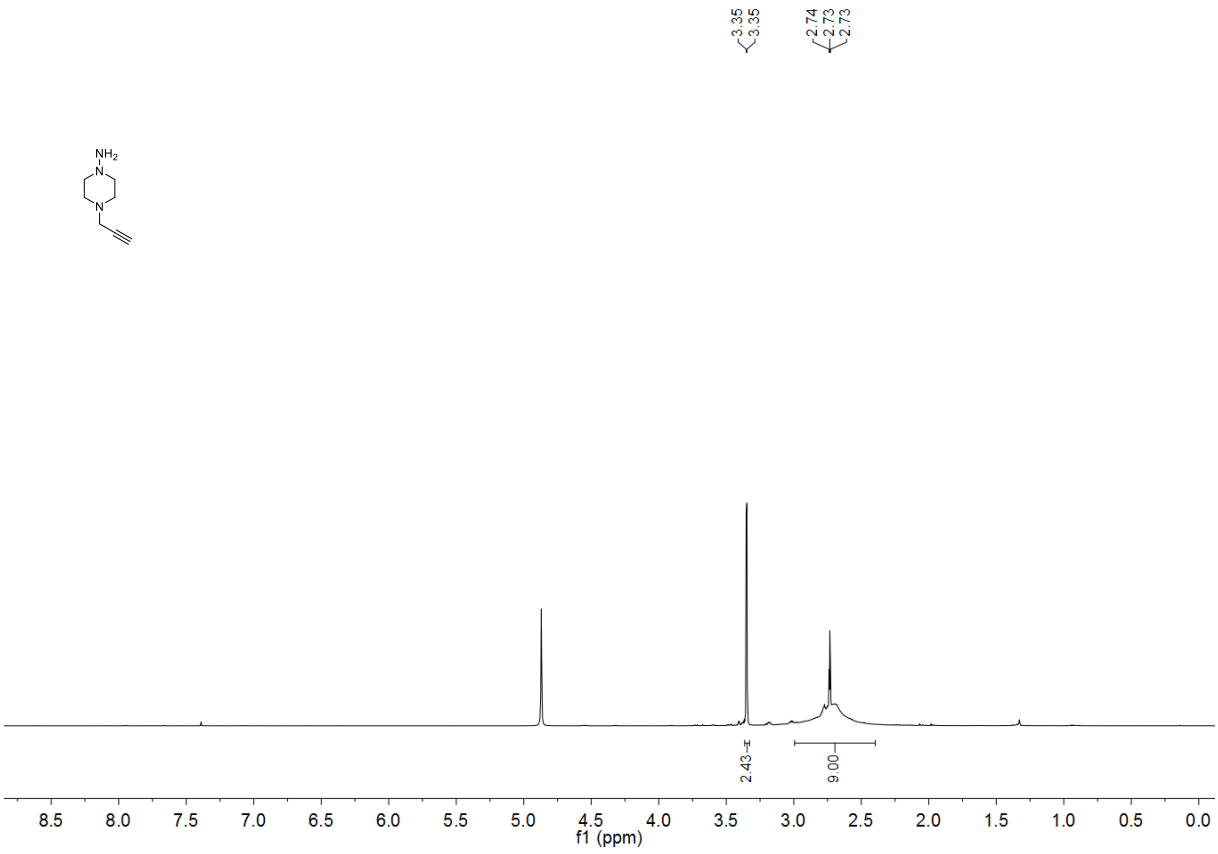

^{1}H NMR (500.13 MHz, 300 K, D_3COD)

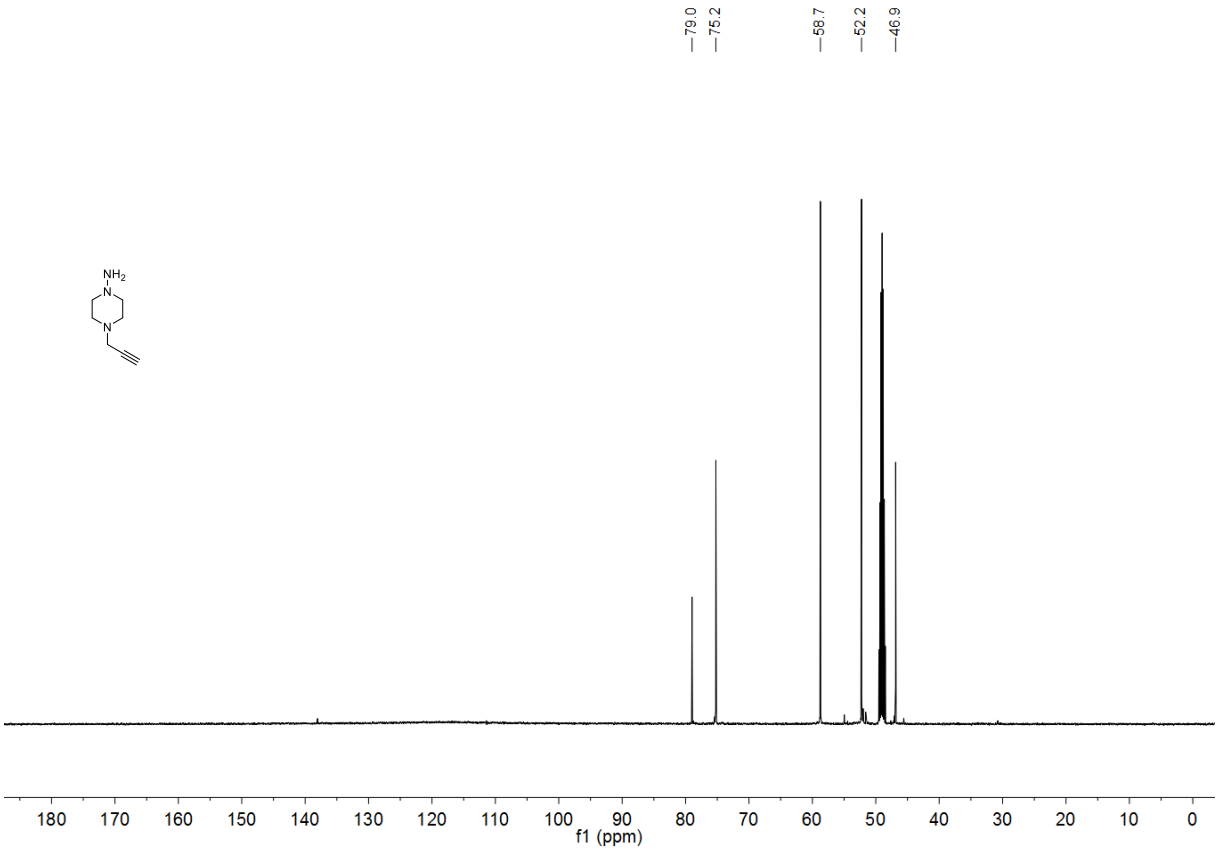

^{13}C NMR (125.77 MHz, 300 K, D_3COD)

Alkinylated Rifampicin (18)

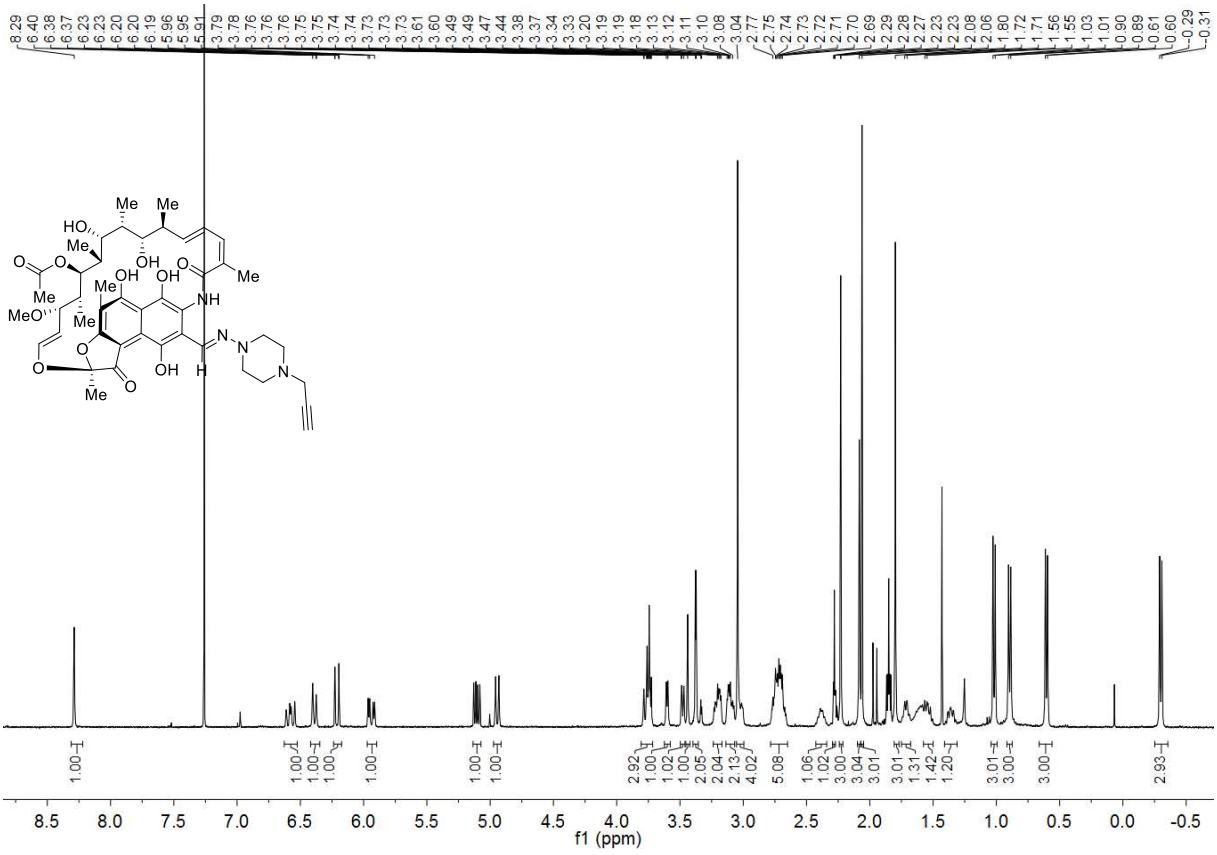

^{1}H NMR (400.13 MHz, 298 K, $CDCl_3$)

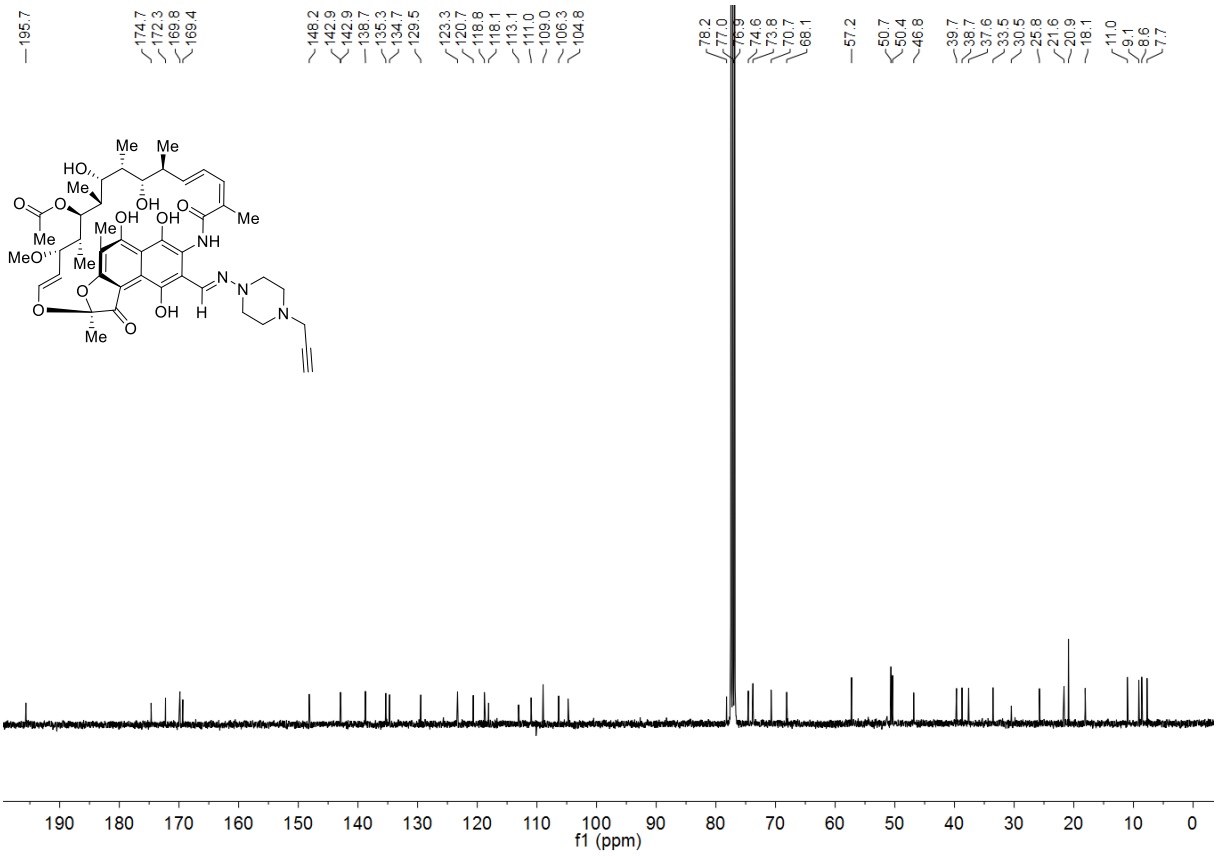

^{13}C NMR (100.62 MHz, 298 K, $CDCl_3$)

Fidaxomicin-Rifampicin Hybrid (19)

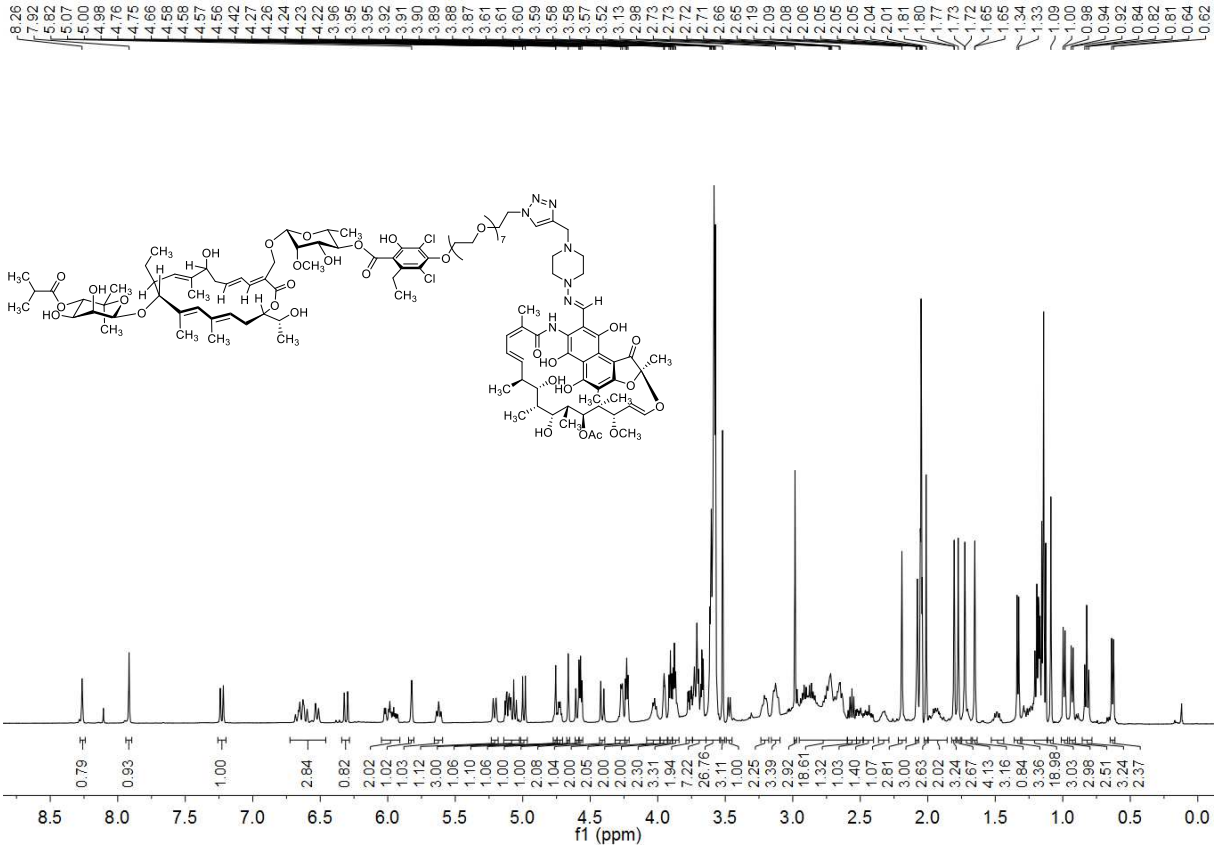

^{1}H NMR (500.13 MHz, 300 K, acetone-d_6)

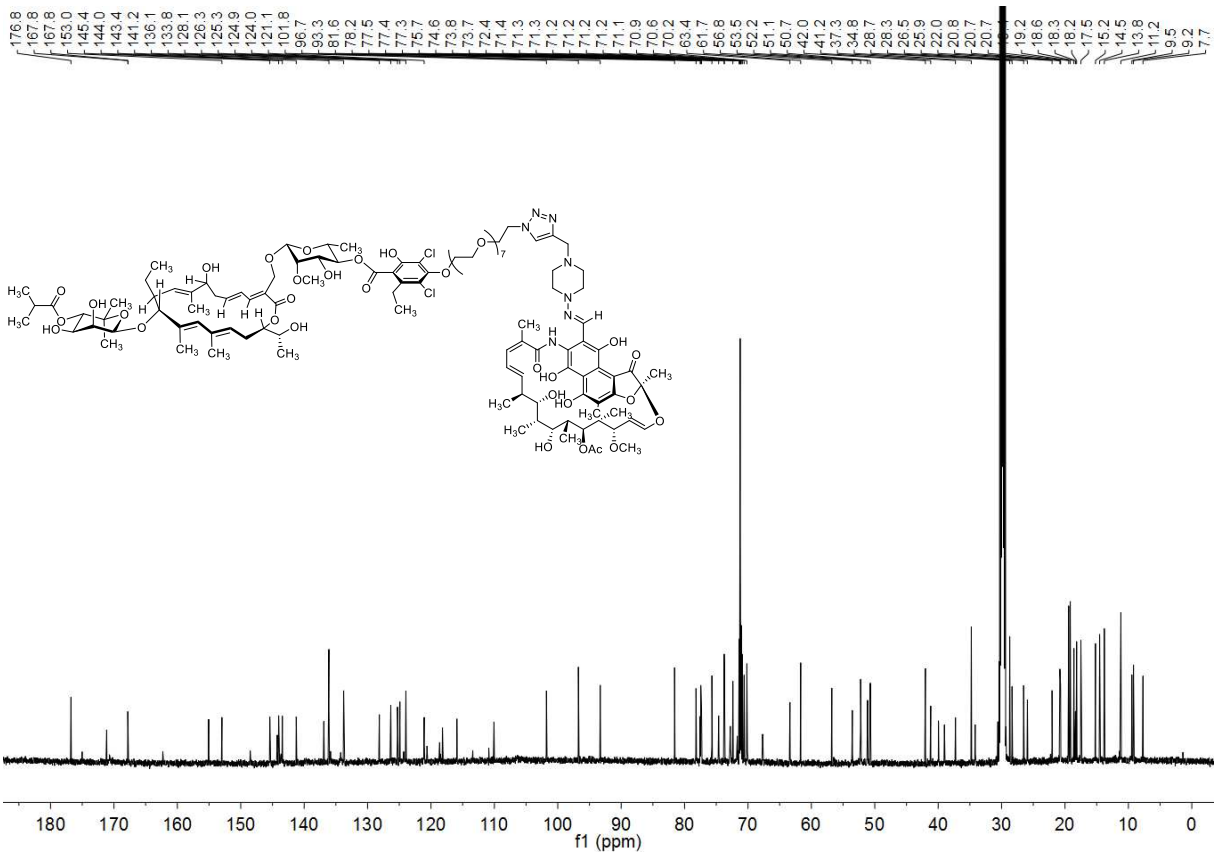

^{13}C NMR (150.94 MHz, 298 K, acetone-d_6)

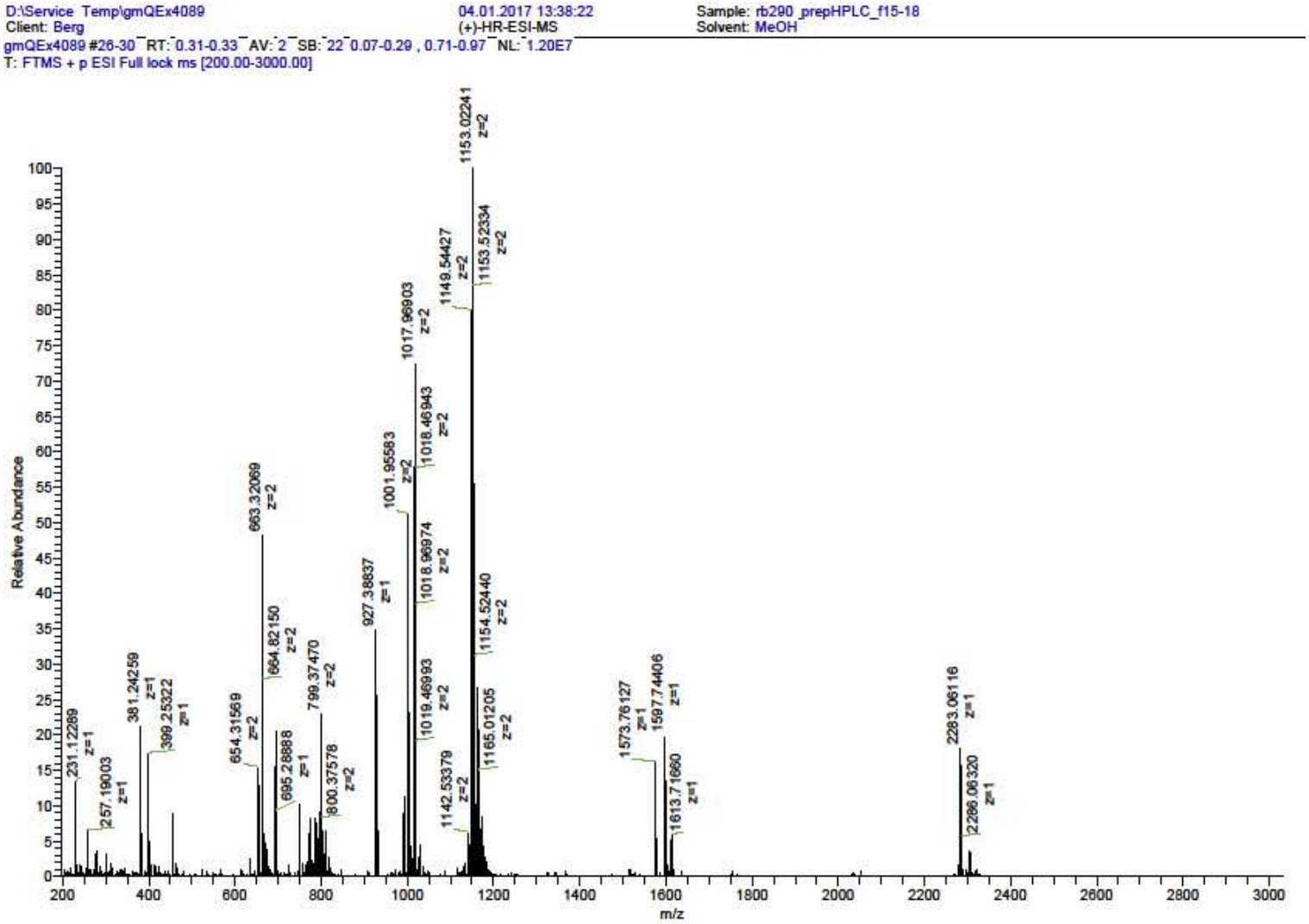

(+)-HR-ESI-MS spectrum of the Fdx-Rif hybrid species: m/z = 1149.54427 can be assigned to the dication $[M+NH_4+H]^{2+}$ of the Fdx-Rif hybrid $C_{113}H_{163}Cl_2N_7O_{37}$, M_{exact} = 2280.04654.

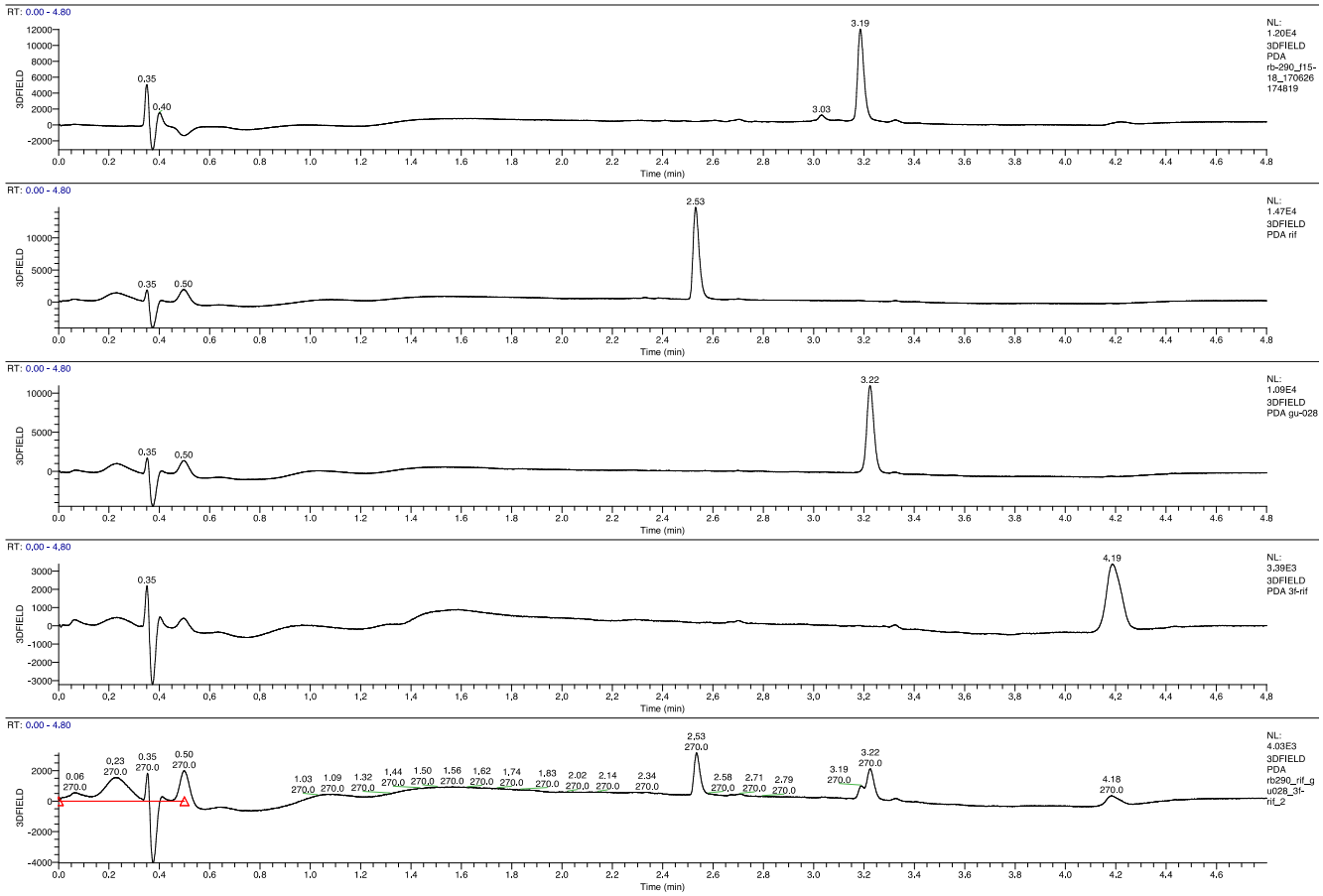

a) Fdx-Rif-Hybrid (50 µg mL^{-1}, MeOH)

b) Rifampicin (50 µg mL^{-1}, MeOH)

c) Rif-alkyne (50 µg mL^{-1}, MeOH)

d) 3-Formylrifampicin (50 µg mL^{-1}, MeOH)

e) Co-injection of a)–d) (10 µg mL^{-1} per compound, MeOH)

UHPLC chromatograms of a) the Fdx-Rif hybrid (same sample as for biological testing) and plausible contaminants b) rifampicin; c) alkynylated rifampicin; d) 3-formylrifampicin. Part e) shows the resulting chromatogram from co-injection of aliquots of solutions from a)–d) [from a 50 µg mL^{-1} sample of a)–d) was taken an aliquot sample of 200 µL and 200 µL MeOH was added to give a total sample volume of 1 mL with a concentration of 10 µg mL^{-1} per compound).

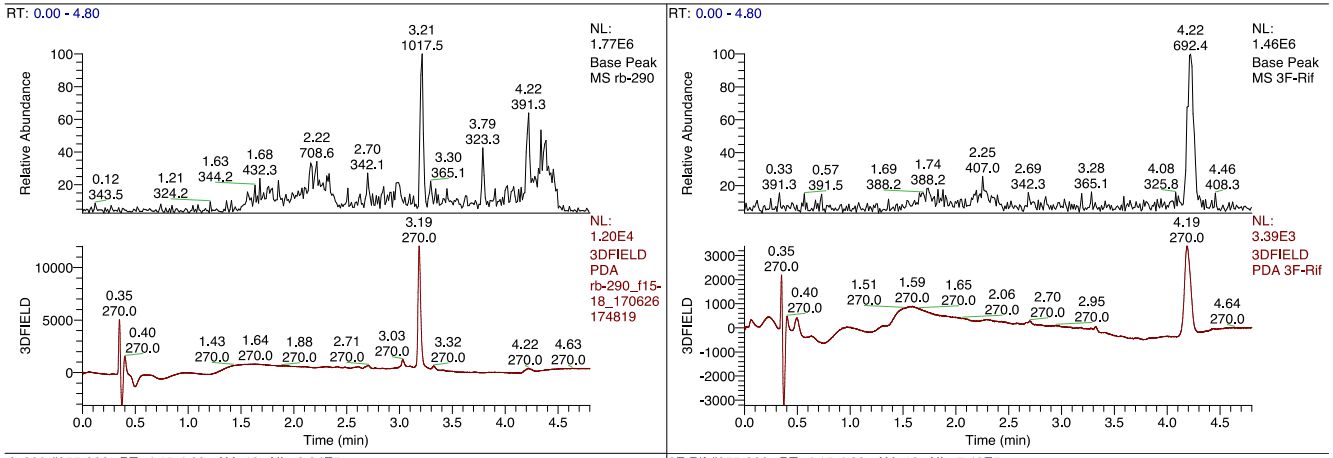

UHPLC chromatograms with UV trace

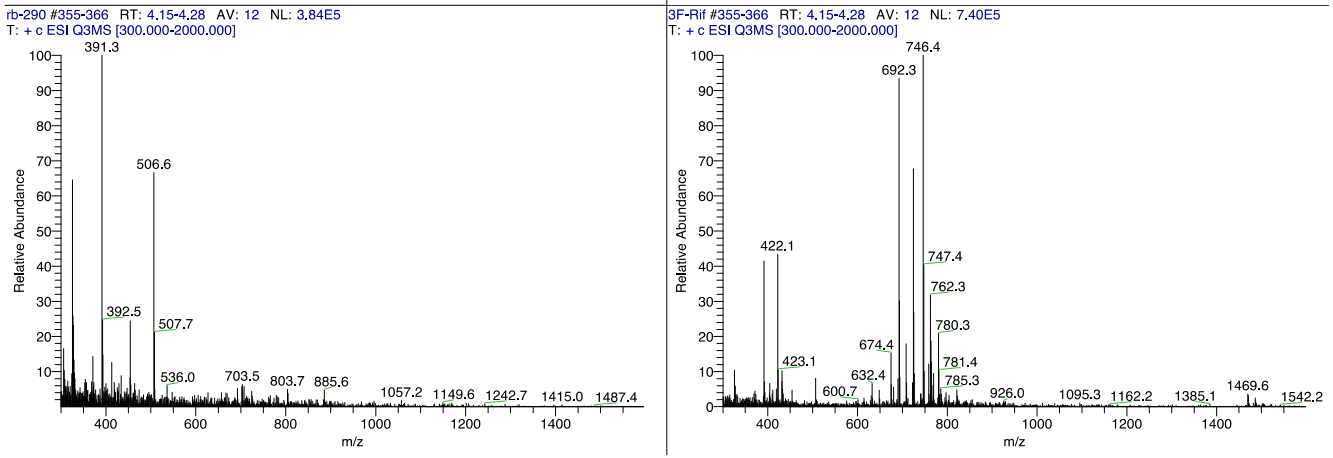

(+)-ESI-MS mass spectra at the indicated retention times

Chromatogram of the Fdx-Rif hybrid and (+)-ESI-MS spectrum of the peak at 4.15–4.28 min

Chromatogram of 3-formylrifampicin and (+)-ESI-MS spectrum of the peak at 4.15–4.28 min

Comparison of the UHPLC chromatograms and mass spectra of Fdx-Rif hybrid and 3-formylrifampicin: Although there is a minor bump at R_t = 4.22 min in the UV trace of Fdx-Rif hybrid (left side), the mass spectrum of this peak is not the one expected for 3-formylrifampicin (right side).